THE UNIVERSITY OF QUEENSLAND

AUSTRALIA

Remote Sensing for Multi-scale Mangrove Mapping

Muhammad Kamal

BSc. (Hons) (UGM), MGIS. (UQ)

A thesis submitted for the degree of Doctor of Philosophy at

The University of Queensland in 2015

School of Geography, Planning and Environmental Management

Abstract

Understanding the relationships between the size of mangrove vegetation features and the optimum image pixel size required to map these features is essential to support effective mapping and monitoring activities in this environment. Currently mangroves are under pressure from anthropogenic and natural disturbances, and up-to-date and accurate spatial information is required to support their management. Addressing ecological problems at the correct spatial scale is essential in mangrove environments. There is a lack of knowledge on the types and biophysical properties of mangroves, which can be mapped at different image spatial resolutions. This thesis integrated the spatial and temporal dimension of remote sensing data into a spatio-temporal continuum of mangrove ecology and developed guidelines for multi-scale image-based mangrove mapping. Three objectives were addressed to achieve the aim: (1) characterising mangrove spatial structure to produce an optimum pixel resolution scheme for image-based mangrove mapping; (2) assessing the applicability of the scheme to selected images for mangrove composition and leaf area index (LAI) mapping; and (3) developing guidelines for multi-scale mangrove mapping. The research sites were located in Moreton Bay, Australia, and Karimunjawa Island, Indonesia. Landsat TM, ALOS AVNIR-2, and WorldView-2 images were used for both sites; with additional LiDAR data and a very high-spatial resolution aerial photograph for Moreton Bay.

After two introductory chapters, chapter three focused on the development of a method for estimating the optimum pixel size to map different sizes of mangrove features accurately. The extent of dominant mangrove structural features including tree/shrub crowns, canopy gaps and vegetation formation or community, could be detected using semi-variogram analysis applied to image datasets with different spatial resolutions. The findings showed a gradual loss of mangrove information detail with increasing pixel size. Specific mangrove features could be optimally mapped from a specific pixel size and spectral bands or indices. A pixel size of $\leq$ 2 m was suitable for mapping canopy and inter-canopy-related features within mangrove vegetation features (such as shrub crown, canopy gaps and single tree crowns), while a pixel size of $\geq$ 4 m was appropriate for mapping mangrove vegetation formation, communities and larger mangrove features. An optimum pixel resolution scheme was produced for mangrove mapping that served as a basis for an inversion approach to map mangrove features using remote sensing image datasets.

Chapters 4 and 5 focused on the application of the optimum pixel size scheme to the selected images with different spatial resolutions, to map mangrove composition and LAI, respectively. Object-based image analysis successfully produced mangrove composition maps at discrete spatial

scales. The findings suggested that the accuracy of the maps was a result of the interaction between the image spatial resolution, the scale of the targeted objects and the number of land cover classes on the map. This task confirmed that the conceptual spatial and temporal hierarchical organisation of mangroves provided an essential aid for effective multi-scale mangrove composition mapping. For LAI mapping, the effect of different image pixel sizes and mapping approaches (i.e. object- and pixel-based) to estimate LAI was investigated. The results suggested that the optimum pixel size to estimate LAI correlated with the dominant object size in the area of interest and the field plot size. The object-based approach significantly increased the LAI accuracy as opposed to the pixel-based approach; with the optimum segmentation size corresponding to the size of the dominant objects in the image scene.

Chapter six synthesised the findings from chapters 3, 4, and 5 and developed guidelines for multi-scale image-based mangrove mapping. Through these guidelines, the relationships between remote sensing and mangrove ecology could be shown explicitly; and at the same time, they provided an effective and efficient way to select the best image datasets and mapping techniques to map mangrove feature(s) at a relevant spatial and temporal scale. These targeted mangrove features can be used as a basic mapping unit for other applications, such as LAI and biomass estimation, carbon storage calculation, species distribution and so on.

This thesis has successfully integrated the field of remote sensing with mangrove ecology and developed rigorous and robust guidelines that provide a fundamental basis for multi-scale image-based mangrove mapping. It also signifies the operational use of remote sensing data for multi-scale mangrove mapping to produce science- and management-ready environmental information at relevant spatial and temporal scales. In a practical context, this guideline will help mangrove scientists and managers select the appropriate image datasets for mapping, measuring and monitoring mangrove environments. To ensure the wider applicability of the guidelines, the methods presented in this thesis need to be tested at other mangrove sites with different environmental settings, using a wider range of image datasets and processing techniques.

Declaration by author

This thesis is composed of my original work, and contains no material previously published or written by another person except where due reference has been made in the text. I have clearly stated the contribution by others to jointly-authored works that I have included in my thesis.

I have clearly stated the contribution of others to my thesis as a whole, including statistical assistance, survey design, data analysis, significant technical procedures, professional editorial advice, and any other original research work used or reported in my thesis. The content of my thesis is the result of work I have carried out since the commencement of my research higher degree candidature and does not include a substantial part of work that has been submitted to qualify for the award of any other degree or diploma in any university or other tertiary institution. I have clearly stated which parts of my thesis, if any, have been submitted to qualify for another award.

I acknowledge that an electronic copy of my thesis must be lodged with the University Library and, subject to the policy and procedures of The University of Queensland, the thesis be made available for research and study in accordance with the Copyright Act 1968 unless a period of embargo has been approved by the Dean of the Graduate School.

I acknowledge that copyright of all material contained in my thesis resides with the copyright holder(s) of that material. Where appropriate I have obtained copyright permission from the copyright holder to reproduce material in this thesis.

Publications during candidature

Peer-reviewed papers

Kamal, M & Phinn, SR 2011, 'Hyperspectral data for mangrove species mapping: a comparison of pixel-based and object-based approach', *Remote Sensing,* vol. 3, pp.2222-2242. [DOI: 10.3390/rs3102222].

Klein, CJ, Jupiter, SD, Selig, ER, Watts, ME, Halpern, BS, **Kamal, M**, Roelfsema, C & Possingham, HP 2012, 'Forest conservation delivers highly variable coral reef conservation outcomes', *Ecological Applications,* vol. 22, pp.1246-1256. [DOI: 10.1890/11-1718.1].

Kamal, M, Phinn, S & Johansen, K 2014, 'Characterizing the spatial structure of mangrove features for optimizing image-based mangrove mapping', *Remote Sensing,* vol. 6, pp. 984-1006. [DOI: 10.3390/rs6020984].

Kamal, M, Phinn, S & Johansen, K 2015, 'Object-based approach for multi-scale mangrove composition mapping using multi-resolution image datasets', *Remote Sensing - special issue on "Remote Sensing of Mangroves: Observation and Monitoring",* vol. 7, pp. 4753-4783. [DOI: 10.3390/rs70404753].

Kamal, M, Phinn, S & Johansen, K (in revision) 'Assessment of multi-resolution image data for mangrove leaf area index mapping', submitted to *Remote Sensing of Environment*.

Book chapter

Lucas, R, Lule, ADV, Asbridge, E, Kuenzer, C, Zuniga, MTR, Thomas, NM & **Kamal, M** (submitted), Spatial Ecology of Mangroves. In: Rivera-Monroy, VH, Lee, SY, Kristensen, E & Twilley, RR (eds.), *Mangrove Ecosystems: A Global Biogeographic Perspective (Structure, Function and Services)*, Springer, Berlin.

Conference proceedings

Kamal, M, Phinn, S & Johansen, K 2013, 'Assessment of mangrove spatial structure using high-spatial resolution image data', *In:* Proceedings of the IEEE International Geoscience and Remote Sensing Symposium (IGARSS), 21-26 July 2013, Melbourne, Australia, pp. 2609-2612. [DOI: 10.1109/IGARSS.2013.6723357].

Kamal, M, Phinn, S & Johansen, K 2013, 'Extraction of multi-scale mangrove features from WorldView-2 image data: an object-based image analysis approach', *In:* Proceedings of the 34th Asian Conference on Remote Sensing (ACRS), 20-24 October 2013, Bali, Indonesia, pp. 653-659.

<u>Publications included in this thesis</u>

Publication citation – incorporated as Chapter 3.

Kamal, M, Phinn, S & Johansen, K 2014, 'Characterizing the spatial structure of mangrove features for optimizing image-based mangrove mapping', *Remote Sensing*, vol. 6, pp. 984-1006. [DOI: 10.3390/rs6020984].

Contributor	Statement of contribution
Muhammad Kamal (Candidate)	Data processing and analysis (100%) Research direction and manuscript writing (80%)
Stuart Phinn	Research direction and manuscript review (10%)
Kasper Johansen	Statistical analysis, manuscript review and editing (10%)

Publication citation – incorporated as Chapter 4.

Kamal, M, Phinn, S & Johansen, K 2015, ‘Object-based approach for multi-scale mangrove composition mapping using multi-resolution image datasets’, *Remote Sensing - special issue on “Remote Sensing of Mangroves: Observation and Monitoring”*, vol. 7, pp. 4753-4783. [DOI: 10.3390/rs70404753].

Contributor	Statement of contribution
Muhammad Kamal (Candidate)	Data processing and analysis (100%) Research direction and paper writing (80%)
Stuart Phinn	Research direction and manuscript review (10%)
Kasper Johansen	Object-based mapping, manuscript review and editing (10%)

Publication citation – incorporated as Chapter 5.

Kamal, M, Phinn, S & Johansen, K (in revision) ‘Assessment of multi-resolution image data for mangrove leaf area index mapping’, *Remote Sensing of Environment*.

Contributor	Statement of contribution
Muhammad Kamal (Candidate)	Data processing and analysis (100%) Research direction and paper writing (80%)
Stuart Phinn	Research direction and manuscript review (10%)
Kasper Johansen	Manuscript review and editing (10%)

Contributions by others to the thesis

Professor Stuart Phinn and Dr Kasper Johansen, through their advisory role, contributed to the research direction and research design as well as providing editing and revision of publication manuscripts and this thesis.

Statement of parts of the thesis submitted to qualify for the award of another degree

None

Acknowledgements

My journey to accomplish this thesis would not have been possible without the permission and will of God, who sent those kind-hearted people to support the completion of my study. This long scientific journey brought me into deeper acknowledgement and understanding that *"... and you (i.e. mankind) have not been given of knowledge except a little*" (Sūrah al-Isrā', 17:85).

First and the foremost, I would like to thank my advisers, Professor Stuart Phinn and Dr Kasper Johansen for their expert guidance and tremendous support throughout my PhD study, their patience in correcting my manuscripts and inspiring advice, which always kept me motivated. Stuart, thanks for always encouraging me to keep thinking positively during my difficult times; and Kasper, thanks for always pushing me to the limit. Both of you are my role models in the academic life.

I would like to acknowledge the Australia Awards Scholarships (previously AusAID) for awarding me the Australian Development Scholarship (ADS – now Australia Awards Scholarships (AAS)) to pursue my PhD degree. Thanks to Laura Anderson, Claudia Morales, Sue Quarton and Vicky Otsu for their helpful assistance. My gratitude goes to the School of Geography, Planning and Environmental Management at The University of Queensland (GPEM-UQ) for providing the research facilities and funding for fieldwork, conferences and publications.

I extend my sincere thanks to the staff of the School of GPEM-UQ for their great support. Thanks to Patrick Moss, Judy Nankiville, Jurgen Overheu, Alan Victor, Lorraine Liang, Suhan Chin, Michael Tobe and Nivea Hall whose help and consideration were so important. Thanks to Arnon Accad and Ralph Dowling (Queensland Herbarium), Melissa Cooper (Brisbane City Council), Rachael Attard (Port of Brisbane), Tracy Rowbotham (DERM), and Novi Adi whose help made my fieldwork possible in Australia. For Indonesia side, thanks to Puji Astuti and Tukiman (Karimunjawa National Park), Pramaditya Wicaksono, Dimar Wahyu Anggara, and Muhammad Hafizt for the great help during my fieldwork. I would also thank Julie Sanderson for editing my thesis.

Thanks to my colleagues and friends at the Remote Sensing Research Centre (RSRC - formerly Biophysical Remote Sensing Group (BRG)) for sharing a good academic environment: Chris Roelfsema, Scarla Weeks, Joanne Edkins, Javier Patino, Emily Shaw, Eva Kovacs, Santosh Bhandari, Robert and Marites Canto, John Armston, Mitchell Lyons, Johanna Speirs, Chris Rohner, Ana Redondo, Fabrice Jaine, Michael Hewson, Rodney Borrego, Novi Adi, Martina Reichstetter, Ralph Trancoso, Jiban Deb, Muhammad Hoque, Mohammad Redowan, Jasmine Muir, Sabrina (Dan) Wu, Denise Perez and Danang Surya Candra. Thanks also to Beben Benyamin, Fenty Forsyth and all of my Indonesian friends who made me feel ‘‘at home’’ during my stay in Brisbane.

From my home institution, the Cartography and Remote Sensing Study Program at the Faculty of Geography Universitas Gadjah Mada (UGM), I would like to thank Professor Totok Gunawan, Professor Hartono, Dr Suharyadi, and Dr Projo Danoedoro and all of my colleagues who always encouraged me to study for my PhD and for sharing their passion in the academic life.

Lastly, my final appreciation goes to my family. Thanks to my late father for his wisdom and spirit in always keeping my dreams alive and my mother for her continuing prayers. I cannot thank you enough for all that you have done for me. Most importantly, I would also like to express my love and gratitude to my lovely wife, Risti Indriastuti, who always prays and provides continuing support during my study, unconditionally. Likewise to my wonderful kids Salma Karimah Kamal and Muhammad Azman Kamal, thanks for simply being the sunshine of my days and apologies for not having much time to share with you during my study. You are all my sources of strength.

Keywords

Remote sensing, mangroves, multi-scale, object-based image analysis, hierarchy, spatial resolution, spatial ecology.

Australian and New Zealand Standard Research Classifications (ANZSRC)

ANZSRC code: 090905

Photogrammetry and Remote Sensing, 80%

ANZSRC code: 050199

Ecological Applications not elsewhere classified, 10%

ANZSRC code: 050206

Environmental Monitoring, 10%

Fields of Research (FoR) Classification

FoR code: 0909

Geomatic Engineering, 80%

FoR code: 0501

Ecological Applications, 10%

FoR code: 0502

Environmental Science and Management, 10%

Table of contents

List of figures

List of tables

Acronyms

ALOS	*Advanced Land Observation Satellite*
ASTER	*Advanced Spaceborne Thermal Emission and Reflection Radiometer*
AVHRR	*Advanced Very High Resolution Radiometer*
AVIRIS	*Airborne Visible/ Infrared Imaging Spectrometer*
BI	*Brightness Index*
BoM	*Bureau of Meteorology*
BRG	*Biophysical Remote Sensing Group*
BTNK	*Balai Taman Nasional Karimunjawa (Karimunjawa National Park Office)*
CASI	*Compact Airborne Spectrographic Imager*
CHM	*Canopy Height Model*
CV	*Coefficient of Variant*
DBH	*Diameter at Breast Height*
DN	*Digital Number*
DSITIA	*Department of Science, Information Technology, Innovation, and the Arts*
DTM	*Digital Terrain Model*
ENVI	*Environment for Visualizing Images*
EVI	*Enhanced Vegetation Index*
FAO	*Food and Agricultural Organisation*
FCC	*Fractional Canopy Cover*
FDI	*Forest Discrimination Index*
FLAASH	*Fast Line-of-sight Atmospheric Analysis of Spectral Hypercubes*
GEOBIA	*Geographic Object-Based Image Analysis*
GPEM	*Geography, Planning and Environmental Management*
GPS	*Global Positioning System*
INRA	*Institut National de la Recherche Agronomique*
ISME	*International Society for Mangrove Ecosystems*
JAXA	*Japan Aerospace Exploration Agency*
LAADS	*Level 1and Atmosphere Archive and Distribution System*
LAI	*Leaf Area Index*
LiDAR	*Light Detection and Ranging*
MIR	*Middle Infrared*
MLC	*Maximum Likelihood Classification*
MLCNN	*Maximum Likelihood Classification combined with Nearest-Neighbour*
MODIS	*Moderate Resolution Imaging Spectroradiometer*

MSE	*Mean Square Error*
NASA	*National Aeronautics and Space Administration*
NDVI	*Normalised Difference Vegetation Index*
NIR	*Near-Infrared*
NN	*Nearest-Neighbour*
OA	*Overall Accuracy*
OQ	*Overall Quality*
PA	*Producer's Accuracy*
PCA	*Principal Component Analysis*
RMSE	*Root Mean Square Error*
RTM	*Radiative Transfer Model*
SAVI	*Soils Adjusted Vegetation Index*
SP	*Scale Parameter*
SPOT	*Satellite Pour l'Observation de la Terre*
SR	*Simple Ratio*
SV	*Semi-variogram*
SVI	*Spectral Vegetation Index*
SVM	*Support Vector Machine*
TM/ETM+	*Thematic Mapper/ Enhanced Thematic Mapper+*
TOA	*Top of Atmosphere*
UA	*User's Accuracy*
UQ	*University of Queensland*
USGS	*United States Geological Survey*
UTM	*Universal Transverse Mercator*
VI	*Vegetation Index*
VNIR	*Visible and Near-Infrared*
WV-2	*WorldView-2*

CHAPTER 1:

INTRODUCTION AND SIGNIFICANCE OF THE RESEARCH

This chapter provides the general context that motivated the research presented in the thesis.

No paper publication is associated with this chapter.

1.1. Overview of the Research Context

Mangroves have been identified among the most important objects in wetland ecosystems, forming a link between terrestrial and marine systems in tropical and subtropical regions. They are highly productive ecosystems that typically dominate the intertidal zone of low energy tropical and subtropical coastlines (Kathiresan & Bingham 2001; Alongi 2002). Mangroves perform a range of ecological and economical functions such as protection of coastal environment, provision of nursery habitat for the juveniles of aquatic organisms, support for aquatic food chains, maintenance of coastal water quality, provision of wildlife reserves and attracting tourists (Lugo & Snedaker 1974; Hutchings & Saenger 1987; Robertson & Duke 1987; Green et al. 1998b; Giri et al. 2011). However, their health and resilience are under intense ecological pressure from anthropogenic and natural disturbances. Major threats to mangroves include logging for fuel and timber (Gopal & Chauhan 2006), conversion to other land uses such as agriculture, aquaculture, industrial and urban development (Alongi 2002; Manson et al. 2003; Giri et al. 2008) and the relative sea level rise (Gilman et al. 2008). Approximately 36% of the global mangrove area was lost during the past two decades (FAO 2007). Predictions suggest that in the next 100 years, about 30-40% of coastal wetlands will be lost (McFadden et al. 2007) and 100% of mangrove forest (Duke et al. 2007) if the present loss continues. These threats and losses of mangroves are leading to the increasing demand for retrieving up-to-date and accurate information on mangrove forest. This information is crucial for mangrove inventory and mapping, monitoring the state of existing mangrove forest, assessing change (deforestation), estimating blue carbon storage and ensuring their sustainable management (Green & Mumby 2000; Wang & Sousa 2009b; Heumann 2011b).

Over the past 20 years, remote sensing data have been used extensively to map and monitor mangrove environments (Heumann 2011b; Kuenzer et al. 2011). It provides key advantages for mangrove studies including: (1) indirect access to mangrove habitats that are temporarily inundated and often inaccessible due to geographical location in intertidal zones (Ramsey III & Jensen 1996; Davis & Jensen 1998), (2) enabling extrapolation of observation results at specific sampling sites into an entire image extent (Hardisky et al. 1986; Kuenzer et al. 2011), (3) providing a synoptic overview and repeated coverage of mangrove sites (Giri et al. 2007), and (4) the ability to deliver data at multi-scale levels to address key problems in coastal areas (Malthus & Mumby 2003). The recent development of remote sensing and image processing allows exploration of various types of image datasets as well as types of mapping techniques, or combinations of them, to map mangrove environments (Heumann 2011b; Kuenzer et al. 2011). Problems arise when there is a need to match the scale of the analysis to the scale of the phenomenon under investigation because environmental inferences are scale-dependent (Wiens 1989). So there are substantial knowledge gaps dealing with remote sensing approaches for mangrove mapping including knowing what type of mangrove information is able to be mapped from specific image resolutions and the level of detail in that information.

From a spatial ecology perspective, mangrove ecosystems - as for to other vegetation ecosystems - are perceived as having spatial and temporal hierarchical organisation and this hierarchical approach have been used to understand this ecosystem for more than three decades (Feller et al. 2010). The central concept of the theory focuses on the differences in structure and process rates between levels. Based on these differences, ecosystems are viewed as being stratified into discrete levels of interacting subsystems, with attributes occurring at specific spatial and temporal scales (Delcourt et al. 1983; Müller 1992; Lee & Grant 1995; Farnsworth 1998). Geospatial technology and analysis tools, including remote sensing data and its mapping techniques, are required to address emerging issues in spatial ecology from local to global scales (Naveh & Lieberman 1994; Skidmore et al. 2011). Most of the image-based mangrove mapping conducted derived information at a specific scale, with little attention given to the variation of information obtained across different image resolutions (i.e. the ability of a remote sensing system to record and display fine spatial, spectral, radiometric and temporal details (Campbell 2002)). Having this information in place will help scientists focus their research on the ecological questions that are appropriate to each level of spatial resolution (Delcourt et al. 1983; Phinn 1998) and managers to focus on the conservation needs at the relevant levels of spatial and temporal scales (Schaeffer-Novelli et al. 2005). The multi-scale mapping capability of remote sensing has the potential to address the spatial hierarchical organisation of mangroves, in order to identify and characterise the type of information obtainable about mangroves at each hierarchical level, and provide mangrove maps at a variety of spatial scales.

The knowledge gaps define three key issues: (1) how to integrate the remote sensing perspective into mangrove spatial and temporal hierarchical organisation, (2) how to select and optimise the use of image datasets so that the data will most effectively address a particular research problem at a specific spatial scale (Warner et al. 2009), and (3) how to utilise synergetic data from multiple remote sensing images to improve the accuracy of mangrove mapping (Blasco et al. 1998; Malthus & Mumby 2003; Heumann 2011b; Kuenzer et al. 2011). Among various mangrove parameters able to be mapped using remote sensing data, two parameters provide the most fundamental information, mangrove structural feature composition and leaf area index (LAI). Mangrove structural feature composition shows the assemblage of mangrove features at different spatial scale and extent, such as tree crown/species, canopy gaps, vegetation formation and community, and serve as a good indicator of geomorphic and environmental change (Souza-Filho & Paradella 2003). Likewise, LAI is an important biophysical parameter for assessing evapotranspiration, carbon cycling, habitat conditions and forest health (Pierce & Running 1988; Kovacs et al. 2005). Yet, as an increasing number of various resolutions of image datasets become available, selection of the most appropriate image resolution for specific mapping purpose becomes more difficult (Cao & Lam 1997; Warner et al. 2009). These image datasets support the mapping of vegetation features at different spatial scales or multi-scale mapping, which is essential for ecosystem inventory and management. To use remote sensing data effectively for multi-scale mapping in a mangrove environment, it is essential to understand the relationships between image resolutions, mapping techniques and the information obtained.

In summary, further work is needed to understand the multi-scale mapping ability of remote sensing data for the production of spatially-explicit information about mangroves at a variety of spatial scales, to support better mangrove science and management. The work carried out in this thesis began to address the multi-scale issues in mangrove mapping using remote sensing data to understand the link between image spatial resolutions and the type and detail of mangrove information able to be extracted from the image. The results were applied as the basis for multi-scale mangrove composition and LAI mapping, in order to develop a guideline for multi-scale mangrove mapping.

1.2. Knowledge Gap and Problem Statement

Ideally, in order to use remote sensing data effectively for mangrove mapping, there should be existing knowledge of what type of mangrove information could be derived at a specific image spatial resolution (or scale of observation). Given a set of remotely-sensed data, one would know the expected type of information derived from this specific datasets; or *vice versa*, in order to map certain mangrove features, one would select a certain type of image datasets that could optimally detect this specific feature. Many attempts have been made to explore various types and resolutions of remotely-sensed data for mapping mangrove composition and structural parameters. Studies focusing on the explicit relationships between image resolutions and the type and level of detail of mangrove composition and structural information contained at different scales, are limited. In this regard, different image resolutions (spatial and spectral) will result in different levels of interpretability, information detail and accuracy of mangrove information acquired. The research problem can be stated as follows: *there is a substantial lack of knowledge related to the relationships between image resolutions, mapping approaches and the level of information detail able to be produced for mangrove environments.*

1.3. Research Aim and Objectives

The aim of this research is to establish guidelines for multi-scale mangrove structural feature composition and LAI mapping using multi-resolution image datasets. To address the research problem and question, the project is divided into three objectives:

1. To characterise mangrove spatial structure identifiable at different spatial scales for image-based mangrove mapping.
2. To assess the capability of selected remotely-sensed datasets and mapping techniques to produce mangrove structural feature composition and LAI maps at different spatial scales, and assess the accuracy of the mapping results.
3. To develop guidelines for multi-scale mapping of mangrove structural feature composition and LAI suitable for multiple locations.

1.4. Remote Sensing for Mangrove Mapping

Several topics directly associated with the research problem are covered in the literature review to substantiate the need for this research. A basic understanding on the definition, global distribution and characteristics of mangrove ecosystems able to be detected from image data will be established. Common themes, key findings, limitations and gaps in previous research are identified for mangrove mapping techniques using remotely-sensed data. The multi-scale/resolution issues across different image resolutions as a basis for multi-scale analysis will also be addressed.

1.4.1. Definition and Distribution of Mangrove Ecosystems

There are varied definitions of mangroves used across the literature as a result of problems in non-precise identification of mangrove objects and taxonomical classification (Bunt et al. 1982; Blasco et al. 1998). According to Duke (2006, p. 12), a mangrove is defined as *"a tree, shrub, palm or ground fern that is generally higher than one half-metre in height, and normally grows above mean sea level in the intertidal zone of marine coastal environments and estuarine margins"*. The definition above gives a comprehensive and clear delimitation of the object and can be appropriately applied in this study. The term mangrove refers to both trees living in the intertidal zones and to the communities they form (Tomlinson 1994). When referring to the habitat, the term "mangroves", "mangrove forest", or "mangal" is used. The term "mangrove" is also used as an adjective, so that individual trees in the "mangroves" are referred to as a "mangrove tree" (Duke 1992). Apart from the variation of interpretation of the term "mangrove" (Blasco et al. 1998), this study will focus on the "mangrove forest" or intertidal community of trees as the object that can be physically recognised by remote sensing sensors.

Throughout the world mangrove ecosystems occupy intertidal areas between 30ºN and 30ºS and are located within 124 countries (FAO 2007); with 73 species and hybrids as true mangroves and occupying a total estimated area of 137,760 km^2 (Giri et al. 2011). The distribution of mangroves indicates a tropical dominance with major latitudinal limits relating best to major ocean currents and the 20°C seawater isotherm in winter (Figure 1.1). The largest mangrove extent is in Asia (42%) followed by Africa (20%), North and Central America (15%), Oceania (12%) and South America (11%); where Indonesia, Australia, Brazil, Mexico and Nigeria combined have roughly 46.8% of the world's mangrove forests (Giri et al. 2011). The halophytic mangroves typically fringe the transition zone between sea and land in intertidal coastal regions, estuaries and reef environments, which are characterised by strong wind, high temperature, varying inundation and anaerobic muddy soil (Lugo & Snedaker 1974; Kathiresan & Bingham 2001).

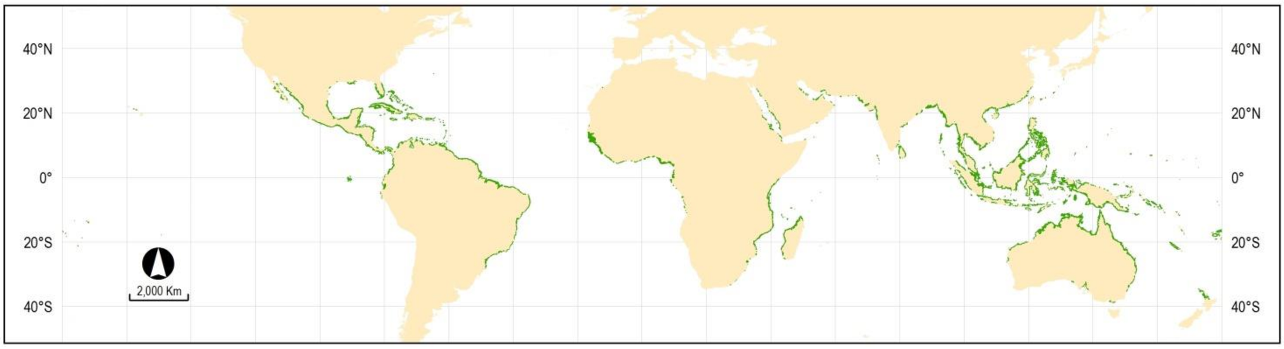

Figure 1.1. Global distribution of the world's mangrove forest; mangroves shown in dark green (Giri et al. 2011; data source: http://data.unep-wcmc.org/datasets/4).

1.4.2. Spatial and Temporal Organisation of Mangroves

The distribution and structure of mangrove forest are influenced by several environmental factors with varying impacts over different spatial and temporal scales (Duke et al. 1998; Twilley et al. 1999). At the global spatial scale, mangrove distributions are limited by temperature (Alongi 2002). They are restricted in areas where mean air temperatures are higher than 20°C and the seasonal range does not exceed 10°C (Duke et al. 1998). At the regional scale, the diverse landform of coastal regions can be considered as a biodiversity component of mangrove ecosystems (Twilley et al. 1996). These regions can be classified into distinct geomorphological units that describe the influence of geophysical processes on the ecological characteristics of mangroves (Thom 1982). The extent and characteristics of mangroves in this scale may be determined by complex interactions between landscape position, rainfall, sea level, sediment dynamics and natural disturbances (storm, pest, or predator) (Alongi 2002, 2008; Eslami-Andargoli et al. 2009).

At the local scale, the micro-topographic factors of a region determine the hydrologic and chemical conditions of soil that control the patterns of forest physiognomy and zonation (Twilley et al. 1996). Lugo and Snedaker (1974) classify the local patterns of mangrove structure into riverine, fringe, basin, hammock and dwarf forests. Finally, for an individual tree, several factors operate collectively to control plant growth including temperature, nutrients, solar radiation, oxygen and water (Clough 1992). Together these can be used to integrate the different scales of environmental factors that control the attributes of mangrove forest structure (Figure 1.2). Changes in any of these factors are likely to affect the spatial patterns and community structure of mangroves.

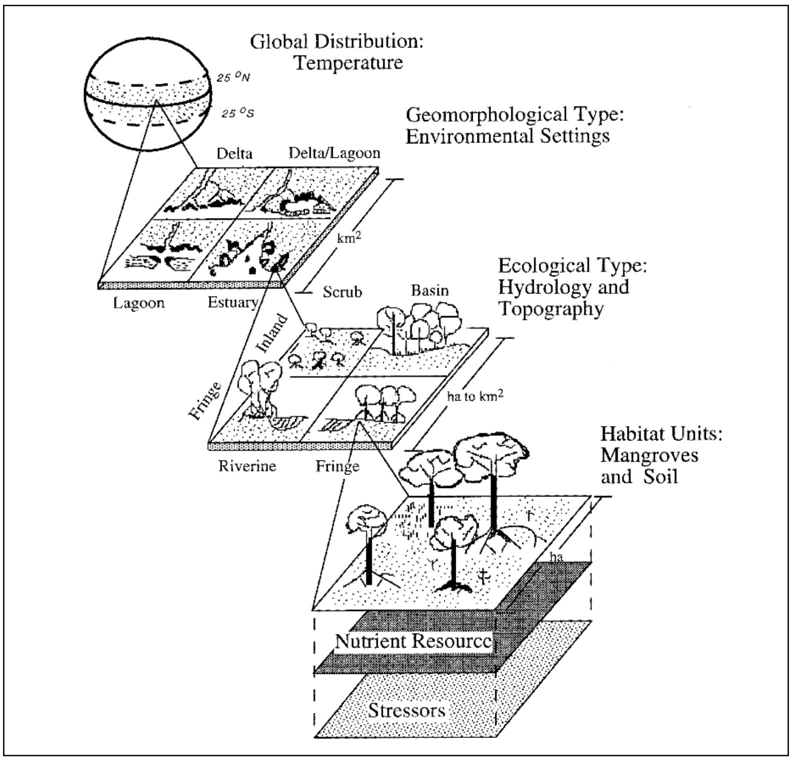

Figure 1.2. Hierarchical organisation of the patterns of mangrove structure and function over different spatial extents (Twilley et al. 1999, p. 406, with permission from Elsevier).

Ecologists have perceived mangrove ecosystems as having hierarchical organisation and have used this hierarchical approach to understand this ecosystem for more than three decades (Feller et al. 2010). This hierarchical organisation was built based on the hierarchy theory (Twilley et al. 1999). It is as a comprehensive theory about the relationships between ecological processes and the spatial and temporal patterns observed in the landscape (Cullinan et al. 1997). It simplifies complex and multi-scaled systems into several single phenomenon and single spatio-temporal scale. By limiting the focus into a specific phenomenon at a specific space and time, it is possible to address the associated problem appropriately (Fox 1992). From the mangrove management point of view, the existing multiple hierarchical levels of mangroves mean that management strategies should be developed to address conservation needs at the relevant levels of ecological organisation and spatial-temporal scale (Schaeffer-Novelli et al. 2005). Management strategies that are successfully implemented at one level may not be applicable for other levels. Therefore, it is best to establish policies to address any given environmental problem at the relevant spatial and temporal level (Fox 1992). Twilley et al. (1999) proposed explicit eco-geomorphic hierarchical levels of dynamic processes in mangrove ecosystem at different spatial and temporal scales (Figure 1.3). This hierarchical organisation of mangroves will be used a guide to characterise mangrove vegetation structure organisation across varying scales within a remote sensing context.

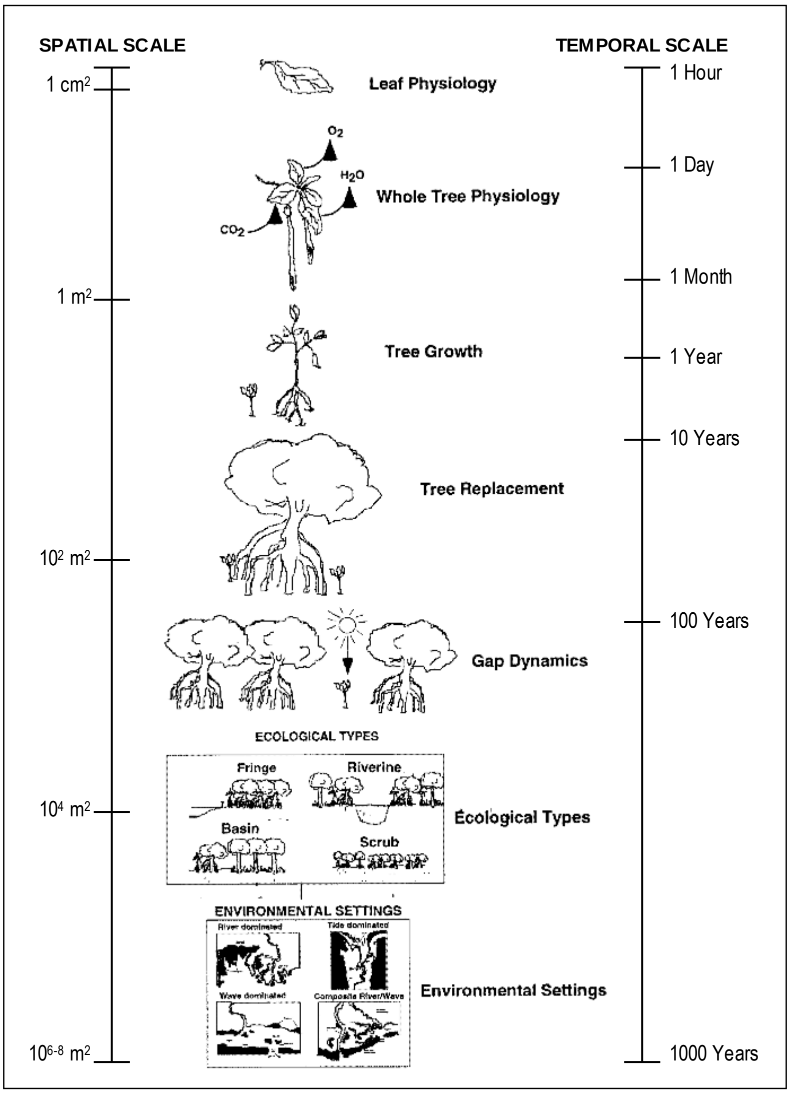

Figure 1.3. Spatial and temporal hierarchical organisation of processes in mangrove ecosystems (Twilley et al. 1999, p. 407, with permission from Elsevier).

On a temporal scale, natural changes occur in mangrove ecosystems at the level of minutes to hours for microbial and physiological processes, of month to years for tree growth and replacement and of decades to centuries for regional forest changes (Twilley et al. 1996). Like most tropical tree species, mangroves are recognised as difficult to age but stands exhibiting different phases can be distinguished (Lugo 1997). Several studies have demonstrated that hierarchy in spatial and time scales chosen for analysis is essential for portraying species and community dynamics, identifying factors that control community structures over different time scales (Farnsworth 1998) and making recommendations for restoring mangrove forests (Twilley et al. 1999). Both spatial and temporal dimensions are the typical advantages attributed to remotely-sensed data. The appropriate use of these data for ecosystem studies will reveal more about the mechanism of pattern changes that contribute to ecosystem dynamics.

1.4.3. Characteristics for Identifying Mangroves using Remotely-Sensed Data

Understanding of the characteristics of an object under investigation, with regard to its appearance on the image, is the foundation of successful implementation of remote sensing data for any mapping purpose. Several characteristics of mangroves have potential to be used as interpretation keys to identify mangrove forest from adjacent environments, or to discriminate features within mangroves using remote sensing data. This includes mangrove location and zonation patterns, textural properties of the canopy and spectral reflectance characteristics of the canopy.

Mangroves exhibit zonation patterns in a number of different geographic regions (Hutchings & Saenger 1987; Tomlinson 1994). The most conspicuous feature of mangrove distribution is their sequential change in tree species parallel to shore and estuarine margins. Zonation of plant communities in intertidal habitats is particularly notable and often results in specific bands of vegetation occurring parallel to the shoreline (Alongi 2008). The nature and extent of these zones are the result of a differential response to physio-chemical gradients that vary across the intertidal area, including topography, geomorphic setting, tidal regime and sediment properties such as salinity, water content, texture, organic matter content, nutrient concentration, texture and chemical composition (Smith 1992; Ellison et al. 2000; Da Cruz et al. 2013; Yang et al. 2013). For example, Smith (1992) described the common mangrove zonation of the Indo-Pacific region as *Aegiceras*, *Avicennia*, and *Sonneratia* in the lowest intertidal zones; *Bruguiera* and *Rhizophora* in the mid-intertidal areas; and *Heritiera*, *Xylocarpus*, and some other species in the higher intertidal areas. However, mangrove zonation is varied from place to place; it may also vary at a local scale, depending on the response to the variation of local processes (Smith 1992; Ellison et al. 2000). The distinctive site and zonation attributes in mangroves provide an important clue in identifying mangrove species using remote sensing images. Often, however, the zones are too narrow to allow discrimination at moderate spatial resolution, particularly where a mix of species occurs. Classification from remote sensing is generally more successful when a single species dominates a zone and where less species occur.

Compared to terrestrial natural forests, the canopy of mangroves is generally smoother as most occur in zones established at the same time; hence mangroves are often of the same age and height (and hence growth form) and of similar species composition. As a consequence, texture measures can be used to differentiate mangrove species types, growth stages and mangrove communities (Ramsey III & Jensen 1996). Image texture gives us information about the spatial arrangement of colour or intensities in an image or selected region of an image (Shapiro & Stockman 2001). Their structural appearance, partially more homogeneous or heterogeneous, depends on several factors such as species composition, distribution pattern, growth form, growth density and stand height. Image texture analysis is often measured using first- and second-order metrics, computed from grey-level co-occurrence matrix within a given window, lag distance and direction (Kayitakire et al. 2006). Such information can be included with spectral data to increase the accuracy of mangrove maps (Wang et al. 2004a; Myint et al. 2008; Wang et al. 2008).

In general, mangrove forests have distinct spectral reflectance characteristics that make them “recognisable” by the optical sensors as being different from adjacent land and sea features (Spalding et al. 2010). Several studies have been carried out utilising the mangrove features’ spectral reflectance to map mangrove ecosystems (Clark et al. 1997; Green & Mumby 2000; Jensen et al. 2007) and species differentiation (Demuro & Chisholm 2003; Held et al. 2003; Hirano et al. 2003; Vaiphasa et al. 2005). However, a closer look into the interaction mechanisms between light and mangrove canopies reveals two main challenges. First, the spectral reflectance of mangroves is strongly influenced by tidal effects on soils, resulting in mixed-pixels; and second, many factors influence the spectral reflectance response that diminishes the accuracy of spectral recognition of mangroves (Blasco et al. 1998; Díaz & Blackburn 2003). According to Diaz and Blackburn (2003), the spectral variations of the canopy reflectance are a function of several optical properties, such as LAI, background reflectance, and leaf inclination. For single species recognition, the canopy spectral reflectance is defined by age, vitality, and phenological and physiological characteristics (Blasco et al. 1998). Furthermore, in mangrove species discrimination, Vaiphasa et al. (2005) and Wang & Sousa (2009a) found that the spectral responses from different mangrove species were too similar, making it difficult to discriminate between mangrove species by spectral properties alone. These findings show the potential usage and limitation of mangrove spectral reflectance to discriminate between mangrove community or species. Therefore, other image interpretation cues such as site, associations and context relationships are necessary in image analysis to increase the mangrove community or species discrimination.

1.4.4. Remote Sensing for Mangrove Biophysical Properties Mapping

Many studies have been carried out to investigate the suitability of various classification algorithms and image types for mangrove mapping with different degree of success. The biophysical properties that are commonly investigated using remote sensing images in mangrove environments include extent and composition, species type, LAI, canopy height, canopy closure, diameter of breast height (DBH) and basal area (Jensen et al. 1991; Ramsey III & Jensen 1996; Green et al. 1997; Davis & Jensen 1998; Manson et al. 2001; Díaz & Blackburn 2003; Jean-Baptiste & Jensen 2006; Kovacs et al. 2010). Table 1.1 provides a synopsis of the data and methods used to map selected mangrove structural features and biophysical properties for the purpose of this research.

Table 1.1. Overview of data and methods used to map selected mangrove biophysical properties*.

	Author(s)	Image data	Method	Biophysical properties
Extent and composition	Jensen et al. (1991)	SPOT XS	Pixel-based (veg indices) and statistical analysis	**Mangrove type**, canopy height, % canopy closure
	Ramsey & Jensen (1996)	Landsat TM SPOT XS & P AVHRR	Pixel-based (veg indices) and statistical analysis	Canopy closure, height, **% species composition**, leaf, litter & canopy reflectance, and understory species type
	Davis & Jensen (1998)	NASA CAMS	Pixel-based (veg indices) and statistical analysis	**Species type**, canopy height, % canopy closure, basal area, average leaf area, and DBH
	Rasolofoharinoro (1998)	SPOT 1 & 2	Pixel-based (vegetation and brightness index, supervised minimum distance and maximum likelihood classifications)	**Mangrove extent and type**
	Gao (1999)	SPOT XS PAN	Pixel-based (supervised maximum likelihood classification)	**Mangrove extent and type**
	Manson et al. (2001)	Landsat TM	Pixel-based (tasselled-cap) combined to topographic maps and aerial photographs	**Mangrove extent**
	Hirano et al. (2003)	AVIRIS	Pixel-based (spectral angle mapper)	**Mangrove species and extent**
	Held et al. (2003)	CASI AIRSAR	Pixel-based (data fusion)	**Mangrove zonation, species type**
	Giri & Muhlhausen (2008)	Landsat MSS TM ETM+ ASTER VNIR	Pixel-based (ISODATA clustering with iterative labelling and post-classification editing)	**Mangrove extent** and change
	Wang et al. (2004a)	IKONOS QuickBird	Object-based (textural roughness), statistical analysis and accuracy assessment	**Species type**
	Conchedda et al. (2008)	SPOT XS	Object based (Nearest Neighbour [NN] classifiers), accuracy assessment	**Mangrove extent** and change
	Myint et al. (2008)	Landsat TM	Object-based (lacunarity measure)	**Mangrove species and extent**
	Kamal & Phinn (2011)	CASI-2	Object-based (rule sets and NN classifiers)	**Mangrove species and community**
	Heumann (2011a)	WorldView-2	Object-based (NN classifiers and decision tree)	**Mangrove community**
	Heenkenda (2014)	WorldView-2 UltraCamD	Object-based (rule sets and support vector machine [SVM]), accuracy assessment	**Mangrove extent and species composition**

Table 1.1. *Continued.*

	Author(s)	Image data	Method	Biophysical properties
Leaf Area Index (LAI)	Green et al. (1997)	Landsat TM SPOT XS	Pixel-based (band ratios, PCA, NDVI) and statistical analysis	**Leaf area index (LAI)**
	Green et al. (1998a)	CASI	Pixel-based (NDVI) and linear regression model to predict LAI	**Leaf area index (LAI)**
	Díaz & Blackburn (2003)	Landsat TM	Pixel-based (veg indices) and laboratory simulation	**Leaf area index (LAI)**
	Kovacs et al. (2004)	IKONOS	Pixel-based (veg indices SR & NDVI) and image-field data statistical relationship analysis	**Leaf area index (LAI)**
	Jean-Baptiste & Jensen (2006)	ASTER	Pixel-based (veg indices SR, NDVI, SAVI) and statistical analysis	Species type, % canopy closure, tree height, DBH, and **LAI**
	Addink (2007)	HyMap hyperspectral	Object-based and ridge regression, results validation	**LAI**, biomass
	Kovacs et al. (2010)	IKONOS, QuickBird, Leica-ADS40	Pixel-based (multi-resolution ISODATA classification) and accuracy assessment	DBH, tree height, stem condition (alive or dead), **LAI**
	Laongmanee (2013)	QuickBird	Pixel-based (veg indices) and image-field data statistical relationship analysis, accuracy assessment	**Leaf area index (LAI)**

*This table is not a comprehensive list of literature on mangrove mapping using remote sensing datasets.

1.4.4.1. Mangrove Extent and Composition

Multispectral remote sensing has been relatively effective at mapping the areal extent and composition of mangroves. For example Landsat (Green et al. 1998b; Manson et al. 2001; Giri & Muhlhausen 2008), SPOT (Gao 1998; Rasolofoharinoro et al. 1998; Gao 1999; Mumby et al. 1999), ASTER (Saito et al. 2003; Vaiphasa et al. 2006; Al-Habshi et al. 2007), IKONOS and QuickBird (Wang et al. 2004a). In the early stage of digital mangrove mapping using remote sensing data, application of the supervised Maximum Likelihood Classifier (MLC) is the most frequent method for classifying mangrove extent and composition based on satellite images (Gao 1998; Green et al. 1998b; Rasolofoharinoro et al. 1998; Gao 1999). The MLC has a well-developed theoretical base which assumes that the statistics for each class in each band are normally distributed and calculates the probability of a given pixel belonging to a specific class (Bolstad & Lillesand 1991). Mangroves, on the other hand, due to its location in the intertidal zone of coastal and estuarine areas have a distinctive spectral response compared to terrestrial vegetation (Blasco et al. 1998), and generally have a smoother canopy texture (Ramsey III & Jensen 1996). Hence, this makes them easy to identify using MLC through class samples. However, classification results were improved by incorporating bands with transformed spectral information, such as PCA (Green et al. 1998b; Kovacs et al. 2001), Tasselled-Cap (Manson et al. 2001), vegetation index (VI) and brightness index (BI) (Rasolofoharinoro et al. 1998). More specifically, the normalised difference vegetation index (NDVI) algorithm is commonly used to separate mangrove and non-mangrove areas, prior to further mangrove ecosystem investigation (Green et al. 1998b). A thorough review of the remote sensing techniques for mangrove extent and composition mapping is provided by Kuenzer et al. (2011) and Heumann (2011b).

Most of the studies in mangrove extent and composition were undertaken using the pixel-based approach. This approach is based on the assumption that the algorithms works solely on the spectral analysis of pixels on an individual basis, which has been criticised by many scientists (Blaschke 2010). Despite its robustness, this approach imposes some limitations, such as the inability of statistical analysis of pixels to represent the concept of object or patch in the image (Blaschke & Strobl 2001) and its inappropriateness for analysing emerging high spatial resolution imagery (Morgan et al. 2010). Object or image object is a group of connected pixels in a scene which represent a meaningful entity (Burnett & Blaschke 2003; Lang 2008), for example mangrove trees. Patch refers to a relatively discrete spatial pattern differing from its surroundings (Blaschke & Strobl 2001), such as a mangrove tree patch in the wetlands ecosystem. The recent development of an object-based approach or geographic object-based image analysis (GEOBIA) provides an alternative solution to solve this problem. This approach was built on the concept of objects, which are contiguous pixels that are grouped based on image properties through an image segmentation process (Baatz & Schape 2000). In its analysis, this approach tries to imitate human perception in interpreting images in digital analysis, which gives more attention to texture, shape and context of the objects rather than concentrating only on the spectral properties of its pixels (Navulur 2007).

Several remote sensing applications in mangrove extent and composition mapping use spatial neighbourhood properties for object-based classification. Wang et al. (2004b) investigate the use of IKONOS images for mangrove species mapping with three different classification methods; maximum likelihood classification (MLC) at the pixel level, nearest neighbor (NN) classification at the object level and a hybrid classification that integrates both methods (MLCNN). The result shows that MLCNN achieved the best average accuracy of 91.4%. Conchedda et al. (2008) applied a multi-resolution segmentation and class-specific rule incorporating spectral properties and relationships between image objects to map land cover in Low Casamance, Senegal using SPOT XS data. The results show a clear separation between the different land cover classes within the research area, as well as within the mangrove classes. Kamal and Phinn (2011) provided an explicit and operational mangrove multi-scale mapping hierarchy using OBIA, which was tested on a CASI-2 hyper-spectral image. The results show the effectiveness of this approach in discriminating mangroves from other objects and differentiating between mangrove species, with an overall accuracy of 76%. More recently, Heumann (2011a) combined GEOBIA and support vector machine (SVM) classification applied on WorldView-2 image to map fringe mangroves in Isabela Island in the Galapagos Archipelago, Ecuador. By implementing a hybrid decision tree classification the overall mapping accuracy of true and associate mangrove species was high (94%) but when used for assessing the species level, the accuracy was poor for some mangrove species (25–29%).

The use of object-based image analysis for mangrove extent and composition mapping is arguably more appropriate and results in better accuracy compared with the pixel-based approach. This approach gives better mimics to human perception of objects and has the ability to integrate attributes important to landscape analysis (such as tone, shape, size, texture and context). In the context of this research, the ability of GEOBIA to incorporate multiple scales in the analysis through the multi-scale segmentation process (Baatz & Schape 2000; Blaschke 2002; Navulur 2007) provides essential support for the analysis of multi-scale issues in mangrove mapping.

1.4.4.2. Leaf Area Index

Leaf area index is one of the most important biophysical parameters for assessing mangrove forest health (Jensen et al. 1991; Giri et al. 2007; Heumann 2011b), which is defined as the single-side leaf area per unit ground area (Green et al. 1997). LAI measurements are valuable input for modelling ecological processes such as photosynthesis, transpiration, evapotranspiration and net primary production, as well as gas, water, carbon and energy interchange within a forest region (Green et al. 1997). Most of the studies in the applications of remote sensing data for mangrove LAI estimation use empirical statistical relationships built between image pixel values (obtained from individual band or transformed image) and field measurements. Such empirical statistical relationships are then used to estimate the distribution of these parameters in the image. For example, Jensen et al. (1991) found that NDVI data derived from SPOT XS has a high correlation with the percentage of mangrove canopy closure (R^2 = 0.913). Using IKONOS, Kovacs et al. (2004) found strong significant relationships between the LAI of red and white mangroves and the simple ratio (SR) and normalised difference vegetation index (NDVI). Regression analyses of the in situ LAI with both vegetation indices revealed significant positive relationships (LAI versus NDVI at 8 m [R^2 = 0.71]; LAI versus NDVI at 15 m [R^2 = 0.70]; LAI versus SR at 8 m [R^2 = 0.73]; LAI versus SR at 15 m [R^2 = 0.72]) at the 8 m and 15 m plot sizes. Despite the strength of these findings, Heumann (2011b) argued that most the study site of these studies was relatively species poor and much of the study area degraded. Therefore, these methods need to be replicated in other areas to test the applicability and consistency of the empirical relationships across different species and conditions.

Recent developments of LAI research have shifted from an empirical and statistical approach to a more complex process-based modelling approach or radiative transfer model (RTM) inversion (Richter et al. 2009; Zheng & Moskal 2009). The process-based model relates fundamental surface parameters of leaves (i.e. LAI, size and shape, relative position, spatial arrangements and distribution) to scene reflectance for a given sun-surface-sensor-geometry (Fang & Liang 2008; Zheng & Moskal 2009). Unlike the empirical methods that uses only two or three spectral bands, the RTM uses the full spectrum of the hyper-spectral sensors (400-2500 nm). Several studies have reported the successful implementation of a physical-based approach to estimate LAI in different environments, such as Qi et al. (2000) in a semi-arid region using a BRDF model and Wang et al. (2013) in agricultural fields using the PROSAIL model. Experimental examples of the physical basis for estimating LAI using RTM, PROSPECT and SAIL are provided by Haboudane et al. (2004), Richter et al. (2009), Herrmann et al. (2011), Verrelst et al. (in press). These physical basis models claimed to address the limitation of the empirical-statistical approach that is the problem with saturation involving the non-linear relationship between LAI and spectral vegetation indices (SVI) (Hasegawa et al. 2010). Nevertheless, some technical shortcomings of these models must be considered, such as the need for an extensive parameterization and the high computational demand (Richter et al. 2009). Different parameter combinations may also produce almost identical spectra, resulting in significant uncertainties in the estimated vegetation characteristics (Atzberger 2004).

Furthermore, most of the studies applying the physical model to estimate LAI were conducted in terrestrial vegetation, and there is no study found yet conducted in mangrove environments. The difficult accessibility to mangroves and the high contribution of the soil and water backgrounds on the canopy spectral reflectance (Ramsey III & Jensen 1996; Blasco et al. 1998) might be the major issue in this environment for apply the physical basis approach. Therefore, this thesis will focus on the implementation of the empirical-statistical approach using SVI as LAI surrogate and applied to multiple pixel sizes and segmentation scales.

1.4.5. Scale Issues in Remote Sensing and Ecology

The issue of *scale effects* have already become one of the most important research focuses of remote sensing (Woodcock & Strahler 1987; Goodchild & Quattrochi 1997; Marceau & Hay 1999; Wu & Li 2009). In geography, the term *scale* refers to both the magnitude of the study (i.e. geographic extent) and the degree of detail (i.e. geographic resolution) (Goodchild & Quattrochi 1997; Lam et al. 2004; Ruddell & Wentz 2009). There are numerous definitions of the term *scale* (Lam & Quattrochi 1992; Ruddell & Wentz 2009; Wu & Li 2009). Throughout this thesis, when discussing remote sensing data, it is defined as the *measurement scale* or *resolution*, which refers to the smallest distinguishable part of an object (Forshaw et al. 1983), or the degree of detail, or the sampling unit. On the other hand, when dealing with mangrove spatial ecology, the term *scale* refers to the *operational scale*, which is the spatial (or temporal) extent at which processes operate in the environment (Cao & Lam 1997; Wu & Li 2009). The spatial domain of scale in the field of spatial ecology is recognised as having two attributes: *extent* and *grain* (Turner et al. 1989), which are similar to the geographic extent and geographic resolution in the definition above. For the sake of simplicity, the discussion of scale in this thesis focuses mainly on the spatial domain.

In remote sensing, scale is translated to the *spatial resolution* of an image (Forshaw et al. 1983). It is defined as "*resolving power"*, which refers to the fineness of detail depicted in an image. It describes the minimum size of an object that can be detected, measured and mapped from an image (Townshend 1981). An example of resolution is the instantaneous field of view (IFOV) of the sensor, which in turn is related to the ground sampling distance or ground resolution element. Another term commonly used in remote sensing is *pixel size*, which refers to the sampling frequency or sampling rate of the image (Warner et al. 2009), and not the actual IFOV of the sensor. Throughout the thesis, both *spatial resolution* and *pixel size* are used interchangeably. Although image pixel size is not identical to the image spatial resolution (Forshaw et al. 1983; Warner et al. 2009), for the sake of simplicity they are used to represent the actual sampling size of the image datasets explored in this thesis.

The scale issues in remote sensing and ecology have been addressed thoroughly by Wiens (1989), Cao & Lam (1997), Marceau (1999), Marceau & Hay (1999), and Wu & Li (2009). The scale represents the window of perception (Marceau & Hay 1999), the ability to observe and reflects the limitation of knowledge through which a phenomenon may be viewed or perceived (Goodchild & Quattrochi 1997). As mentioned previously, conclusions drawn from an analysis at one spatial scale may not be applicable to another scale (Wiens 1989). In remote sensing, changing the spatial resolution (i.e. image pixel size) changes the pattern of reality that can be perceived from an image (Marceau & Hay 1999) and it has a significant impact on the derived information. This issue has been known as the modifiable areal unit problem (MAUP) in the geographic literature (Openshaw 1984). It consists of two aspects; the scale problem and the zoning (or aggregation) problem (Jelinski & Wu 1996). The first aspect concerns changes in the results of spatial analysis with changing scale (i.e. spatial resolution), whereas the second results from the variation of the results of spatial analysis due to different zoning system at the same scale. The MAUP exists both in the field of remote sensing (Marceau et al. 1994a; Arbia et al. 1996) and ecology (Jelinski & Wu 1996).

Since the mid-seventies a series of empirical studies on the scale effects in remote sensing were conducted (Marceau & Hay 1999), and the prime conclusions were that a change in spatial resolution significantly affects classification accuracies. In many cases, the use of higher spatial resolution data resulted in lower overall accuracy, which was due to an increase in within-class spectral variability. This is in accordance with the theory of Strahler et al. (1986) that L-resolution resulting in mixed pixels and H-resolution produces internal variance of the objects. Consequently, scale issues should be carefully dealt with in remote sensing to map multi-scale mangrove features.

1.5. Conceptual Framework: Towards Multi-Scale Image-Based Mangrove Mapping

Integrating the remote sensing spatial (and temporal) resolutions into the mangrove spatial and temporal organisation is essential in order to map, measure and monitor this ecosystem at a correct scale. According to Skidmore et al. (2011), the field of spatial ecology, where geography and ecology intersect, facilitates this approach. It focuses on the spatial pattern of the ecological process and interaction over geographical space and time. From an ecological point of view, mangrove environments are organised in spatial and temporal dimensions (Farnsworth 1998; Twilley et al. 1999; Berger et al. 2008; Feller et al. 2010). Within the spatial domain, various levels of detail of mangrove features can be perceived at different observation scales. Putting this pattern into the remote sensing perspective and mapping mangrove environments at different observation scales (spatial resolutions) will result in different levels of mangrove information. By adopting the explicit mangrove spatial and temporal hierarchy developed by Twilley et al. (1999), a hypothetical linkage between remote sensing and mangrove spatial ecology is proposed in Figure 1.4. It suggests the need for an understanding of the effect of multi-scale variation in mangrove information in order to use remote sensing datasets appropriately, to map mangrove features.

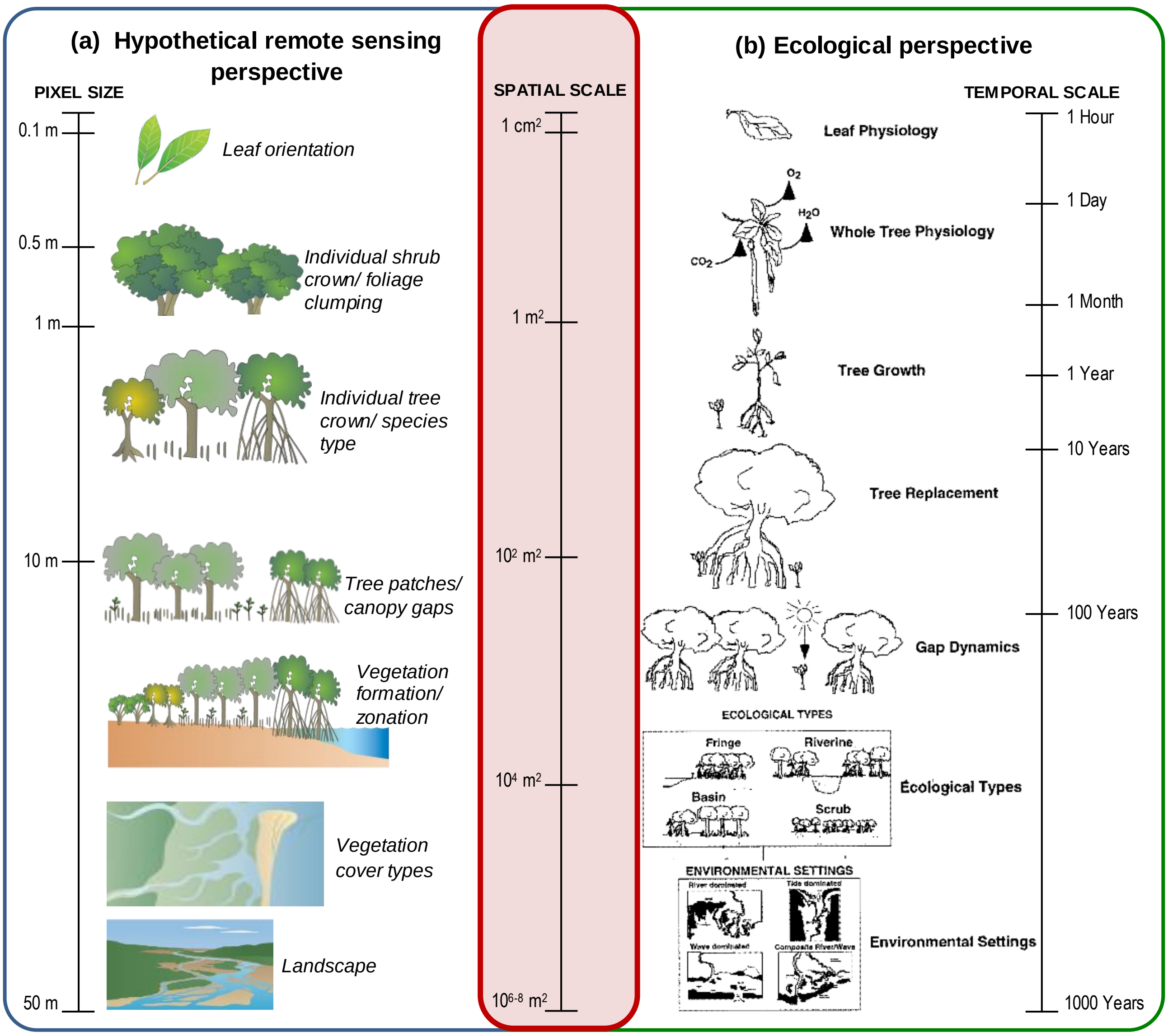

Figure 1.4. Hypothetical relationships of mangrove spatial structure form (a) size of features able to be detected from remote sensing data, and (b) temporal and spatial hierarchical organisation of dynamic processes in mangrove ecosystems (modified from Twilley et al. 1999, p. 407, with permission from Elsevier). *The pictorial symbol is courtesy of the Integration and Application Network, University of Maryland Center for Environmental Science (ian.umces.edu/symbols/).*

After establishing the remote sensing and mangrove hierarchical organisation, the following task is to select an appropriate dataset and image processing techniques. They are the fundamental factors contributing to the successful utilisation of remotely-sensed data for environmental mapping and monitoring. Woodcock and Strahler (1987) conducted preliminary research to reveal the relationship between environment and image spatial structure. They pointed out that the appropriate scale of observations was a function of the type of environment and the kind of information desired. They concluded that the choice of an appropriate scale depended on three factors: (1) the output ground scene information desired; (2) the methods used to extract information from images; and (3) the spatial structure of the scene itself. Based on these parameters, scientists have proposed the concept of scale domain and scale threshold (Marceau & Hay 1999). According to Marceau and Hay (1999), scale can be defined as a continuum through which entities, patterns, and processes can be observed and linked. The scale domain can be considered as the interval in which the phenomenon or the structures are nearly invariable or slowly variable, while they may change dramatically in a different scale domain that is separated by the scale threshold. Therefore, it is necessary to identify these scale thresholds, and to derive the appropriate conditions governing the interactions occurring within and between the levels of organization. Mangrove ecological problems often cannot be handled at a single scale of observation. An understanding of how processes operate at various spatial scales and how they can be linked across scales becomes a primary goal to solve the problems. With regard to the multi-scale research context, the understanding of these concepts would benefit the analysis of optimal spatial resolution to map features at a certain scale, and the scale where the features are likely to occur within an environment. In practice, it is also essential to develop a guideline showing the control of image resolutions and analysis methods on the type and level of information detail able to be mapped in mangrove environments.

1.6. Thesis Structure

The structure of this thesis is organised *by publications*. Chapters 3, 4, and 5 are consecutive publications/ manuscripts following typical publication format (i.e. introduction, data and methods, result and discussion, and conclusion and future work). Some degree of repetition may appear in these chapters as they were written independently. A short description of the thesis chapters are presented below.

Chapter 1: Introduction and Significance of the Research

This chapter introduces the context of the thesis. It includes research background, identification of the knowledge gaps and problem statement, research aim and objectives and relevant literature review on remote sensing for mangrove mapping.

Chapter 2: Research Approach

This chapter describes the study sites, image datasets used, field data collected, and overview of the data processing and analysis applied in the research chapters (Chapters 3, 4, 5, 6). It sets the main assumptions of the research.

Chapter 3: Characterising the Spatial Structure of Mangrove Features for Optimizing Image-Based Mangrove Mapping (Paper 1)

This chapter addresses objective 1. It examines the spatial structure of mangrove features to understand the relationships between mangrove features and the optimum pixel size required to identify and map these features. This paper was published in *Remote Sensing* journal (Kamal et al. 2014).

Chapter 4: Object-Based Approach for Multi-Scale Mangrove Composition Mapping Using Multi-Resolution Image Datasets (Paper 2)

This chapter addresses the first part of objective 2. It applies and evaluates the optimum pixel size scheme from Chapter 4 into the selected image datasets for multi-scale mangrove composition mapping. At the time of thesis publication, this chapter was submitted to *Remote Sensing* journal.

Chapter 5: Assessment of Multi-Resolution Image Data for Mangrove Leaf Area Index Mapping (Paper 3)

This chapter addresses the second part of objective 2. It investigates the effects of different mangrove environmental settings, satellite image spatial resolutions, spectral vegetation indices (SVIs), and mapping approaches for LAI estimation. At the time of thesis publication, this chapter was submitted to *Remote Sensing of Environment* journal.

Chapter 6: Guidelines for Multi-Scale Image-Based Mangrove Mapping

This chapter synthesises the findings from Chapters 3, 4, and 5, and develops the guidelines for multi-scale mangrove mapping.

Chapter 7: Conclusions, Significance and Future Research

This chapter draws together the overall outcomes and contributions of the thesis in the context of the objectives, as well as an overview of the limitations and future work.

CHAPTER 2:

RESEARCH APPROACH

This chapter provides an overview of the research approach used throughout this thesis. It includes descriptions of the study sites, field and image data used and the summary of data processing and analysis for Chapters 3-6.

No paper publication is associated with this chapter.

2.1. Study Sites

There are two study sites in this research (Figure 2.1). The first is a mangrove area at the mouth of the Brisbane River, northern Moreton Bay, South East Queensland, Australia (between 153°3'41" – 153°11'20" E and 27°19'41" – 27°25'31" S). It is a sub-tropical lowland area that includes Whyte Island, Fisherman Island and the Boondall wetlands, approximately 15 km northeast of Brisbane city. This lowland area is classified as subtropical, experiencing warm climate (average daily maximum: 28.9°C, minimum: 20.0°C) with moderate to high rainfall (mean annual rainfall: 1267.7 mm). The highest rainfall events are associated with summer monsoonal depressions (December to February) (BoM 2013).

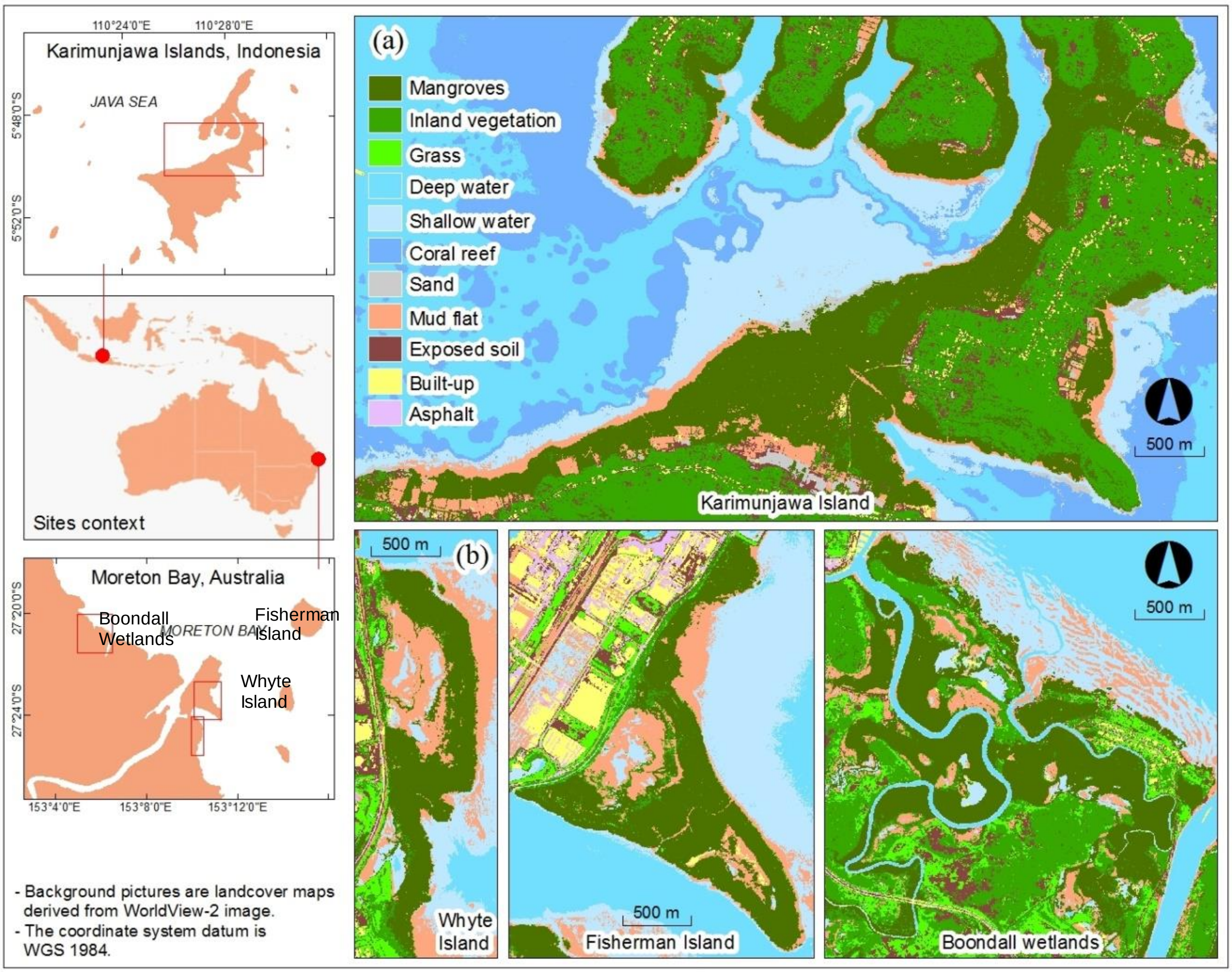

Figure 2.1. Study sites; (a) Karimunjawa Island, Indonesia, and (b) Moreton Bay, Australia.

Moreton Bay is one of Australia's premier wetlands and a Ramsar Convention listed wetland, with extensive stands of mangroves (Environment Australia 2001). This area of Moreton Bay is relatively open to sea water and subject to wave action. As a consequence, the mangrove communities are restricted to protected areas such as river and creek estuaries. However, there are extensive areas of mud flats and shallow water within these areas. These shallow areas provide protective barriers, help to moderate wave action and allow the formation of mangrove communities (Dowling 1986). Mangroves in Moreton Bay are dominated by *Avicennia marina* species, which comprise ~75% of the entire mangrove community (Dowling & Stephen 2001). Some individual *Rhizophora stylosa* are found sporadically as a mid-storey between *Avicennia*, several patches of uniform *Ceriops tagal* stands are found near the creeks in Fisherman Island and Boondall wetlands, and *Aegiceras corniculatum* is found mostly as understorey (Duke 2006). Distinct structural zonations are noticeable in this area; from the saltmarsh area, through the mangroves to the water, the progression is open scrub formation (S3), followed by low-closed forest (I4) and finally closed forest (M4), according to Specht et al. (1995) forest structure classification (see Appendix 1 for the forest structural formation list).

The second site is mangroves at Karimunjawa National Park, located in the Java Sea, between Java Island and Kalimantan Island, Indonesia (between 110°24’10” – 110°30’10” E and 4°47’48” – 5°50’12” S). It is a tropical archipelago of 22 islands (five of which are inhabited) with a total area of 111,625 ha (1285.50 ha of Karimunjawa Island, 222.20 ha of Kemujan Island and 110,117.30 ha of other small islands) (BTNK 2008), approximately 125 km north of Semarang city. It has a humid tropical maritime climate with an average daily temperatures range from 26–30°C and average humidity of 70–85%. The average annual rainfall is 2632 mm; the average monthly rainfall during the dry season (April to September) is 60 mm and during wet season (October to March) is 400 mm.

The Karimunjawa Islands represent several ecosystem types including lowland rain forest, seagrass and algae fields, coastal forests, mangrove forests and coral reefs (BTNK 2001). Generally, coastal areas in Karimunjawa Islands are fringed by coral reefs and mangrove forest that protect the beaches from waves and storms. Mangroves in Karimunjawa National Park exist mainly in the fringing area on the western side of the two main islands; Karimunjawa and Kemujan. According to a Karimunjawa National Park Office report (BTNK 2011) there are 45 mangrove species in this area (27 true mangroves and 18 mangrove associates), with *Rhizophora stylosa* as the dominant mangrove species. Although it is less apparent when compared with Moreton Bay mangroves, three different mangrove structural formations are recognisable from the land to the seaward margin. The first landward formation is dominated by low multi-stem stands (VL4) of *Ceriops tagal* and *Lumnitsera racemosa*. The middle formation is the single and multi-stem low-closed forest (I4) of highly mixed formation of *Ceriops tagal*, *Lumnitsera sp*., *Rhyzophora sp.* and *Bruguiera gymnorrhiza*. Lastly, closer to the shoreline is a formation of multi-stem closed forest (M4) consisting of *Rhizophora mucronata* and some individual *Bruguiera gymnorhiza* and *Xylocarpus granatum*. See appendix 2 for the complete list of mangrove species found.

The reasons for selecting these sites were: (1) both sites are protected areas, thus the existing mangroves are well-preserved (i.e. minimising disturbances), making them ideal for developing and testing mapping approaches for this research; (2) there are distinct mangrove zonation and structural differences from the seaward to the landward, (3) different mangrove species composition and structural forms exist in these areas, making them ideal for site comparison, and (4) similar types of remotely-sensed data with different resolutions are available for both sites. The Moreton Bay site was mainly used to investigate the characteristics of mangrove spatial structure as a basis for multi-scale mangrove mapping. The results of mangrove composition and LAI mapping in both sites were used to develop guideline for multi-scale mangrove mapping suitable for multiple locations.

2.2. Image Datasets

WorldView-2, ALOS AVNIR-2, and Landsat TM datasets were used in this research for both Moreton Bay and Karimunjawa Island sites (Table 2.1). WorldView-2 data was used to examine the spatial structural characteristic of mangrove forest in Moreton Bay and identify the relationships between image spatial resolution and the size of mangrove features (Chapter 3). The validity of the resultant relationships was tested using all of the image datasets to map mangrove composition (Chapter 4) and LAI (Chapter 5) in both sites. The Moreton bay site also used LiDAR data to support mangrove composition mapping; and a very high-spatial resolution aerial photograph (7.5 cm pixel size) with true colour layers (www.nearmap.com) as a reference to analyse the classification accuracy of the produced maps (Chapter 4).

All of the Moreton Bay images were collected within four days in April 2011. However, for Karimunjawa Island, the three images were acquired over a three year period due to cloud cover. The WV-2 images were obtained in an ortho-rectified format, corrected at Level 3X (LV3X); with a root-mean-square error (RMSE) 2D of 0.00 (DigitalGlobe 2013). The TM and AVNIR-2 images were geo-referenced based on the WV-2 image to ensure the high geometric accuracy. All of the Moreton Bay and Karimunjawa Island images were assigned to a UTM zone 56J map projection and UTM zone 49M, respectively.

Table 2.1. Image datasets used in the research.

Image spatial resolution*	Image type	Moreton Bay image acquisition date	Karimunjawa Island image acquisition date	Pixel size	Spectral attributes (nm)	Geometric attributes
Moderate	Landsat TM	14 April 2011	31 July 2009	30 m	Blue (452-518), green (528-609), red (626-693), NIR (776-904), MIR1 (1567-1784), MIR2 (2097-2349)	Level 1T
	ALOS AVNIR-2	10 April 2011	19 Feb 2009	10 m	Blue (420-500), green (520-600), red (610-690), NIR (760-890)	Level 1B2G
Fine	WorldView-2	14 April 2011	24 May 2012	2 m (multi)	Coastal blue (400-450), blue (450-510), green (510-580), yellow (585-625), red (630-690), red edge (705-745), NIR1 (770-895), NIR2 (860-1040),	Level 3X
Very fine	WorldView-2	14 April 2011	24 May 2012	0.5 m (pan)	panchromatic (450-800)	
	LiDAR	24 April 2009	-	2.8 pts/m^2	-	Geo-referenced
	Aerial photo	14 January 2011	-	7.5 cm	RGB image	Geo-referenced

*According to Warner et al. (2009) classification.

The image pixel values (in digital numbers) were then converted to top-of-atmosphere (TOA) spectral radiance (W/cm^{2}sr.nm) using the ENVI 4.8 software (ITT Systems, ITT Exelis, Herndon, VA, USA). This process was carried out following the procedures and correction coefficients described in Chander et al. (2009), Bouvet et al. (2007), and Updike & Comp (2010), for the TM, AVNIR-2 and WV-2 imagery, respectively. Further atmospheric correction was then performed to convert TOA spectral radiance to at-surface reflectance using the Fast Line-of-sight Atmospheric Analysis of Hypercubes (FLAASH) atmospheric correction model for the TM and WV-2 images, with the atmospheric visibility parameter estimated from the *moderate-resolution imaging spectroradiometer* (MODIS) aerosol product (LAADS 2012). A relative dark-object subtraction (DOS) atmospheric correction method was applied using dark, deep, and calm water objects for the AVNIR-2 images due to the lack of satellite scanning position information. The DOS is a simple and efficient approach for atmospheric correction as shown in previous studies (Song et al. 2001; Wang et al. 2004c; Soudani et al. 2006). A very high-spatial resolution aerial photograph (7.5 cm pixel size) with the true colour layers captured on 14 January, 2011 (www.nearmap.com) was used (1) to measure the dimension (*i.e.*, spatial size) of mangrove features investigated (foliage clumping, canopy gaps, tree crown, vegetation formation or community and vegetation cover type) and as a reference to analyse the image spatial structure in Chapter 3, and (2) as a reference to analyse the classification accuracy of the produced maps in Chapter 4.

2.3. Field Datasets

Field survey data from transects perpendicular to the shoreline were obtained to collect selected mangrove information along the different mangrove zonations. The data collected in the field included: (1) mangrove composition (species types and communities), (2) mangrove LAI, and (3) mangrove canopy height. The transect lines represented the variation of mangrove structure within the site, which is commonly stretched perpendicular to coast line from the seaward margin of the mangrove forest to the landward margin following the mangrove zonation (English et al. 1997; Bengen 2002) (Figure 2.2). These transects were established with the aid of high-spatial resolution pan-sharpened WorldView-2 images (0.5 m pixel size), as these images indicate changes or variation in mangrove zonation and geomorphic features. The images were used to design transect lines that were as representative of the general area and also being physically accessible.

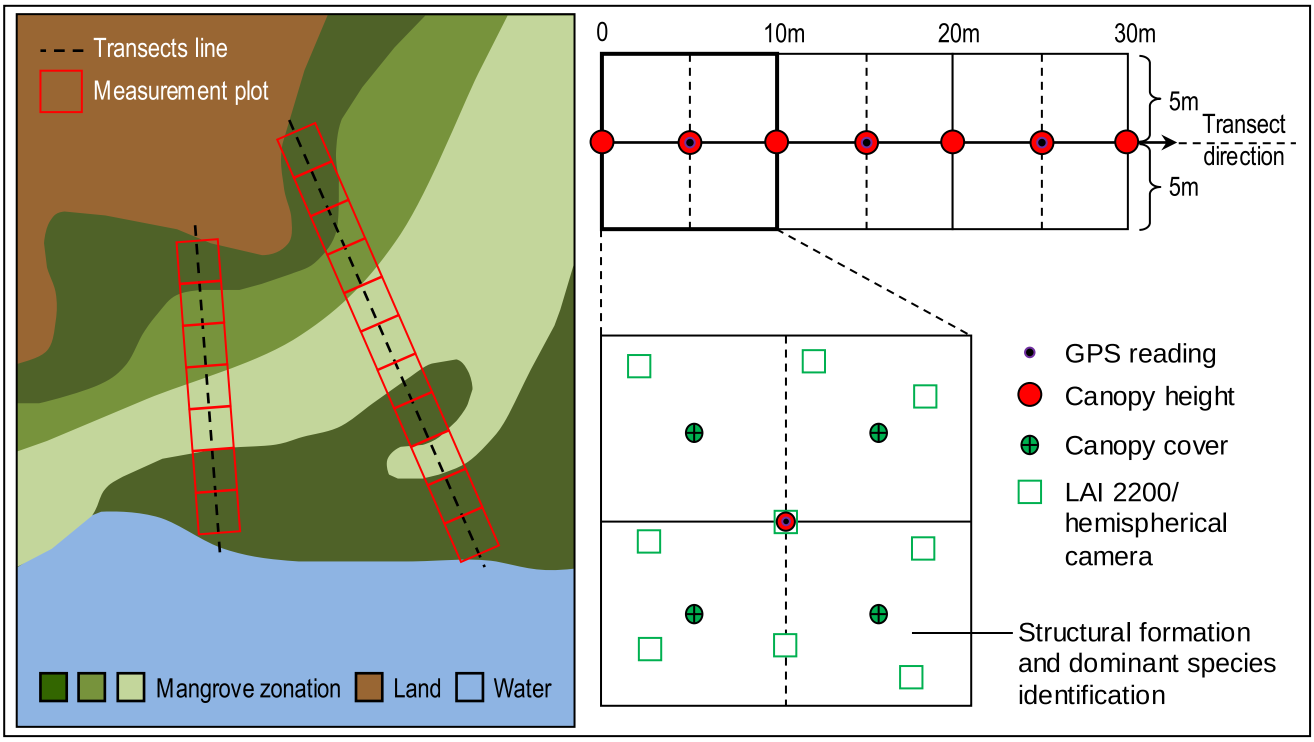

Figure 2.2. Field survey design in mangrove environment; transects are established through the mangrove forest from the seaward edge to the landward margin (modification from English et al. 1997, p. 179).

Fieldwork was conducted in April 2012 at the Moreton Bay sites and July 2012 at Karimunjawa Island. The selection of these dates was to resemble the season in which the WorldView-2 image was captured (i.e. in autumn season [April 2011] and dry season [May 2012] respectively). To record this structural variation, 23 (15 of Moreton Bay and 8 of Karimunjawa) representative 200–300 m transects perpendicular to the shoreline were established to capture the variation of mangrove vegetation structure and composition throughout the study sites (Figure 2.3), following the mangrove fieldwork guidelines established by English et al. (1997). Several types of field data were collected from single quadrats at places where the planned field transects were not accessible. These additional field samples were required to provide as comprehensive as possible measurements of mangrove canopy cover variation over each study site.

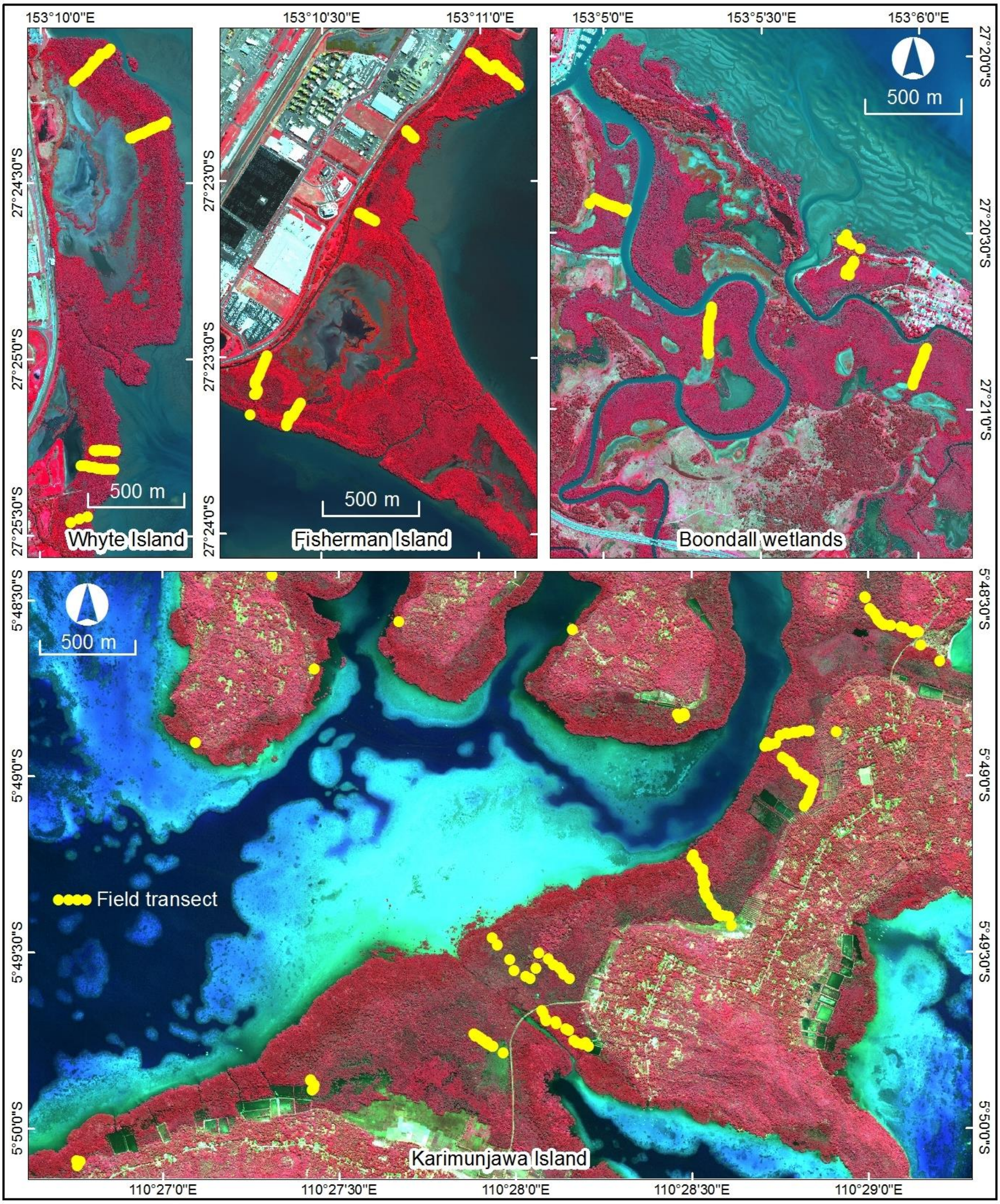

Figure 2.3. Locations of field transects plotted on WorldView-2 image 753 band combinations.

Along each transect, a sequence of 10 m x 10 m quadrats were placed along the centre of the transect lines as a frame to record mangrove zonation patterns and measuring mangrove biophysical properties in the field (Figure 2.2). The size of 10 m x 10 m quadrats was selected based on field observations, indicating homogenous canopy cover within each quadrat. At the same time, the transect width of 10 m was a compromise between measurements corresponding to the pixel size of the imagery data and what was technically feasible. Positions of each sampling plot (at their start and the end points) were measured using a Garmin eTrex Legend H hand-held GPS with an average reading of each point between 400 to 600 seconds, to maximise the GPS signal reception inside the mangrove canopy. Additional control points identifiable from the field and image were used to ensure the precise overlay of the transects to the image. Data collected on each sampling plot included plot position (Global Positioning System, GPS), vegetation structural information (height, percentage of canopy cover and structural formation), dominant species, LAI and field photos.

The canopy height data were measured at every 5 m along the transect using TruPulse 360 laser rangefinder. Any canopy gaps found at the point of measurement were recorded and the closest canopy was measured as additional data. The LAI of mangrove canopy was estimated using LI-COR LAI 2200 Plant Canopy Analyser instrument (LI-COR 2009) along the transect line (Figure 2.4a). A pocket camera and hemispherical camera were used to capture the upward-looking perspective within the canopy (Figure 2.4b). The photos were subsequently analysed using CAN-EYE imaging software (http://www6.paca.inra.fr/can-eye) (INRA 2013) to determine the percentage of canopy cover. Mangrove structural formation on each plot was determined using the Australian vegetation structural formations table (Specht et al. 1995), and dominant species information were identified using mangrove species identification book for Australian mangroves (Duke 2006) and Indonesia mangroves (Kitamura et al. 2004). Field photos were also obtained during the fieldwork to document the important field information.

Mangrove zones at the Moreton Bay study sites are dominated by *Avicennia marina* with some variation in structural characteristics. Some individual *Rhizophora stylosa* are found sporadically as a mid-storey between *Avicennia*, several patches of uniform *Ceriops tagal* stands are found near the creek in Fisherman Island and Boondall wetlands and *Aegiceras corniculatum* is found mostly as understorey. Distinct structural zonations are noticeable in this area; from the saltmarsh area to the coastline, zonation commonly starts with open scrub formation (S3), followed by low-closed forest (I4) and finally closed forest (M4) according to Specht et al. (1995) forest structure classification (see appendix 1). Mangroves at Karimunjawa Island has a higher species diversity, higher canopy densities and consists of taller and more mature trees, as opposed to Moreton Bay mangroves (see

Figure 2.4a and b for photo comparison). Seventeen mangrove species were found during the fieldwork (see appendix 2, Kitamura et al. 2004), with *Rhizophora sp*. being the dominant species in this area. Three different mangrove structural formations were recognised from the landward to the seaward. Low multi-stem stands (VL4) of *Ceriops tagal* and *Lumnitsera racemosa* dominate the area close to landward, followed by the single and multi-stem low-closed forest (I4) of highly mixed formation of *Ceriops tagal*, *Lumnitsera sp*., *Rhyzophora sp*. and *Bruguiera gymnorrhiza*. Closer to the shoreline are formations of multi-stem closed-forest (M4) of *Rhizophora apiculata* and some *Xylocarpus granatum*.

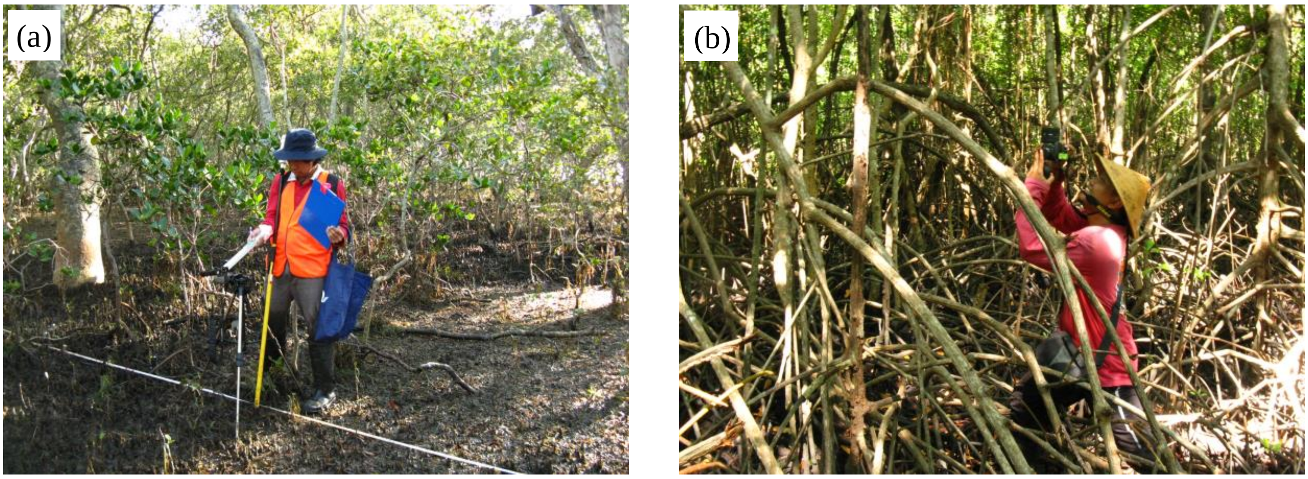

Figure 2.4. Field measurement along the transect in (a) Moreton Bay, with dominant *Avicennia marina* stands, and (b) Karimunjawa Island with *Rhizophora apiculata* stands.

2.4. Data Processing and Analysis

Following the image and field datasets acquisition the guidelines for multi-scale mangrove mapping were developed in three main stages based on these datasets. The first stage determined and quantified the spatial structure of mangrove appearance on images with various pixel sizes (Chapter 3). This stage was intended to characterise the size of mangrove features able to be identified at a certain image pixel size. This approach provided basic understanding to develop an optimum pixel size scheme to be used for mapping mangrove features at multiple scales. The second stage applied the developed optimum pixel size scheme using selected real digital image datasets and mapping methods, to map mangrove composition (Chapter 4) and LAI (Chapter 5). This stage evaluated the applicability of the optimum pixel size scheme to a real mapping scenario and assessed the accuracy of the mapping results. The final stage synthesised the results from the first and second stages (Chapters 3, 4, and 5) and analysed the relationships between image datasets, mapping methods, type of mangrove information and level of accuracy produced (Chapter 6). This relationship provided the foundation to develop the guidelines for multi-scale image-based mangrove mapping, which formed the main aim of this research. An outline of the main stages of processing and analysis is presented in Figure 2.5.

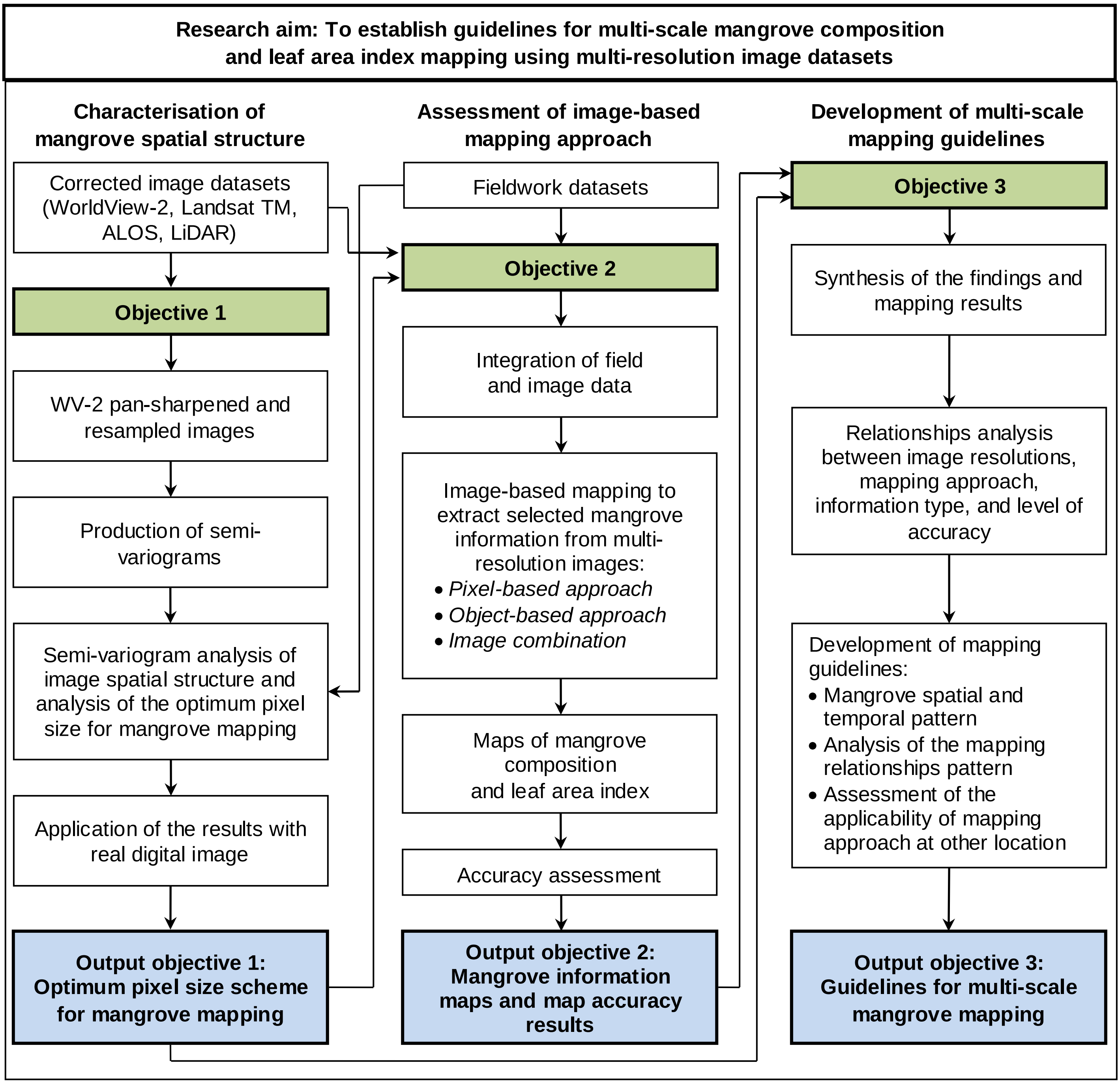

Figure 2.5. Flowchart illustrating the main components and linkages of the data and methods.

2.4.1. Characterisation of Mangrove Spatial Structure

The first objective aimed to provide a fundamental understanding of the spatial arrangement of mangrove features across different scales as a basis for developing an inversion approach, which is information extraction from remote sensing data, in multi-scale image-based mangrove mapping. Examination of how variation in scales (i.e. pixel sizes) controlled the representation of mangrove features was conducted using high spatial resolution WV-2 image data and mainly assessing mangroves at Moreton Bay sites. To analyse the scale domain and scale threshold of mangrove features on the images, semi-variograms were produced for various pixel sizes, spectral bands and mangrove zones. The results of the semi-variogram analysis revealed the relation between mangrove features and the most suitable pixel size to map these features. This finding was used as a basis to select the optimal spatial scales for mapping mangrove features and develop a multi-scale approach for mangrove feature mapping. In order to validate the analysis result, a series of object-based segmentation and classification tests were conducted at selected sites in Moreton Bay mangroves. The final results were a validated optimum pixel size for mangrove mapping and approach for multi-scale mangrove mapping, presented in Chapter 3.

2.4.2. Assessment of Image-Based Mangrove Mapping Approach

Based on the findings from the semi-variograms analyses, the optimum pixel size scheme and multi-scale mapping approach were applied to the selected remotely-sensed data and mapping technique(s) to map mangrove species and structural composition and LAI, and assess the quality of produced maps. This stage contained two parts, (1) multi-scale mangrove composition mapping (Chapter 4) and (2) multi-scale mangrove LAI mapping (Chapter 5). The first part mapped targeted mangrove features at discrete spatial scales using selected image datasets, assessed the accuracy of the mapping results and evaluated the effect of spatial resolutions on the produced maps. The second part investigated: (1) the accuracy of different image datasets for estimating LAI at different sites; (2) the most optimum spectral vegetation index to use for LAI estimation; and (3) whether the GEOBIA approach improved the LAI estimation ability of the pixel-based method. Datasets from TM, AVNIR-2 and WV-2 were used as source images for mapping at both sites. Additional LiDAR data was used for the Moreton Bay site. The information obtained in this stage was the mangrove vegetation features identified in the first stage (Chapter 3), with additional information about mangrove species communities and LAI. Variations of information obtained in the produced maps provided input for the next stage in order to develop guidelines for selecting the most appropriate image datasets to provide mangrove composition and LAI information at different scales.

2.4.3. Development of Multi-Scale Mangrove Mapping Guidelines

The selection of scale or an appropriate spatial resolution is an important factor that contributes to the successful application of remote sensing. To address the challenge in selecting the appropriate image data, the last stage of this research (Chapter 6): (1) analysed the relationships between image resolutions, mapping approaches and the type of information acquired and their accuracy in mapping mangroves, and (2) developed guidelines for multi-scale mangrove mapping based on the findings from stages 1 and 2. Woodcock and Strahler (1987) stated that the appropriate scale of observations was a function of (1) the type of environment, and (2) the kind of information desired. This statement provides a foundation of the relationships analysis in this study. Each of the factors contributing to the selection of an appropriate scale in mangrove mapping was examined. It covered the variation of image resolutions (spatial and spectral), map scales, mapping approaches, types of information and the map accuracy produced. All information associated with the parameters examined was presented in tables and graphics and the pattern of relationships was analysed and synthesised as a tentative guideline for multi-scale mangrove mapping. The final guideline shows the variety of mangrove features identifiable from different image spatial resolutions, the mapping approach used and the accuracy of the produced maps.

CHAPTER 3:

CHARACTERISING THE SPATIAL STRUCTURE OF MANGROVE FEATURES FOR OPTIMISING IMAGE-BASED MANGROVE MAPPING

This chapter uses multi-spatial-resolution images derived from WorldView-2 of Whyte and Fisherman Islands, Brisbane, Australia to understand the relationship between the size of mangrove features and the optimum pixel size to identify and map these features. The results provide a basis for multi-scale mangrove mapping using high-spatial resolution image datasets.

Associated Publications:

Kamal, M, Phinn, S & Johansen, K 2014, 'Characterizing the Spatial Structure of Mangrove Features for Optimizing Image-Based Mangrove Mapping', *Remote Sensing,* vol. 6**,** pp.984-1006. [DOI: 10.3390/rs6020984].

Key Findings:

- *The diameter and area size of dominant mangrove structural features (tree/shrub crown, canopy gaps, vegetation formation or community) can be detected using semi-variogram analysis applied to image datasets.*
- *There is a gradual loss of mangrove vegetation information detail with increasing pixel size.*
- *Specific mangrove features can be optimally identified and mapped from a specific pixel size and spectral band or indices.*
- *A pixel size of ≤ 2 m is suitable for mapping canopy and inter-canopy-related features within mangrove objects (such as shrub crown, canopy gaps and single tree crown).*
- *A pixel size of ≥ 4 m is appropriate for mapping mangrove vegetation formations, communities and larger mangrove features.*
- *The green (510-580 nm) and red-edge (705-745 nm) bands are optimum for determining smaller-sized mangrove features (< 8 m), such as single shrub crowns or foliage clumps, canopy gaps and single tree crowns.*
- *The near infrared1 band (770-895 nm) is more suitable for identifying features ≥ 8 m (e.g. double tree crowns or larger gaps) and the NDVI image is suitable for mapping all targeted features.*
- *The findings of this study provide a basis for an inversion approach to map mangrove features using remote sensing image datasets.*

3.1. Introduction

Remote sensing has been used extensively to map and monitor mangrove environments over the past two decades. It offers some key advantages for mangrove studies, including indirect access to mangrove habitats that are usually hard to access (Ramsey III & Jensen 1996; Davis & Jensen 1998), extrapolation of observation results at specific sample sites over large areas (Kuenzer et al. 2011) and delivery of data at specific spatial and temporal scales (Malthus & Mumby 2003). Recent developments in remote sensing and image processing allow us to explore various types of image datasets, as well as types of mapping techniques, to map mangroves (Heumann 2011b; Kuenzer et al. 2011). However, there is a need to match the scale of the analysis to the scale of the phenomenon under investigation, as environmental inferences are scale-dependent (Wiens 1989). Mapping mangroves at specific spatial scales will help scientists to focus their research on the ecological questions that are appropriate to each level of ecological detail (Delcourt et al. 1983) and managers to focus on the conservation activities at ecologically relevant spatial and temporal scales (Schaeffer-Novelli et al. 2005).

From an ecological perspective, mangrove ecosystems, like other vegetated ecosystems, can be placed within a hierarchical structure (Feller et al. 2010). The central concept of this theory focuses on the differences in structure and process rate between hierarchical levels. Based on these differences, ecosystems are viewed as being stratified into discrete levels of interacting subsystems, with attributes and processes occurring at specific spatial and temporal scales (Delcourt et al. 1983; Müller 1992; Lee & Grant 1995; Farnsworth 1998). Remote sensing is a tool able to deliver information on mangrove characteristics at specific spatial and temporal scales. However, the spatial configuration of mangroves, as measured in an airborne or satellite image, is dictated by spatial structures of mangroves in the field, interacting with imaging sensor characteristics. In order to use satellite or airborne image data to extract information on mangroves at specific scales or features, it is essential to understand the control of mangrove spatial structures on their measurement in an image. This raises the question, “what mangrove features are dominant and able to be mapped at specific levels of image resolution, as controlled by pixel size?” Studies linking the spatial structure of mangroves and the image spatial-resolution are limited.

The selection of scale or an appropriate spatial resolution is an important factor that contributes to the successful application of remote sensing. It depends on several factors, including the information to be extracted from the ground scene, the analysis method to be used to extract the information, the spatial structure of features within the image scene (Woodcock & Strahler 1987), the type of environment being investigated and other relevant constraints (*i.e.*, cost and time) (Phinn et al. 2000). The scale effect is regarded as one of the most important problems in remote sensing studies (Raffy 1994; Goodchild & Quattrochi 1997; Marceau & Hay 1999). The "scale" represents the window of perception (Marceau & Hay 1999), the ability of observation and reflects the limitation of knowledge through which a phenomenon may be viewed or perceived (Goodchild & Quattrochi 1997). Changing the scale of data collection and analysis impacts the measurements and conclusions able to be drawn for an environment and image dataset combination. Consequently, selecting an appropriate or optimal spatial resolution requires information on the spatial characteristics of features within the scene under investigation.

Scientists have developed several methods to select the optimal spatial scale for remote sensing applications, which are tied to selection of pixel sizes and spectral bands, primarily for use in the per-pixel classification. The most widely adopted method is to examine the spatial autocorrelation of the image scene through the analyses of semi-variograms. The semi-variogram is a tool to link models of the ground scene to spatial variation in images (Woodcock et al. 1988a) and is able to detect the most dominant scale(s) of variation in images (Woodcock et al. 1988b). In remote sensing studies, it enables the optimal pixel size for feature mapping in different environments from image data to be specified, for example, in forests (Hyppanen 1996; Treitz & Howarth 2000; Colombo et al. 2004; Wolter et al. 2009), tropical savannahs (Menges et al. 2001; Johansen & Phinn 2006), grasslands (Phinn et al. 1996; He et al. 2006) and wetlands (Wen et al. 2012). Semi-variograms can be used to identify the domains of scale where certain features reside (Cohen et al. 1990; Treitz & Howarth 2000; Johansen & Phinn 2006), which in turn will provide support in selecting the most appropriate image spatial resolution for a specific mapping purpose.

The current status of remotely sensed data (*i.e.*, various types and resolutions) enables multi-scale information to be derived for mapping and monitoring mangroves across spatial-ecological hierarchies. However, as an increasing number of remotely-sensed datasets with different pixel sizes become available, selecting the most appropriate spatial resolution becomes more difficult. In order to select an appropriate spatial resolution for a specific application, the spatial characteristics of the scene should be examined (Chen 2001). The main objectives of this study were to estimate the optimum pixel size for mapping mangrove composition and structural properties and test the applicability of the methods. The examination of spatial characteristics of mangroves was conducted using experimental semi-variograms derived from WV-2 image, in Moreton Bay, Australia, to determine the spatial scales of the mangrove features. This information may provide guidance for selecting the most appropriate image spatial resolution for mapping certain mangrove features and answer the question of which mangrove feature can be mapped from a given spatial resolution, and *vice versa*.

3.2. Data and Methods

3.2.1. Study Site

The study site for this chapter was carried out in mangrove areas at the mouth of the Brisbane River, Northern Moreton Bay, South East Queensland, Australia. For the detailed description of the location refer to section 2.1 of the thesis.

3.2.2. Image and Field Datasets

The image data used as a basis for mangrove spatial structure examination was a WorldView-2 image of the Brisbane River mouth captured on 14 April, 2011 (Table 3.1). The image pre-processing and fieldwork details are presented in sections 2.2 and 2.3 of the thesis.

Table 3.1. Characteristics of image data used in Chapter 3.

Image Type	WorldView-2 (WV-2)	Aerial Photograph (AP)
Acquisition date	14 April 2011	14 January 2011
Acquisition time	00:10:47.59 UTC (10:10:47.59 AEST)	
Product type and level	Ortho, LV3X	Ortho-rectified
Geometric attributes	UTM 56 J in meters	GCS WGS 1984
Radiometric attributes	16 bits per-pixel	
Spectral attributes	Coastal (400–450 nm) Blue (450–510 nm) Green (510–580 nm) Yellow (585–625 nm) Red (630–690 nm) Red edge (705–745 nm) NIR1 (770–895 nm) NIR2 (860–1040 nm) PAN (450–800 nm)	True colour image (red, green, blue)
Pixel size	Multi-spectral 2 m, panchromatic 0.5 m	7.5 cm

The fieldwork was conducted during April, 2012, to measure selected mangrove vegetation structures and composition variables in the study area. Fifteen representative 200–300 m long field transects were established perpendicular to the shoreline (Figure 3.1a, b). On each transect, plots of 10 m × 10 m quadrats were sampled along the transect lines as a frame to record mangrove zonation patterns and measure mangrove biophysical properties in the field, including transect and plot positions, vegetation structural information (canopy height and vegetation formation type), dominant species and field photos. The structural characteristics measured along the transect in each of three mangrove field sample sites are presented in Table 3.2.

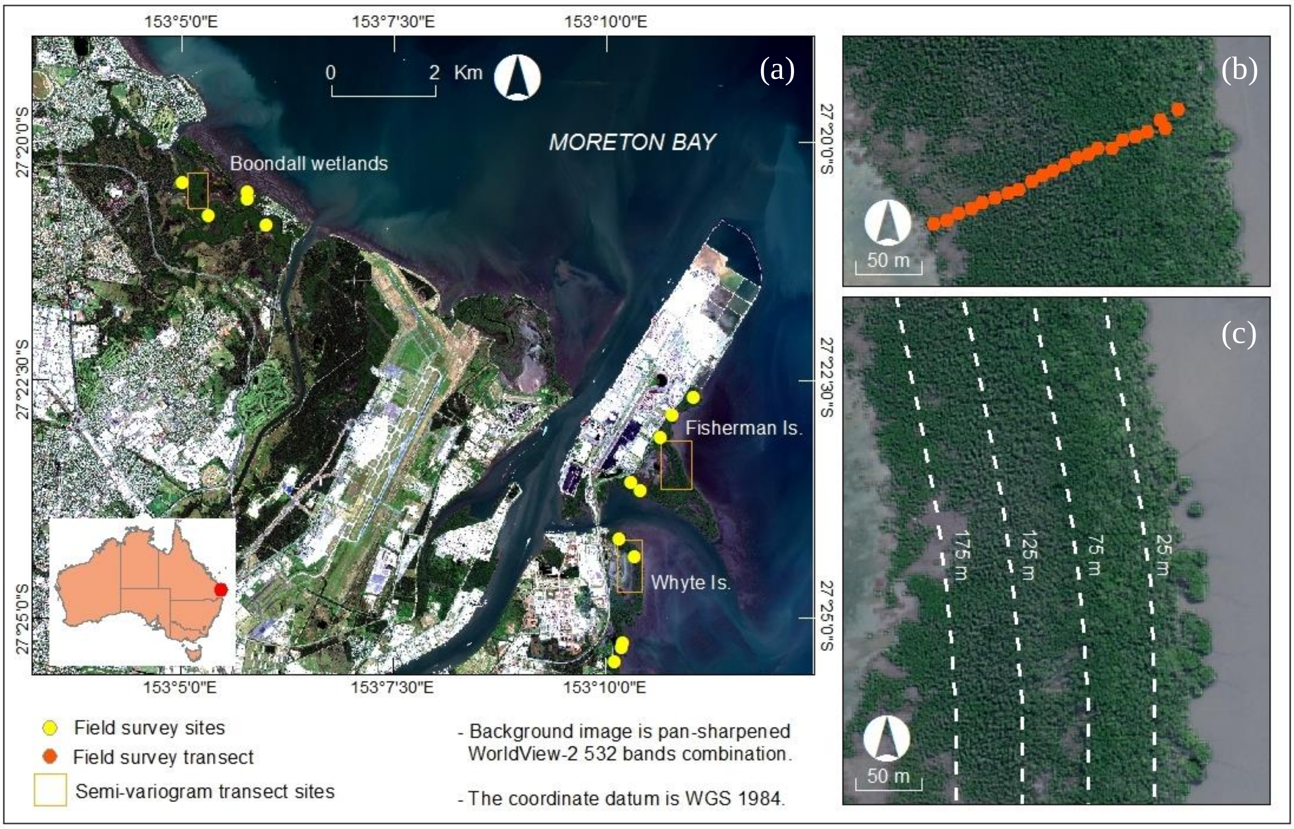

Figure 3.1. (a) Study sites: mangroves at Moreton Bay area, Brisbane, Australia; (b) an example of field survey transect, orange circles represent location of 10 m x 10 m quadrats, and (c) transects of image pixels running parallel to the coastline used to derive the semi-variograms shown for Whyte Island.

Table 3.2. Mangrove vegetation structural characteristics of Moreton Bay mangroves, sampled at three sites, derived from field data sampled across the main vegetation zonation boundaries.

Distance from Coastline	Whyte Island	Fisherman Island	Boondall Wetlands
175 m (S3)	Open scrub, 1–3 m height, multi stem, gaps > canopy cover, *Sarcocornia quinqueflora*, water or soil understory, low density canopy cover, dominant species *Avicennia marina.*	Open scrub, 2.5–4 m height, single or multi stem, gaps < canopy cover, *Sarcocornia quinqueflora*, water or soil understory, low density canopy cover, dominant species *Avicennia marina.*	Open scrub, 1.5–5 m height, single or multi stem, gaps > canopy cover, *Sarcocornia quinqueflora*, water or soil understory, medium density canopy cover, dominant species *Avicennia marina.*
125 m (I4a)	Low-closed forest1, 4–7 m height, single or multi stem, gaps < canopy cover, *Avicennia marina* seedling or *Aegiceras corniculatum* understory, medium density canopy cover, dominant species *Avicennia marina.*	Low-closed forest1, 4–9 m height, single stem, gaps < canopy cover, *Avicennia marina* seedling or *Aegiceras corniculatum* understory, high density canopy cover, dominant species *Avicennia marina.*	Low-closed forest1, 5–7.5 m height, single stem, gaps < canopy cover, *Avicennia marina* seedling or *Aegiceras corniculatum* understory, high density canopy cover,dominant species *Avicennia marina.*

Table 3.2. *Continued.*

Distance from Coastline	Whyte Island	Fisherman Island	Boondall Wetlands
75 m (I4b)	Low-closed forest2, 6–8 m height, single stem, gaps < canopy cover, clear understory, very high density canopy cover, dominant species *Avicennia marina* with some individual *Rhizophora stylosa.*	Low-closed forest2, 8–10 m height, single stem, gaps < canopy cover, clear understory, high density canopy cover, dominant species *Avicennia marina* with some individual *Rhizophora stylosa* and patches of *Ceriops tagal*.	Low-closed forest2, 7–9 m height, single stem, gaps < canopy cover, clear or *Avicennia marina* seedling understory, high density canopy cover, dominant species *Avicennia marina* with some individual *Rhizophora stylosa.*
25 m (M4)	Closed forest, 10–12 m height, single or multi stem, gaps < canopy cover, clear understory, high density canopy cover, dominant species *Avicennia marina* trees.	Closed forest, 8–11 m height, single or multi stem, gaps < canopy cover, clear understory, high density canopy cover, dominant species *Avicennia marina* trees.	Closed forest, 8–10.5 m height, single or multi stem, gaps < canopy cover, clear understory, high density canopy cover, dominant species *Avicennia marina* trees with some patches of *Ceriops tagal*.

3.2.3. Methods

Figure 3.2 summarises the methods used to measure the spatial structure of mangrove features in the study area. The work flow is divided into three steps. Step 1 is necessary to prepare the data and create a series of images with different pixel sizes as a basis for multi-scale level examination of mangrove spatial structure. Step 2 deals with measuring and analysing the spatial structure of mangrove vegetation from the pre-processed images using semi-variograms. Step 3 applies and evaluates the results from step 2 into image datasets for mapping mangrove features using GEOBIA.

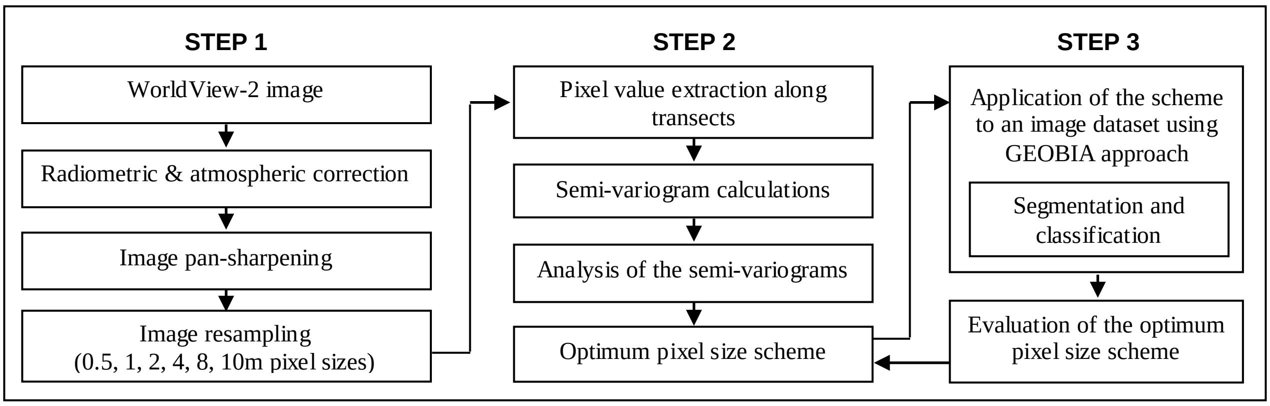

Figure 3.2. Overview of Chapter 3 methods.

3.2.3.1. Image Dataset Preparation

Pan-sharpening algorithms were applied to the atmospherically corrected images to obtain a higher spatial resolution image for input to the spatial structure analysis. Six different pan-sharpening algorithms (*principal component, multiplicative, Brovey, wavelet, Gram-Schmidt and colour* *normalised*) from commercial image processing software were investigated to determine their quality in terms of preserving pixel values of the atmospherically corrected multi-spectral data. Several image quality metrics were applied, including root mean square error, standard deviation, relative shift of the mean and coefficient of correlation (Vijayaraj et al. 2004; Jayanth et al. 2012) (Appendix 3). The overall evaluation of the image quality metrics shows that the Gram-Schmidt pan-sharpening algorithm produced the pixel values closest to the original multi-spectral data and therefore this method was used to produce a sharpened image for spatial structure analysis.

To enable analysis of the spatial structure of mangroves at multiple specific-scales and to examine the effect of different pixel sizes on the derived information, the Gram-Schmidt pan-sharpened image (0.5 m pixels) was resampled to a pixel size of 1 m. As well, the original multi-spectral image (2 m pixels) was resampled to 4 m, 8 m and 10 m pixel sizes using an averaging algorithm. According to Bian and Butler (1999), the pixel aggregation method is more appropriate for processing remote sensing images because a pixel value is assumed to be the averaged value over the associated area on the ground. This process produced a total of six different image pixel sizes (0.5 m, 1 m, 2 m, 4 m, 8 m and 10 m). The reasons for selecting these pixel sizes were to detect specific details of mangrove features and create an approximation of the currently available image datasets. All of processing above used ENVI 4.8 image processing software.

3.2.3.2. Measurement of Mangrove Spatial Structure through Semi-Variogram

The semi-variogram (γ) is a spatial statistical graph of semi-variance, which is the measured difference in variance value between pairs of regionalised variable samples in relation to their spatial separation with a given relative orientation. It provides a concise and unbiased description of the scale(s) and pattern(s) of spatial variability, in both remotely-sensed data and field data (Curran 1988; Curran & Atkinson 1998). If applied to remotely-sensed data; the semi-variogram is used to examine the relationship between the digital number (*DN*) or pixel value of *n* pixel pairs at a distance *h* (the lag distance) apart. The equation for semi-variance $\gamma(h)$ is:

$$\gamma(h) = \frac{1}{2n}\sum\{DN(x) - DN(x+h)\}^2 \qquad \text{(Eq. 3.1)}$$

where $\gamma(h)$ represents half of the mathematical expectation of the squared differences of pixel pair values at a distance, *h,* and *DN* refers to spectral reflectance or vegetation index in this study. Hence, for image spectral data, $\gamma(h)$ estimates the variability of DNs, as a function of spatial separation.

In creating semi-variograms, the distance of each lag determines the number of the pixel pairs in the transect sample. By increasing the lag distance, the pixel pairs on a transect are fewer; which in turn decreases the confidence level of the analysis (Curran 1988). To alleviate this problem, Webster (1985) suggested to use lag distances shorter than a fifth of the transect length for the semi-variogram interpretation. The analysis of semi-variograms requires two assumptions. First, spatial stationarity, which assumes that the correlation between variables is a function of the lag distance between pixels and not because of the variation in spatial positions of the transect (Bailey & Gatrell 1995; Phinn et al. 1996; Treitz & Howarth 2000). Second, ergodicity, which assumes that spatial statistics taken over the area of the image as a whole are unbiased estimates of those parameters (Jupp et al. 1988). Both of these assumptions are appropriate in digital remotely-sensed images; first, because of the variation in scan angle and terrain effects are minimal and regarded as stationary in increments, and second, the reflectance surface is considered stochastic (Jupp et al. 1988). According to Curran (Curran 1988), all image bands and directions should be examined in order to define the minimum range of the semi-variogram and therefore the minimum spatial resolution of the feature element. There are two sampling methods used in creating semi-variograms (Cohen et al. 1990; Feng et al. 2010): (1) transect method, where the semi-variogram is calculated along a single, representative row or column of pixels from each selected image; and (2) matrix method, where the semi-variogram is calculated for all the row and column pixels in each image. For canopy structure analysis, the transect sampling method provides more detailed sill variation and periodicity and also a smaller range distance compared with the matrix method (Cohen et al. 1990). It was as a result of averaging the semi-variograms for all row and column directions in matrix method. Therefore, the first sampling method was adopted for this study in order to depict structural information inherent within each of the mangrove zones.

The approach used for examining spatial structure in this study was similar to the one conducted by Cohen *et al.* (1990), and Johansen and Phinn (2006). Several transects were created over the image datasets (original and resampled WV-2 images) to generate semi-variograms. All eight bands of the WV-2 image (Table 3.1) and the derived normalised difference vegetation index (NDVI) images were used to generate the semi-variograms. According to image visual inspection and semi-variogram evaluation (Kamal et al. 2013) four bands – green, red-edge, near infrared1 (NIR1) and NDVI – were identified as sensitive to mangrove vegetation variations and having the least redundant information among other bands. As a result, these bands were used for further analysis of the semi-variograms. The semi-variogram transects were located parallel to the coastline to represent the homogenous areas within each mangrove zone (i.e., areas assumed to have similar vegetation structural properties). In this study, 12 representative transects located parallel to the coastline at a distance of 25 m, 75 m, 125 m and 175 m from the coastline were used to develop semi-variograms within zone structures (Figure 3.1c). The distance of the transect lines varied between 500 m and 1000 m, depending on the length of the mangrove zonation. All transects were evaluated at six different pixel sizes (0.5 m, 1 m, 2 m, 4 m, 8 m and 10 m). Earth Resources Data Analysis System (ERDAS IMAGINE) 2013 was used to extract pixel values along the semi-variogram transects and GS+ geostatistical software for semi-variance calculation.

3.2.3.3. Interpretation of Semi-Variograms

In order to interpret a semi-variogram, it is necessary to understand the terms and characteristics associated with the semi-variogram (Figure 3.3). The range (a) of semi-variograms is the distance at which samples become independent and it is controlled by the size of dominant objects in an image. The height of the sill (*s*), where the semi-variogram levels off, is considered proportional to the density of objects and the scene-scale level of variance. The form of semi-variograms is controlled by the pattern and distribution of objects in an image (Woodcock et al. 1988a, 1988b; Jupp et al. 1989; Bailey & Gatrell 1995). These descriptors of semi-variograms are usually used together to interpret the appropriate spatial resolution for mangrove elements.

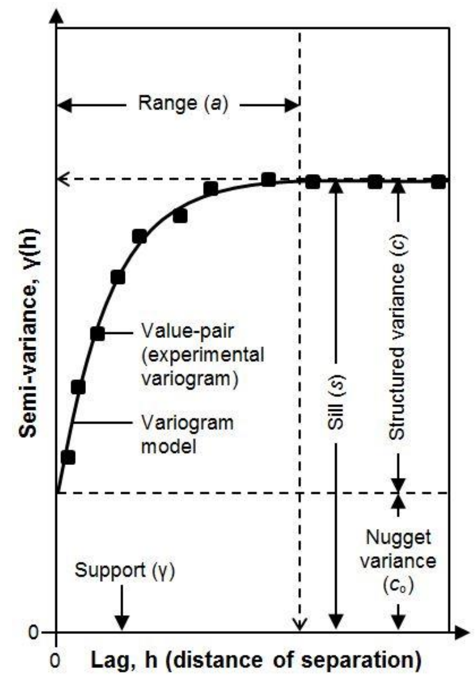

Term	Symbol	Definition
Semi-variance	γ(h)	Half the averaged variances between pixels at distance h apart.
Support	γ	Area, shape and orientation of space represented by each sample datum.
Lag	h	Distance (and direction in two or more dimensions) between sampling pairs.
Sill	*s*	Maximum value of γ(h) model.
Range	*a*	Point on x axis where γ(h) model reaches maximum. Places closer than the range are related statistically, places further apart are not.
Nugget variance	c_0	Point where γ(h) model intercepts the y axis. Represents a component of the variation that is spatially uncorrelated.
Structured variance	*c*	Sill minus nugget variance.
Gradient	*m*	The slope for γ(h) model with a linear component.

Figure 3.3. An example of a semi-variogram with descriptors and the definition of terms (Curran & Atkinson 1998; Johansen & Phinn 2006).

The advantage of using semi-variograms in remote sensing is the ability to relate descriptors to the spatial characteristics of the scene (Atkinson & Curran 1997). The range and sill were extracted from all semi-variograms of transects located parallel and perpendicular to the coastline using the green, red-edge, NIR1 and NDVI bands. Six different image pixel sizes were evaluated to detect the scale at which certain features within each mangrove zone occurred. The range provides a measure of the size of the elements or features in the mangrove environment in the image and has been identified as a useful indicator for selecting the optimal spatial resolution for discriminating features embedded in the semi-variogram (Curran 1988; Woodcock et al. 1988b). Visual inspection of the field data and visual interpretation of the image were conducted in order to relate the semi-variogram range values to the mangrove vegetation structure dimensions (foliage clumping, canopy gap and tree crown size, vegetation formation, or community and vegetation cover type). This information provides guidance for developing a scheme in selecting the optimum image spatial resolution for extracting specific mangrove features and serves as a basis for an inversion mapping approach. A total of over 1500 semi-variograms were analysed in this study. The findings from the semi-variogram analysis revealed the spatial characteristics of mangrove vegetation features and the optimum pixel sizes to map these features.

3.2.3.4. Application of the Analysis Results

To test the applicability and validate the results, GEOBIA was applied to the original and resampled WV-2 images with the segmentation and classification being driven by parameters obtained from the semi-variogram analysis. GEOBIA offers some fundamental advantages in the context of this study including: (1) image objects can be created at multiple, yet specific, hierarchical spatial scales (e.g., tree community consists of several single tree canopies) (Hay et al. 2003; de Jong & van der Meer 2005), (2) numerous attributes can be obtained from the image objects, such as an object's statistics, geometry and context, (3) the result better mimics human perceptions of real-world objects (Morgan et al. 2010), and (4) image objects reduce the salt-and-pepper effect in pixel-based classifications (Blaschke et al. 2000).

The image segmentation and classification were applied to the original and resampled WV-2 images to evaluate the applicability of the semi-variogram results. The segmentation and classification routines were carried out using eCognition Developer software v. 8.7.0. A series of scale parameters from 5 to 100 were tested for the mapping of mangrove features with a weight of 5 applied to the green, red, red-edge and NIR1 bands to enhance the influence of bands that are sensitive to vegetation reflectance in the segmentation. A trial-and-error approach and visual inspection of the segmentation results, with the help of a very-high-spatial resolution aerial photograph (7.5 cm pixel size), were performed to determine the mangrove features that could be depicted from different scale parameters and image pixel sizes.

A supervised rule-based classification was applied to implement the optimum pixel size scheme for mangrove feature mapping based on the WV-2 images. The rule sets were developed using the objects' spectral information, geometry of the objects and contextual hierarchy of the classes. The first hierarchy layer was used to separate mangrove and non-mangrove features, the second layer was for dividing the mangrove area into trees and gaps (and shadows) and the third layer was used for the classification of objects within the mangrove tree class. These hierarchical layers were applied to all image pixel sizes being examined. The result of the mapping was used to evaluate the image selection scheme and inversion mapping approach.

3.3. Results and Discussion

3.3.1. Relation of Semi-Variograms to Mangrove Vegetation Structure Properties

Visual characteristics of the images demonstrate the gradual loss of mangrove spatial structure detail with increasing pixel sizes (Figure 3.4). The descriptive statistics for each image show the divergence between the original (0.5 m and 2 m) and resampled image (1 m, 4 m, 8 m and 10 m). While the mean values of the bands in the resampled image exhibit some random variations, the coefficient of variance (%CV) decreased with decreasing spatial resolution relative to the original images. The coastal and yellow bands for the first resampling group (from 0.5 m to 1 m) and all bands for the second resampling group (from 2 m to 10 m) also follow this pattern. Figure 3.4 shows that an image with lower spatial resolution has lower data variability and therefore contains less information compared with a higher spatial resolution image.

The spatial structural information of mangrove elements (or features) detectable from the original and resampled WV-2 images was related to the semi-variogram descriptors (range, sill and form). Figure 3.5 (preliminary version published in (Kamal et al. 2013)) shows the representative semi-variogram plot of the NIR1 image band at six different pixel sizes and the average mangrove feature sizes measured from field-work and the aerial photograph. It reveals similar results to those presented in other studies examining the effects of changes in image pixel size on image information content (Woodcock et al. 1988b; Cohen et al. 1990; Garrigues et al. 2006; Johansen & Phinn 2006; Chen & Henebry 2009). Specifically, there is a gradual loss of information detail with the increasing pixel size (Figure 3.4 and 3.5). The forms of semi-variogram changes with the varying pixel sizes describe the effect of data regularisation on the spatial heterogeneity component. The decreasing height of the sill characterises the loss of spatial variability when the spatial resolution of the image decreases, which is also evident in the image statistics in Figure 3.4.

The original and resampled WorldView-2 images.

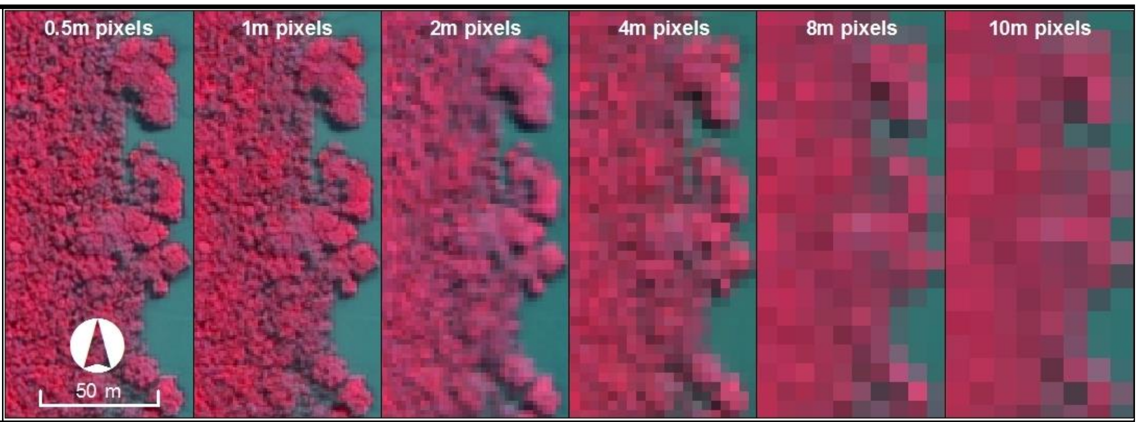

Image statistics	0.5m Mean	0.5m %CV	1m Mean	1m %CV	2m Mean	2m %CV	4m Mean	4m %CV	8m Mean	8m %CV	10m Mean	10m %CV
WV-2 image bands: Coastal	0.0605	0.64	0.0605	0.63	0.0628	0.53	0.0628	0.52	0.0625	0.51	0.0628	0.50
Blue	0.0684	0.68	0.0683	0.68	0.0710	0.58	0.0710	0.56	0.0707	0.54	0.0710	0.53
Green	0.0876	0.59	0.0875	0.59	0.0908	0.51	0.0908	0.50	0.0904	0.48	0.0909	0.47
Yellow	0.0879	0.67	0.0879	0.66	0.0915	0.56	0.0914	0.55	0.0911	0.53	0.0915	0.52
Red	0.0778	0.79	0.0778	0.79	0.0814	0.66	0.0814	0.65	0.0811	0.63	0.0815	0.62
Red-edge	0.1429	0.50	0.1428	0.50	0.1479	0.54	0.1478	0.53	0.1472	0.52	0.1482	0.51
NIR1	0.2109	0.60	0.2108	0.60	0.2172	0.67	0.2171	0.66	0.2162	0.65	0.2179	0.63
NIR2	0.1909	0.63	0.1908	0.63	0.1967	0.70	0.1966	0.69	0.1958	0.67	0.1973	0.66
NDVI	0.3617	1.11	0.3611	1.10	0.3029	1.34	0.3043	1.33	0.3055	1.32	0.3104	1.29

Note: The mean image spectral reflectance and NDVI values were represented at a scale of 0–1, %CV: coefficient of variance.

Figure 3.4. Subsets of mangrove on Whyte Island at pixel sizes of 0.5 m, 1 m, 2 m, 4 m, 8 m and 10 m displayed with a band combination of R:7, G:5, B:3, and their associated descriptive statistics.

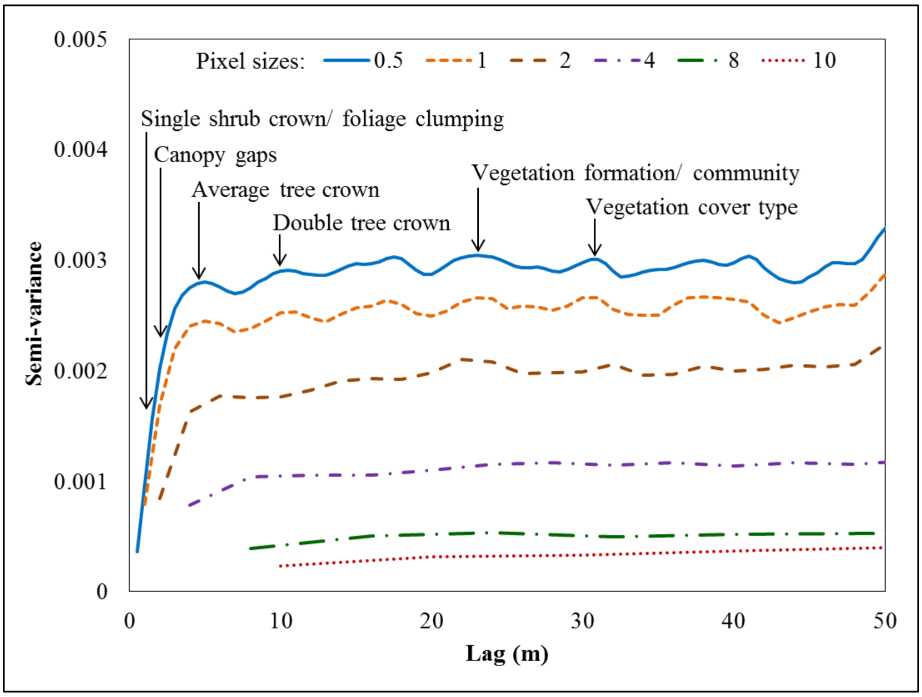

Figure 3.5. Subset of NIR1 semi-variogram showing the mangrove features responsible for the semi-variogram range and form up to a 50 m lag distance.

At a pixel size of 0.5 m, the form of semi-variograms appears to be controlled by inter-canopy features including individual shrubs and tree crowns, foliage clumping and smaller inter-canopy gaps. At a pixel size of 1 m, the individual shrub and tree crowns are still distinguishable but the detailed foliage clumping and inter-canopy gaps become more difficult to identify. Single shrub crowns and foliage clumping identified from the image and field data correspond to the semi-variogram lag distance of 1.5 m and the inter-canopy gaps at 2 m. Pixel sizes 0.5 m and 1 m had similar semi-variogram forms, meaning the variation of information of the pattern and distribution of mangrove features within these sizes are comparable, but they have different sill height which is attributed to the different level of pixel value variance in the image scene (see image statistics in Figure 3.4). Although these two pixel sizes offer similar capability, detailed information on structural properties and sharper visual image appearance increases the likelihood of correctly identifying mangrove inter-canopy features.

The range of the semi-variograms for pixel sizes 0.5, 1 and 2 m are at 5, 6 and 6 m respectively, which is approximately equal to the average diameter of single mangrove tree crowns. This indicates that single mangrove tree crowns may be distinguished at a maximum pixel size of 2 m. At a pixel size of 4 m the average single tree crown is no longer apparent, although some individual larger canopies of mangrove tree and gaps that are more than 10 m in diameter can still be identified. Based on field observations, it is likely that the range of about 8–10 m corresponds to groups of two tree crowns and these can be identified at pixel sizes of 4 m. The semi-variogram range of pixel sizes of 8–10 m are approximately 20 m and 30 m, respectively, which correspond to the average size of mangrove vegetation formation or community at 23 m and larger mangrove cover types at 30 m. At a pixel size of 4 m and larger, the canopy-related information is gradually lost. These sizes are more appropriate for mapping larger mangrove communities, mangrove patches and separating mangroves from non-mangrove cover types.

Overall, there are noticeable patterns of semi-variogram peaks and troughs with different sill heights across varying pixel sizes. According to Figure 3.5, the variation of structural information within mangrove stands can be preserved only with pixel sizes of 0.5 m to 2 m, where the semi-variogram contains periodic peaks and troughs along the graph. On the other hand, from pixel sizes of 4 m to 10 m, these variations are lost and result in relatively flat graphs with minimum or no information on within mangrove structural properties. This finding indicates that pixel sizes of 2 m and smaller are appropriate for mapping small size features and the internal variation of mangrove canopy (such as single shrub crown, foliage clumping, canopy gaps and average tree crowns), whereas pixel sizes of 4 m and larger are more appropriate for mapping larger mangrove features (such as groups of tree crowns, vegetation formations or communities, and cover type).

3.3.2. Relation of Semi-Variograms to Mangrove Zone Features

Variation in spatial structural information between mangrove zones, that is, areas with consistent structure and composition parallel to the coastline, were examined using transects located parallel to the coastline at varying distances from the three Moreton Bay sites. The semi-variograms were derived from transects of 1000 m along the mangrove zonation, which were located at distances of 25 m, 75 m, 125 m and 175 m from the edge of outer mangrove stands. These distances were selected to be as representative as possible of mangrove zonation to depict the internal mangrove zonation structural properties. Among the three transect locations; two of them produced similar semi-variograms. Therefore, only two of the transect locations are discussed here, which are Fisherman Island and Boondall wetlands (Figure 3.6).

The transect at 125 m from the coastline on Fisherman Island had high sill values and was the second highest for all of the bands. It corresponds to a low-closed forest mangrove formation where there are mixed stems of *Avicennia marina* trees (I4a) with high canopy cover and some canopy gaps. For the Boondall wetlands, this transect distance was at the third highest level of the semi-variogram sill height. The mixed-stem low-closed forest (I4a) formation in Boondall has a lower canopy cover and more canopy gaps, making it appear to have low contrast in the image. Finally, transects located at a distance of 175 m from the coastline had the lowest semi-variogram sill values and this pattern is noticeable for all bands and all locations. These transects cover the open scrub *Avicennia marina* zone with low density of canopy cover and uniform canopy layers. Some gaps with *Sarcocornia quinqueflora*, water or soil are also frequently found in this zone, which may contribute to decreasing the reflectance intensity of the pixels.

Semi-variograms located along the mangrove zones revealed different spatial structural characteristics of mangrove features within each zonation. As shown in Figure 3.7, the average range of semi-variograms of all evaluated bands for transects located along the mangrove zonation at the Moreton Bay sites exhibit different patterns. The average range values of open scrub formation (S3) were higher for all of the image bands (2.7–8.1 m) compared with the other formations where low-closed forest1 (I4a) had the lowest average range value (2.5–5.2 m), and low-closed forest2 (I4b) together with closed forest (M4) had a similar range value (3.1–6.6 m and 2.6–6.6 m, respectively). The high average range values on the open scrub formation (S3) were attributed to the large variation in the size of *Avicennia marina* scrub patches interleaved with large gaps of ground or water frequently found in this zone (see image on Figure 3.7). Conversely, the low average range values of the low-closed forest1 (I4a) were caused by the foliage clumping and the narrow canopy gaps (1–2 m) between individual tree crowns (approximately 5 m in diameter) that dominate this zone.

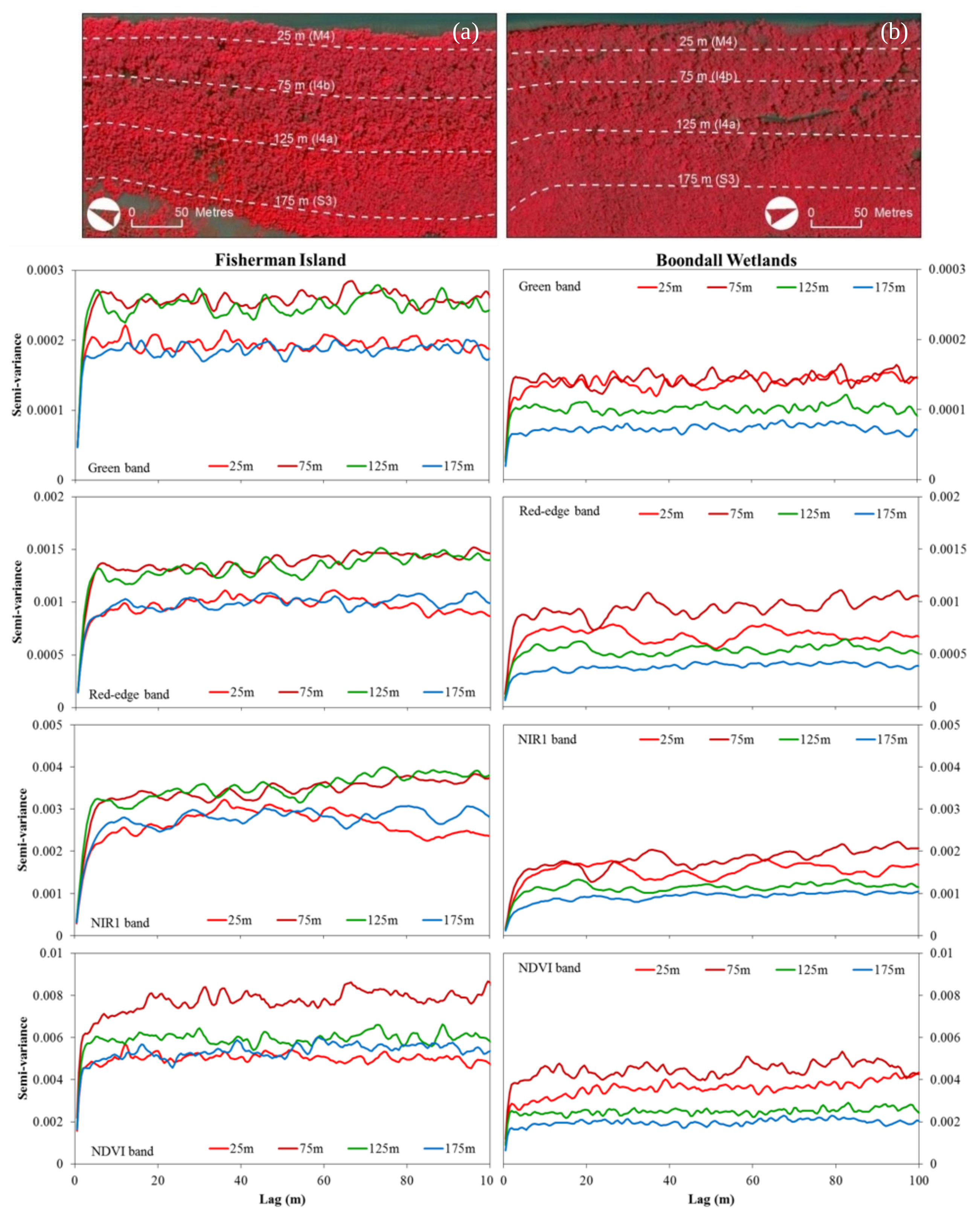

Figure 3.6. Subset of pan-sharpened images of (a) Fisherman Island and (b) Boondall wetlands showing the transects along the mangrove zonations and semi-variograms created from transects along the mangrove zonation at distances of 25 m, 75 m, 125 m and 175 m from the coastline using the 0.5 m pan-sharpened WV-2 image.

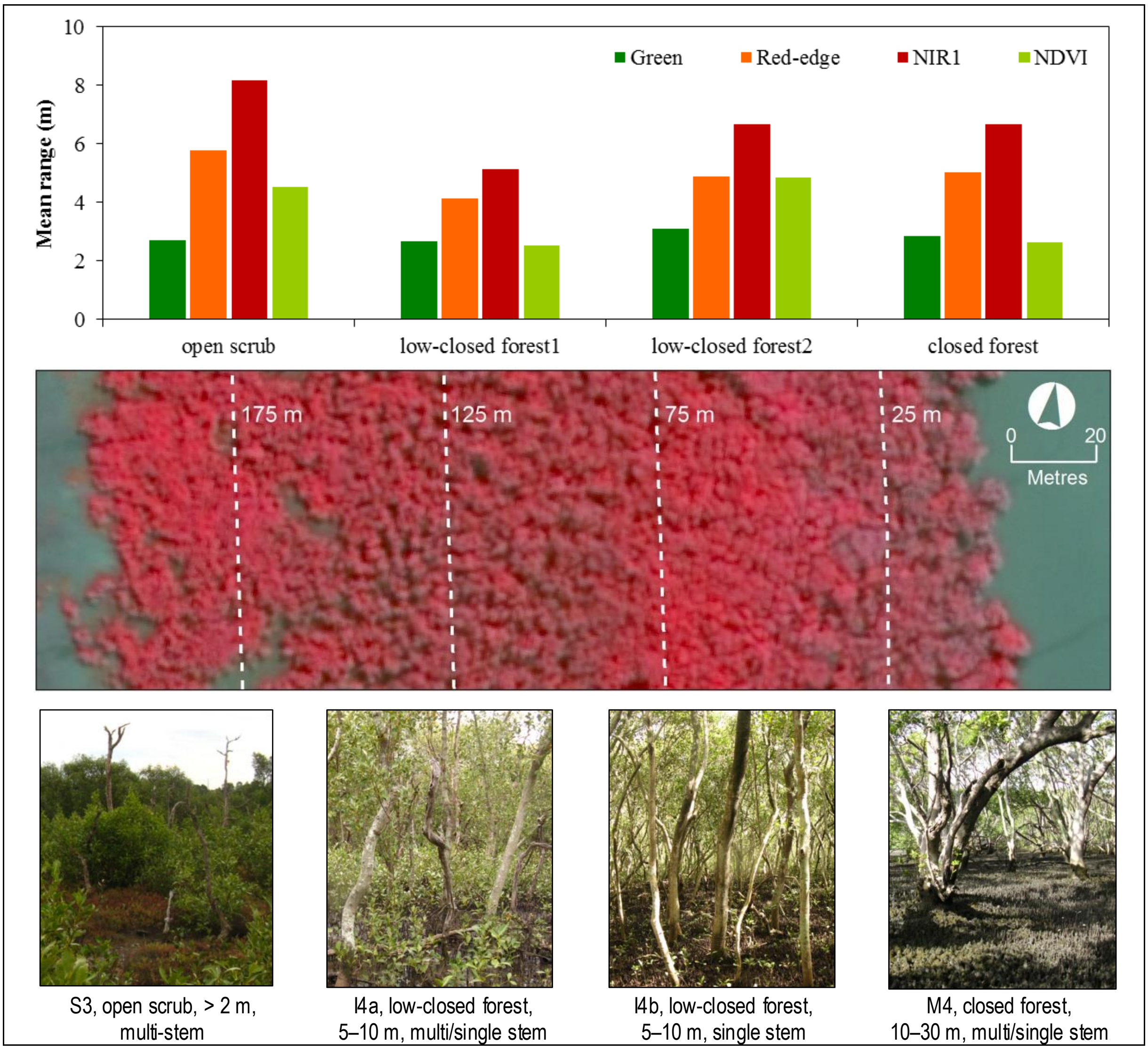

Figure 3.7. Mean semi-variogram range values sampled at 0.5 m pixel size for the green, red-edge, NIR1 and NDVI bands, based on four transects located at 175 m (S3), 125 m (I4a), 75 m (I4b) and 25 m (M4) from the coastline of Moreton Bay mangroves.

3.3.3. Optimum Pixel Size for Mangrove Mapping

Several transects were established along the mangrove zonation at the Moreton Bay sites to create semi-variograms to depict the variation of spatial size of the structural features of mangroves. The information on the characteristics of the spatial structure of mangrove features obtained from semi-variogram interpretation and analysis provides the basis for establishing the relationship between mangrove feature sizes and optimum spatial resolution (i.e., image pixel size) to map these features. According to techniques used in the previous semi-variogram analyses, seven mangrove vegetation structures were apparent in the study area and detectable from the WV-2 image data. These included single shrub crowns, small foliage clumping within the canopy or intra-canopy, smaller canopy gaps, average single tree crowns, double tree crowns or larger gaps, vegetation structural formations/communities and vegetation cover types. By integrating semi-variogram interpretation results at specific pixel sizes along mangrove zonations, with field data and image interpretation, it was apparent that each of these mangrove features resided within a certain range distances and could be detected only at specific image pixel sizes.

Figure 3.8 illustrates the relationships between the range of mangrove features, the optimum pixel size and the most appropriate spectral bands able to identify and map these features. The mangrove structural features were plotted on the y axis from the largest scale at the bottom, to the smallest scale at the top of the axis. Seven plot boxes inside the graph depict where the mangrove features on the y axis reside along the feature range distance (bottom x axis); and the downward bar charts from the x axis at the top illustrate the influence of the associated pixel size on the plot boxes of mangrove features. The most appropriate spectral bands were placed as dot point indicators beside the associated mangrove feature. For example, the average single tree crown has semi-variogram range values between 4 m and 8 m. This feature can be identified using image pixel sizes of 0.5 m, 1 m and 2 m but is unable to be identified at a pixel size of 4 m or larger. Therefore, in this case, an image with a pixel size of 2 m is the optimum option to map the average mangrove tree crown as it is the largest pixel size able to identify individual tree crowns and green, red-edge and NDVI bands will be the most suitable for discriminating this feature. For routine mapping purposes, using image datasets with a smaller pixel size might increase the cost, both for resources and processing and may produce the result that is similar to a product derived from the optimum pixel size.

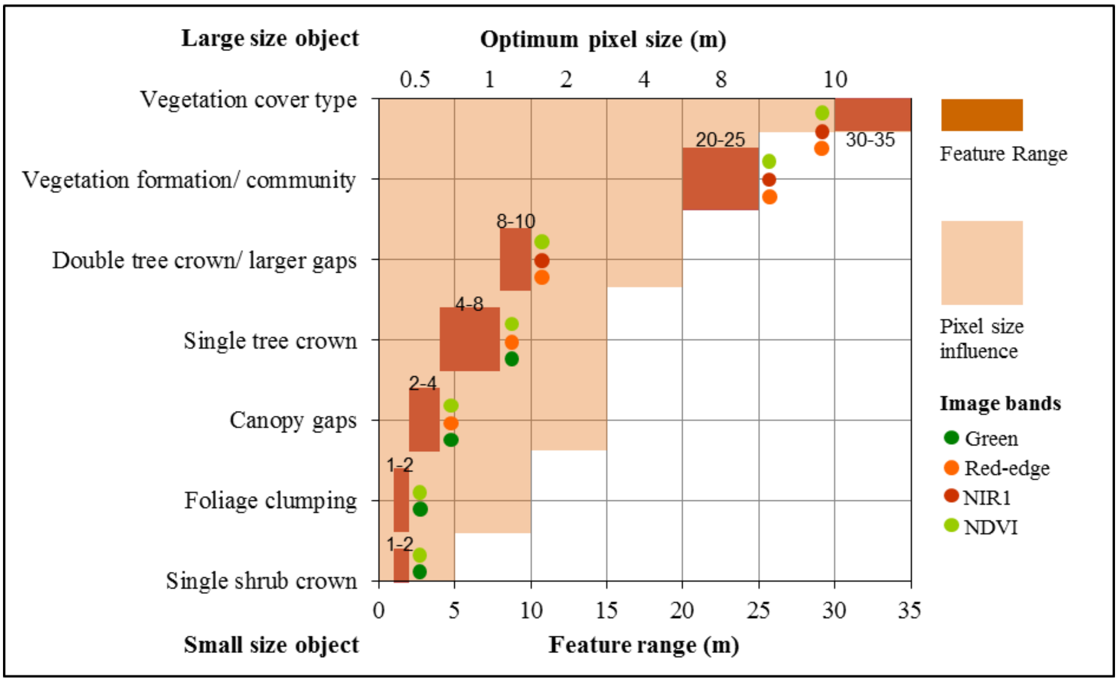

Figure 3.8. Relationship between mangrove features, feature ranges, optimum pixel sizes and the most sensitive image bands to map mangrove features.

3.3.4. Application of the Optimum Pixel Size Scheme

The pattern of mangrove feature information obtained from different scale parameters applied to different image pixel sizes was interpreted from the image segmentation results (Figure 3.9). In accordance to the results of the semi-variogram analysis; the lower value of the scale parameter or the smaller pixel size, the more mangrove information could be extracted from the image. According to the interpretation results, single shrub crowns could be recognised only at a pixel size of 0.5 m with the segmentation scale parameter ≤ 30, and at a pixel size of 1 m with the scale parameter ≤ 10. At a pixel size of 2 m, the smallest obtainable mangrove objects were canopy gaps and single tree crowns with a segmentation scale parameter ≤ 10 and 20–30, respectively. At a scale parameter ≥ 40 the segment size was too large and failed to identify single tree crowns. Most of the pixel sizes ≥ 2 m could only differentiate objects larger than the average size of single tree crowns, including double/multiple tree crowns, larger gaps, vegetation formation and community and vegetation cover types; with the exception of scale parameters ≤ 10 at a pixel size 4 m, which still allowed discrimination of single tree crowns. In general, there was an obvious relationship between mangrove information detail and the pixel and segmentation scale parameter size, where smaller pixel sizes or segmentation scale parameters will allow more detailed mapping of mangrove features.

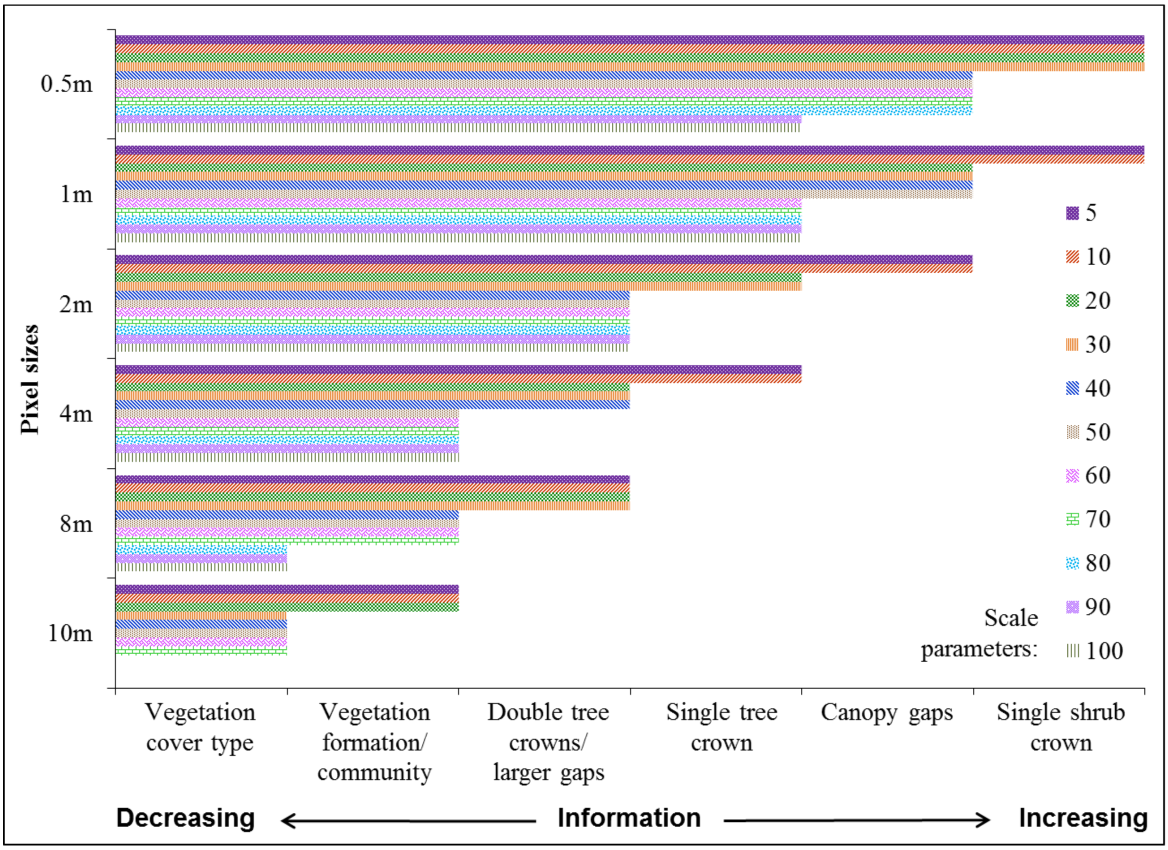

Figure 3.9. Graph of mangrove features detectable at a number of scale parameters derived from different WV-2 image pixel sizes.

The size of dominant objects able to be delineated in the segmentation process from six different pixel sizes was identified and the result related with the measured feature dimension in the field. The dominant segment sizes and the corresponding pixel sizes were found to correspond well to the result of the optimum pixel sizes from the semi-variogram analysis (Columns c and f in Table 3.3). The result indicated that the theoretical finding of the optimum pixel sizes from the SV was empirically proven on the image dataset through image segmentation.

Table 3.3. Optimum pixel sizes interpreted from semi-variogram and image segmentation results.

Mangrove Features	Average Features Size (m) in the Field	Optimum Image Pixel Size (m) from SV	GEOBIA Segmentation		
			Dominant Object Size (m^2)	Estimated Feature Dimension (m)	Optimum Image Pixel Size (m) from GEOBIA
(a)	(b)	(c)	(d)	(e)	(f)
Single shrub crown	1–2	0.5	1.5	1.2	0.5
Canopy gaps	2	1	4	2	1
Single tree crown	4	2	16	4	2
Double tree crowns/ larger gaps	8	4	48	6.9	4
Vegetation formation/ community	20–25	8	128	11.3	8
Vegetation cover type	30–40	10	700	26.4	10

The classification results showed that the use of each image pixel size enabled the discrimination of the smallest mangrove object according to the previously developed optimum pixel size scheme (Figure 3.8). Figure 3.10 shows some selected examples of the classification results applied to the image at pixel sizes of 0.5 m, 2 m and 8 m to depict information of shrub crown, single tree crown, and mangrove formation, respectively. A very-high-spatial resolution aerial photograph was used as a reference to assess and evaluate the quality of mangrove feature mapping. This was used as there was no existing map containing mangrove vegetation features for the study area and the aerial photograph interpretation was accepted to be correct (due to the features evident at very high resolution) without any form of accuracy assessment (Congalton 1991).

At a pixel size of 0.5 m individual shrub crowns were discriminated from other features but the classification was unable to identify each single shrub crown in groups of shrub (Figure 3.9a) due to the short distance between the crowns and the shape similarity. Single stands of tree crowns could be identified at a pixel size of 2 m, although the segments were blocky due to the bigger pixel size (Figure 3.10b). Individual trees in the mangrove forest were difficult to distinguish because of their closed canopy and similarity to neighbouring objects (i.e. tree crowns). Four mangrove formations found in the study area were clearly separated at a pixel size of 8 m (Figure 3.10c), with some isolated segments found within the formation. According to the qualitative segmentation assessment, the optimum pixel size scheme worked well when applied to the image datasets used in this study. As the segmentation and classification example was used purely as a proof of concept, further improvements to the segmentation and classification process are still possible to improve the mapping accuracy and repeatability across other areas.

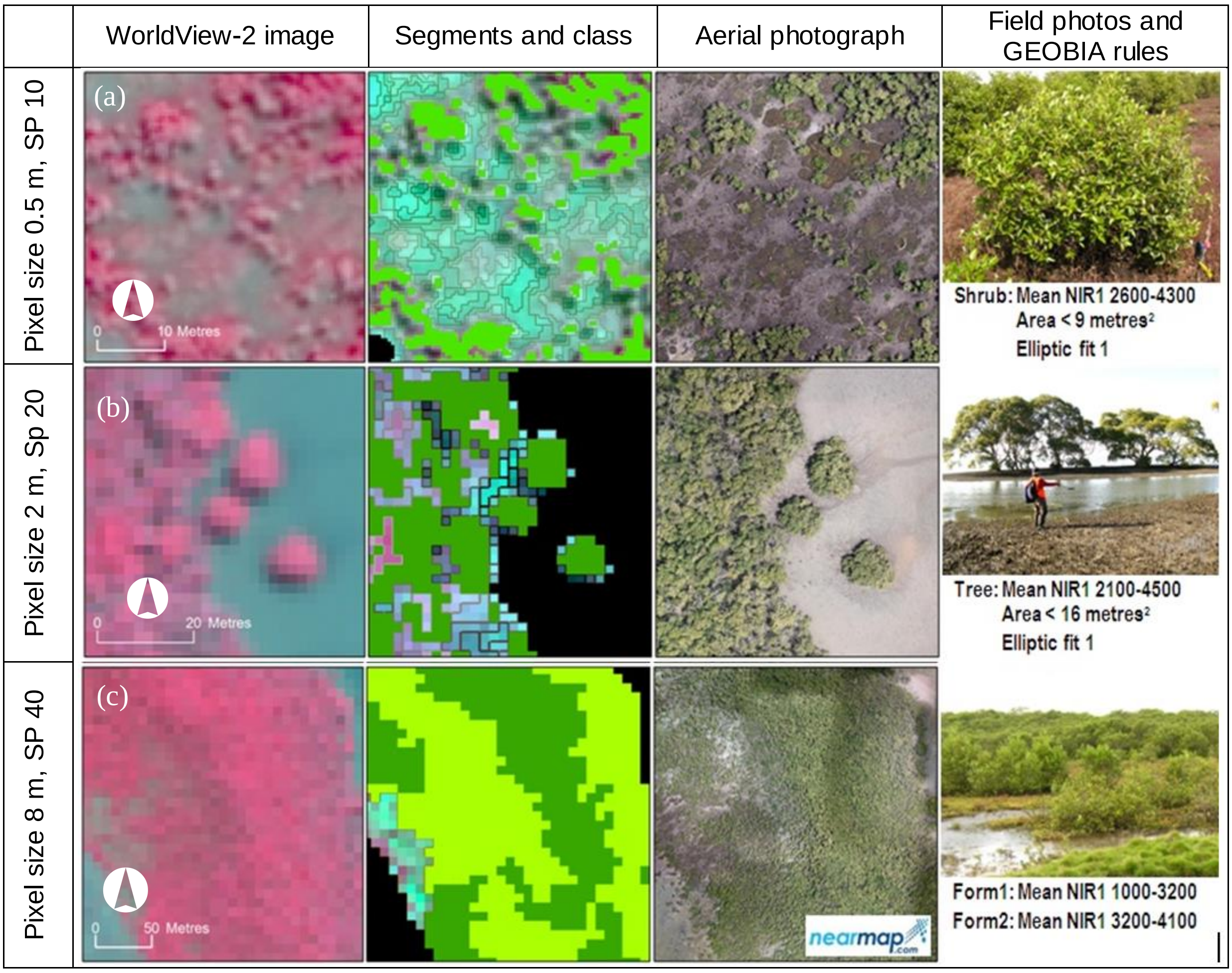

Figure 3.10. Example of mangrove features segmented and classified (green polygons) from images with different image pixel sizes and scale parameters (SP).

3.4. Conclusions and Future Research

This study showed that scale-specific, ecologically relevant information on mangroves could be detected using experimental semi-variogram analysis. This approach indicated the size of dominant mangrove features able to be identified from a specific pixel size and the optimum spectral bands to use to detect and map these features. The results show that there was a gradual loss in mangrove vegetation structural information, as indicated by the mangrove features measured, with increasing pixel size. When applied to the original and resampled WV-2 images, a pixel size ≤ 2 m was suitable for mapping canopy and inter-canopy-related features within mangrove objects (such as shrub crowns, canopy gaps and single tree crowns). A pixel size of ≥ 4 m was more appropriate for mapping mangrove vegetation formation, communities and larger mangrove features. The green and red-edge bands were optimum for discriminating smaller sized mangrove features (< 8 m), such as single shrub crowns or foliage clumping, canopy gaps and single tree crowns. The near infrared1 band was more suitable for identifying features ≥ 8 m (e.g. double tree crowns or larger gaps) and the NDVI image was suitable for mapping all targeted features.

The findings of this study provide a basis for an inversion approach to mangrove feature mapping using high-spatial resolution image datasets. The mapping application results demonstrated that the optimum pixel size scheme from the semi-variogram analysis was effectively applied through image segmentation and classification using object-based image analysis. The optimum pixel analysis result from the image segmentation interpretation was highly correlated with the semi-variogram results and the classification result identified the smallest features that could be discriminated at the corresponding pixel size.

The results of this work were limited to the study site in Moreton Bay, Australia, with sub-tropical mangroves. For future research, the application of the experimental semi-variogram method to other mangrove environments is necessary to assess the consistency of the method. Other emerging method such as wavelet transform method (WTM) and fractal method (FM) need also be explored to detect the domain of scale of objects in mangrove environments. In terms of the mapping application, further development of object-based classification rule sets is essential for improving the detection of multi-scale mangrove features and determining the transferability and general applicability of the findings.

CHAPTER 4:

OBJECT-BASED APPROACH FOR MULTI-SCALE MANGROVE COMPOSITION MAPPING USING MULTI-RESOLUTION IMAGE DATASETS

This chapter applies the optimum pixel resolution scheme for mapping mangrove features as defined in Chapter 3, by developing and evaluating an object-based approach to map mangrove features at appropriate scales from multi-resolution images (TM, AVNIR-2, WV-2 and LiDAR data) in Moreton Bay (Australia) and Karimunjawa Island (Indonesia). Five levels of mangrove features were mapped including vegetation boundary, mangrove stands, mangrove zonation, individual tree crowns and species community. The results demonstrate the effectiveness of a conceptual hierarchical model in mapping specific mangrove features at discrete spatial scales. The findings of this chapter provide a conceptual guidance of multi-scale mangrove mapping and technical demonstration to produce scale-specific mangrove information.

Associated Publications:

Kamal, M, Phinn, S & Johansen, K (2015) ‘Object-based approach for multi-scale mangrove composition mapping using multi-resolution image datasets’, *Remote Sensing - special issue on “Remote Sensing of Mangroves: Observation and Monitoring”*, vol. 7, pp. 4753-4783. [DOI: 10.3390/rs70404753].

Key Findings:

- *Conceptual spatial and temporal hierarchical organisation of mangroves provides an essential aid for effective multi-scale mangrove composition mapping.*
- *The use of GEOBIA through the mangrove image objects hierarchy enables the production of mangrove composition maps at discrete spatial scales, with an acceptable level of accuracy.*
- *The spatial variation of mangrove vegetation determines the level of information that can be mapped using remote sensing images.*
- *Image spatial and spectral resolutions dictate the level of information detail able to be obtained from the image dataset.*
- *Combining the image spectral reflectance value with contextual information significantly increases the accuracy of the mapping.*
- *The development and application of the GEOBIA rule-set is sensor, site, and time dependent.*
- *Mapping smaller objects requires a more complex rule-set and results in more within-class variability.*
- *The accuracy of the produced maps is a result of the interaction between the image spatial resolution, the scale of the targeted objects and the number of classes on the map.*

4.1. Introduction

Spatial information on the distribution, composition and condition of mangroves at appropriate spatial scales is essential to support the understanding and management of mangrove ecosystems and their biodiversity. Remote sensing with the correct selection of sensors and image processing methods provides an efficient, rapid, accurate and often cost-effective source of mangrove information (Green et al. 1998b; Green et al. 1998a; Giri et al. 2007). In mangrove mapping, remote sensing approaches have some advantages compared with the conventional terrestrial surveys. These include provision of indirect access to remote or inaccessible mangrove sites (Davis & Jensen 1998), the ability to extrapolate measurements from specific sampling points to larger areas (Hardisky et al. 1986), provision of synoptic and repeated coverage of sites (Giri et al. 2007) and the ability to deliver data at multiple spatial scales or levels of ecological detail (Malthus & Mumby 2003). In the last two decades, remote sensing has been exploited to map various types of mangrove information from global mangrove status (Giri et al. 2011) and regional mangrove extent and dynamics (Giri et al. 2007; Bhattarai & Giri 2011), to local mangrove species composition (Wang et al. 2004a; Kamal & Phinn 2011; Koedsin & Vaiphasa 2013; Heenkenda et al. 2014) and biophysical applications (reviews in Heumann (2011b) and Kuenzer (2011)). Most mangrove studies using remote sensing techniques produced single scale-specific information, depending on the spatial resolution of the dataset(s) used. Remote sensing studies using a diversity of information within mangrove forests are still uncommon (Held et al. 2003). In this study, a multi-scale mapping approach was presented to produce mangrove maps at multiple spatial scales by integrating existing knowledge on the spatial hierarchical structure of mangrove ecosystems, field data, multi-spatial resolution images and GEOBIA techniques.

Providing multi-scale information about mangroves, where each scale corresponds to an ecological organisation of structure or process, is necessary to properly address issues related to management and conservation at relevant scales in this environment and it remains the major challenge in remote sensing for all environments (Krause et al. 2004). The production of meaningful multi-scale mangrove information from remote sensing data requires an understanding of the organisation of mangrove composition, structure and processes in different spatial scales. From an ecological perspective, environmental inferences are scale-dependent (Wiens 1989) and conclusions reached at one scale of analysis may not be easily applied to other scales (Marceau & Hay 1999; Schaeffer-Novelli et al. 2005). In theory, mangrove ecosystems are perceived as having spatial and temporal hierarchical organisations; from the landscape setting down to individual tree and leaf structures, which change at timescales from centuries to hours (Duke et al. 1998; Farnsworth 1998; Twilley et al. 1999). This hierarchical approach has been used to understand mangrove ecosystems for more than three decades (Feller et al. 2010). The central concept of this theory focuses on the differences in structure and process rates between levels. Based on these differences, mangrove ecosystems are viewed as being stratified into discrete levels of interacting subsystems, with attributes occurring at specific spatial and temporal scales.

Remote sensing data and correct application of image processing techniques can provide data at multiple spatial scales or levels based on single or multiple images (Blaschke 2002; Burnett & Blaschke 2003; Blaschke et al. 2014). In this case, the spatial resolution of the imaging sensor and scale(s) of features in the environment imaged dictates the level of detailed information that can be produced (Woodcock & Strahler 1987; Woodcock & Harward 1992; Marceau & Hay 1999). Remote sensing can provide information on mangroves at multiple scale levels depending on the user's need. By synthesising the knowledge of the hierarchical structures of mangroves (Farnsworth 1998; Twilley et al. 1999; Berger et al. 2008; Feller et al. 2010) with the empirical study of the optimum pixel size to extract mangrove features from remotely-sensed images (Kamal et al. 2014), explicit relationships between spatial and temporal scales of mangrove features and the corresponding image spatial resolution at which to map these features, can be established (Figure 4.1). This relationship guides the image analysts or interpreters to select the optimal image spatial resolution in order to accurately map a specific mangrove feature.

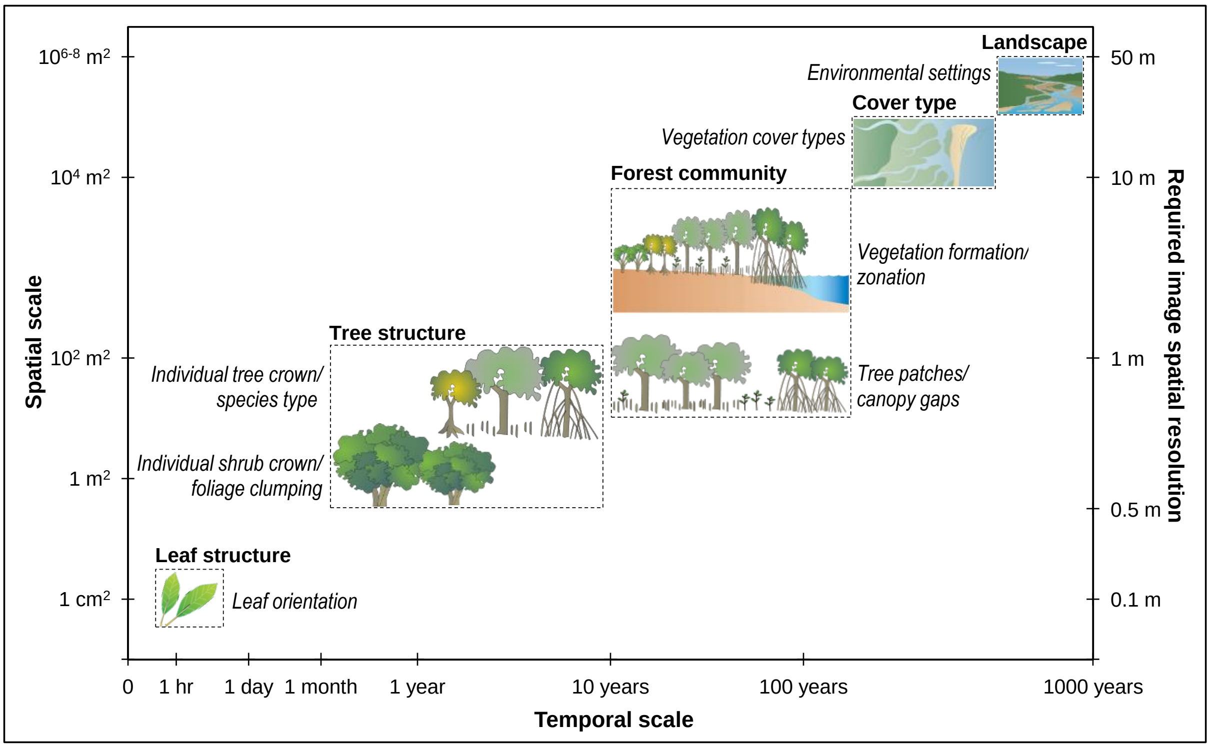

Figure 4.1. Conceptual temporal and spatial hierarchical organisation of mangrove features identifiable from remotely-sensed images and the required image pixel resolution for mapping the features. (*Symbols are courtesy of the Integration and Application Network, University of Maryland Center for Environmental Science - ian.umces.edu/symbols/*).

A GEOBIA approach facilitates multi-scale object recognition from a single image or across several images (Blaschke 2002; Blaschke et al. 2014). It enables an image to be segmented into a hierarchical network of image objects that addresses the limitation of specific pixel-level information in the pixel-based mapping approach (Blaschke & Strobl 2001). In GEOBIA the image data can be divided into homogenous image objects at a number of discrete spatial scales which are organised in an interrelated hierarchy, where larger objects consist of several smaller objects (Müller 1997; Burnett & Blaschke 2003). These image objects can represent meaningful multi-scale features of different sizes, shapes and spatial distribution within an image scene such as individual trees, tree patches and forest (Castilla & Hay 2008) (Figure 4.1). Image classification based on image objects provides more relevant information than per-pixel classification, as it provides a more appropriate scale to map environmental features at multiple spatial scales (Gamanya et al. 2007).

Numerous studies in GEOBIA have reported that the application of the multi-scale hierarchical concept in the mapping process provides more accurate and useful information (Hay et al. 2005; Blaschke 2010). However, one of the main issues in GEOBIA is the selection of an appropriate spatial scale for image segmentation to ensure the image object classes are mapped consistently at one scale (i.e. individual trees), and do not overlap, but fit hierarchically with classes that apply to other scales (e.g. tree patches). In this case, high-spatial resolution imagery (< 5 m) is generally suitable for multi-scale object-based segmentation and classification (Johansen et al. 2009; Blaschke 2010). This paper developed and evaluated the GEOBIA approach for mapping mangrove composition at multiple scales using multi-spatial resolution image data. Three objectives were addressed in this study: (1) to map targeted mangrove features at multiple spatial-scales (vegetation boundary, mangrove stands, mangrove zonation, individual tree crowns and species community) using a GEOBIA approach applied to multiple image datasets (TM, AVNIR-2, WV-2, and LiDAR); (2) to assess the accuracy of the mapping results; and (3) to evaluate the effect of image spatial resolutions on the produced maps. In a broader context, this study demonstrates the capability of remote sensing data to provide mangrove information at multiple spatial scales to fulfil the needs of mangrove management and conservation at various spatial and ecological scales.

4.2. Data and Methods

4.2.1. Study Area

The study sites for this chapter were in two mangroves areas; the mouth of the Brisbane River, northern Moreton Bay, South East Queensland, Australia and Karimunjawa National Park, Central Java, Indonesia. For detailed descriptions of these locations refer to section 2.1 of the thesis.

4.2.2. Image Datasets

This study used TM, AVNIR-2 and WV-2 multispectral images of the mouth of the Brisbane River and Karimunjawa Island to cover the variation of image spatial resolutions investigated, with the addition of LiDAR data and aerial photos for the Moreton Bay sites (Table 4.1). The image pre-processing details are presented in section 2.2 of the thesis.

Table 4.1. Image datasets used in Chapter 4.

Image type	Moreton Bay image acquisition date	Karimunjawa Island image acquisition date	Pixel size	Spectral attributes (nm)	Geometric attributes
Landsat TM	14 April 2011	31 July 2009	30 m	Blue (452-518), green (528-609), red (626-693), NIR (776-904), MIR1 (1567-1784), MIR2 (2097-2349)	Level 1T
ALOS AVNIR-2	10 April 2011	19 Feb 2009	10 m	Blue (420-500), green (520-600), red (610-690), NIR (760-890)	Level 1B2G
WorldView-2	14 April 2011	24 May 2012	2 m (multi), 0.5 m (pan)	Coastal blue (400-450), blue (450-510), green (510-580), yellow (585-625), red (630-690), red edge (705-745), NIR1 (770-895), NIR2 (860-1040), panchromatic (450-800)	Level 3X
LiDAR	April 2009	-	2.8 pts/m^2	-	Geo-referenced
Aerial photo	14 January 2011	-	7.5 cm	RGB image	Geo-referenced

The Gram-Schmidt spectral sharpening image fusion technique (Laben & Brower 2000) was applied to produce a pan-sharpened WV-2 image with a 0.5 m pixel size. This pan-sharpening technique was selected because it preserved the original spectral information of the image, and could be simultaneously applied to multispectral bands. A Canopy Height Model (CHM), Digital Terrain Model (DTM), and fractional canopy cover (FCC) were derived from the LiDAR data using lasheight, lasgrid and lascanopy modules from LAStools (rapidlasso Gmbh., Germany). The CHM and DTM were used in combination with the multispectral images to define the boundary of mangroves and produce a mangrove structural composition map for the Moreton Bay site. Finally, a very high-spatial resolution aerial photograph (7.5 cm pixel size) with true colour layers (www.nearmap.com) of Moreton Bay was used as a reference to analyse the classification accuracy of the produced maps.

4.2.3. Field Datasets

Fieldwork was conducted during April 2012 (for Moreton Bay sites) and July 2012 (for Karimunjawa Island) to collect information on vegetation structure and composition in the study areas. There were 21 (200–300 m long) field transects established perpendicular to the shoreline to record the variation of mangrove vegetation structure and species composition at different zones (Figure 2.3 of the thesis). These field transects were purposively selected to represent the variation of local mangrove zonation and at an accessible location. A detailed fieldwork description is presented in section 2.3 of the thesis.

Four distinct mangrove zonations were identified from the high-spatial resolution images for both study sites and verified by field visits (Table 4.2). For Moreton Bay mangroves, *Avicennia marina* is the dominant mangrove species throughout each zonation but different mangrove structural formations occur within each zone. From the shoreline towards land, these zones represent mature closed forest, low-closed forest with single stems (some individual *Rhizophora stylosa* or *Ceriops tagal* were found in this zone), low-closed forest with single/multi stems and open scrub. At the Karimunjawa Islands site, the dominant mangrove structural formation is closed forest, with a greater variety of mangrove species throughout the zonations. Tall trees of *Rhizophora apiculata* dominate the fringing shoreline area, followed by zones of highly-mixed *Bruguiera gymnorhiza, Bruguiera cylindrical, Xylocarpus granatum* and *Excoecaria agallocha.* The third and fourth zonations were mixes of *Ceriops tagal* and *Lumnitzera racemosa* with different vegetation structural formations.

Table 4.2. Mangrove canopy height, formation type, canopy cover and dominant species derived from field data sampled across the vegetation zones at four study sites.

Mangrove zones*	Whyte Island	Fisherman Island	Boondall Wetlands	Karimunjawa Islands
Zone 1	10-12 m, closed forest (M4) with single or multi-stems, high density canopy cover, *Avicennia marina* trees.	8-11 m, closed forest (M4) with single or multi-stems, high density canopy cover, *Avicennia marina* trees.	8-10.5 m, closed forest (M4) with single or multi-stems, very high density canopy cover, *Avicennia marina* trees with some patches of *Ceriops tagal.*	11-15 m, closed forest (M4) with single or multi-stems, very high density canopy cover, *Rhizophora apiculata* trees with some individual *Bruguiera gymnorhiza.*
Zone 2	6-8 m, low-closed forest (I4) with single stem, very high density canopy cover, *Avicennia marina* trees with some individual *Rhizophora stylosa.*	8–10 m, low-closed forest (I4) with single stem, high density canopy cover, *Avicennia marina* with some individual *Rhizophora stylosa* and patches of *Ceriops tagal*.	7–9 m, low-closed forest (I4) with single stem, very high density canopy cover, *Avicennia marina* with some individual *Rhizophora stylosa.*	10-13 m, closed forest (M4) with single stems, very high density canopy cover, *Bruguiera gymnorhiza, Bruguiera cylindrical, Xylocarpus granatum* and *Excoecaria agallocha.*
Zone 3	4–7 m, low-closed forest (I4) with single or multi stems, medium density canopy cover, *Avicennia marina.*	4–9 m, low-closed forest (I4) with single stem, high density canopy cover, *Avicennia marina.*	5–7.5 m, low-closed forest (I4) with single stem, very high density canopy cover, *Avicennia marina.*	7-10 m, low-closed forest (I4) with single or multi stems, high density canopy cover, *Ceriops tagal* and *Lumnitzera racemosa*.

Table 4.2. *Continued.*

Mangrove zones*	Whyte Island	Fisherman Island	Boondall Wetlands	Karimunjawa Islands
Zone 4	1–3 m, open scrub (S3) with multi stems, low density canopy cover, *Avicennia marina.*	2.5–4 m, open scrub (S3) with single or multi stems, low density canopy cover, *Avicennia marina.*	1.5–5 m, open scrub (S3) with single or multi stems, medium density canopy cover, *Avicennia marina.*	4-9 m, low multi-stem forest (VL4) with multi-stems, medium density canopy cover, *Ceriops tagal* and *Lumnitzera racemosa*.

*Zone 1, 2, 3, and 4 for Moreton Bay sites are centered at about 25, 75, 125, and 175 m respectively from Coastline; and 25, 150, 250, and 350 m for the Karimunjawa site.

4.2.4. Mangrove Vegetation Structure Characterization

Prior to the mapping process, it is essential to perform an exploratory analysis to understand the spatial variability of the vegetation structure at different targeted locations and environment settings. This approach identifies the expected levels of detail able to be obtained from each site. Semi-variograms were used to analyse the spatial structure of mangroves at the Moreton Bay and Karimunjawa Island sites. Semi-variograms are used for measuring the degree of dissimilarity between observations as a function of distance (Woodcock et al. 1988a). A review of its application in remote sensing was provided by Curran and Atkinson (1998). As demonstrated by Cohen (1990), Johansen and Phinn (2006) and Kamal et al. (2014), the semi-variogram can be used to explore and describe the spatial variation of objects of interest in the image data in various forest environments. The equation for semi-variance $\gamma(h)$ is:

$$\gamma(h) = \frac{1}{2n}\sum\{DN(x) - DN(x+h)\}^2 \qquad \text{(Eq. 4.1)}$$

where $\gamma(h)$ represents half of the mathematical expectation of the squared differences of pixel pair values at a distance h. For image spectral data, $\gamma(h)$ estimates the variability of pixels digital number (DN), as a function of spatial separation. The semi-variograms in this chapter were derived from 21-line transects positioned across the mangrove zonations on the WV-2 image, coinciding with the field transects. All of WV-2 pan-sharpened bands were used to produce semi-variograms but only the green band was presented because it depicted the highest level of detail of mangrove vegetation information compared with the other bands (Kamal et al. 2014).

4.2.5. Overview of the GEOBIA Approach

The GEOBIA mapping process started with developing a conceptual hierarchical structure of mangrove objects based on published literatures on mangrove spatial structure and the analysis described in section 4.2.4, field work data and local knowledge (Figure 4.2). It shows the organisation of mangrove features at various spatial scales and represents the objects of interest to be mapped. Inclusion of specific scales of mapped features is one of the main advantages of GEOBIA, which does this in a multi-scale hierarchical network of image objects derived through image segmentation (Hay et al. 2003; de Jong & van der Meer 2005). Based on the conceptual hierarchy, five levels of mangrove features were selected (see output section in Figure 4.2). To perform the multi-scale mangrove mapping, eCognition Developer 8.7 (Trimble 2011) was exploited to develop the rule set and for executing the object-based routine.

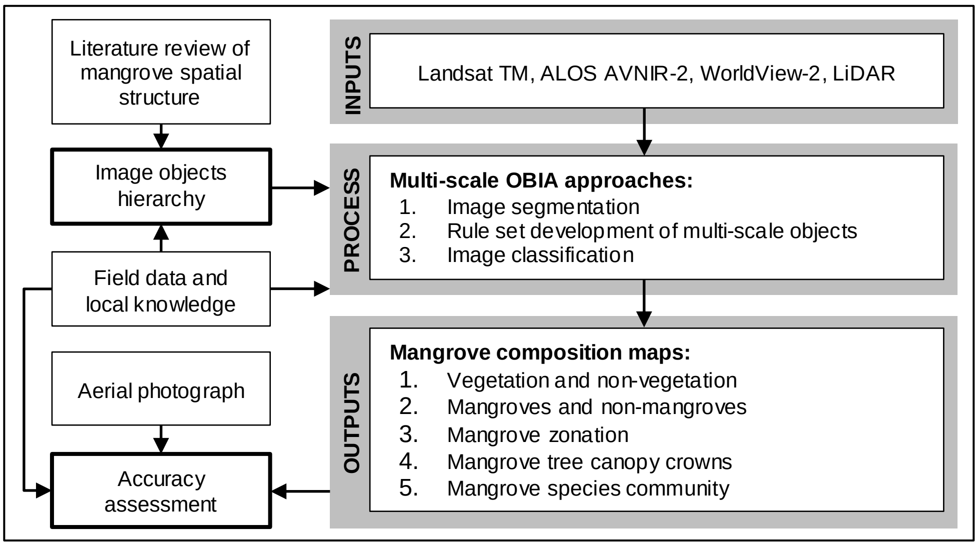

Figure 4.2. Flowchart of the mangrove composition mapping process applied in Chapter 4.

4.2.5.1. Classification Hierarchy and Rule Set Development

Developing conceptual hierarchical levels of the objects of interest is essential in multi-scale mapping using GEOBIA (Baatz & Schäpe 1999; Blaschke 2002; Burnett & Blaschke 2003). This hierarchy shows the spatial organisation of the objects in the landscape or image scene from a larger landscape unit into the smaller objects or component units. The landscape scaling ladder concept (Wu 1999; Blaschke 2002; Burnett & Blaschke 2003) was implemented to break down the complexity of targeted mangrove information into manageable units that still linked across scales (Figure 4.3). In the hierarchy, the “super-level” objects act as containers for the “sub-levels” and work within parent and child relationships; while objects at the same level have a neighbourhood relationship (Blaschke 2002; Trimble 2011). There are several advantages to having this hierarchy in place, as it provides a logical sequential mapping process, has a clear multi-scale context for the targeted objects and their relationships and provides control over the process within a certain level and object container.

From the object hierarchy it is possible to develop a strategy and procedure to identify and map the targeted objects individually, which was documented in the form of rule sets. For example, conceptually mangroves can be found within vegetation features in the image and it also serves as the container of several lower hierarchical levels such as mangrove zonations, tree crowns and canopy gaps and individual tree species. At this stage, it is also necessary to identify some potential properties commonly embedded in these features in the image, which could be spectral, textural, and/or contextual spatial information of the targeted features. The contextual spatial information or contextual information in GEOBIA refers to the relative relationship of pixel to objects on the scene (Lang 2008; Blaschke 2010), such as distance and proximity to an object, relative height or elevation, pixel location in relation to objects, etc. Together, the conceptual object hierarchy and mapping strategy provide a feasible scenario to apply in the rule set processes to address the predefined research problem. Table 4.3 shows the documented multi-scale mapping scenario, membership rules and the classification processes developed for the Moreton Bay mangrove site. This is explained in more detail in the corresponding sections. The detailed rule set for Karimunjawa Island is provided in Appendix 4, the produced maps are presented in Appendix 5 and a comparison of the results is discussed in section 4.3.5.

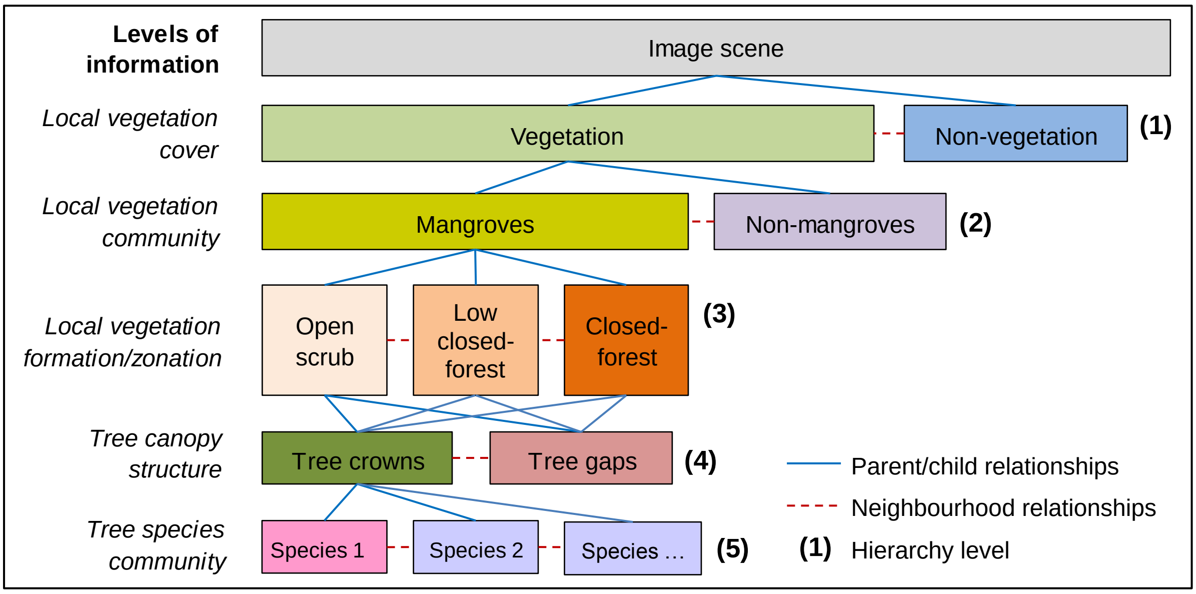

Figure 4.3. Image objects hierarchy for multi-scale mangrove mapping, objects relationships, and the levels of information at each hierarchy level.

Table 4.3. Summary of the membership rules used in the multi-scale mangrove classification rule sets for Moreton Bay mangroves. The numbers in the table correspond to section numbers in the method section of this paper.

No.	Information		Landsat TM	ALOS AVNIR-2	WorldView-2	WorldView-2 and LiDAR
2.5.2	Vegetation		Layer arithmetic Multi-threshold seg. FDI > 100	Layer arithmetic Multi-threshold seg. FDI > 200	Layer arithmetic Multi-threshold seg. FDI > 0	Layer arithmetic Multi-threshold seg. FDI > 0
	Non-vegetation		Not "Vegetation"	Not "Vegetation"	Not "Vegetation"	Not "Vegetation"
2.5.3	Mangroves		Within "Vegetation" Chessboard seg: 1 Mean *4* = 1500-3500 Mean *5* = 900-1450	Within "Vegetation" Chessboard seg: 1 Mean *3* = 300-550 Mean *4* = 1000-3000	Within "Vegetation" Chessboard seg: 1 (*7*-*5*)/(*3*-*5*) = 8-22 Mean *5* ≤ 720	Within "Vegetation" Chessboard seg: 1 (*7*-*5*)/(*3*-*5*) = 8-22 Mean *5* ≤ 720 Mean DTM ≤ 1.5
	Non-mangroves		Not "Mangroves"	Not "Mangroves"	Not "Mangroves"	Not "Mangroves"
2.5.4	Zonation bands			Within "Mangroves" Multiresolution seg. (SP:10, s:0.1, c:0.5)	Within "Mangroves" Multiresolution seg. (SP:25, s:0.1, c:0.5)	Within "Mangroves" Multiresolution seg. (SP:25, s:0.1, c:0.5)
		Zone 1	-	1.5 ≤ *4*/(*3*+*1*) ≤ 4 Coast dist ≤ 75m	0 > *7*/(*5*+*6*) ≤ 1.36 Coast dist ≤ 75m	Mean CHM > 10 FCC ≤ 1
		Zone 2	-	2.5 < *4*/(*3*+*1*) ≤ 6 25>Coast dist≤100m	*7*/(*5*+*6*) ≥ 0 25>Coast dist≤100m	7 < CHM ≤ 10 0.95 > FCC ≤ 1
		Zone 3	-	1.5 ≤ *4*/(*3*+*1*) ≤ 4 Coast dist > 100m	0 > *7*/(*5*+*6*) ≤ 1.36 Coast dist > 100m	3 < CHM ≤ 7 FCC ≤ 0.98 Coast dist > 75
		Zone 4	-	1.5 ≤ *4*/(*3*+*1*) ≤ 6 Coast dist > 100m	*7*/(*5*+*6*) > 1.36 Coast dist > 100m	CHM ≤ 3 FCC ≤ 0.98
2.5.5	Tree canopy	Canopy gaps	-	-	Within "Mangroves" Chessboard seg: 1 Within "Mangroves" Mean PC1 ≥ 500 Mean PC2 < -250	Within "Mangroves" Chessboard seg: 1 Mean CHM ≤ 3
		Tree crowns	-	-	Not "Canopy gaps" Seed based on local maxima of NIR1. Grow seed by ratio to neighbour < 1.2. Opening the seed.	Not "Canopy gaps" Seed based on local maxima of CHM. Grow seed by ratio to neighbour < 1.5. Opening the seed.
2.5.6	Individual species		-	-	Within "Tree crowns". Nearest Neighbour classification with samples taken from the individual tree crown.	

FDI: Forest Discrimination Index, NIR: near-infrared, MIR: mid-infrared, DTM: digital terrain model, CHM: canopy height model, FCC: fractional canopy cover, PC: principal component, SP: scale parameter, s: shape, c: compactness, italic numbers represent band order for the associated images, the conditional operator used on each membership rule was "and(min)".

4.2.5.2. Vegetation and Non-Vegetation Separation

The first classification level in the multi-scale mapping process generated a mask to separate vegetation and non-vegetation features (i.e. water bodies, soils and other artificial surfaces) in the image. In this study, the Forest Discrimination Index (FDI) developed by Bunting and Lucas (2006) was modified for WV-2 image to separate vegetation and non-vegetation as follow:

$$FDI = NIR1 - (Red + Green) \qquad \text{(Eq. 4.2)}$$

This equation was derived by examining the spectral reflectance pattern of targeted features from the WV-2 image bands that had the greatest spectral separation between vegetation and non-vegetation features. The near infra-red1 (NIR1) band, as expected, provided a consistently high spectral response of all types of healthy vegetation and gave the greatest spectral separation between features (Figure 4.4a). Water and artificial surfaces (building roofs and asphalt) had high spectral reflectance in the green band (band 3) and lower spectral reflectance in the red band (band 5), but greater separation from vegetation features. In this case, the sum of the green and red bands could be greater, lower or equal to the value of the near infrared1 band. Therefore, for the WV-2 image, FDI values greater than zero represent all types of vegetation features and zero or negative values represent non-vegetation features (Figure 4.4b). Different threshold values were applied to other images due to variation of object spectral reflectance responses between images (Table 4.3). Layer arithmetic and multi-threshold segmentation algorithms were used to implement this process in eCognition Developer 8.7 software.

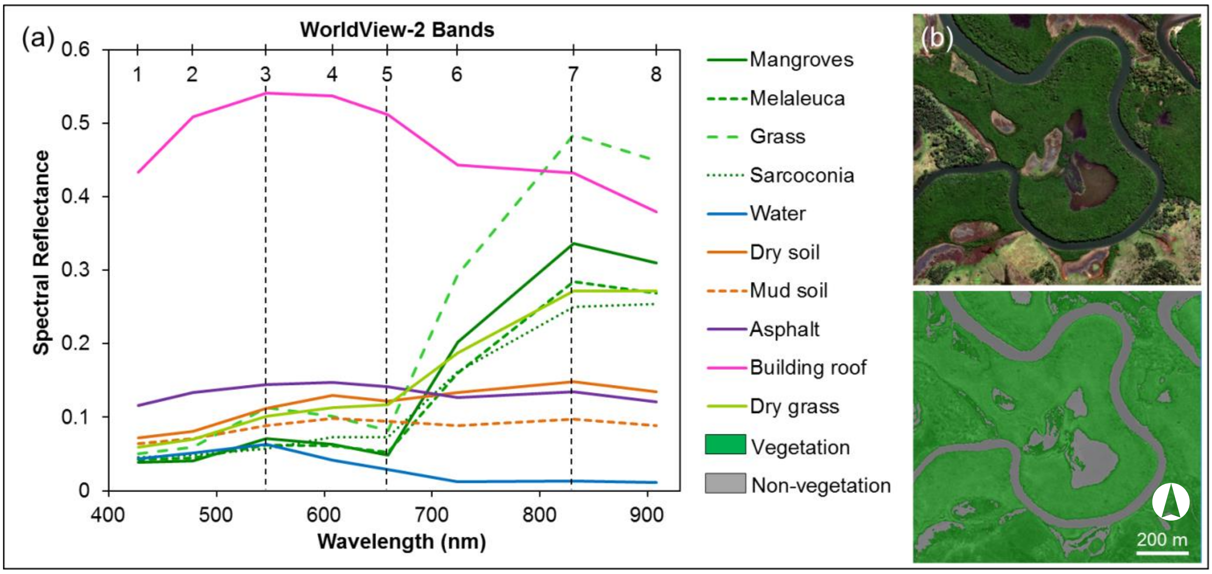

Figure 4.4. Spectral reflectance profiles extracted from WV-2 image: (a) major land cover types in Moreton Bay site, and (b) comparison of true colour WV-2 image and the FDI classification result.

4.2.5.3. Mangroves and Non-Mangroves Discrimination

Figure 4.5 summarises the sequences of mangrove composition mapping using WV-2 images in this chapter. Mangroves and non-mangroves within the vegetation class were separated by combining thresholds of image bands or band algorithms that were sensitive to mangrove features. For spectral recognition of mangroves, the near-infrared reflectance spectrum revealed different reflectance levels related to the internal leaf structure and facilitated in the discrimination of mangroves from other objects (Kuenzer et al. 2011). It is also evident from the spectral reflectance profile in Figure 4.4a that mangroves and other vegetation objects are distinguishable by their spectral profiles; specifically in the green, red and NIR bands of the WV-2 image where the spectral separation are optimal.

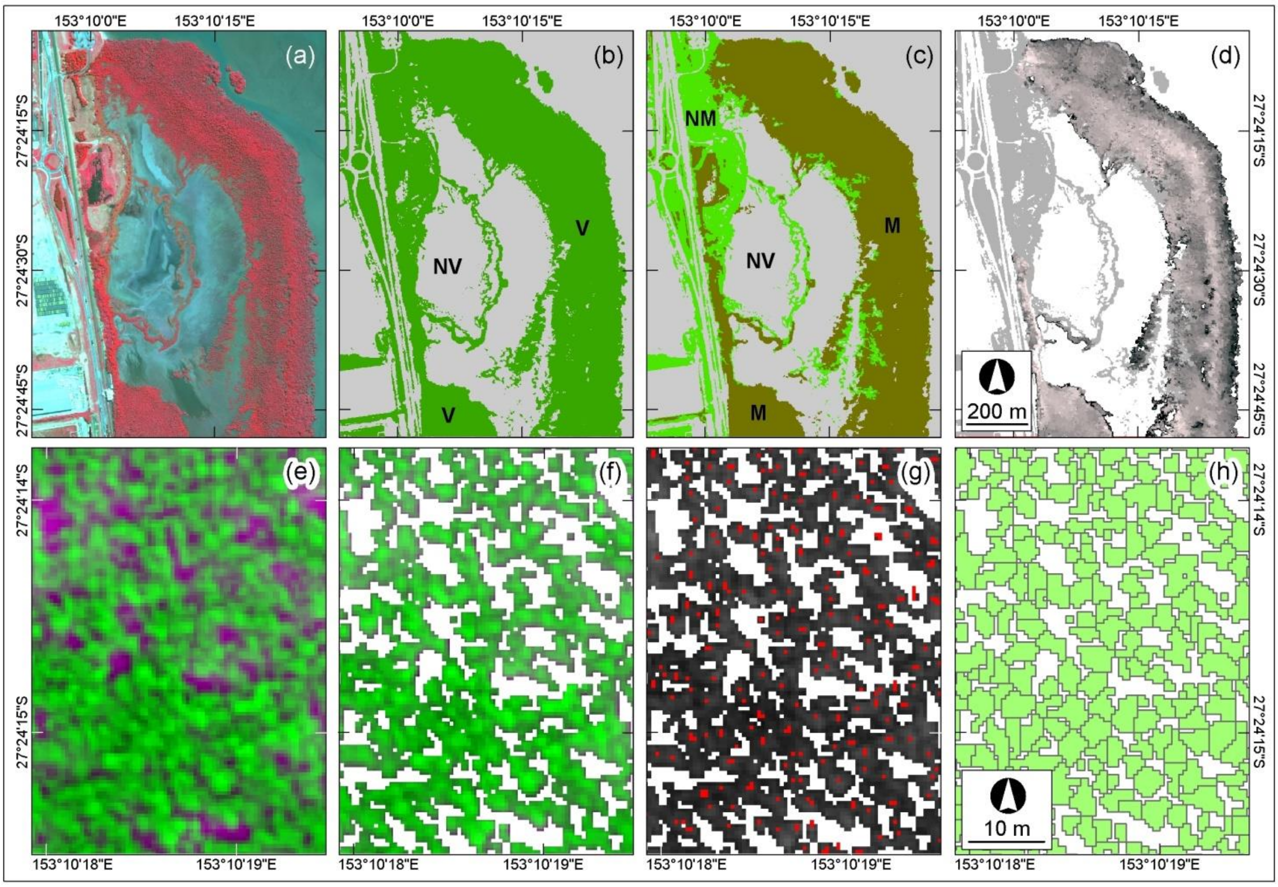

Figure 4.5. Subset of Whyte Island maps showing the mapping sequences. (a) WV-2 standard false colour composite, (b) vegetation (V) and non-vegetation (NV) discriminated using FDI, (c) spectral-based mangroves (M) and non-mangroves (NM) separation, and (d) band combination image to enhance the mangrove zonations. Tree crown delineation process showing (e) colour composite of PC1, PC2, PC1 (RGB), (f) masked canopy gaps (white), (g) tree canopy seeds (red) on top of NIR band, and (h) tree crown polygons resulting from region growing algorithm.

At the Moreton Bay site, a ratio of the spectral reflectance distance between NIR to red, and green to red ([NIR-red]/[green-red]) was found to be effective in separating mangrove from non-mangrove objects in the WV-2 imagery (Figure 4.5c). The NIR and red bands were also useful for discriminating mangrove objects in the AVNIR-2 imagery, as were the NIR and the first mid infrared (MIR1) band for the TM image (Table 4.3). To enable comparison with the spectral-based only approach, the contextual information in the form of a DTM derived from LiDAR data was also used in this process in combination with the WV-2 image. The DTM was used to set an elevation boundary above sea level for mangrove habitats commonly occurring in the lower parts of tidal flats in coastal or riverine areas, which are frequently inundated by saline water. Limiting the delineation to the typical elevation of mangrove habitats will increase the accuracy of the classification and compensate for limitations of spectral-based recognition.

4.2.5.4. Mangrove Zonation Pattern Delineation

Mangrove zonation boundaries at the study sites follow the topographic contours, which are possibly indicative of tidal inundation levels (Duke et al. 1998). From the field survey, it was established that these zonations represent a variation of canopy cover density, stem structure, dominant species and tree height (Table 4.2). Optical remote sensing data can often distinguish different mangrove zones based on the spectral reflectance of dominant mangrove species within each zone (Lucas et al. 2007). Multi-resolution segmentations were applied to the mangrove class to aggregate the zonation pattern. Using the AVNIR-2 and WV-2 images, a combination of band ratios and the distance from the coastline (Table 4.3) facilitated the differentiation of mangrove zonation boundaries (Figure 4.5d). However, due to the large pixel size and the narrow mangrove zonation bands, TM was unable to differentiate the zonation pattern. As a comparison, the CHM and fractional canopy cover (FCC) derived from LiDAR data were also incorporated to differentiate the mangrove zonations based on tree height and canopy cover density.

4.2.5.5. Mangrove Tree Canopy Crowns and Gaps Delineation

To delineate individual mangrove tree crowns and gaps the “valley following” (Gougeon 1995) and “region growing” (Culvenor 2002) approaches were modified and applied in the eCognition Developer software. The basic principle of tree crown delineation is well-described using three dimensional “radiometric topography” analogy of tree crowns (Culvenor 2002). The valleys (local minima) that have lower spectral reflectance (i.e. in the NIR or panchromatic band) represent the boundary of tree crowns, while the peaks, which have local maxima, are treated as seeds and will be grown towards the boundary of the valleys. The polygons created from this region-growing approach are the tree crowns. There are two implicit assumptions in these approaches; (1) the tree crown should be visually recognisable as a discrete object on the image (i.e. the pixel size of the image must be smaller than the average size of the tree), and (2) the tree crown is brighter (or has a higher pixel value) than the edge of the crown (Culvenor 2003). Therefore, the pan-sharpened WV-2 image with a pixel size of 50 cm was used to delineate the tree crowns.

There were three main steps to delineate mangrove tree crowns. The first step was to find tree canopy gaps between trees as the boundary of the tree crowns. It is common in mangrove forest to have irregular stands and canopies with groups of trees often clumped into a single wider canopy, making the delineation of canopy gaps through shadow (local minima) growing difficult. Therefore, PC1 and PC2 of the image, which accounted for 99.84% of the variance, were used to emphasise the difference in appearance between soil backgrounds or canopy gaps and mangrove tree canopies (Figure 4.5e, f). The second step was to find the tree top (local maxima) from the original NIR1 band and treat them as crown seeds (Figure 4.5g), and then grow it toward the canopy gaps border. A ratio of NIR1 spectral values of the adjacent pixels to the crown seed was used to grow the crown region in a looped iteration until the crown seed polygons reached the canopy gaps border. This rule set was developed to adapt the sample sites' mangrove pattern, where there were noticeable canopy gaps between tree canopies. Modifications might be needed to apply this rule set to mangrove forests with limited canopy gaps. Finally, the delineated tree crowns were refined using a pixel-based morphological opening operation to smooth the edge of the tree crown polygons (Figure 4.5h). As a comparison, the LiDAR data were used to delineate tree crowns based on the patterns of canopy height derived from the CHM.

4.2.5.6. Mangrove Tree Species Identification

Delineated tree crowns were classified into main mangrove species found at the study sites using the pan-sharpened WV-2 multi-spectral image bands using a supervised nearest neighbour (NN) classifier. The extra textural information in the pan-sharpened imagery is important to include due to the different vegetation structural characteristics of mangrove species. The boundary of the tree species communities is also more apparent with smaller pixels. An approach similar to the one developed by Gougeon and Lackie (2006), where representative sample objects of each mangrove species were collected individually from the tree crown polygons, was applied and used to generate signatures for each class. The nearest neighbour (NN) algorithm looks for the closest sample object in the feature space for each image object (Trimble 2011). A standard NN algorithm was used based on the mean value of red, green, blue, PC2 layers and the standard deviation of layer NIR1, with the selection of the object samples guided by the field species identification. However, due to the domination of *Avicennia marina* stands in Moreton Bay mangroves, it is difficult to identify the other species using this approach. Therefore, this classifier was applied to discriminate between different communities of *Avicennia marina* in Moreton Bay mangroves.

4.2.5.7. Mangrove Composition Mapping Validation

The accuracy assessment of GEOBIA requires assessment of the geometric accuracy (shape, symmetry and location) of the created image objects (Schopfer & Lang 2006), because the geometry of image objects is an inherent property resulting from image segmentation. Only limited numbers of published works describe the area-based accuracy approach developed for GEOBIA (Blaschke 2010). Among the significant results in this field were studies done by Zhan et al. (2005) and Whiteside et al. (2010) who developed a framework for assessing the quality of geometric properties of image objects based on the error matrix idea. An area-based accuracy assessment (Table 4.4) was used to measure the degree of similarity between the results of the classification and reference data from different aspects, including overall quality, user's accuracy and producer's accuracy (Zhan et al. 2005). In addition, the overall accuracy measure, which is defined as the ratio between the correctly classified area and the total area of observation, was also calculated. To perform this calculation, the reference data used in this measurement should have an area dimension matching the classified objects (Zhan et al. 2005; Whiteside et al. 2010).

Table 4.4. Area-based accuracy assessment equations (Zhan et al. 2005; Whiteside et al. 2010).

Measure	Equations	Equation number
Overall Quality (OQ)	$\frac{\lvert C \cap R \rvert}{\lvert \neg C \cap R \rvert + \lvert C \cap \neg R \rvert + \lvert C \cap R \rvert}$	4.3
User's Accuracy (UA)	$\frac{\lvert C \cap R \rvert}{\lvert C \rvert}$	4.4
Producer's Accuracy (PA)	$\frac{\lvert C \cap R \rvert}{\lvert R \rvert}$	4.5
Overall Accuracy (OA)	$\frac{\lvert C \cap R \rvert}{\lvert C \cup R \rvert}$	4.6

C is the area of the classified object and R is the area of the reference object, $C \cap R$ is the area of intersection between C and R, $\neg C \cap R$ is the area of R not covered by C, $C \cap \neg R$ is the area of C that is not covered by R, and $C \cup R$ is the area covered by both objects.

The accuracy assessments were performed for map results of levels 1 to 4 (see Figure 4.3) against the thematic maps derived from manual interpretation of a very-high-spatial resolution aerial photograph (7.5 cm pixel size) of the Moreton Bay mangroves. All of these features can be accurately discriminated and delineated from this imagery. This approach was selected due to the lack of reference information for the study sites for the accuracy assessment. The image interpretation results from the very high-spatial resolution aerial photographs were accepted to be correct without any form of accuracy assessment (Congalton 1991). However, the accuracy assessment for Karimunjawa Island was not performed due to the lack of the reference maps and very-high resolution aerial imagery. Following the approach by Whiteside et al. (2010), a circular buffer with a 50 m radius of 30 random point samples within the “class domain areas” were created to calculate the area-based accuracy assessment. The circular buffer was used for practical reasons to create the area samples, and the number of points and buffer radius were chosen with regard to the size of the objects on the map being accuracy assessed. The resulting circular polygons were used to clip both the classified image objects and visually-interpreted reference map for area comparisons (Figure 4.6). A similar approach was implemented for the accuracy assessments of levels 3, 4, and 5. However, for level 3, only 10 random points were plotted and used a buffer radius of 20 m within each zonation because of the smaller area of the object class being validated. Ten random points with a 10 m radius buffer was used for levels 4 and 5. However, at the mangrove species level, the South East Queensland mangrove composition maps (1:25.000) produced by the Queensland Herbarium (Dowling & Stephens 1998) were used as reference data. This map was produced from aerial photograph interpretation combined with extensive fieldwork, which shows the mangrove species communities and their description of the Moreton Bay area.

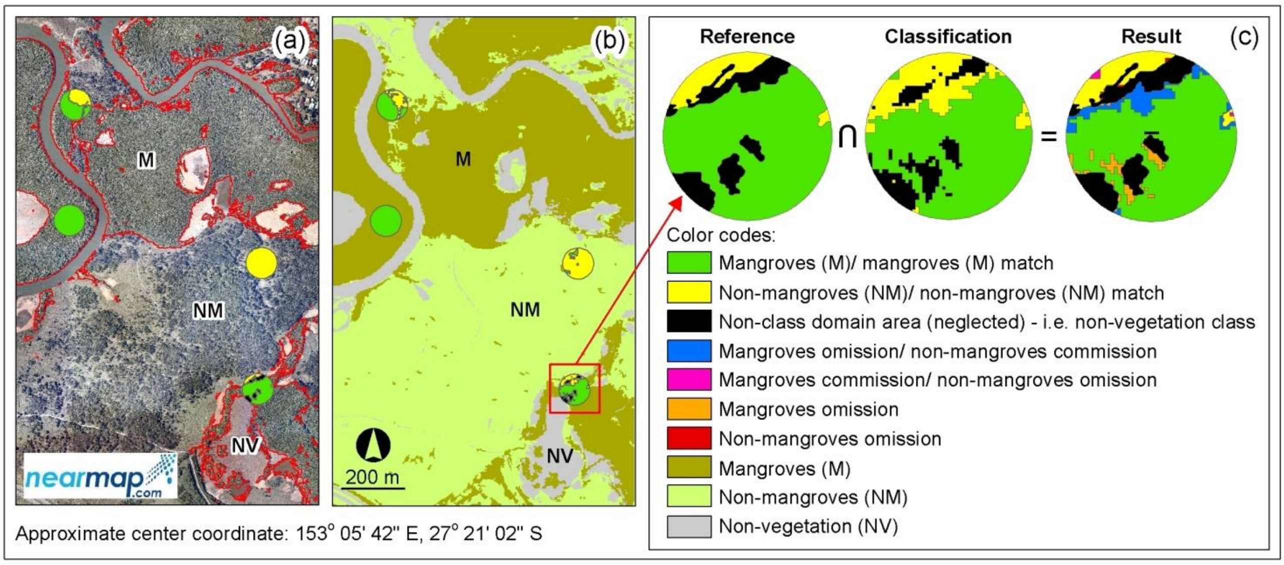

Figure 4.6. Example of mangroves and non-mangroves area-based accuracy assessment; (a) reference map, (b) classified map from WV-2 image, and (c) classes produced from the area intersection process.

4.3. Results and Discussion

4.3.1. Mangrove Spatial Structure from Semi-Variogram Analysis

The particular interest of this study was the forms of the semi-variograms, namely sill and periodicity. They are related to the density of objects and scene-scale level of variance (Woodcock et al. 1988b; Jupp et al. 1989), and provide an indication of a repetitive spatial pattern along the transect (Curran 1988; Woodcock et al. 1988b). Figure 4.7 showed that Fisherman and Whyte Island mangroves have higher sill and periodicity than the Boondall wetland and Karimunjawa Island mangroves. This pattern was attributed to the high variation in the degree of openness of the mangrove canopy and the significant canopy gaps present in the Fisherman and Whyte islands mangroves, allowing individual tree crowns to be detected. On the other hand, mangroves in the Boondall wetlands were dominated by low-closed *Avicennia marina* forest of homogeneous stems with very high-density canopy cover and the mangroves in Karimunjawa Island mainly consisted of closed-mature mangrove trees with overlapping canopy crowns (Table 4.2). It was noticeable from the image (Figure 4.7c and d) that it has a smooth texture with minimum gaps between tree stands and some clumping of tree groups, preventing detection of individual tree crowns from the image. From the semi-variogram analysis, it was hypothesised that mangroves on Fisherman and Whyte islands have higher vegetation structural variability compared with the others, providing a higher level of information for mangrove mapping (i.e. up to the tree canopy crown level).

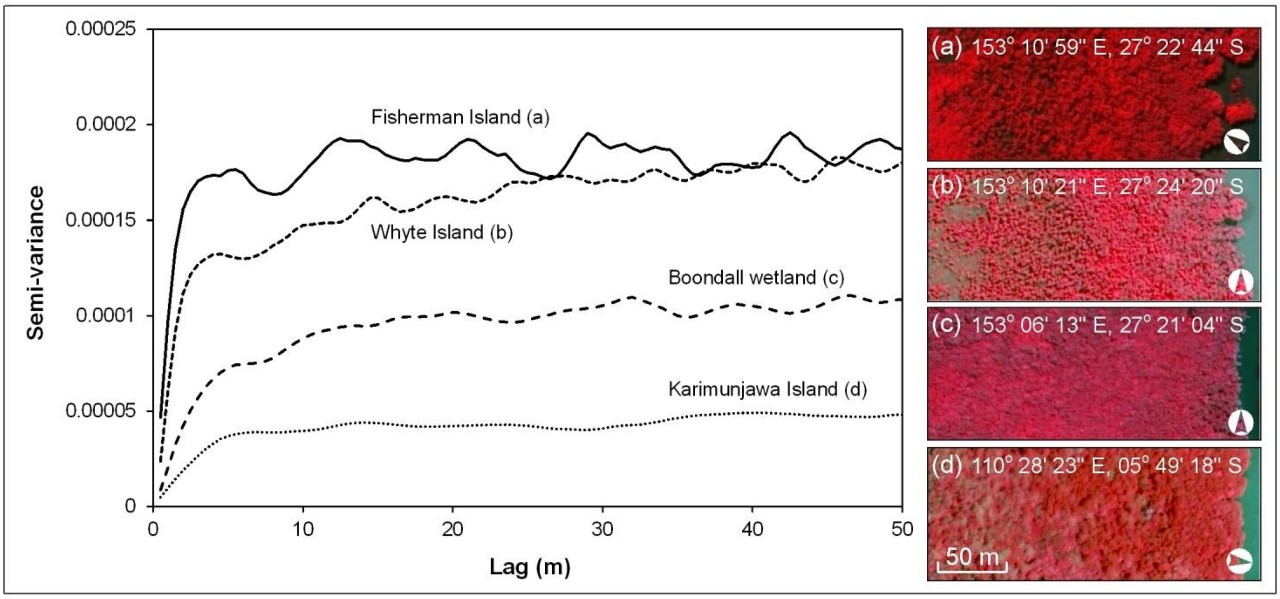

Figure 4.7. Subsets of green band semi-variograms up to 50 m lag distance, showing the variation of vegetation structure at different sites. Coordinates represent the approximate centre of each image.

4.3.2. Mangrove Composition Maps

The results of this study demonstrated that the GEOBIA approach was able to produce various mangrove feature information details from single and multiple images by integrating field data, operator local knowledge and a conceptual hierarchical model of multi-scale mangrove features in the rule set (Figure 4.8). The results showed that the developed rule set was able to map targeted mangrove composition objects from images with different spatial resolutions. Only limited studies have implemented the explicit hierarchical model of objects in mangrove mapping (Murray et al. 2003; Krause et al. 2004; Kamal & Phinn 2011; Heenkenda et al. 2014). This study demonstrated the effectiveness of having a conceptual hierarchical model for mangrove mapping. It also described the ability and limitation of the images and the mapping approach in depicting information of mangrove composition. Nevertheless, membership rules/thresholds in the rule set required adjustment for each image (see Table 4.3). The results also show the required image pixel resolution aspect in the conceptual spatial hierarchical organisation of mangroves features identifiable from remotely-sensed images (Figure 4.1).

Image spectral reflectance was the main criteria used to map vegetation and mangrove stands from the optical images (TM, AVNIR-2 and WV-2). The FDI algorithm successfully discriminated between the vegetation and non-vegetation class (level 1) with a high degree of overall accuracy for TM (89%), AVNIR-2 (93%) and WV-2 (97%) (see Table 4.5 in section 4.3.3). This pattern was also visually evident in Figure 4.8a to c, where the vegetation class boundary was more accurately represented in WV-2 than the TM and AVNIR-2 images. The strip of *Sarcocornia quinqueflora* grass located in the middle of the saltmarsh was successfully mapped by WV-2 image (Figure 4.8c), but not by other images. The FDI algorithm was found to be sensitive to all typical vegetation spectral reflectance, regardless of the health of the vegetation. For example, the dry *Sporobulus virginicus* background grass, lacking the red-edge and absorption feature in the red part of the spectrum, which is typical for healthy green vegetation spectral reflectance (Carter 1994; Bunting & Lucas 2006) (Figure 4.4), was classified as vegetation. In general, the FDI algorithm was transferrable from WV-2 to the other images but it required adjustment of the vegetation threshold for each image (Table 4.3).

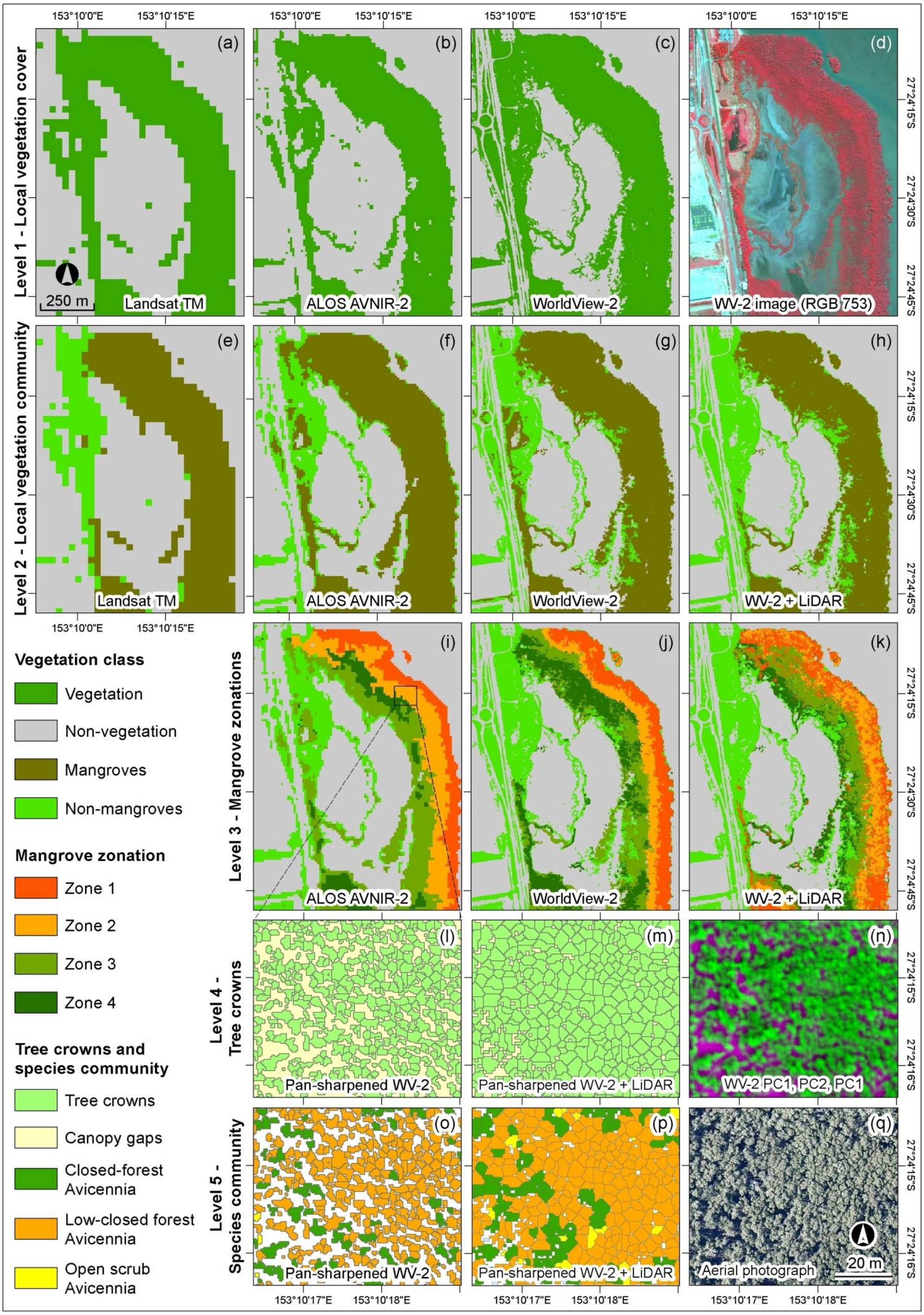

Figure 4.8. Example subsets of mangrove composition maps at Whyte Island, Moreton Bay, showing all hierarchy levels produced from different image sources.

The mangrove stands (level 2) were differentiated within the vegetation class created in level 1. The spectral reflectance of mangroves is strongly influenced by tidal effects and soil background, resulting in mixed pixels (Blasco et al. 1998; Díaz & Blackburn 2003). As a consequence, it makes the application of a pixel-based approach in mangrove stands problematic. However, the combination of image bands and context information in the rule set in GEOBIA allows effective recognition of mangrove objects in the image (Heumann 2011a; Kamal & Phinn 2011; Heenkenda et al. 2014). For the spectral only approach, the green, red, NIR and MIR bands provided a useful tool to discriminate mangrove stands from other vegetation objects. Exploratory work to find the best image band algorithm and associated threshold for each band, representing mangrove stands, suggested that each image has a unique combination of band algorithm and threshold to successfully separate mangrove from non-mangrove objects. However, the results showed some *Casuarina glauca* trees were misclassified as mangrove tree stands due to their similar spectral reflectance (see along the port highway in Figure 4.8e to g as examples). To refine the arbitrarily-defined spectral-based rule set, the DTM derived from LiDAR was included in the rule set as contextual information about the mangrove habitat. A threshold of DTM $\leq$ 1.5 m above mean sea level was found to be useful in combination with the WV-2 spectral-based rule set and applicable to all Moreton Bay mangrove sites. This additional information significantly improved the accuracy of the mangrove delineation (Figure 4.8h) by 9% (Table 4.5).

Within the mangrove class, the zonation pattern in Moreton Bay was difficult to map using image spectral information only. The zonation pattern in Moreton Bay represents variations of *Avicennia marina* vegetation structure (i.e. canopy density, tree stem, tree height) across the mangrove stand. Hence, the mangrove zonation pattern differentiation based on image spectral reflectance suggested by Lucas et al. (2007) was not applicable in this case. To address this issue, in theory, the inclusion of textural or contextual information might help the classification. However, the finding showed that the textural information of the image did not facilitate the zonation discrimination. It might be attributed to the fact that some of the mangrove zones have highly mixed vegetation structure stands with a number of canopy gaps (i.e. S3 and M4 in Moreton Bay), making it difficult to differentiate the zonation based on image texture. Instead, the distance from the coastline was incorporated in combination with the spectral-based rule set to delineate each zone (Table 4.3), and this approach worked reasonably well (Figure 4.8i and j). The use of the CHM and FCC derived from LiDAR data were also investigated. The results showed that the mangrove zonation was oversimplified using the AVNIR-2 or WV-2 imagery and well-represented using a combination of WV-2 and LiDAR data (Figure 4.8i, j, k, respectively). However, the accuracy assessment results suggested a low accuracy of the zonation maps. It was attributed to the inaccuracy in defining the mangrove zonation boundary, due to the mixed vegetation stands between zones.

The mangrove tree crowns and species community levels were mapped using pan-sharpened WV-2 image only (0.5 m) and a combination of pan-sharpened WV-2 with LiDAR data (2 m). Most of the mangrove tree canopies are very dense and have overlapping canopy arrangements. As a result, the definite borders of tree canopies were difficult to detect and delineate from the image. To minimise the tree canopy border demarcation error, a rule set was specifically developed to (1) enhance the differentiation between canopy gaps and trees, and (2) find the tree crown seed and grow the seed towards the tree crown border within the tree class (Table 4.3). Figure 4.8n shows that PC bands 123 enhanced the differentiation of tree and canopy gaps. The tree crowns produced from the pan-sharpened WV-2 showed more realistic polygon boundaries compared with the result from the combination of pan-sharpened WV-2 and LiDAR data, with an overall accuracy of 68% and 64%, respectively (Table 4.5). Although LiDAR data provided a clear tree crown pattern along with the canopy height information, the optimum pixel resolution resampled from the point clouds was limited to 2 m. According to the result evaluation, the LiDAR data worked very well on large canopies (i.e. 8 m diameter or larger), but were unabled to depict small individual trees crowns less than 8 m in diameter (see the result in comparison with Figure 4.8q). The LiDAR result in Figure 4.8m showed a very dense canopy with fewer and smaller canopy gaps compared with the pan-sharpened WV-2 result (Figure 4.8l). Therefore, as suggested by Gougeon (1995) and Culvenor (2003), high-spatial resolution image data with pixels significantly smaller than the tree canopy size is an essential requirement for tree crown delineation.

The mangrove species community maps were created based on the tree crown boundaries produced from the previous level. The NN algorithm successfully classified the *Avicennia marina* community. Visually, the map results follow the mangrove zonation pattern from the previous level. However, there were noticeable misclassified open scrub *Avicennia* in the WV-2+LiDAR produced map. Although there was a clear difference pattern on the produced maps (Figure 4.8 o and p), the results from the accuracy assessment did not show much difference between them (54% and 53%, respectively). The large scale of the reference map (1:25,000), as opposed to the image resolution (0.5 and 2 m), was likely to be the source of this inaccuracy.

4.3.3. Accuracy Assessments of the Maps

The area-based accuracy assessment calculated the area of the correctly classified class relative to the class domain area. In this study, an entire image was used for the domain area of level 1, vegetation class for level 2, and so on. Table 4.5 summarises the results of the area-based accuracy assessment descriptive statistics for all mangrove composition levels in the study. The overall quality (OQ) shows the class-related area accuracy; for instance, the area of correctly classified vegetation was 85% out of the total area of vegetation in level 1. On the other hand, the overall accuracy (OA) calculated the percentage of all correctly classified classes (vegetation and non-vegetation) in comparison to the total class domain area (an entire image).

Table 4.5. Summary of the area-based accuracy descriptive statistics in percentage (%).

Level	Class	Landsat TM				ALOS AVNIR-2				WorldView-2				WV2+LiDAR			
		OQ	PA	UA	OA	OQ	PA	UA	OA	OQ	PA	UA	OA	OQ	PA	UA	OA
1	Vegetation	85	92	92	89	90	93	97	93	95	99	97	97				
	Non-vegetation	70	82	83		81	94	86		90	92	97					
2	Mangroves	74	79	92	82	76	81	93	82	80	94	84	85	91	99	99	94
	Non-mangroves	66	88	72		66	85	75		63	69	88		87	98	97	
3	Zone 1					55	57	92	46	72	75	96	53	72	75	95	59
	Zone 2					59	59	100		45	45	98		60	61	96	
	Zone 3					38	38	99		49	50	97		39	39	99	
	Zone 4					34	34	100		44	44	99		68	68	99	
										PS WV-2				PS WV-2+LiDAR			
4	Tree crowns									64	81	76	68	56	64	82	64
	Canopy gaps									34	65	41		24	36	42	
5	Avicennia (CF)									65	82	75	54	57	87	62	53
	Avicennia (LCF)									58	87	64		65	77	81	
	Avicennia (OS)									22	23	94		4	4	20	

OQ: overall quality, PA: producer's accuracy, UA: user's accuracy, OA: overall accuracy, PS: Pan-sharpened, CF: closed-forest, LCF: low closed-forest, OS: open scrub.

The percentage of OQ and OA have a similar pattern throughout the levels. For local mangrove features (levels 1 and 2), both OQ and OA have high accuracy levels, with increasing accuracy for the higher spatial resolution images (63–95% and 82–97%, respectively). It indicated the effectiveness of the mapping approach and the superiority of the high-spatial resolution images. The OQ and OA of "within mangrove features" (levels 3 to 5) showed lower accuracy levels (4–72% and 46–68%, respectively), suggesting that the rule set developed at these levels was unable to classify the targeted objects properly. Heumann (2011a) reported similar results, where the overall acuracy of mangrove stands was 94.4% and dropped to about 25% at mangrove species level. The producer's accuracy (PA) depicts the omission error or the probability of a reference object being correctly classified, whereas the users's accuracy (UA) or commission error indicates the probability that an object classified on the map actually represents that category on the ground (Congalton 1991). For instance, for the delineation of tree crowns using the pan-sharpened WV-2 image, 81% of the tree crown areas were correctly classified as tree crown, but only 76% of the areas called tree crown on the map were actually tree crowns on the ground.

Overall, the area-based accuracy assessment was simple to implement and easy to interpret. The result of this accuracy assessment approach was not only checking the thematic category of the object, but also representing the spatial accuracy of object boundaries compared with the reference. However, it calculated one class at a time (Zhan et al. 2005) rather than all of the accuracy samples in one attempt, making the calculation more time-consuming. The locations of the areal sampling for calculation were also limited to the class domain area. Therefore, in accordance with the findings of Whiteside et al. (2010), this may contribute to limiting the area sampled and hence inclusion in the area-based accuracy assessment.

4.3.4. Multi-Scale Mangrove Composition Mapping

The effects of the *L*- and *H*-resolution model of remote sensing data (Strahler et al. 1986) to the produced mangrove maps were evident in this study. The results indicated that low-resolution images had limited ability to depict mangrove features compared with the high-resolution images (Figure 4.8). The TM image (30 m) was only able to differentiate mangrove stand objects (Figure 4.8e); and the AVNIR-2 (10 m) and WV-2 images (2 m) were able to map different mangrove zonation patterns (Figure 4.8i and j). The pan-sharpened WV-2 (0.5 m) and LiDAR, on the other hand, were able to map more detailed mangrove features to the level of mangrove tree crowns and species communities (Figure 4.8l to o). A decrease in image spatial resolution affects spectral heterogeneity of the image, since it creates mixed pixels (Strahler et al. 1986; Woodcock & Strahler 1987) and is therefore less sensitive to the spatial complexity and hampers the ability to discriminate small objects relative to the pixel size (Strahler et al. 1986; Rocchini 2007).

The comparison of overall accuracy per image (Figure 4.9a) indicated that WV-2 imagery has the highest overall accuracy for all of the levels. For levels 1 and 2 there were clear increases in accuracy when increasing image spatial resolution. Levels 3 to 5 also confirmed this pattern. The decrease in overall accuracy when combining WV-2 and LiDAR data was attributed to the 2 m resampling of LiDAR point cloud. It is important to note that a comparatively large number of spectral bands available with a limited spectral range for the WV-2 image also enabled more flexibility in applying the GEOBIA rule set (Heenkenda et al. 2014). Increasing the spectral resolution provides additional explanatory information in object recognition (Rocchini 2007), which in turn increases the classification accuracy.

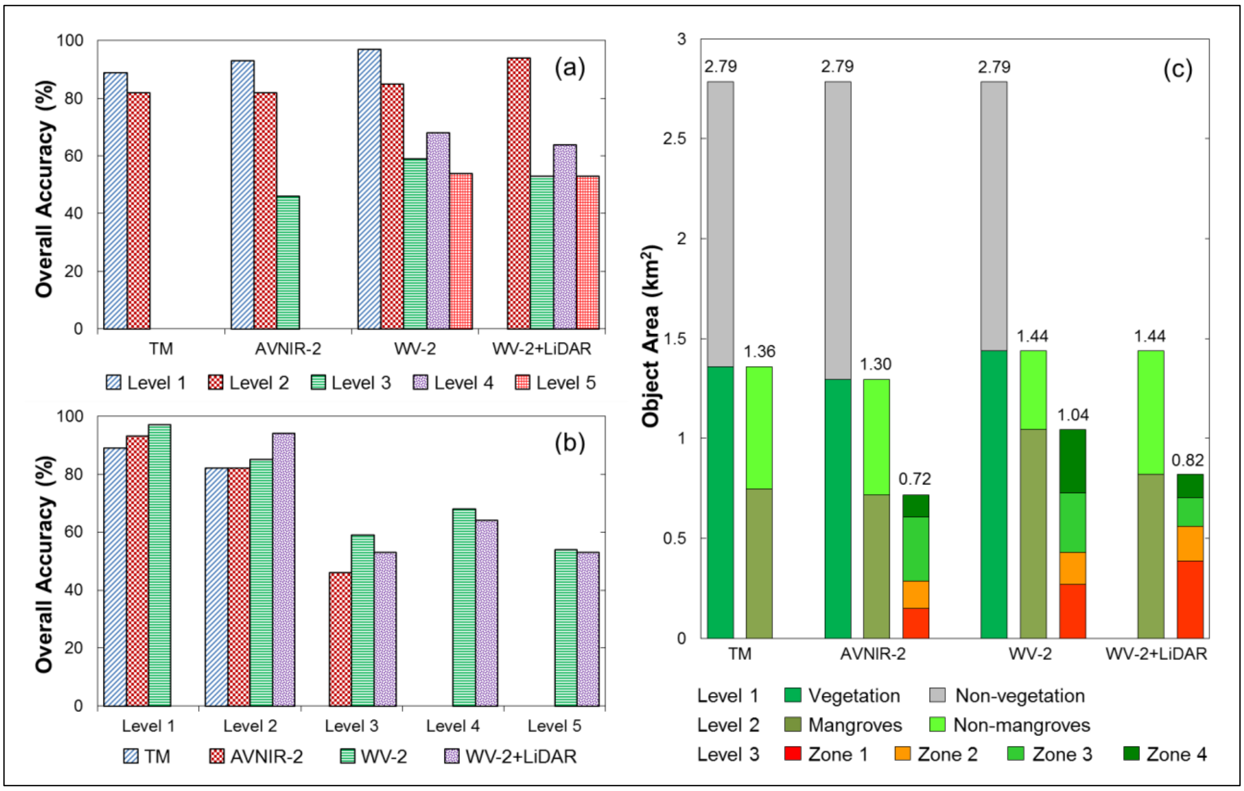

Figure 4.9. Comparison of the overall accuracy result of (a) different images and (b) different levels, and (c) area of the produced maps for level 1, 2, and 3 in Whyte Island, Moreton Bay.

Looking at the variation across levels, the overall accuracy decreased with increases in the mapping level (i.e. finer scale or smaller object size) (Figure 4.9b). There are several possible explanations for this pattern. First, smaller object sizes (i.e. zonations, tree crowns and individual species) required more complex classification rule sets to map the land-cover classes. The inaccurate definition of the rule set will affect the accuracy of the mapping. Second, smaller object sizes increase within-class variability, which decreases the spectral separability of classes and potentially decreases the accuracy (Markham & Townshend 1981; Chusnie 1987). This effect is well-known in pixel-based approaches (Rocchini 2007) and may also affect the GEOBIA approach. Third, it is suggested that a higher number of classes involved in a classification tends to reduce the accuracy of the results (Andrefouet et al. 2003; Roelfsema & Phinn 2013). A larger number of targeted land-cover classes requires a more complex definition of each object category for effective separation and increases the "boundary effect" (Markham & Townshend 1981). As the targeted objects become smaller, the proportion of segments falling on the boundary of objects will increase and hence potentially decrease the mapping accuracy. The object area comparison in Figure 4.9c showed the area difference of land-cover classes between images (indicated by the numbers on top of the bar graph) was increased by the increasing number of targeted object classes. At level 1 the area was similar across images. At levels 2 and 3 the area increased to 0.14 km^2 and 0.32 km^2, respectively. The relatively large area of mangroves mapped from the WV-2 image was attributed to the decreasing boundary effect due to the high spatial resolution of the image.

4.3.5. Applicability of the Approach to Other Sites

The next question following the success of the implementation of the mapping approach is whether the approach can be applied elsewhere. Developing an approach or algorithm that can be universally implemented is one of the major challenges in remote sensing applications. Unfortunately, this situation is difficult to achieve and rarely occurs because of varying environmental conditions, seasonality, sensor viewing geometry, level of pre-processing, spatial resolution and image sensor types. Most of the mapping procedures and algorithms employing remote sensing data are site and sensor specific. The transferability of the conceptual hierarchical model of multi-scale mangrove features and its rule set were investigated to another site on Karimunjawa Island using the same image datasets (TM, AVNIR-2, and WV-2). All image datasets were pre-processed to the same level using the same correction methods, to ensure a fair comparison.

In theory, the conceptual hierarchical model developed indicates the “domains of scale” (Wiens 1989) of mangrove features and provides a logical multi-scale mapping guideline that can be applied everywhere. When it comes down to the technical mapping aspect, the result might be unexpected. The finding showed only the first three hierarchical levels could be mapped. This limitation was in accordance with the results of mangrove spatial pattern analysis discussed in section 4.3.1 (Figure 4.7). According to field observations, mangroves on Karimunjawa Island are richer in species composition, have higher canopy density and consist of taller and more matured trees than the Moreton Bay mangroves. The dense and highly overlapping tree canopies prevented the delineation of the individual tree crowns. Therefore, the difference of environmental settings and local variation of mangrove composition affected the implementation of the model.

A direct transfer of the rule set from Moreton Bay to Karimunjawa Island was not possible. At level 1, the FDI algorithm successfully discriminated vegetation and non-vegetation objects from all of the images but required modification in the membership thresholds. Mangrove and non-mangrove separation and mangrove zonation delineation were performed using different processes and membership rules in the rule set compared to the Moreton Bay site. Apart from the environmental setting, the canopy reflectance depends on a numbers of factors and varied across location and time (Atzberger 2004). Thus, the image spectral response might also contribute to the rule set modification requirements.

4.4. Conclusions and Future Research

This study demonstrated that scale-specific, ecologically relevant information on mangroves can be mapped using a GEOBIA approach. The conceptual hierarchical model of multi-scale mangrove features was successfully implemented and facilitated the development of rule sets for mangrove mapping. The results show that higher spatial resolution images and this approach can map detailed information on mangroves. The TM image was only able to differentiate mangrove stand objects, while AVNIR-2 and WV-2 imagery allowed different mangrove zonation patterns to be mapped. The pan-sharpened WV-2 and LiDAR data could be used to map more detailed mangrove features, including individual mangrove tree crowns and species communities. However, it was also noted that the superiority of WV-2 imagery was also attributed to the relatively large number of spectral bands.

Developing an efficient rule set requires an understanding of the spectral, physical and contextual characteristics of the targeted object(s). All of these aspects might work individually or in combination with each other in order to define and demarcate targeted objects. The findings showed that the inclusion of contextual information significantly increased the accuracy of the mapping. However, the development of rule sets is image and site dependent. Different algorithms and threshold values might be applied to different images to map similar objects due to variation of object spectral reflectance responses between images. Modification of algorithms and membership thresholds was also needed to map similar objects at different locations, due to the different environmental settings, local mangrove composition variations and the site-specific spectral response.

In terms of the accuracy of the produced maps, the findings suggest that the accuracy of maps was defined by interactions between image spatial resolution, the scale of the targeted objects and the number of object land-cover classes mapped. As expected, higher image resolution (spatial and spectral) provided more detailed information on mangroves. Although it was achievable using the high resolution images, mapping smaller objects required a more complex rule set to be developed due to the increased within-class variability that potentially decreases the mapping accuracy. Incorporation of a larger number of object categories adds more complexity to the class definition and increases the boundary effect, which in turn will decrease the mapping accuracy.

The findings of this study provide conceptual guidance for multi-scale mangrove mapping and a technical demonstration of how to produce scale-specific mangrove information. This information is essential to address mangrove ecological problems at a relevant spatial scale. However, the results of this study are limited to the selected images, mapping techniques and mangrove sites. Further research is needed to include a wider range of images and mapping techniques. The potential of including image texture in this processing approach also needs to be explored further. Finally, to ensure the transferability of the conceptual hierarchical model, this approach needs to be tested at locations rich in mangrove species with distinctive individual tree canopies.

CHAPTER 5:

ASSESSMENT OF MULTI-RESOLUTION IMAGE DATA FOR MANGROVE LEAF AREA INDEX MAPPING

This chapter investigates the effects of different mangrove environmental settings, satellite image spatial resolutions, spectral vegetation indices (SVIs) and mapping approaches for LAI estimation. The accuracies of WV-2, AVNIR-2 and TM (2 m, 10 m and 30 m pixel sizes) subject to different pixel averaging windows (3x3, 5x5, 7x7, 9x9 pixels) and segmentation scales (10, 20, 30, 40, and 50) were assessed for estimating LAI at the Moreton Bay (Australia) and on Karimunjawa Island (Indonesia) study sites. Results show that LAI estimation using remote sensing data varied across sites, sensors pixel size and segmentation scales. The findings of this chapter provide an understanding of the relationship between pixel resolutions and the spatial variation of mangrove vegetation for estimating mangrove LAI. In other words, the results guide the optimal selection of optical remote sensing datasets to estimate and map mangrove LAI.

Associated Publications:

Kamal, M, Phinn, S & Johansen, K (in revision) 'Assessment of multi-resolution image data for mangrove leaf area index mapping', *Remote Sensing of Environment*.

Key Findings:

- *Mangrove LAI variation is dependent on the location, spatial variation of mangrove vegetation (i.e. homogeneous or heterogeneous) and the tree growth stage.*
- *LAI values are independent of the mangrove formation (i.e. scrub, low-closed forest, closed forest, etc.). Instead, the LAI value depends on the local spatial variation of mangrove phenological stages and canopy cover.*
- *Overall, the regression analysis shows significant coefficient of determination (R^2) values ranging from 0.50 to 0.83 across sensors, segmentation scales and SVIs.*
- *NDVI and AVNIR-2 is the best LAI predictor for the two selected study sites and associated field sampling approach.*
- *The optimum pixel size to estimate mangrove LAI correlates with the dominant object size in the area of interest (the average mangrove canopy size is 10 m) as well as the ground resolution element of the collected field data.*
- *The results from the WV-2 pixel averaging show that pixel window size corresponding to the extent of the field plots (i.e. 5x5 or 7x7, equivalent to about 10 m x 10 m to 14 m x 14 m pixel sizes) yield better LAI estimation than individual pixels (2 m x 2 m).*
- *Image segmentation significantly increases the accuracy of LAI estimates.*
- *The optimum image segmentation scale is defined by the scale of the targeted objects, the spatial variation of the landscape, the local image spectral variation and the extent of the image.*
- *The optimum segmentation size to estimate LAI corresponds to the size of the dominant objects in the scene and the ground resolution element of the collected field data.*

5.1. Introduction

Leaf area index is one of the most important biophysical parameters for assessing mangrove forest health (Jensen et al. 1991; Giri et al. 2007; Heumann 2011b). It is defined as the one-sided leaf area per unit surface area (m^2/m^2), and therefore is a dimensionless number (Pierce & Running 1988; Green et al. 1997; Lymburner et al. 2000; Addink et al. 2007). The importance of LAI in vegetation studies is well-recognised. It is an indicator of ecological processes (rates of photosynthesis, transpiration and evapotranspiration) (Pierce & Running 1988), net primary production (Meyers & Paw 1986, 1987; Clough et al. 1997) and rates of energy exchange between plants and the atmosphere (Gholz et al. 1991). It can be used to predict future growth and yield (Gholz 1982) and assists in monitoring changes in canopy structure due to pollution and climate change (Gholz et al. 1991; Fassnacht et al. 1997). Due to its significance in describing a fundamental property of the plant canopy in its interaction with the atmosphere and solar radiation (Bréda 2008), the ability to estimate LAI provides a valuable means to understand and estimate the physical condition of mangroves. This is even more essential as at least 35% of the global mangrove area was reported lost during the past two decades (FAO 2007), exceeding losses reported for tropical rain forests and coral reefs (Valiela et al. 2001). Predictions suggest that in the next 100 years, about 30-40% of coastal wetlands will be lost (McFadden et al. 2007), and 100% of mangrove forest (Duke et al. 2007) if the present rate of loss continues.

The alarming status of the global mangrove forest losses corroborates the need to develop cost-effective techniques for rapid mangrove LAI mapping. Direct measurements of LAI in mangroves gives very accurate results but it is difficult, labour intensive, costly in terms of time and money and some of the methods used are destructive (Green et al. 1997; Bréda 2008). As an alternative, indirect and spatially explicit LAI extraction from remote sensing data provides a more practical method to estimate and repeatedly map LAI. It provides an estimate of LAI at repeated times over local to global scales (Fang & Liang 2008). Although still limited in number, several studies have indicated the successful implementation of optical remote sensing data for mangrove LAI mapping from various sensors, for example Landsat TM or ETM+ (Ramsey III & Jensen 1996; Green et al. 1997; Díaz & Blackburn 2003; Ishil & Tateda 2004), SPOT XS (Ramsey III & Jensen 1996; Green et al. 1997), AVHRR (Ramsey III & Jensen 1996), ASTER (Jean-Baptiste & Jensen 2006), IKONOS (Kovacs et al. 2004; Kovacs et al. 2005; Kovacs et al. 2010), QuickBird (Kovacs et al. 2009; Kovacs et al. 2010), CASI (Green et al. 1998a), Leica-ADS40 (Kovacs et al. 2010), and ALOS PALSAR (Kovacs et al. 2013).

The estimation of mangrove LAI using optical remote sensing data has been based on empirical or semi-empirical statistical relationships formulated between in-situ LAI measurements and the image pixel values, from at-surface spectral reflectance or in the form of spectral vegetation indices (SVIs). The indices are designed to enhance the sensitivity of the spectral reflectance contribution of vegetation while minimising the soil background reflectance or atmospheric effects (Fang & Liang 2008; Huete 2012). These empirical statistical relationships are then used to estimate the distribution of LAI in an image. For example, Green et al. (1997) found that using a linear regression, the normalised difference vegetation index (NDVI) derived from SPOT XS has high a correlation with LAI (R^2 = 0.74, p < 0.001, n = 29) in South Caicos and Caicos Bank, British West Indies. Using QuickBird imagery and a linear regression, Kovacs et al. (2009) found significant relationships between LAI and the simple ratio (SR) and the NDVI (R^2 = 0.63 and 0.68, respectively, p < 0.0001, n = 225) in the Teacapán–Agua Brava–Las Haciendas estuarine–mangrove system, Mexican Pacific.

With regards to the advancement of remote sensing technology, a plethora of imaging sensors with various spatial (and spectral) resolutions are available, with pixel sizes ranging from sub-meter to hundreds of meters, from narrow hyper-spectral bands to broad band multi-spectral images. At the same time, the rapid development of image processing techniques suitable for high spatial resolution image data, e.g. GEOBIA has also shifted the way image mapping is performed (Blaschke & Strobl 2001; Blaschke 2010). As opposed to the conventional pixel-based methods, GEOBIA produces meaningful objects that are represented by a cluster of neighbouring homogenous pixels through image segmentation based on the spectral information and local pattern or textural information (Baatz & Schape 2000; Blaschke & Strobl 2001; Benz et al. 2004). One of the advantages of image segmentation in GEOBIA is its flexibility to adjust the scale of the targeted objects (Benz et al. 2004; Trimble 2011). Currently, there are a very limited number of studies investigating the effects of image segmentation scales on LAI mapping.

Based on the premise that the selection of an appropriate image spatial resolution is essential for the successful application of remote sensing (Woodcock & Strahler 1987; Phinn et al. 2000), this study assessed the effects of different image spatial resolutions and pixel aggregation (i.e. image segmentation) to estimate LAI in two different mangrove habitats using spectral vegetation indices. The specific objectives were to investigate: (1) whether different remote sensing data affected the estimation of LAI in different mangrove habitats; (2) which of the remote sensing datasets and spectral vegetation indices provided the most accurate estimation of LAI, and (3) whether GEOBIA improved LAI estimation compared to pixel-based models.

5.2. Data and Methods

5.2.1. Study Area

The study sites for this chapter were conducted in two mangroves areas; the mouth of the Brisbane River, northern Moreton Bay, South East Queensland, Australia and Karimunjawa National Park, Central Java, Indonesia. For the detailed description about the location refer to section 2.1.

In the context of this study, the Moreton Bay site is dominated by homogenous mangrove species stands, while the Karimunjawa site represents heterogeneous species stands. In both sites, mangrove zonations were noticeable at different distances from the coastline towards the landward limit of the mangroves. These locations were selected to understand the variation in LAI at different mangrove vegetation structure and environmental settings and to investigate the optimum pixel size to estimate LAI at multiple sites.

5.2.2. Image Datasets

This study used TM, AVNIR-2 and WV-2 multispectral images of the mouth of the Brisbane River and Karimunjawa Island to cover the variation of image spatial resolutions investigated (Table 5.1). The image pre-processing details are presented in section 2.2 of the thesis.

Table 5.1. Image datasets used in Chapter 5.

Image type	Moreton Bay image acquisition date	Karimunjawa Island image acquisition date	Pixel size	Spectral attributes (nm)	Geometric attributes
Landsat TM	14 April 2011	31 July 2009	30 m	Blue (452-518), green (528-609), red (626-693), NIR (776-904), MIR1 (1567-1784), MIR2 (2097-2349)	Level 1T
ALOS AVNIR-2	10 April 2011	19 Feb 2009	10 m	Blue (420-500), green (520-600), red (610-690), NIR (760-890)	Level 1B2G
WorldView-2	14 April 2011	24 May 2012	2 m (multi), 0.5 m (pan)	Coastal blue (400-450), blue (450-510), green (510-580), yellow (585-625), red (630-690), red edge (705-745), NIR1 (770-895), NIR2 (860-1040), panchromatic (450-800)	Level 3X

5.2.3. Fieldwork and LAI Measurements

Fieldwork was conducted on April 2012 at the Moreton Bay sites and July 2012 on Karimunjawa Island. The selection of these dates was aimed to resemble the season in which the WV-2 images were captured (i.e. autumn [April 2011] and dry season [May 2012], respectively). Twenty-three field transects perpendicular to the shoreline were laid out on both sites (Figure 5.1) to collect structural measurements of the mangroves along different zonations, following the mangrove fieldwork guideline established by English et al. (1997). A detailed fieldwork description is presented in section 2.3 of the thesis. Field data were also collected from individual quadrats (indicated by single circles in Figure 5.1) at locations where the setup of a field transect was not possible due to access restrictions. These additional field samples were collected to increase the variation of mangrove canopy cover within sampled quadrats.

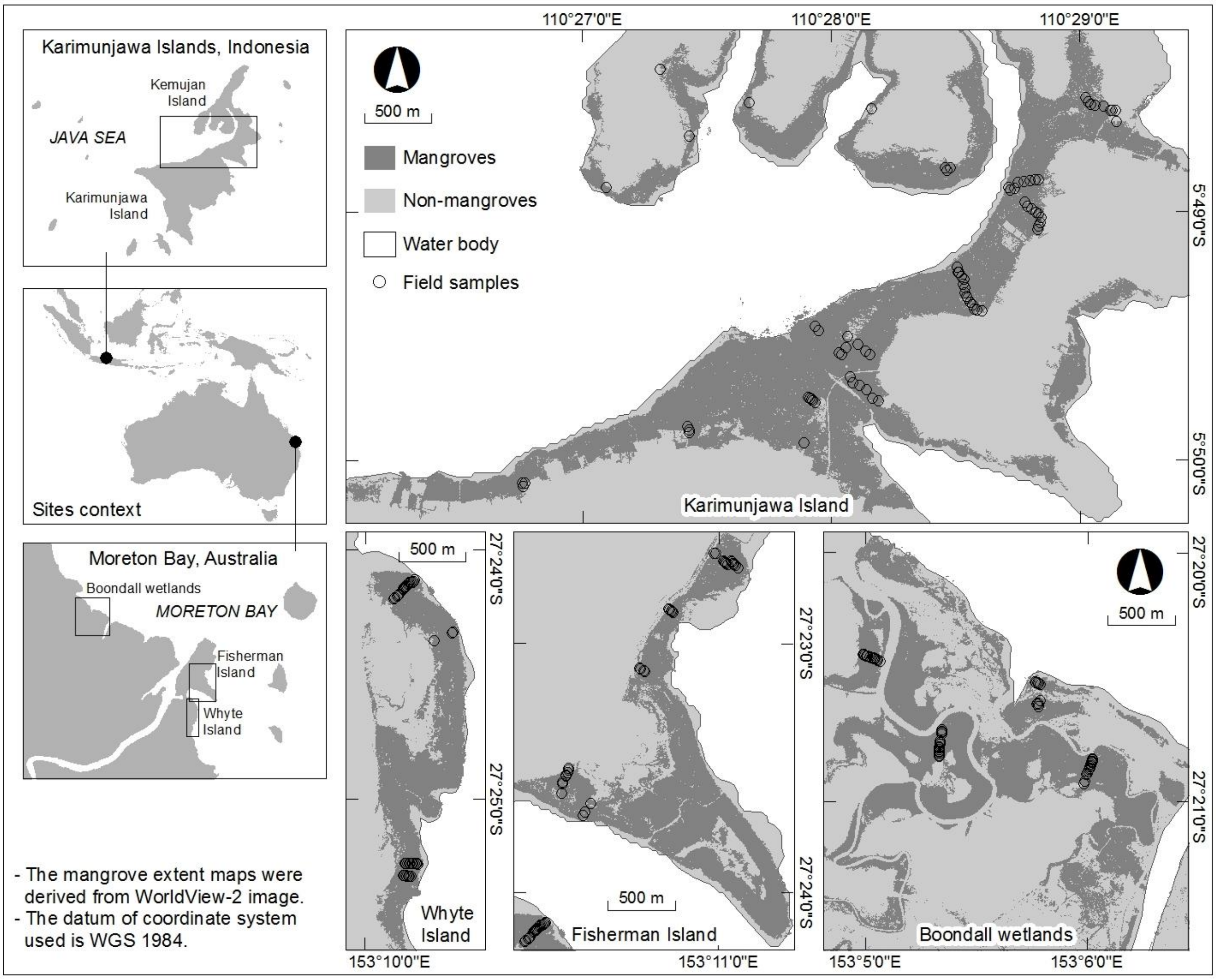

Figure 5.1. Study sites showing the extent of mangroves and the location of LAI field measurements.

In-situ LAI was estimated using the LI-COR LAI-2200 Plant Canopy Analyser (LICOR Inc., Lincoln, NE, USA). This instrument measures simultaneously diffuse radiation by means of fish-eye light sensor (148° field of view) in five concentric light-detecting silicon rings, sampling five concentric sky sectors (with central zenith angle of 7°, 23°, 38°, 53° and 68° respectively) (LI-COR 2009). This indirect and non-destructive instrument determines in situ effective LAI (LAIe, for simplicity this chapter uses the term LAI) using the gap fraction of a canopy, which is the fraction of view in some directions from beneath a canopy that is not blocked by foliage. Gap fractions are then calculated by dividing the below-canopy readings by the above-canopy readings at the five angles of view (Welles & Cohen 1996). LAI is then estimated by inversion of a Poisson model, comparing the transmittances, calculated simultaneously for each sky sector, measured above and below the canopy (LI-COR 2009). A detailed description of the instrument and its theoretical background is provided by Welles and Norman (1991) and Weiss et al. (2004).

In this study, the fish-eye lenses of the instruments were covered by a view cap with a 270° opening, in order to block off the operator from the sensor field of view and maintain the light signal under the dense mangrove canopy (LI-COR 2009). One LAI-2200 instrument was placed in a clearing during the field campaign to record above-canopy readings in auto log mode once every minute. The other LAI-2200 instrument was used to record the below-canopy readings at nine random points, which were averaged, within each quadrat along the field transects. All measurements were taken at a height of about 1 to 1.5 m above the ground. The LAI values were then calculated by the FV2200 LI-COR software based on the above- and below-canopy readings. The best time to obtain the most accurate results of LAI measurements using LAI-2200 instruments is under conditions of totally diffuse light with the sun at or below the horizon (at dusk or dawn). This condition needs to be met in order to avoid the additional light from brightly sunlit leaves that will reduce the accuracy of LAI estimation (Welles & Norman 1991; Cutini et al. 1998). Unfortunately, during the field campaign it was impractical to collect the data at this timeframe in the mangrove forest due to the rapid tidal fluctuations and logistic difficulties in accessing the sites. The data were collected during low tides that lasted for about three hours on most of the days. The data were collected when the sun angle was still low (from 6 am to 9 am, or 3 pm to 6 pm), with the instrument wands facing the opposite direction to the sun. This procedure was performed to avoid the direct sunlight recorded by the sensor and make sure the below- and above-canopy readings had the same light direction and intensity. A total of 196 quadrat samples were collected during the fieldwork campaign; 120 samples at the Moreton Bay site and 76 samples for Karimunjawa Island (see Figure 5.1 for the field samples distribution).

5.2.4. Spectral Reflectance Characteristics for Estimating LAI

In LAI estimation based on empirical-statistical models, the characteristic parameters (also referred to as “estimators”) that have significant correlations with the LAI are computed first from the canopy spectrum. Then, the statistical relationships are constructed between the characteristic parameters and the known LAI values in sample plots. This statistical predictive model is then used to compute the LAI values throughout the whole image. Spectral vegetation indices (SVIs) are designed to depict distinctive spectral characteristics of vegetation, e.g., high reflectance in near-infrared bands and absorption in red bands, with a one-dimensional index. The objective of developing SVIs are to enhance spectral features sensitive to a vegetation property while reducing disturbance by combining a few spectral bands into an SVI (Glenn et al. 2008). Variables that describe the characteristic spectra of vegetation are also used for LAI estimation, for instance: red through position, red-edge inflection position (Pu et al. 2003), area of red-edge peak, and near infrared (NIR)-platform position (Filella & Penuelas 1994) (Figure 5.2).

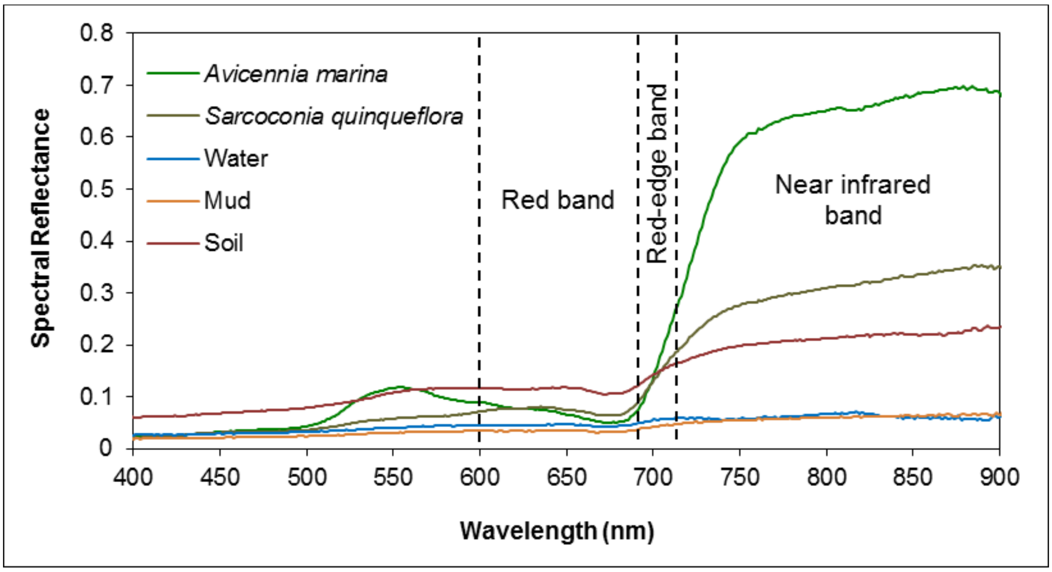

Figure 5.2. Average spectral reflectance plot of the main objects in the study area measured by ASD Handheld 2 portable spectrometer.

The electromagnetic energy in the red part of the spectrum is strongly absorbed by the plant leaves pigments (maximum absorption of chlorophyll a and b at 662 nm and 642 nm, respectively), and the high reflectance in the NIR part of the spectrum (700-1300 nm) results primarily from foliar reflection from the internal structure of the plant leaves (Jensen 2005). The steep reflectance increase occurring in the red-edge part of the spectrum (680-730 nm) physiologically marks the transition between the photosynthetically affected region of the spectrum (chlorophyll absorption spectrum), and the region with high reflectance values of the NIR plateau affected by plant cell structure or leaf layers (Herrmann et al. 2011). The position of the red-edge provides an indication of plant condition that might be related to several canopy factors such as LAI, nutrients, water and chlorophyll contents, seasonal patterns, and biomass (Pu et al. 2003; Cho & Skidmore 2006). Different SVIs were defined for different purposes, and optimized to assess a process of interest. However, in LAI estimation, all of them are affected by the problem of saturation. SVIs generally tend to exhibit less sensitivity for LAI values that are higher than 2, depending on the type of SVIs (Carlson & Ripley 1997; Haboudane et al. 2004; Zarco-Tejada et al. 2005).

5.2.5. Image Processing and Statistical Analysis

The atmospherically corrected images were used to compute four SVIs using algorithms given in Table 5.2. Semi-empirical relationships were developed between the vegetation index pixel values and the in-situ LAI measurements (i.e. a pixel-based LAI modelling). All of the SVIs used in this study were computed using red and near-infrared bands of the three different image datasets, with the addition of the blue band for the Enhanced Vegetation Index (EVI). The SR and NDVI were selected as representative of intrinsic vegetation properties (Mather & Koch 2011). The Soil Adjusted Vegetation Index (SAVI) was included to adjust for soil colour, while EVI represented a background and atmospherically corrected vegetation index (Huete et al. 2002; Colombo et al. 2003). To focus on the mangroves, other objects in the image were masked out before the calculation of the SVIs. To investigate the effect of changing pixel size based on a single image, a mean filter with window sizes of 3x3, 5x5, 7x7, and 9x9 pixels was applied to the WV-2 image derived SVIs. The mean filter averaged the neighbouring pixel values surrounding the centre pixel and assigned the mean value to the centre pixel to simulate the different pixel sizes. The resultant pixel values at the centre of each field quadrats were then used to estimate LAI.

Table 5.2. Spectral vegetation indices used in LAI estimation.

Vegetation index	Algorithm		Source
Simple Ratio	$SR = \frac{\rho_{nir}}{\rho_{red}}$	(Eq. 5.1)	(Birth & McVey 1968)
Normalised Difference Vegetation Index	$NDVI = \frac{\rho_{nir} - \rho_{red}}{\rho_{nir} + \rho_{red}}$	(Eq. 5.2)	(Rouse et al. 1974)
Soil Adjusted Vegetation Index	$SAVI = (1 + L)\frac{(\rho_{nir} - \rho_{red})}{(\rho_{nir} + \rho_{red} + L)}$	(Eq. 5.3)	(Huete 1988)
Enhanced Vegetation Index	$EVI = G\frac{(\rho_{nir} - \rho_{red})}{(\rho_{nir} + C_1\rho_{red} - C_2\rho_{blue} + L)}$	(Eq. 5.4)	(Huete et al. 2002)

ρ_{nir}, ρ_{red}, and ρ_{blue} are near-infrared, red, and blue spectral reflectance, respectively. For the SAVI, L is a canopy background adjustment factor set at 0.25, because of the high density of mangrove canopy. For the EVI, G, C_1, C_2, and L are coefficients to correct for aerosol scattering, absorption, and background brightness (set at 2.5, 6, 7.5, and 1, respectively).

Several image segmentations were applied to the high-spatial resolution WV-2 image to understand the effect of pixel aggregation through different segmentation sizes for estimating LAI (i.e. an object-based LAI modelling). Segmentation is the process of clustering together neighbouring pixels with similar spectral characteristics to minimise the internal spectral and spatial heterogeneity of the objects. eCognition Developer 8.7 software (Trimble 2011) was used to perform the multi-resolution segmentation with scale parameters of 10, 20, 30, 40, and 50. The band weights were set equally to 1, and the shape and compactness parameters were set to 0.1 and 0.5, respectively. The selections of the parameter setting were intended to focus on the influence of the scale parameter variation alone and minimise the influence from other factors.

Semi-empirical relationships between in-situ LAI and both pixel- and object-based SVIs were investigated using regression analysis, following the regression-based LAI estimation used by (Green et al. 1997) and (Kovacs et al. 2004). The LAI-2200 averaged measurement points were plotted on the images using their associated GPS locations. These in-situ measurement points were used to extract the pixel values of the SVI images for the regression analysis. To develop the regression model, field sample points were randomly selected at a distance of at least 20 m apart to avoid a clustered spatial distribution of the model samples. This process resulted in 57 model samples for Moreton Bay and 39 for Karimunjawa Island.

5.2.6. Results - Validation

Validation is the process of assessing the accuracy of products by independent means (Justice et al. 2000; Tian et al. 2002). In this study, the uncertainty of LAI estimated from the three types of satellite imagery was assessed by analytical comparison against the remaining in-situ LAI measurements as reference data. After the models were created, the estimated LAI values produced from the SVI models were compared with the in-situ LAI validation samples by means of the Pearson's correlation (r) and root mean square error (RMSE) of the validation models (Jensen & Binford 2004; Soudani et al. 2006; Laongmanee et al. 2013). The measurements with the smallest RMSE were assumed to be the most accurate. In this process, 63 independent validation samples were used for Moreton Bay and 37 for Karimunjawa Island. To aid the assessment of prediction error, linear models and scatter plots between modelled and in-situ observed LAI were produced and plotted in a 1:1 graph.

5.3. Results and Discussion

5.3.1. Mangrove LAI Estimation

For the homogenous mangrove stands at the Moreton Bay site, the in-situ LAI values ranged from 0.26 to 3.23 (n = 120, mean = 1.97, SD = 0.45), while for the heterogeneous stands on Karimunjawa Island the LAI values ranged from 0.88 to 5.33 (n = 76, mean = 2.98, SD = 1.04). The in-situ LAI values were plotted against NDVI to visualise their distribution (Figure 5.2a-d). It is evident that Karimunjawa Island mangroves had a comparatively wider range of LAI values and had more LAI variation (Figure 5.3b) than the Moreton Bay mangroves (Figure 5.3a). According to field observations, mangroves on Karimunjawa Island are more diverse in species composition, have higher canopy densities and consist of taller and more mature trees than the Moreton Bay mangroves.

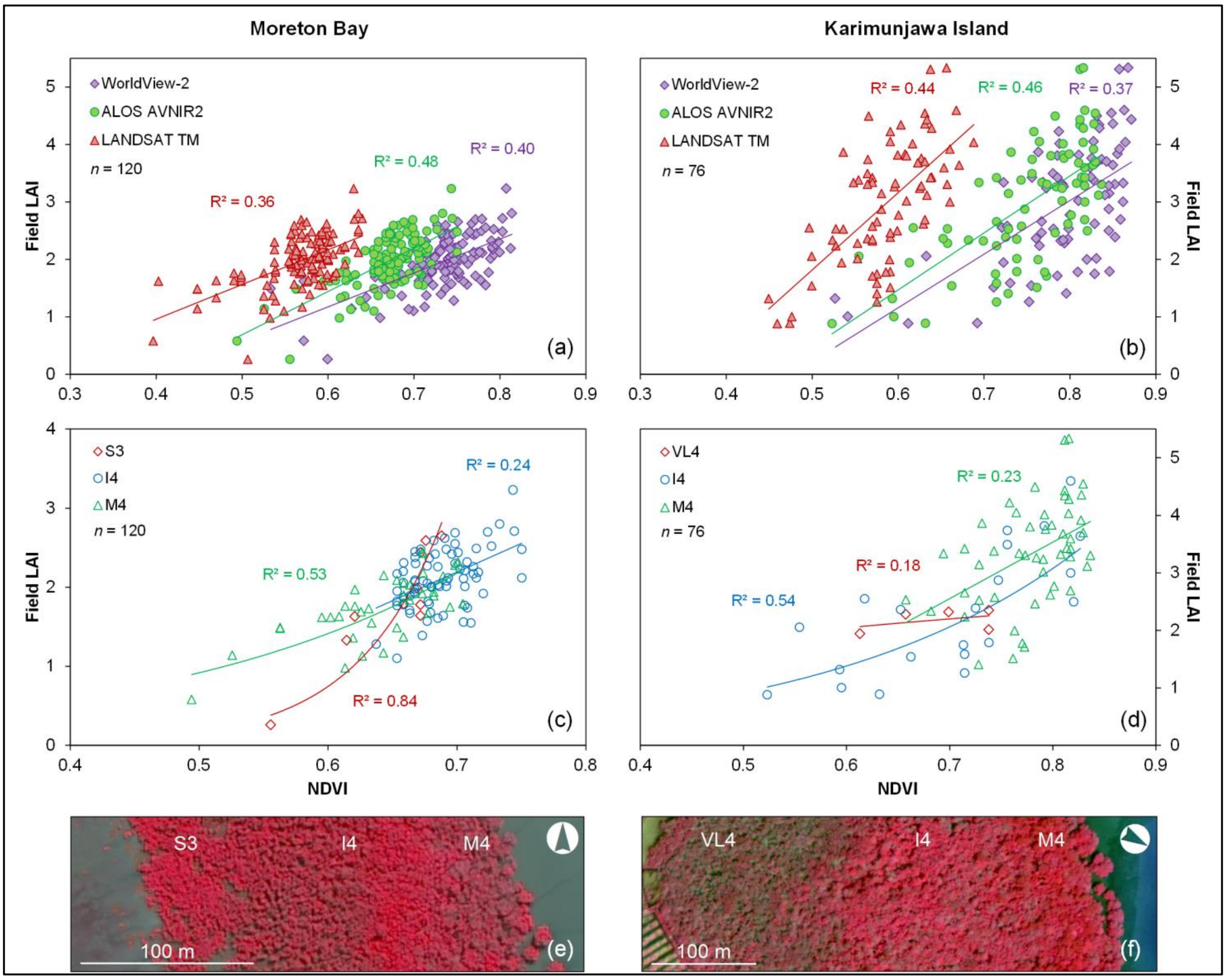

Figure 5.3. Plots of LAI variation based on AVNIR-2 NDVI across different sensors and locations (a, b), the variation of LAI within mangrove structural formation against NDVI (c, d), and subsets of WV-2 image showing the mangrove formation zones for (e) Moreton Bay and (f) Karimunjawa Island.

Looking at the LAI variation between mangrove zones in Moreton Bay (Figure 5.3c), the mean LAI values of low-closed forest (I4) of *Avicennia marina* were higher than the open scrub formation (S3) or closed forest (M4) formation (2.10, 1.81, and 1.73, respectively). The I4 formation consists of closely-spaced single or multi-stem tree stands of 4-10 m height, with overlapping leaves resulting in high density canopy cover (Figure 5.3e). The S3 and M4 formations, on the other hand, mainly consist of individual trees with many canopy gaps between mangrove stands, making the LAI values less than I4. The different LAI pattern across the mangrove formation was also apparent on Karimunjawa Island (Figure 5.3d). Closed forest (M4) had higher mean LAI values compared with the low multi-stem stands (VL4) and low-closed forest (I4) formation (3.33, 2.18, and 2.33, respectively). From field observations, the M4 formation at the seaward margin was dominated by tall (11-15 m) *Rhizophora mucronata* trees with high canopy density a limited canopy gaps (Figure 5.3f). In accordance with the finding of Ramsey III and Jensen (1996), the varying LAI values within the mangrove formations suggested that the LAI value range is independent of the mangrove structural formation or species composition. Instead, the local phenological stages and spatial pattern of mangrove vegetation may dictate the distribution of the LAI values (Addink et al. 2007).

5.3.2. In-Situ LAI Versus SVIs

The in-situ LAI measurements were regressed against its corresponding four SVIs values derived from different sensors and segmentation sizes within the study sites. The resulting coefficient of determination (R^2) for each regression model is presented in Table 5.3. All of the regression models had a positive relationship between observed LAI and SVIs. The F-statistic for the models and the t-statistic for slopes suggested that the relationships were statistically significant at $p < 0.001$ (with $n = 57$ for Moreton Bay, and $n = 39$ for Karimunjawa Island). Kuenzer et al. (2011) and Heumann (2011b) suggested using more complex mathematical models to work with natural mangrove forests, as the linear regression model may not be appropriate due to the natural variation of mangrove phenology stages. Therefore, the data were fitted into different regression models (both linear and non-linear). Only the models achieving the highest coefficient of determination (R^2) are presented in Table 5.3 and used for further processing. The complete list of the LAI models are presented in the Appendix 6, and some of the selected LAI map results are presented in the Appendix 7.

Table 5.3. The coefficient of determination (R^2) of the regression models for different sensors and segmentation sizes. All of the highest R^2 values are underlined.

Moreton Bay ($n = 57$, $p < 0.001$)												
SVIs	Image sensors (pixel-based)							WV-2 segmentation scale parameters (SP) (object-based)				
	WV-2					AVNIR-2	TM	SP10	SP20	SP30	SP40	SP50
	Original	3x3	5x5	7x7	9x9							
SR	0.63^3	0.69^3	0.73^3	0.74^3	0.70^3	$\underline{0.81}^3$	0.68^3	0.64^3	0.62^3	0.66^3	$\underline{0.70}^3$	0.69^3
NDVI	0.63^1	0.72^3	0.75^3	0.77^3	0.77^3	$\underline{0.83}^3$	0.70^3	0.65^1	0.63^1	0.67^1	$\underline{0.72}^3$	0.71^3
SAVI	0.55^1	0.69^3	0.76^3	0.78^3	0.78^3	$\underline{0.81}^1$	0.71^3	0.57^1	0.54^1	0.57^1	$\underline{0.64}^3$	0.61^1
EVI	0.50^3	0.68^3	0.76^3	0.78^3	0.77^3	$\underline{0.81}^3$	0.70^3	0.53^3	0.52^1	0.55^1	$\underline{0.61}^3$	0.59^1
						Average segment size (m^2):		9.6	43.9	100.0	174.6	266.2
Karimunjawa Island ($n = 39$, $p < 0.001$)												
SR	0.58^3	0.64^3	0.64^3	0.61^3	0.59^3	$\underline{0.80}^3$	0.63^3	0.59^3	0.57^3	$\underline{0.64}^3$	0.59^3	0.55^3
NDVI	0.62^2	0.68^2	0.70^2	0.68^2	0.66^2	$\underline{0.82}^2$	0.65^3	0.63^2	0.68^2	$\underline{0.71}^2$	0.66^2	0.64^2
SAVI	0.60^2	0.68^2	0.71^2	0.70^2	0.70^2	$\underline{0.77}^1$	0.69^3	0.59^2	0.64^2	$\underline{0.65}^2$	0.64^2	0.60^2
EVI	0.60^3	0.68^3	0.70^1	0.69^2	0.68^2	$\underline{0.77}^1$	0.69^3	0.59^3	0.61^2	$\underline{0.65}^3$	0.62^3	0.57^3
						Average segment size (m^2):		15.3	68.8	151.7	271.9	433.6

Regression model: [1]Linear, [2]Exponential, [3]Logarithmic

For the comparison of pixel-based models across sensors, the finding showed that AVNIR-2 with the pixel size of 10 m, yielded the highest R^2 values (from 0.77 to 0.83) for all the SVIs, followed by TM (from 0.63 to 0.71) and WV-2 (from 0.50 to 0.63). Within the WV-2 image pixel averaging simulation, the window size of 7x7 and 5x5 pixels were found to have the highest R^2 values for Moreton Bay and Karimunjawa Island, respectively. The wider averaging window (7x7 pixels) providing optimum WV-2 results for Moreton Bay may be caused by the mangrove stands being more homogenous compared with the mangrove stands in Karimunjawa Island where an averaging window size of 5x5 provided optimum results. It can be hypothesised that the window size corresponding to the field plot size is less important in an area with homogenous stands, whereas a heterogeneous field site would need to spatially match the corresponding extent on the image to account for the stand variation. This result corresponds to the findings of Laongmanee et al. (2013), who assessed the effect of different simulated pixel sizes (2.5 m, 5 m, 10 m, 15 m, 20 m, 25 m and 30 m) from QuickBird imagery to estimate mangrove LAI in the Bangpu restoration project, Samut Prakan, Thailand. They found that the optimum LAI estimation was achieved with a pixel size of 10 m (with the adjusted R^2 = 0.797 for the green vegetation index). According to the field observation, the size of about 10 m x 10 m represents the average size of tree canopy or group of smaller tree canopies at both sites. This combined with the field plot size is likely to contribute to the results, indicating that an AVNIR-2 pixel size of 10 m or a WV-2 averaging window size of 5x5 or 7x7 pixels corresponded to the field quadrats of 10 m x 10 m. An averaging window size of 9x9 pixels (18 m x 18 m) becomes too large in relation to the 10 m x 10 m field quadrats, which results in a drop in the field derived LAI and image derived SVI correlation. However, a systematic investigation of the effect of different field plot sizes is beyond the scoop of this study.

For TM models, the large pixel size results in mixed pixels. Their lower R^2 values might be attributed to the larger pixel size, resulting in the averaging of LAI values over a 900 m^2 area, which is nine times larger than the field plot size of 10 m x 10 m. On the other hand, the WV-2 models produced the lowest R^2 values due to two main reasons. First, high levels of heterogeneity are caused by the smaller pixel size, which according to Weiss and Baret (2014) could affect the estimation accuracy of the LAI. Second, it can be difficult to match up the 2 m x 2 m of WV-2 pixels with the 10 m x 10 m field plot, especially when considering the 5–6 m uncertainty in GPS position. The results of WV-2 pixel averaging (i.e. reducing the pixel heterogeneity) show that a pixel size at the approximate size of the field plots or slightly larger yielded the highest LAI estimation ability. This pattern was consistent at both study sites, indicating that the results were invariant to the mangrove environmental setting but was dictated by the local dominant size of the mangrove tree canopy and field plot size. Hence, this finding suggested that the optimum pixel size for LAI estimation and mapping of local mangroves for the field sampling scheme in this study was 10–15 m.

All of the best regression models based on the field LAI and SVIs derived from AVNIR-2 image data were plotted in Figure 5.4 along with their regression functions. Using this sensor, the SVI regression models for Moreton Bay had high R^2 values, ranging from 0.81 to 0.83. The NDVI yielded the highest R^2 at 0.83, and there were only subtle differences between the SVIs (Figure 5.4a). Of the Karimunjawa Island SVIs, NDVI also yielded the highest R^2 value of 0.82. The SAVI and EVI models produced slightly lower R^2 values (both 0.77) than NDVI and SR (0.82 and 0.80, respectively) (Figure 5.4b). Similar results were also found by Soudani et al. (2006) for LAI estimation in coniferous and deciduous forest stands, where NDVI resulted in the highest correlation coefficient (r) at the SPOT-4 resolution (20 m). Using a simple radiative transfer model applied to an agricultural area, Carlson and Ripley (1997) also concluded that NDVI was indicative of LAI values. The slightly lower coefficient of determination variation of SAVI and EVI might be related to the field data sampled from different phenological stages, from low mangrove canopy cover in the shrub formation to the very dense canopy in the closed forest formation at the seaward margin. Therefore, it may reduce the estimation ability of soil line-based vegetation indices (Colombo et al. 2003).

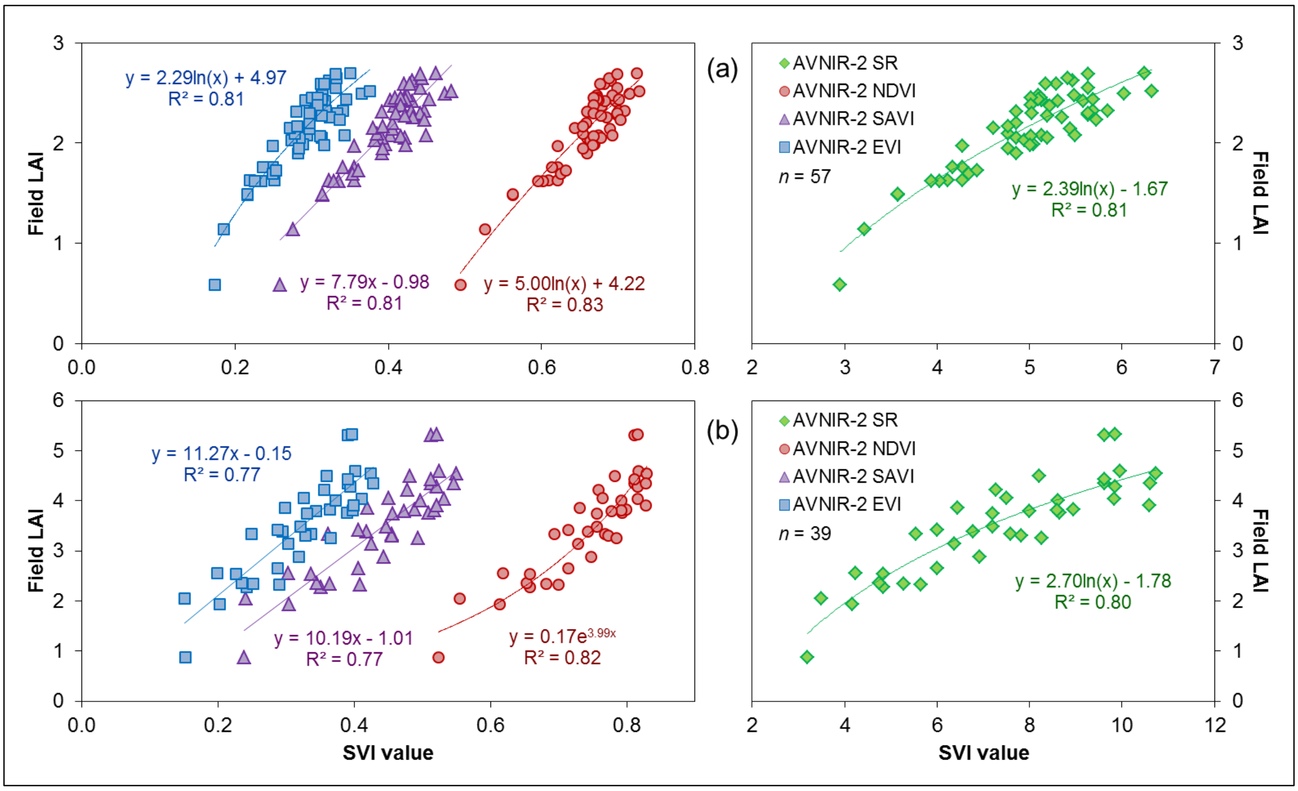

Figure 5.4. Regression models of in-situ LAI vs. SVIs from AVNIR-2 image in (a) Moreton Bay and (b) Karimunjawa Island.

Excluding the water and other non-mangrove features, the SVIs regression functions were applied to the AVNIR-2 image to understand the results of different estimation ability of the models (Figure 5.5), and to compare with the results from the segmentation-based LAI estimation. The range of mapped LAI values using the four SVI models was from 0.2 to 5.3. This was within the mangrove LAI ranges previously studied, for example 3.0 to 5.7 (Araújo et al. 1997), 2.2 to 7.4 (Clough et al. 1997), 0.8 to 7.0 (Green et al. 1997), and 0.01 to about 3.5 (Kovacs et al. 2009).

From visual inspection, there was not much spatial distribution differences found among the maps. However, the stacked bar graph in Figure 5.5f revealed that the LAI ranges covered different areas (in km^2) using the four different SVI models. The most noticeable difference was that the NDVI model predicted a larger area of lower LAI values of 0–3 compared to the SR, SAVI, and EVI models (total of 1.11 km^2 compared to 0.94, 0.85 and 0.90 km^2, respectively). Consequently, the NDVI based map had a smaller area of higher LAI values (3–4) (3.23 km^2 compared to 3.41 [SR], 3.49 [SAVI] and 3.44 [EVI] km^2).

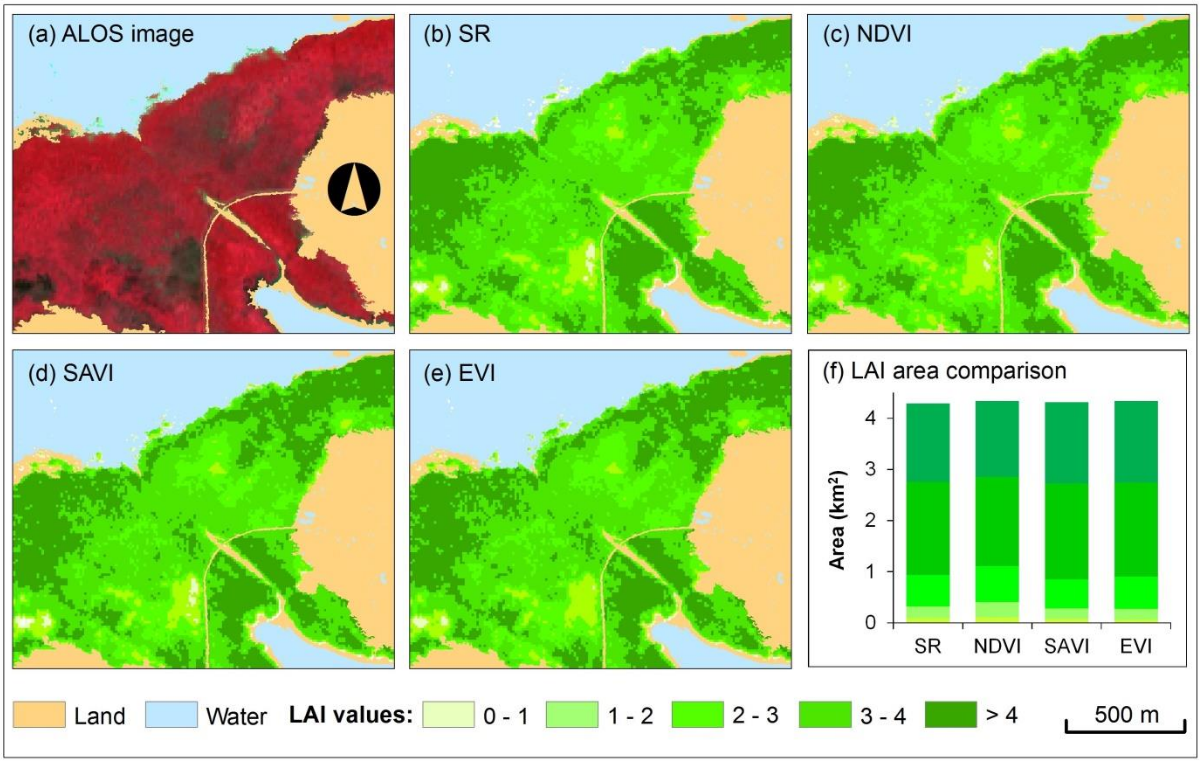

Figure 5.5. Subset of AVNIR-2 composite 432 showing part of mangroves in Karimunjawa Island (a), map comparison of estimated LAI from SVIs (b – e), and LAI area comparison derived from SVIs (f). The aggregation of LAI ranges into five classes is for visualisation and comparison purposes only.

5.3.3. Effect of Image Segmentation Size on the LAI Estimation

Multi-resolution segmentations were carried out for the mangrove areas at both study sites by aggregating pixels at several scale parameters (10, 20, 30, 40, and 50) from the WV-2 images. The coefficient of determination (R^2) from the regression modelling between the different segmentation sizes and in-situ LAI are presented in Table 5.3, with $p < 0.001$. Image with the smallest pixel size (i.e. WV-2) was used because the optimal pixel size to derive the image objects should be considerably smaller than the targeted objects (Fisher 1997; Addink et al. 2007), which in this case were mangrove canopies.

From Table 5.3, the optimum R^2 for the Moreton Bay and Karimunjawa Island sites from the different SVIs models were achieved at a scale parameter of 40 (R^2 from 0.61 to 0.72) and 30 (R^2 from 0.64 to 0.71), respectively. Overall, significant R^2 increases were achieved with the object-based models compared with the WV-2 pixel-based models and NDVI yielded the highest R^2. Their regression functions of NDVI are presented below:

$$\text{LAI} = 4.6372 * \ln \text{NDVI}_{seg40} + 3.6422 \quad \text{(Eq. 5.6)}$$

$$\text{LAI} = 0.0625 * e^{4.9924(\text{NDVI}_{seg30})} \quad \text{(Eq. 5.7)}$$

Other than the scale of the targeted objects and the spatial variation of the landscape (Addink et al. 2007), the difference in the optimum scale parameter obtained was possibly determined by the local image spectral variation and associated image object extent in relation to the 10 m x 10 m field sampling plots. However, if the R^2 and the average segment size (m^2) derived from the segmentation were plotted, it revealed a specific relationship between study sites (Figure 5.6a, b). The red lines on the graph projected the scale parameters with the optimum R^2 to the average segment size (m^2), and the pattern suggested that they had a similar average segment size (174.65 m^2 for Moreton Bay and 151.70 m^2 for Karimunjawa Island). Assuming the square root of the average size is the pixel dimension, it would result in 13.2 m and 12.3 m, respectively; which is close to the size of AVNIR-2 pixels. By examining the example of image segmentation results (Figure 5.6c, d), the tree canopy and gaps were well delineated.

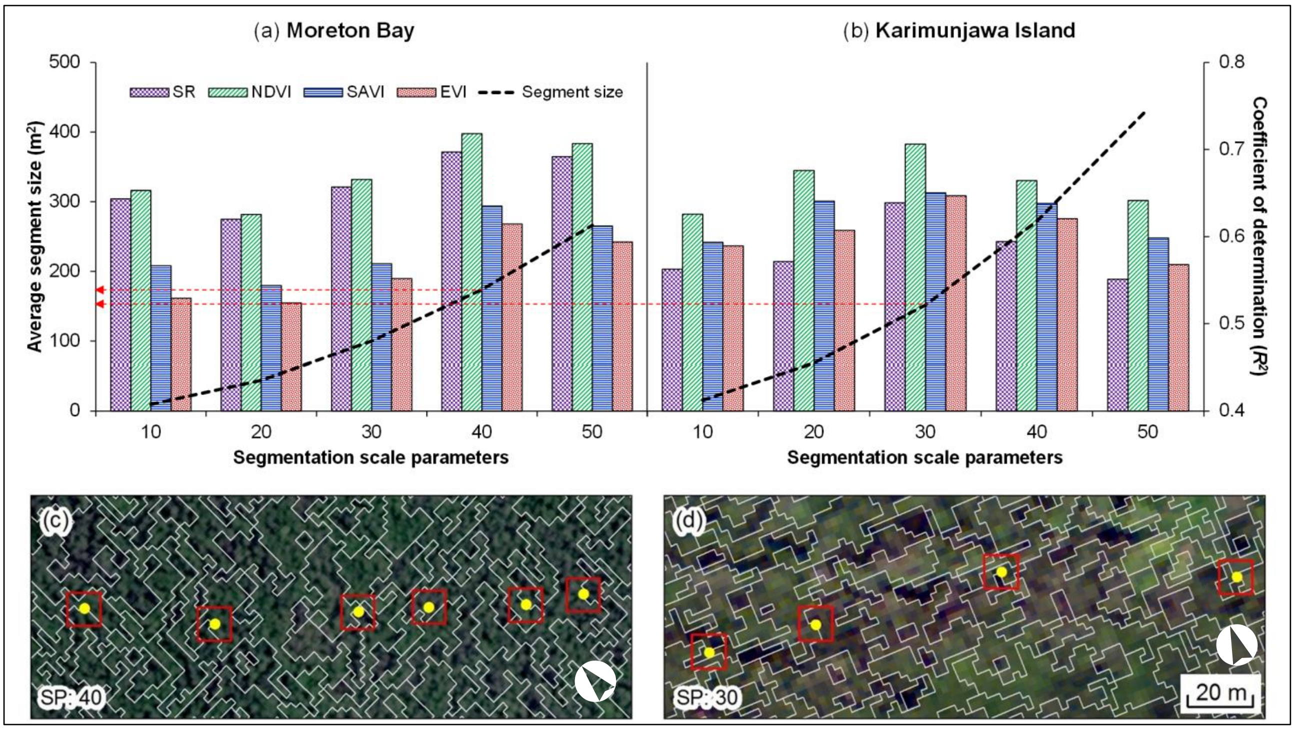

Figure 5.6. Effect of segmentation size (black-dashed line) on the coefficient of determination (R^2, in bar graphs) at (a) Moreton Bay and (b) Karimunjawa Island; and the corresponding example of image segments along the field plots (c and d). The red-dashed lines indicated the average segment size at the highest R^2 values, the red boxes and yellow points are field quadrats and the centre of quadrats, respectively.

At a pixel size of 2 m x 2 m of the WV-2 imagery, the relationship to the field derived LAI values obtained from 10 m x 10 m plots produced lower R^2 values than the use of larger image objects based on the WV-2 imagery. That is most likely because this resulted in a larger overlap of spatial extent between the image SVI values and field derived samples of LAI. However, as a larger scale parameter is used, which results in larger objects, the spatial extent from where image SVI values are derived becomes too large to correspond to the 10 m x 10 m field plots. It can then be expected that the R^2 value will start to drop again with increasing object sizes. The 10 m x 10 m field plots did, in some cases, represent partial mangrove canopy and partial canopy gaps. Therefore, the larger objects, which are still spectrally homogenous due to the multi-resolution segmentation process, will correspond to the part of the 10 m x 10 m field plot that represents either the mangrove canopy or canopy gap. Field plots of 10 m x 10 m that are homogenous in nature are likely to correlate better with the overlapping segmented object, whereas heterogeneous 10 m x 10 m plots may be divided by two or more objects. For these heterogeneous field plots, the selected object matched with the corresponding field derived LAI value may not, in these cases, have correlated as well, hence reducing the overall R^2 value. Using a pixel size of 10 m or an averaging window size of 7x7 WV-2 image pixels to derive each SVI value may correlate better with the 10 m x 10 m field derived LAI values, as these pixels/pixel windows cut across heterogeneous parts of the mangroves, whereas the segmented objects do not. It is therefore not surprising that WV-2 derived objects produce better results than individual WV-2 pixels, and that images with a pixel size of 10 m or an averaging window of e.g. 7x7 WV-2 image pixels produce better results than the WV-2 derived objects.

Table 5.3 shows that semi-empirical-statistical modelling of LAI using an object-based approach provided better LAI estimation ability for the WV-2 image data, as opposed to the pixel-based approach. A similar result was reported by Atzberger (2004) for LAI estimation using the inversion model of object-signatures, where the RMSE dropped from 0.81 (pixel-based) to 0.59 (object-based). It was also evident that the different level of image aggregation (i.e. image segmentation) resulted in different accuracies for estimating LAI from four of the spectral vegetation indices. Image segmentation averages the spectral values of neighbouring homogenous pixels of an image into a single image object segment, based on the image spectral features as well as the object geometry (Benz et al. 2004; Blaschke 2010). It means the detailed information contained within each pixel is lost. However, at a certain aggregation level, the image objects derived from the segmentation might turn out to be relevant (Addink et al. 2007). In our case, the segmentation at a scale parameter of 40 for Moreton Bay and 30 for Karimunjawa Island for NDVI images appeared to be the optimum for estimating LAI. These scale parameters confirmed that the LAI estimation ability was determined by the average size of the objects of interest (i.e. mangrove canopy) and the field plot size.

5.3.4. Independently Measured Versus Estimated LAI

The relationships between the independent samples of in situ observed LAI and the estimated LAI from four SVIs derived from the three different images and the optimum segmentation (SP 40 and 30) were calculated (Table 5.4). This section focused on the results of the AVNIR-2 imagery and the segmentation models, because they produced the best results from the previous analysis. The WV-2 and TM models were included for comparison only. For the pixel-based models of AVNIR-2, the validation results revealed that the difference in RMSE between the models was small for each site. The RMSE values of LAI for the AVNIR-2 imagery of Moreton Bay were 0.54 (SR and NDVI) and 0.55 (SAVI and EVI) and for Karimunjawa Island were 1.32 (SR), 1.31 (NDVI), 1.36 (SAVI), and 1.38 (EVI). The NDVI had the lowest RMSE values. The Pearson's correlation values for all of the AVNIR-2 pixel-based models ranged from 0.79 to 0.86. To examine whether one model was statistically better than the others to estimate LAI, a one-way ANOVA test was performed based on the validation samples for AVNIR-2. At a 95% confidence level, it suggested that none of the four SVIs models for Moreton Bay or Karimunjawa Island were statistically different ($F(3,248) = 0.025$, $MSE = 0.002$, $p < 0.05$ and $F(3,144) = 0.039$, $MSE = 0.024$, $p < 0.05$, respectively). It confirmed the previous finding (section 5.3.3) that all of the SVIs performed almost similarly for estimating LAI. Similar results were reported by Kovacs et al. (2004) for SR versus NDVI, and Laongmanee et al. (2013) for the Green Vegetation Index (GVI), EVI and NDVI. However, NDVI was the most accurate estimator of LAI values for our study areas.

Table 5.4. LAI model validation results. The bold text indicates the focus of the discussion.

Moreton Bay (n = 63, p < 0.001)									
Images		SR		NDVI		SAVI		EVI	
		r	RMSE	r	RMSE	r	RMSE	r	RMSE
WorldView-2		0.73	0.52	0.73	0.52	0.68	0.50	0.66	0.49
ALOS AVNIR-2	Pixel-based	**0.80**	**0.54**	**0.81**	**0.54**	**0.80**	**0.55**	**0.79**	**0.55**
LANDSAT TM		0.72	0.56	0.71	0.56	0.73	0.56	0.73	0.55
SP 40	Object-based	**0.70**	**0.54**	**0.69**	**0.54**	**0.68**	**0.54**	**0.68**	**0.53**
Karimunjawa Island (n = 37, p < 0.001)									
Images		SR		NDVI		SAVI		EVI	
		r	RMSE	r	RMSE	r	RMSE	r	RMSE
WorldView-2		0.64	1.19	0.64	1.15	0.68	1.15	0.64	1.22
ALOS AVNIR-2	Pixel-based	**0.85**	**1.32**	**0.86**	**1.31**	**0.83**	**1.36**	**0.82**	**1.38**
LANDSAT TM		0.81	1.23	0.78	1.24	0.78	1.23	0.77	1.23
SP 30	Object-based	**0.71**	**1.15**	**0.71**	**1.12**	**0.66**	**1.14**	**0.66**	**1.16**

r is the Pearson's correlation, RMSE is the root mean square error, and SP is the scale parameter of segmentation.

The validation results from the object-based models showed different patterns to the pixel-based results. Overall, the Pearson's correlation of the object-based models (ranged from 0.66 to 0.71) appeared to be lower than the pixel-based models. Compared with the pixel-based WV-2 LAI estimates, the image segmentation increased the accuracy of the LAI model for Karimunjawa Island as indicated by the increasing Pearson's correlation coefficients and decreasing RMSE values, with NDVI as the best estimator (RMSE = 1.12). On the other hand, for Moreton Bay, the segmentation showed a slight decrease in estimation accuracy of the models as indicated by increasing RMSE values (from 0.49–0.52 to 0.53–0.54). The size of segments potentially contributed to the slight change in RMSE values. In the relatively narrow mangrove area of Moreton Bay, by increasing segment size, several validation samples occurred within a segment with a single vegetation indices value. The aggregation of samples affected the distribution of the validation data and hence increased the RMSE values. Therefore, to avoid the field sample aggregation, it is recommended to also consider the distribution of the field samples when selecting the scale of image segmentation.

To assess the validation results visually, linear statistical models and scatter plots between field observed and NDVI modelled LAI (for pixel-based and object-based models) were applied for both study sites (Figure 5.7). Generally, the NDVI models show good prediction ability by following the

1:1 line pattern. An obvious over-estimation was found at lower and middle ranges of LAI for Moreton Bay and most of the estimation for Karimunjawa Island. LAI over-estimation in mangroves may be caused by the dark organic detritus covering the sediment (Green et al. 1997) and the presence of mangrove seedlings on the forest floor. These substances were commonly found on the mangrove forest floor at both study sites and were potentially adding to the mangrove canopy spectral reflectance recorded by the sensors. The under-estimated high LAI values in Moreton Bay were associated with the tall closed forest of *Avicennia marina*. This mangrove formation is located at the seaward margin and has more frequent inundation by the tide. As a result, muddy sediments and water on the forest floor occurred in many of these areas and organic detritus and mangrove seedlings were less apparent. The influence of wet mud and water in this mangrove formation might reduce the NIR reflectance and hence SVI values, and reduce the ability of the sensors to estimate LAI (Blasco et al. 1998; Díaz & Blackburn 2003).

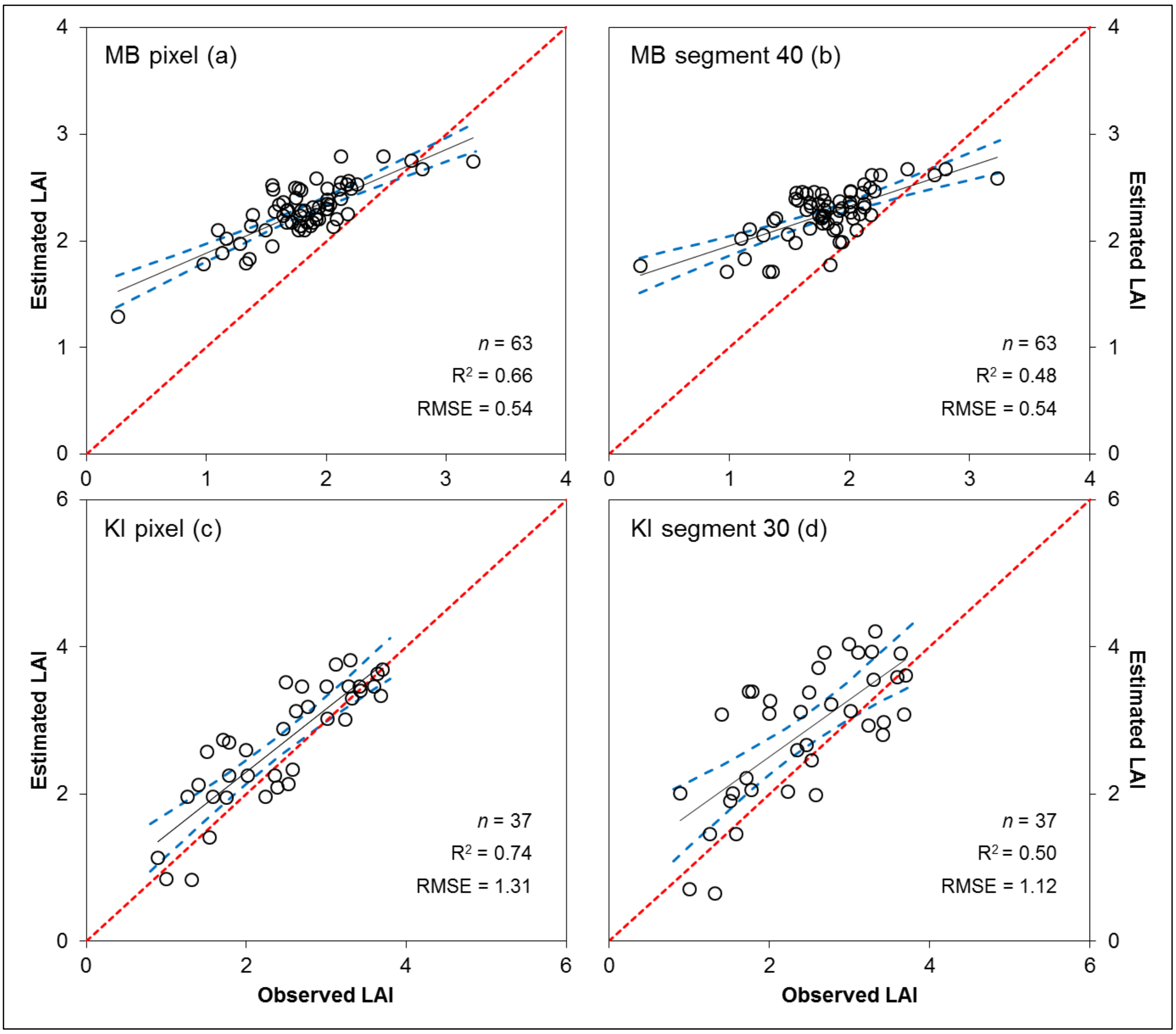

Figure 5.7. Plots of observed vs predicted LAI (m^2/m^2) for Moreton Bay (a, b) and Karimunjawa Island (c, d); using AVNIR-2 for pixel-based and WV-2 for object-based. The red-dashed line represents 1:1 line and the black line and area between blue-dashed lines represent the regression line and 95% confidence interval respectively. The observed values are in situ LAI data that were not used for model development.

5.3.5. Multi-Scale Mangrove LAI Mapping

The semi-empirical LAI estimation from different sensors at the same location yielded different results (Figure 5.8). AVNIR-2 imagery (Figure 5.8b) and a segmentation scale of 30 for WV-2 imagery (Figure 5.8e) were used as the benchmarks for mangrove LAI estimation on Karimunjawa Island. Generally, the LAI spatial distributions for the pixel-based models were quite similar, especially for the medium (2–4) and high (>4) LAI values. As expected, the derived map from a high-spatial resolution WV-2 image was noisy (Figure 5.7a), because of the high level of pixel heterogeneity (Strahler et al. 1986; Weiss & Baret 1999) reducing its mangrove LAI estimation ability in relation to the 10 m x 10 m field sampling units (R^2 = 0.62, RMSE = 1.15). On the other hand, the low-spatial resolution of TM (i.e. pixel resolution larger than the targeted elements) caused spatial aggregation of the estimated LAI values, and also decreased its ability to estimate mangrove LAI (R^2 = 0.65, RMSE = 1.24).

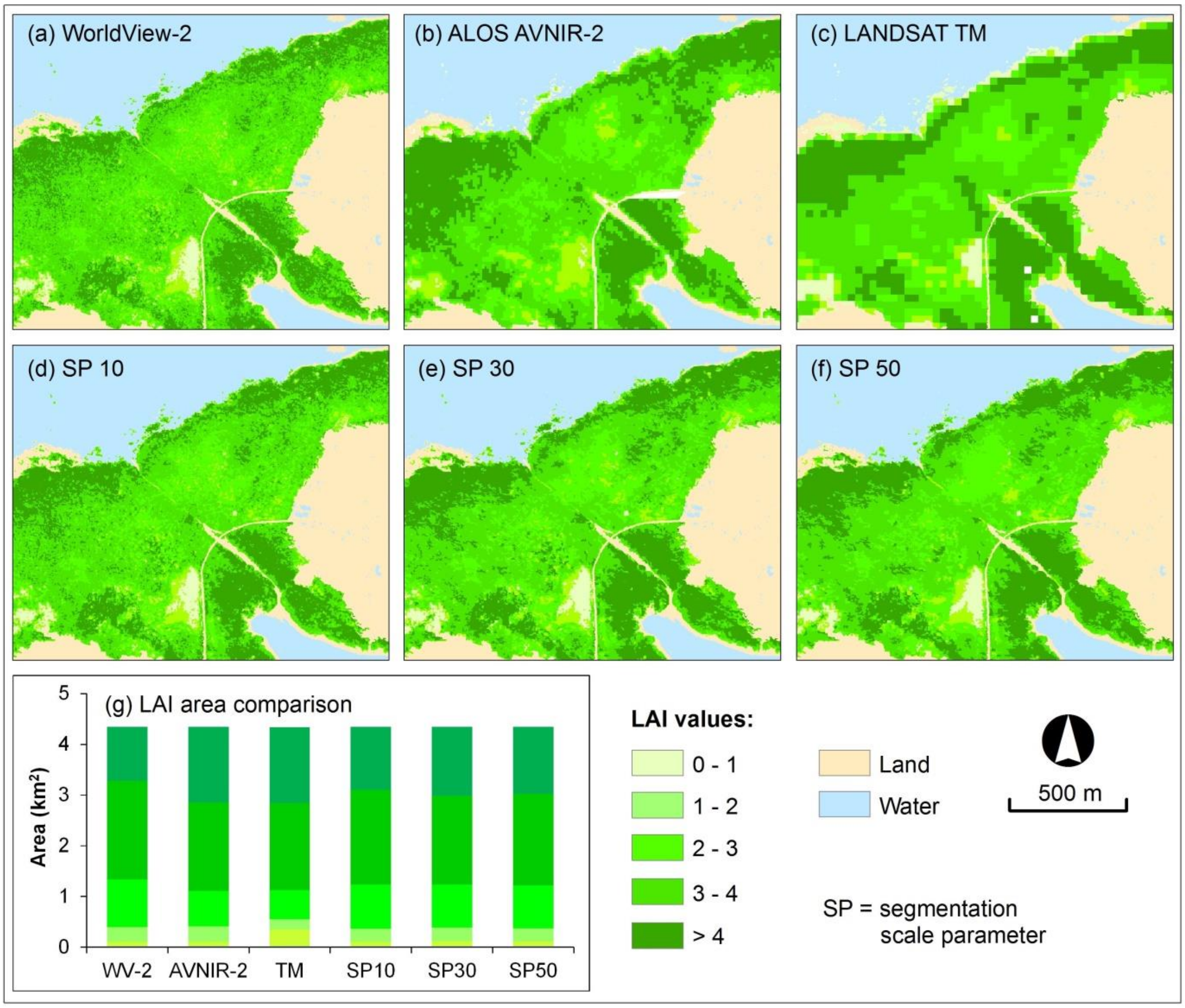

Figure 5.8. Estimated LAI map comparison from different sensors (a – b) and segmentation size (d – f) and the LAI area comparison (f) at Karimunjawa Island. The aggregation of LAI ranges into five classes is for visualisation and comparison purposes only.

The difference in LAI ranges between the three sensors is clearly shown in the LAI area graph (Figure 5.8g). In the WV-2 model, LAI values of 2–3 were overestimated (0.94 compared with 0.69 km^2 in AVNIR-2) and LAI values of > 4 were underestimated (1.06 compared with 1.49 km^2 in AVNIR-2). For the TM model, there were similarities between the WV-2 and TM models, except the overestimation of the LAI values of 0–1 (0.34 compared to 0.11 km^2 in the AVNIR-2 imagery). According to Soudani et al. (2006), the discrepancies between the sensors are influenced by several factors including variation in spectral response, view and illumination conditions, temporal variation of canopy properties and atmospheric effects. More specifically, Teillet et al. (1997) found that the variation of NDVI across different sensors was significantly affected by the differences in spectral bandwidth, especially in the red band. The acquisition date difference among the sensors (especially for Karimunjawa Island [Table 5.1]) might also contribute to the discrepancies of the results. The five-month time span of the image acquisition in this site may have changed the vegetation condition to some extent.

For the estimated LAI values derived from object-based models, the SP30, SP10 and SP50 were compared with the pixel-based WV-2 map. As expected, all of the segmentation maps followed the LAI distribution pattern of the pixel-based WV-2 model. The only difference observed was the variation of the aggregation pattern of LAI classes as a result of the different image objects (i.e. segment) sizes. Larger scale parameter values produced a more distinct and compact class separations, as a result of the increasing aggregation level. However, by looking at the LAI area comparison (Figure 5.8g), there were only slight area differences between SP10, SP30 and SP50. This is most likely because the different segmentation scale parameters affected the LAI objects sizes but not the overall spatial extent of the LAI intervals. So, the areas within a given LAI value interval were clustered into larger objects with similar LAI values by the larger scale parameters and while still maintaining the object boundary between areas with differing LAI values.

5.4. Conclusions and Future Research

This study investigated the effects of different spatial resolutions and aggregation sizes on LAI estimation accuracies from satellite images and field data in two mangrove environments. The ability of WV-2, AVNIR-2 and TM sensors were compared and contrasted to estimate LAI, as well as different pixel averaging windows (3x3, 5x5, 7x7, 9x9 pixels) and segmentation scale parameters (10, 20, 30, 40, and 50) applied to the WV-2 image, using four spectral vegetation indices (SR, NDVI, SAVI and EVI). The analysis of the relationships between in-situ LAI and SVIs from different sensors and segmentation size were investigated by means of regression models.

This study found that LAI estimation accuracy from remote sensing data was site specific. The different mangrove environments (i.e. homogenous versus heterogeneous stands) have different LAI value distribution patterns. The LAI value distributions for the homogenous mangrove stand has less variation compared to the heterogeneous stands, which influence the LAI regression models. Looking into more detail within the mangrove stand, the LAI values were overlapping between formations. Hence, LAI values were independent of the mangrove formation (i.e. scrub, low-closed forest, closed forest, etc.). Instead, the LAI value depends on the local spatial variation of mangrove phenological stages and canopy cover. Overall, the relationship between in situ LAI model samples and SVIs across sensors and segmentation scales were adequate to estimate LAI, with the R^2 range from 0.50 to 0.83. In relation to the field plots of 10 m x 10 m, the regression analysis results showed that the pixel size of different sensors affects the ability to estimate LAI. In this case, it was found that the optimum sensor, in relation to the collected field data to estimate and map mangrove LAI for both of the study sites, was AVNIR-2 with 10 m pixel sizes. This pixel size corresponded to the average size of the dominant mangrove object, i.e. mangrove tree canopy or groups of smaller tree canopies) as well as the ground resolution element of the collected field data.

The results from the WV-2 pixel averaging showed that pixel window size corresponding to the extent of the field plots (i.e. 5x5 or 7x7, equivalent to about 10 m x 10 m to 14 m x 14 m pixel sizes) yielded better LAI estimation than individual pixels (2 m x 2 m). Similar results were also found from the object-based segmentation of WV-2 image. It demonstrated that semi-empirical statistical modelling of LAI using an object-based approach improved the estimation ability (i.e. increasing R^2 from the pixel-based approach). It was also confirmed that the optimum segment sizes were about the size of the field plots and the average mangrove canopy size for both sites. Therefore, the optimum pixel size to estimate LAI is strongly dependant on the spatial patterns and size of the dominant canopy of the area of interest and the field sampling size. NDVI achieved better LAI prediction in most cases compared with the other SVIs, although not statistically different. It was also evident from the validation results that the use of NDVI for estimating LAI produced the lowest RMSE. The findings of this study provide an understanding of the relationship between pixel resolutions, field plot size and the spatial variation of mangrove vegetation for estimating mangrove LAI. The results of this study may serve as a guide to optimally select the optical remote sensing datasets to estimate and map mangrove LAI.

The results of this work were limited to the study sites in Moreton Bay and on Karimunjawa Island with similar average canopy sizes. To verify the findings, similar research, focusing on the more detailed effects of spatial aggregation for different mangrove spatial patterns or canopy sizes, needs to be conducted in the future. It is also important to further investigate the influence of different field plots sizes in relation to imagery with multiple spatial resolutions for semi-empirical LAI estimation. Lastly, it is necessary to investigate the ability of LiDAR data for estimating LAI to support the context of this research.

CHAPTER 6:

GUIDELINES FOR MULTI-SCALE IMAGE-BASED MANGROVE MAPPING

This chapter summarises the findings from previous research chapters (Chapters 3, 4 and 5) and analyses the relationships between image resolutions, mapping approaches, the type and level of information acquired and their accuracy in mapping mangroves. It synthesises the resultant knowledge to develop guidelines for multi-scale image-based mangrove mapping.

Key Findings:

- *This chapter confirms that remote sensing spatial and temporal dimensions can be fitted into the spatio-temporal ecological hierarchical organisation of mangroves.*
- *This chapter also reveals the relationships between image spatial resolution, level of information detail and the accuracy of the resultant maps of mangrove properties.*
- *The multi-scale image-based mangrove mapping guidelines provide an effective and efficient way to select the best image datasets to map mangrove feature(s) at a relevant scale and can be viewed from either an information-driven (user) or image datasets-driven (producer) perspective.*

No paper publication is associated with this chapter

6.1. Introduction

Selecting the most appropriate image spatial resolution and mapping techniques for mangrove mapping is essential to support mapping, management and monitoring in this environment. In this thesis, the analysis of the most appropriate image spatial resolution and mapping techniques for mangrove composition and LAI mapping was built on the exploratory approach developed in the framework for selecting appropriate remote sensing data for environmental monitoring and management by Phinn (1998). First, a conceptual spatial and temporal hierarchical organisation of mangroves was established, from the landscape scale down to individual plants (presented as part of Chapter 1). The concept synthesises the knowledge of the eco-geomorphic hierarchical interactions that occur in both directions (Twilley et al. 1999) and provides a means to interpret the image datasets. Second, utilising the approach of Cohen et al. (1990) and Johansen & Phinn (2006), the high-resolution WV-2 image data (original and pan-sharpened) were resampled to several larger pixel sizes in order to examine the relationship between image pixel size and the mangrove features able to be mapped (Chapter 3). Semi-variogram analysis was conducted to find the scale of the targeted mangrove features in relation to the different image pixel sizes. Third, the domain of scales of the targeted mangrove features were related to the mangrove conceptual hierarchical model and exploratory mapping was conducted using selected image datasets and processing techniques for mangrove composition and LAI mapping (Chapters 4 and 5). The specific output from this stage determines the scale characteristics of the selected mangrove features and the pixel size at which these features can be detected, mapped and measured using remote sensing image data. The final stage will provide a basis for specifying optimal image datasets and processing techniques for multi-scale mangrove mapping.

Selecting the most appropriate image datasets to map a targeted attribute or answer a specific question in mangroves, or any other vegetation ecosystem, is a challenging task. To answer questions of *which remote sensing datasets are the best to map certain mangrove features, or what mangrove information could be obtained from a remote sensing dataset,* one requires some relevant knowledge and experiences. The solution requires an understanding of (1) the nature of the object being investigated (Marceau et al. 1994b), (2) the typical appearance of the object in the scene, (3) the expected output information detail, (4) the information extraction techniques required (Woodcock & Strahler 1987), (5) the characteristics of the image data, (6) the known ability of the data (Lefsky & Cohen 2003), and (7) the project constraints (i.e. time and cost) (Phinn et al. 2000). The decision of which image datasets and processing techniques should be used to deliver the best product is a result of the interaction between these factors.

At the same time, the recent development of remote sensing technology provided a wide range of image datasets available both commercially and for research purposes. As a result, the selection of image datasets for a specific application became more difficult. Warner et al. (2009) mentioned three related issues that added to the complexity of selecting image datasets. First, there are fundamental physical and engineering trade-offs that limit the details of the data from the ground scene able to be recorded by the imaging system sensors. Given the limited resources, a trade-off has to be made regarding the spatial, spectral, temporal and radiometric resolution of an image that can be acquired (Key et al. 2001). Second, finding the balance between the level of detail of the image source and expected derived information is not an easy task. Data with too little detail will reduce the quality of analysis. On the other hand, data with too much detail results in lower overall accuracy due to an increase in within-class spectral variability (Chusnie 1987; Marceau & Hay 1999). Third, it is necessary to match the scale of analysis to the scale of the phenomenon under investigation (Wiens 1989). Environmental inferences are scale-dependent, so conclusions reached at one scale of analysis may not be easily applied to other scales (Marceau & Hay 1999; Schaeffer-Novelli et al. 2005). Therefore, an understanding of the effect of scale variation in the mangrove information is needed in order to use remote sensing datasets appropriately to map mangrove features at a relevant scale(s).

“Scale” is one of the major research areas in the field of ecology and remote sensing (Wiens 1989; Goodchild & Quattrochi 1997; Marceau & Hay 1999). From an ecological point of view (as discussed in the section 1.4.2), mangrove environments can be organised in spatial and temporal dimensions. Along the spatial dimension continuum, a specific size of mangrove features resides at a specific observation scale, from the landscape scale to individual tree level. Putting this pattern into a remote sensing perspective, mapping mangrove environments at different observation scales (i.e. spatial resolutions) will result in different levels of mangrove information. This relation leads to several overlapping scale issues between remote sensing and mangrove ecology (Figure 6.1), which are addressed in this thesis. The underlying conceptual question for this relationship is how the spatial and temporal resolution variation of remote sensing image data fit the mangrove spatio-temporal hierarchical organisation. By understanding how mangroves are ecologically organised in spatial and temporal dimensions and the capability of different resolutions of remote sensing data to detect and map mangrove features, the linkage between these two disciplines can be established. Once the conceptual linkage is established, technical questions remain such as which image spatial resolution can detect targeted mangrove feature(s), or vice versa, what can be mapped from a specific image spatial resolution and how to map targeted mangrove feature(s) from selected remote sensing image datasets.

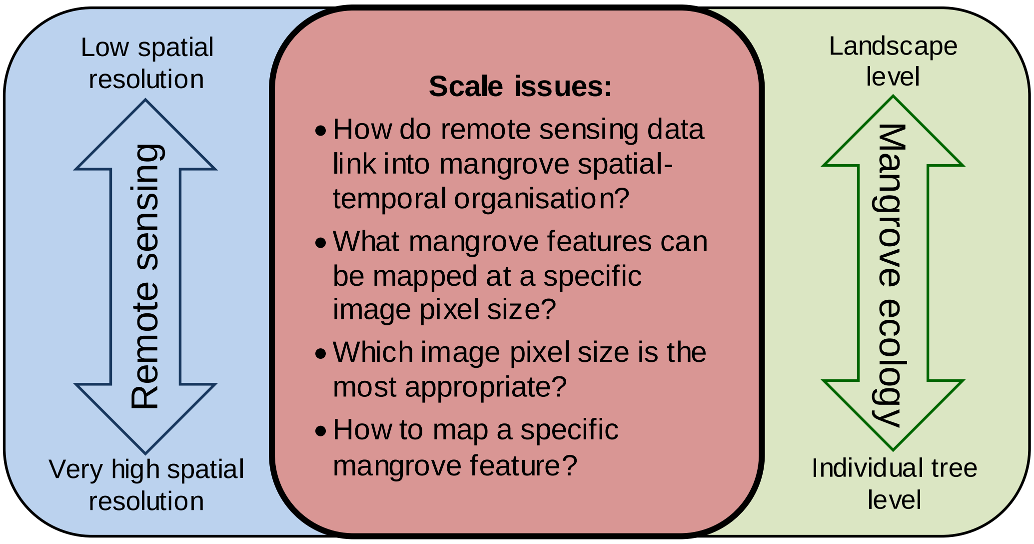

Figure 6.1. Overlapping scale issues between remote sensing and mangrove ecology addressed in this thesis.

Mapping mangroves at specific spatial scales will help scientists to focus their research on the ecological questions that are appropriate to each level of ecological detail (Delcourt et al. 1983), and assist managers to focus on the conservation activities at ecologically relevant spatial and temporal scales (Schaeffer-Novelli et al. 2005). In the field of mangrove mapping, there is a substantial knowledge gap dealing with remote sensing approaches; questions remain about what type of mangrove information can be mapped at specific image resolutions and the level of detail that information can provide. The challenging task of selecting the most appropriate image datasets for mangrove mapping corroborate the need for conducting a systematic study to reveal the relationship between image spatial resolution and the mangrove features able to be mapped. This chapter addresses this issue by synthesising the findings from previous research chapters (Chapters 3, 4, and 5) and utilising relevant information on image-based mangrove mapping from the relevant literature. The result is presented in the form of a guideline for multi-scale mangrove mapping.

6.2. Integrating Remote Sensing into the Spatio-Temporal Organisation of Mangroves

According to Delcourt et al. (1983), in vegetation studies, different physical and biological processes influence the vegetational patterns observed at each spatial-temporal scale. An obvious implication of this hypothesis is that the hierarchical scale pattern of mangroves would be visible from remote sensing data (Cullinan et al. 1997). Based on the ecological spatial and temporal hierarchical organisation of mangroves (presented in section 1.4.2), the hypothetical relationships between remote sensing and the mangrove hierarchy were proposed (Figure 1.4). The pixel size domain required to detect the mangrove features was summarised from literature on mangrove and vegetation mapping using image datasets. By examining the pattern of where the specific image spatial resolution is frequently used to map certain vegetation features, the pixel size of the image datasets was then placed alongside the spatial scale of the feature's spatial scale continuum. The particular focus of this thesis is the mangrove features that compose mangrove vegetation communities from individual tree level up to the landscape level. It includes individual shrub crown or foliage clumping, individual tree crown and species type, tree patches or canopy gaps, vegetation formation and zonation, vegetation cover types and the larger environmental setting of the mangrove forest.

Chapter 3 of this thesis provides *a proof of concept* of the pixel size domain in the hypothetical relationships by characterising the spatial structure of mangrove vegetation features based on the examination of six different image pixel sizes. Semi-variogram analyses were performed to reveal the spatial size or scale domain pattern of the mangrove vegetation features. By examining the semi-variograms range and form, the dominant size of mangrove vegetation features in relation to the spatial distance (i.e. lag distance) can be identified. Smaller pixel sizes detect more mangrove features than larger ones. Single shrub crowns and foliage clumping were detected at a pixel size of 0.5 m or lower and canopy gaps and single tree crowns at 1 m or 2 m. Larger features, such as tree patch or larger gaps were identified with a pixel size of 4 m, vegetation formation or zonation were identified at 8 m and vegetation cover type at 10 m or larger. At the same time, the actual size of the targeted mangrove features were measured from the field and aerial photograph, and identified from the semi-variogram analysis (Table 3.3).

Figure 6.2 synthesises the link between remote sensing and ecological mangrove hierarchical organisation, which is an updated version of Figure 4.1. This figure provides an overview of the spatial and temporal dimensions of both remote sensing and ecological mangrove hierarchy, along with the example of associated image datasets commercially available and commonly used for vegetation mapping and monitoring (see Appendix 8 for the detailed image characteristics). A summary of spatio-temporal mangrove structures and processes and the required image resolution related to Figure 6.2 was presented in Table 6.1. It shows the detailed ecological structure and processes of mangroves at each level, summarised from Holling (1992), Duke et al. (1998), Farnsworth (1998), Twilley et al. (1999), and Feller (2010). Through this figure and table, the relationship between these two fields can be shown explicitly; and at the same time it provides guidance for selecting appropriate image resolutions (spatial and temporal) to map specific mangrove features. These mangrove features can be used as a base mapping unit for other applications, such as LAI, biomass and carbon storage estimation, species distribution, and so on.

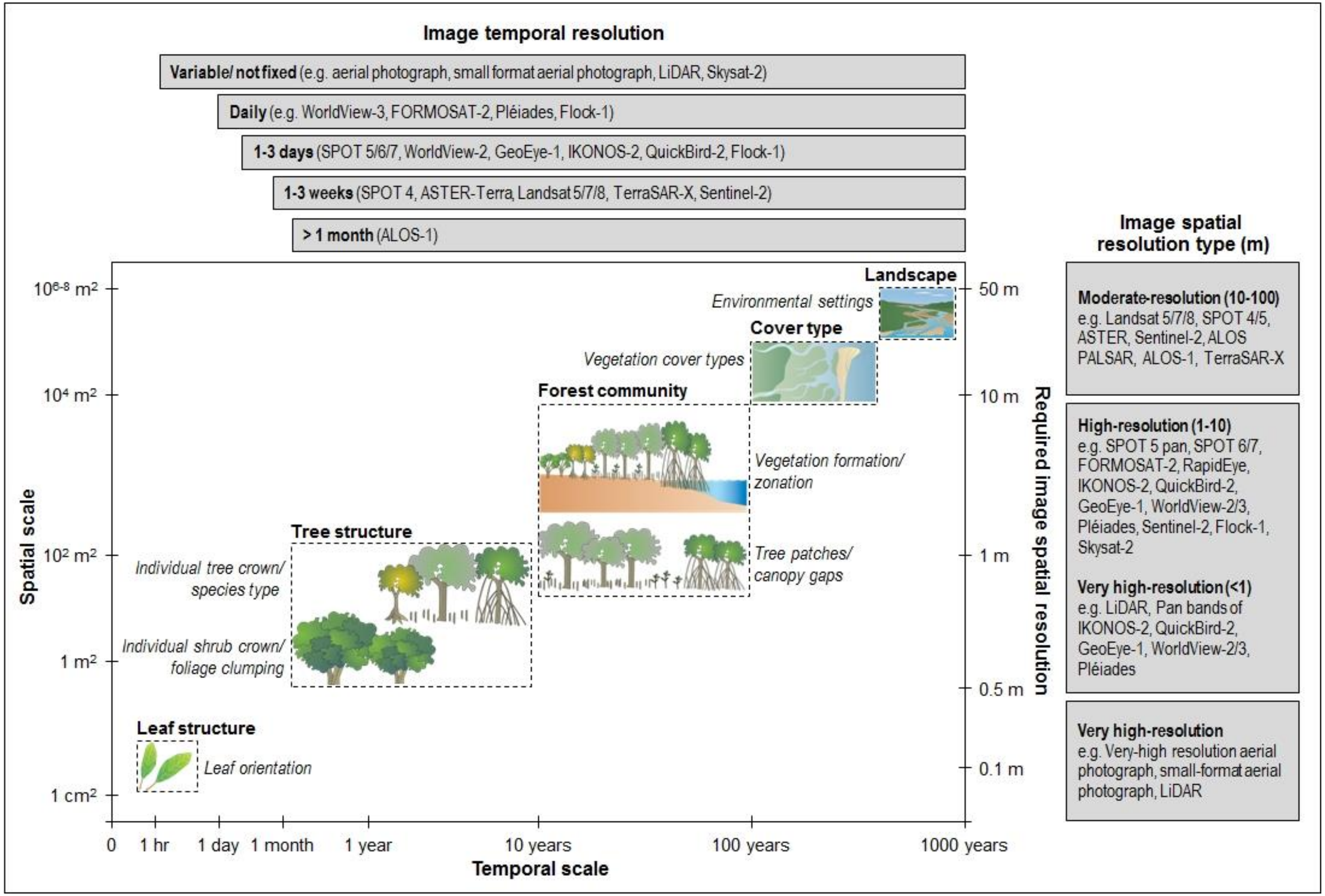

Figure 6.2. Temporal and spatial hierarchical organisation of mangrove features identifiable from remotely-sensed images and the required image spatial resolution and image types for mapping the features. (*Symbols are courtesy of the Integration and Application Network, University of Maryland Center for Environmental Science - ian.umces.edu/symbols/*).

Table 6.1. Spatio-temporal hierarchical levels of mangrove structure and process, and the corresponding required remote sensing datasets.

Feature level	Scales		Categories of structure processes	Structure variables	Structure processes	Required image resolution	
	Space	Time				Spatial	Temporal
Leaf	0.01 – 0.1 m^2	1 hr – 1 day	Plant physiological process	Leaf and branches clusters, orientations, and ages	Photosynthesis, respiration, decomposition, nutrient uptake	< 0.5 m	1 hr – 1 day
Individual shrub crown/ foliage clumping	0.1 – 10 m^2	1 month – 10 years	Auto-ecological process	Tree crown forms and sizes, tree species	Plant growth, seed production, foraging on vegetation, decomposition	0.5 – 2 m	$\geq$ 1 day
Individual tree crown/ species type	10 – 100 m^2	1 year – 10 years					
Tree patches/ canopy gaps	100 – 1000 m^2	10 – 100 years	Plant competitive process of gaps dynamics	Dominant and sub-dominant tree	Tree growth, competition, mortality, vegetation effects on micro-climate	1 – 4 m	> 1 month
Vegetation formation/ zonation	1 – 10 km^2	10 – 100 years	Meso-scale disturbance and dispersal process	Plant community structure, tree age and density, micro-topography	Physiognomic differences, disturbance, dynamics, seed dispersal	4 – 10 m	> 1 month
Vegetation cover types	10 – 100 km^2	100 – 500 years	Watershed process	Topography: vegetation, water, bare soil	Erosion, watershed hydrology, meso-climatic interaction with vegetation	10 – 30 m	> 1 month
Environmental setting	> 100 km^2	500 – 1000 years	Evolutionary process	Precipitation, temperature, bed rock	Evolution, geomorphology, planetary dynamics	30 – 50 m	> 1 month
Sources:	(Holling 1992; Duke et al. 1998; Farnsworth 1998; Twilley et al. 1999; Feller et al. 2010)					(Kamal et al. 2014)	

6.3. Relationships Between Image Data, Mapping Approach and Map Accuracy

The relationships analysis in this study built upon a statement by Woodcock and Strahler (1987, p. 312) that: "*the appropriate scale of observations is a function of the type of environment and the kind of information desired*". More specifically, the choice of an appropriate scale depends on four factors; (1) the output ground scene information desired, (2) the methods used to extract information from images, (3) the spatial structure of the object on the scene, and (4) the type of environment being investigated (Woodcock & Strahler 1987; Phinn et al. 2000). Each of those factors significantly contributes to the successful implementation of remote sensing-based environmental mapping and monitoring.

Within the context of this study, the relationships derived from image analysis and mapping processes in Chapters 3, 4 and 5 were investigated. The output map products from these chapters can be considered in two main categories. First, mangrove composition maps covering the mangrove vegetation features able to be detected from remote sensing data, from landscape scale down to individual trees. The results include vegetation boundary, mangrove stands, mangrove zonation, individual tree crowns and species community. Second, mangrove LAI maps produced from different image spatial resolutions and locations. In terms of mapping technique, GEOBIA was used to derive mangrove composition information based on a single image dataset or by images combination. For the LAI mapping, both pixel-based and object-based models were used to estimate the LAI values of the mangroves.

Chapters 4 and 5 of this thesis were the empirical implementations of the relationships between remote sensing and mangrove ecological hierarchy (Figure 6.2) into real image datasets. The relationships between image datasets, mapping approach, information derived and map accuracy was presented in Table 6.2. For the mangrove composition mapping, images with a smaller pixel size were able to detect, identify and map more mangrove features accurately than the larger pixel size. Referring back to the conceptual framework of the pixel sizes relative to objects in the scene by Strahler et al. (1986), the effects of H- and L-resolution were evident in this study. Although image segmentation can reduce the scene variance by merging several relatively homogeneous pixels into a segment (Blaschke et al. 2000), the pattern of increasing accuracy by increasing spatial resolution of the image was obvious. For example, there was an increase in the accuracy of regional land-cover type and local vegetation community maps clearly observable from Table 6.2 through the increase of image spatial resolution. Therefore, image spatial resolution (i.e. pixel size) significantly affects the accuracy of mangrove feature maps.

Table 6.2. Relationships between image spatial resolution, mangrove features and mapping accuracy.

Mapping approach		Mangrove features	Image datasets: Moderate resolution, multispectral Landsat TM	Moderate resolution, multispectral ALOS AVNIR-2	High resolution, multispectral WorldView-2	High resolution, multispectral WorldView-2 + LiDAR	Very high resolution, multispectral WV-2 (pan-sharpened) +LiDAR	Very high resolution, multispectral WV-2 (pan-sharpened)
		Increasing image spatial resolution →						
Mapping approach	Mangrove composition (object-based)	**Regional land-cover type** (vegetation and non-vegetation)	**89%**	**93%**	**97%**	* Chadwick 2011	**	**
		Local vegetation community (mangroves and non-mangroves)	**82%**	**82%**	**85%**	**94%**	**	* Heenkenda et al. 2014
		Local mangrove zonation (mangrove zonation and formation)	ND	**46%**	**53%**	**59%**	**	* Heenkenda et al. 2014
		Tree canopy structure (tree crowns and gaps)	ND	ND	ND	ND	**64%**	**68%**
		Individual tree species (mangrove tree species) ↓ Increasing information detail	ND	ND	ND	ND	**53%**	**54%**
	Mangrove Leaf Area Index (pixel-based)		**0.74**	**0.83**	**0.68**	**	**	**
	Mangrove Leaf Area Index (object-based)		**	**	**0.70**	**	**	**

Mangrove composition accuracy figure was based on the overall accuracy calculation in Table 4.5.
Mangrove LAI accuracy figure was based on the Pearson's correlation average of the sites from the LAI model validation in Table 5.4.
* : unable to assess; assumed to have high accuracy based on the previous studies using similar image type.
** : not performed.
ND: Not Detected (i.e. unable to detect the object).

Accuracy colour code:										
Overall accuracy (%):	0-10	10-20	20-30	30-40	40-50	50-60	60-70	70-80	80-90	90-100
Pearson's correlation:	0-0.1	0.1-0.2	0.2-0.3	0.3-0.4	0.4-0.5	0.5-0.6	0.6-0.7	0.7-0.8	0.8-0.9	0.9-1.0

By interpreting Table 6.2 in more detail, the mapping accuracy pattern for mangrove composition along the image and mangrove features domains suggested that:

- low spatial resolution images had less ability to depict mangrove features than high-resolution images
- the accuracy of composition mapping increased by increasing the image spatial resolution
- the accuracy of mapping decreased with the increased level of mangrove feature details and the number of mangrove vegetation feature classes
- images with a large number of spectral bands enabled more flexibility in classifying targeted objects, which in turn increased the accuracy of the map
- the effects of within-pixel heterogeneity in the high-spatial resolution images could be eliminated using image segmentation at the correct scale, while maintaining the boundary of the targeted objects
- the inclusion of contextual information increased the accuracy of the maps.

Summarising from the points above, the relationships between image resolutions (spatial and spectral), detail level and number of classes of targeted information and accuracy in mangrove composition mapping is presented as Figure 6.3. The behaviour of image spatial and spectral resolution and the number of classes and level of information detail in relation to mapping accuracy are inversely related. The map accuracy increases with increasing image spatial and spectral resolution but it decreases with increasing numbers of classes and levels of information detail. The discussion about this trend was provided in detail in section 4.3.4.

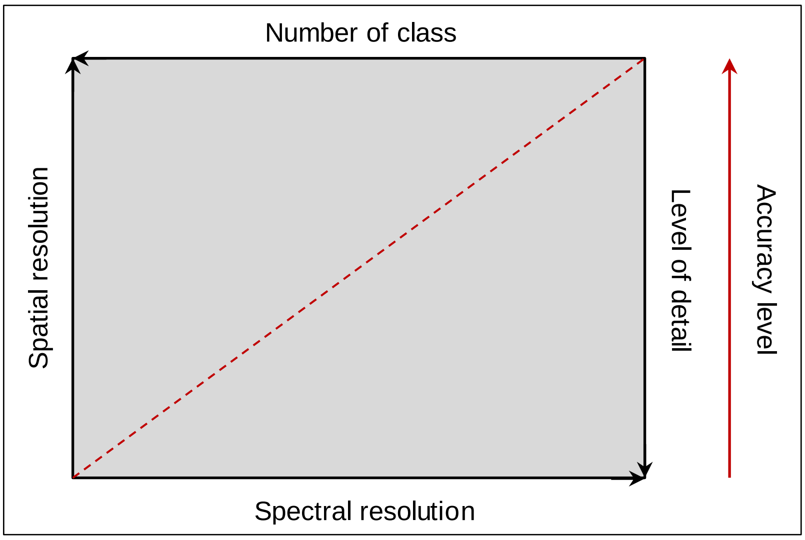

Figure 6.3. Relationships of image resolutions, level of information details and map accuracy resulted from the empirical mangrove composition mapping. The arrows on the axes indicate an increase of the variable values and the red-dashed line shows the accuracy trend.

The accuracy pattern for mangrove LAI mapping shown in Table 6.2 was different to the mangrove composition pattern. According to the examination of different pixel sizes from three different images (TM, AVNIR-2 and WV-2) for LAI estimation, there was no clear pattern of the estimation accuracy in relation to the variation of pixel sizes. The main conclusions were:

- high image spatial resolution does not necessarily provide a better estimate of LAI compared to a lower spatial resolution
- the optimum pixel size or average segment size for LAI estimation corresponds to the dominant mangrove object size in the area of interest
- the optimum pixel size is also influenced by the field LAI sampling size (i.e. plot or quadrat)
- an object-based approach slightly improved the LAI estimation accuracy compared with the pixel-based approach.

6.4. Guidelines for Multi-Scale Mangrove Mapping

This section provides condensed guidelines for the selection of the most suitable remote sensing datasets and processing technique in order to map and monitor different mangrove features. The main part of the section gives an overview of the capabilities of different image datasets and techniques to detect, characterise, map and monitor mangrove features, and can be used to initially constrain the choice of methods to a few techniques that seem most feasible for mangrove mapping.

There is no unique spatial resolution appropriate for the detection and discrimination of all objects on an image scene (Marceau et al. 1994b). Most of the image scenes consisted of multiple objects with variation of sizes. Depending on the object of interest, selections of image datasets are often arbitrary. Different problems require different image resolution and mapping approaches and the highest resolution is not required for all situations. A set of guidelines for selecting the most appropriate image dataset was developed based on the remote sensing-embedded spatio-temporal organisation of mangroves (Figure 6.2) and the table of relationships analysis (Table 6.2). Aside from the limitations of the study (i.e. image datasets and mapping techniques used), the proposed guidelines will clarify questions about the relationships between image types and the targeted information. This includes; (1) what type and level of mangrove information can be extracted, (2) what are the appropriate image datasets, and (3) what type of mapping technique can be used appropriately to derive the targeted information. The scheme for the optimum multi-scale mangrove mapping is presented in Table 6.3.

Table 6.3. Guideline for selecting an image dataset for mangrove mapping. Colours of the box show corresponding selection flow.

1. Identify the targeted objects				2. Determine the resolutions of image dataset (with image examples)			3. Determine the processing technique	Study example
Feature level	Feature size	Variable to map	Output scale	Spatial	Spectral	Temporal		
Individual shrub crown	0.1 – 10 m²	Shrub/ foliage clumping Species Community Composition	1:1,000 – 1:5,000	**0.5 – 2 m** *Aerial photograph, WorldView-2/3, GeoEye-1, QuickBird, Pléiades, IKONOS-2 pan, Skysat-2, FORMOSAT-2 pan, LiDAR*	*All*	Single date: *All*	Object-based Pixel-based Hybrid approach	(Heenkenda et al. 2014) (Everitt et al. 2008) (Heenkenda et al. 2014)
		Height Biomass Carbon stock			*LiDAR*	Single date: *LiDAR*	LiDAR processing	(Wannasiri et al. 2013)
		Change detection			*All*	Multi dates: Variable: *AP, LiDAR* Daily: *WV-3, FORMOSAT-2* 1-5 days: *WV-2, QB-2* 1-4 weeks: *IKONOS-2, Pléiades*	Object-based Pixel-based Hybrid approach	- - -
Individual tree crown	10 – 100 m²	Tree crown Species Community Composition	1:1,000 – 1:5,000	**0.5 – 2 m** *Aerial photograph, WorldView-2/3, GeoEye-1, QuickBird, Pléiades, IKONOS-2 pan, Skysat-2, FORMOSAT-2 pan, LiDAR*	*All*	Single date: *All*	Object-based Pixel-based Hybrid approach	(Wang et al. 2004a) (Wang et al. 2004b) (Heenkenda et al. 2014)
		Height Biomass Carbon stock			*LiDAR*	Single date: *LiDAR*	LiDAR processing	(Chadwick 2011)
		Change detection			*All*	Multi dates: Variable: *AP, LiDAR* Daily: *WV-3, FORMOSAT-2* 1-5 days: *WV-2, QB-2* 1-4 weeks: *IKONOS-2, Pléiades*	Object-based Pixel-based Hybrid approach	- - -
Tree patches/ canopy gaps	100 m² – 1 km²	Tree patch Community Zonation Composition Cover density LAI	1:2,000 – 1:10,000	**1 – 4 m** *Aerial photograph, WorldView-2/3, GeoEye-1, QuickBird, Pléiades, IKONOS-2, Skysat-2, Flock-1, FORMOSAT-2 pan, ALOS PRISM, SPOT 6/7 pan, LiDAR*	*All*	Single date: *All*	Visual interpretation Object-based Pixel-based Hybrid approach	(Dahdouh-Guebas et al. 2006) (Proisy et al. 2007) (Neukermans et al. 2008) (Heumann 2011a)
		Height Biomass Carbon stock			*LiDAR*	Single date: *LiDAR*	LiDAR processing	(Zhang 2008)
		Change detection			*All*	Multi dates: Variable: *AP, LiDAR* Daily: *WV-3, FORMOSAT-2* 1-5 days: *WV-2, QB-2, SPOT 6/7* 1-4 weeks: *IKONOS-2, Pléiades* >1 month: *ALOS PRISM*	Visual interpretation Object-based Pixel-based Hybrid approach	(de Oliveira Vasconcelos et al. 2011) - - -
Vegetation formation/ zonation	1 – 10 km²	Extent Local distribution Zonation Composition Cover density LAI	1:10,000 – 1:20,000	**4 – 10 m** *RapidEye, FORMOSAT-2, ALOS AVNIR-2, SPOT 4 pan, SPOT 5/6/7, Sentinel-2, ALOS PALSAR, LiDAR*	*All*	Single date: *All*	Visual interpretation Object-based Pixel-based	(Saito et al. 2003) (Conchedda et al. 2008) (Gao 1999)
		Height Biomass Carbon stock			*LiDAR, PALSAR*	Single date: *LiDAR, PALSAR*	LiDAR and PALSAR processing	(Lucas et al. 2008)
		Change detection			*All*	Multi dates: Variable: *LiDAR* Daily: *RapidEye, FORMOSAT-2* 1-5 days: *SPOT 6/7* 1-4 weeks: *SPOT 4/5* >1 month: *ALOS AVNIR, ALOS PALSAR*	Visual interpretation Object-based Pixel-based	(Manson et al. 2003) (Conchedda et al. 2007) (Nguyen et al. 2013)
Vegetation cover types	10 – 100 km²	Extent Regional distribution Cover density LAI	1:20,000 – 1:60,000	**10 – 30 m** *FORMOSAT-2, ALOS AVNIR-2, SPOT 4, SPOT 5/6/7, Landsat 5/7/8, Sentinel-2, ALOS PALSAR, TerraSAR-X*	*All*	Single date: *All*	Visual interpretation Object-based Pixel-based	(Benfield et al. 2005) (Myint et al. 2008) (Manson et al. 2001)
		Height Biomass Carbon stock			*PALSAR, TerraSAR*	Single date: *PALSAR, TerraSAR*	PALSAR and TerraSAR processing	(Lucas et al. 2010)
		Change detection			*All*	Multi dates: Daily: *FORMOSAT-2* 1-5 days: *SPOT 6/7* 1-4 weeks: *TerraSAR, Landsat 5/7/8, SPOT 4/5* >1 month: *ALOS PALSAR*	Visual interpretation Object-based Pixel-based	(Manson et al. 2003) (Conchedda et al. 2008) (Giri & Muhlhausen 2008)

The structure of the guidelines in Table 6.3 was ordered based on the typical steps followed in remote sensing projects. It starts with identifying the goals of the project that includes targeted objects, the average size of targeted objects, variability of the object commonly mapped and the expected output map scale. It can also be extended to the cost and budget to decide what image data can be obtained in the next step. The feature level and size were derived from Table 6.1 and serve as the mapping unit of the targeted object. The relationship between output map scale and image spatial resolution was determined using the "rule of thumb" by Tobler (1987) and a guideline by McCloy (2005). It suggests the detectable size (in meters) on a map is obtained by dividing the map scale denominator with 1000; the spatial resolution is half of the detectable size. For instance, using a 2 m image pixel size, one can create a map up to the scale of 1:4000 (2 m x 2 x 1000).

The second step is to determine the image resolutions needed to map the targeted object. The spatial resolution dimension was derived from Figure 6.2 and Table 6.1 and acts as the first filter in selecting the image. Several commercially available images associated with the required spatial resolution were used as examples. To narrow down the image selection, spectral and temporal resolutions of the image were incorporated. The spectral dimension indicates whether the targeted object needs to be mapped using a specific wavelength or sensor (refer to Appendix 8 for the detailed description) and the temporal dimension provides selection of the temporal limitation of the images. The final step is to select the appropriate processing technique to derive the targeted information from the selected image. Due to the unlimited options of the processing techniques available, the guidelines show only the general divisions of image processing commonly and potentially used to complete the tasks, along with some related studies as reference.

This set of guidelines can be viewed from either an information-driven (user) or image datasets-driven (producer) perspective. The first is as the sequence explained above, which starts from the selection of the targeted information and following up by the image type and processing technique selection. The second starts by selecting the image and following the box colour to figure out (1) what type of mangrove features can be mapped from the image, (2) at what scale level, and (3) which processing technique should be used. For example, due to a major flood, one needs to map the change in the mangrove species community at tree level within a week. By following the blue boxes in the second row, the best image for this purpose can be seen to be either WorldView-2 or QuickBird-2; the mapping technique could be pixel-based, object-based or a combination of both. Putting this example the other way around, one can see from the table that a WorldView-2 image is able to map the listed mangrove features at tree level detail with an expected map scale up to

1:4000. Therefore, these guidelines provide an effective and efficient way to select the best image datasets to map mangrove feature(s) at a relevant scale.

A key point associated with developing guidelines is to assess its applicability and transferability from one situation to another – between sites, between countries or between scales (MacKay et al. 2009). In remote sensing-based mangrove mapping, the widely applicable and transferable mapping approach is still in question (Blasco et al. 1998; MacKay et al. 2009; Heumann 2011b; Kuenzer et al. 2011). To address this issue, the guideline was developed from the findings of multi-scale mangrove mapping conducted at Moreton Bay (Australia) and Karimunjawa Island (Indonesia), which have different environment settings and mangrove characteristics. These guidelines have been designed to be as simple and flexible as possible, yet cover the aspects needed for selecting the image. Therefore, if needed, they can accommodate any modifications and adjustments in relation to its applicability and transferability to other mangrove environments.

6.5. Conclusions and Future Research

The objective of this chapter was to address the challenge of selecting an appropriate image dataset and processing algorithm for mangrove mapping. This aim was initially accomplished by analysing the relationships between image resolutions, mapping approaches and the type of information acquired and their accuracy in mapping mangroves. The results were used to develop guidelines for multi-scale mangrove mapping based on the findings from Chapters 3, 4, and 5. Providing this information is essential to assist the mapping, measurement, monitoring and modelling of mangroves at the relevant spatial and ecological scales, which in turn provides support to build understanding of mangrove ecosystems and how they are changing.

This chapter confirmed that remote sensing spatial and temporal dimensions can be fitted into the spatio-temporal hierarchical organisation of mangroves (Figure 6.2). The guidelines serve as a basis for selecting image datasets to appropriately map and address mangroves problems at a relevant scale. This chapter also revealed the relationships between image spatial resolution, level of information detail, and the accuracy of the resulted maps (Table 6.2). Smaller pixel sizes tend to depict more detailed features and have higher map accuracy; however, smaller mangrove features and more feature classes decrease the accuracy of the maps. By synthesising these findings, the guidelines for selecting an image dataset for mangrove mapping were proposed.

The guidelines address the lack of knowledge on the relationships among image resolutions and types, mapping approaches and the level of information detail able to be produced in the mangrove environment. They summarise how remotely-sensed data can be used most effectively and most accurately to map mangrove information. From a practical point of view, this guideline assists in; (1) selecting the most appropriate image datasets for the optimal mapping of mangrove composition and LAI at specific scales, and (2) providing direction on the types of information that can be derived from a specific image dataset and how to obtain this information. It covers the aspects of project goals and expectations, image resolution dimensions, available processing techniques and some examples from literature. Depending on the need, the guidelines can be viewed from the user's or producer's perspective.

The results of this chapter were limited by the number and type of images and mapping techniques tested and the mangrove environmental settings used. For future research, to develop more comprehensive mangrove mapping guidelines able to work with globally available image datasets, a wider range of image datasets from multispectral, hyper-spectral and RADAR need to be tested. Likewise, a more detailed assessment of mapping techniques need to be applied to map targeted features, to provide a more detailed mapping technique selection. Future work will also focus on improving the transferability of the guidelines to other mangrove environmental settings.

.

CHAPTER 7:

CONCLUSIONS, SIGNIFICANCE AND FUTURE RESEARCH

This chapter revisits the main findings of the thesis and discusses their specific contribution to the field of remote sensing for mangrove mapping and monitoring. Limitations of the studies are also presented and the directions for future works are suggested.

No paper publication is associated with this chapter

7.1. Summary

Mangroves have a wide range of ecosystem values ecologically, economically and socially. In the recent decades, their existence is under intense pressure from anthropogenic and natural disturbances with an alarming loss rate. There is a significant need to map mangroves and monitor the changes accurately for basic mangrove ecology and their management. It requires a basic understanding of the condition and distribution of mangroves to take the necessary steps to prevent further habitat loss in the future. Remote sensing provides a means for spatially extensive, non-destructive, repeatable, multi-scale and multi-temporal assessment of mangrove status and condition. Advances in remote sensing technology in the past 15 years allow us to explore various types of image datasets with different resolutions, as well as mapping techniques to map mangrove environments. However, effective use of remote sensing data requires a match of the scale of analysis to the scale of the phenomenon under investigation. As an increasing number of airborne and satellite image data types become available for free and commercial use, selection of the most appropriate image resolutions and processing techniques becomes more difficult. At present, there are a limited number of studies and there is still no explicit guideline to answer the question of "*what type of mangrove information can be derived from specific image datasets"*; or vice versa, "*in order to map a particular mangrove feature, which type of image datasets could optimally detect the specific feature?*" This PhD thesis, addresses this knowledge gap by combining remote sensing data dimensions with the mangrove ecological hierarchy and providing guidelines for multi-scale image-based mangrove mapping.

Essential to the effective science and management of mangroves is an understanding of their spatial and temporal ecological structure and process. Based on the differences in process rates, mangrove systems are viewed as being stratified into discrete levels of interacting subsystems, from the landscape scale down to individual plants. On the other side, the detectability of mangrove objects from remote sensing data is dependent on the spatial resolution of the image. In this thesis, the "scale domain" (i.e. range of size) of mangrove objects detectable from remote sensing images was identified and tested to map mangrove composition and LAI in Moreton Bay (Australia) and Karimunjawa Island (Indonesia). This thesis combined the spatial and temporal dimension of remote sensing data into the spatio-temporal continuum of the mangrove hierarchy. It identified the scale domain of the targeted mangrove features and linked it to the optimum image resolutions able to map these features. This resulted in the first explicit relationship between remote sensing and mangrove spatial ecology at multiple spatial and temporal scales. This relationship provided a fundamental basis for selecting the most appropriate image dataset to map specific features of mangroves.

By synthesising this relationship with findings from the empirical mapping tasks and literature, a guideline for multi-scale image-based mangrove mapping was established. It provided a systematic and efficient procedure to select the best image datasets and mapping techniques to map mangrove feature(s) at a relevant spatial and temporal scale. In a broader context, this thesis signifies the utility of remote sensing for mangrove mapping and builds a solid foundation for the implementation of multi-scale image-based approaches to map and monitor mangrove ecosystems. This will produce environmental information ready for scientific and management uses to address ecological problems at relevant spatial and temporal scales.

7.2. Main Findings and Outcomes

The following restates the PhD objectives, followed by the main findings and outcomes that address the objectives of this thesis.

Objective 1: To characterise mangrove spatial structure identifiable at different spatial scales for image-based mangrove mapping.

The major output from objective one was a method that enables the estimation of the optimum pixel size for accurately mapping different sizes of mangrove features. In the case of this thesis, semi-variogram analyses were applied to six simulated image pixel sizes (0.5 m, 1 m, 2 m, 4 m, 8 m and 10 m) of WorldView-2 to investigate the pattern of mangrove features detectable from image datasets. The results showed that semi-variograms detected the variations in the structural properties of mangroves in the study area (Moreton Bay, Australia). Its forms were controlled by the image pixel size, the spectral bands used and the spatial structure of the scene object (e.g., tree or gaps). In terms of the pixel size effect, there was a gradual loss of mangrove vegetation information detail with increasing pixel size and a specific mangrove feature can be optimally identified and mapped from a specific pixel size and spectral band or indices. Specifically, a pixel size of ≤ 2 m was suitable for mapping canopy and inter-canopy-related features within mangrove objects (such as shrub crowns, canopy gaps and single tree crowns), while a pixel size of ≥ 4 m was appropriate for mapping mangrove vegetation formation, communities and larger mangrove features. The major outcome of the analysis results is an optimum pixel resolution scheme for mangrove mapping that provides a basis for multi-scale mangrove mapping and the selection of appropriate remote sensing image datasets for mangrove mapping. Through this study, a better understanding of the relationship between the size of mangrove features and the optimum image pixel size is achieved. Future research is needed to test the consistency of the method at other mangrove environments.

Objective 2: To assess the capability of selected remotely-sensed datasets and mapping techniques to produce mangrove composition and LAI maps at different spatial scales and assess the accuracy of the mapping results.

This objective provided a "proof of concept" of the optimum pixel resolution scheme for mangrove feature mapping developed in objective one. It was empirically applied to some selected image datasets (TM, AVNIR-2, WV-2 and LiDAR) to map mangrove composition and LAI in Moreton Bay (Australia) and Karimunjawa Island (Indonesia). For the first task, the major output was the implementation of the scheme to map five levels of mangrove features, including vegetation boundary, mangrove stands, mangrove zonations, individual tree crowns and species communities. The result demonstrated that GEOBIA, through the mangrove image objects hierarchy, successfully produced mangrove composition maps at discrete spatial scales, with a reasonable level of accuracy. The level of information detail able to be obtained from the image dataset was dictated by image spatial and spectral resolution. Inclusion of contextual information (i.e. DTM or CHM) significantly increased the accuracy of the maps. It is also demonstrated that the accuracy of the produced maps was a result of the interaction between the image spatial resolution, the scale of the targeted objects and the number of land-cover classes of the map. The major outcome of this task is a demonstration that the conceptual spatial and temporal hierarchical organisation of mangroves provides an essential aid for effective multi-scale mangrove composition mapping. This information is necessary to address mangrove ecological problems at relevant spatial scales.

The major output of the second task was the demonstration of LAI variation in maps produced from different image datasets, spectral vegetation indices and mapping approaches (i.e. object- and pixel-based). From an ecological perspective, mangrove LAI variation was dependent on the location, spatial variation of mangrove vegetation (i.e. homogeneous or heterogeneous) and the tree growth stage. From a remote sensing perspective, the optimum pixel size to estimate mangrove LAI correlates to the dominant object size in the area of interest (e.g. the average mangrove canopy size) and the associated field plot size used to correlate field and image data. NDVI was found to be the best estimator of LAI. Based on the mapping approach investigation, image segmentation significantly increased the accuracy of LAI estimates; with the optimum segmentation size for LAI estimates corresponding with the size of the dominant objects on the scene. The major outcome of this task is an understanding of the relationship between pixel resolutions and the spatial variation of mangrove vegetation for estimating mangrove LAI. In other words, the results of this study serve as a guide for the optimal selection of the optical remote sensing datasets to be used to estimate and map mangrove LAI.

Objective 3: To develop guidelines for multi-scale mapping of mangrove composition and LAI suitable for multiple locations.

This objective analysed and synthesised the findings from objective one and two. It combined all of the knowledge obtained in the previous objectives to develop a guideline for multi-scale image-based mangrove mapping. The major outputs of this objective were: (1) a graphical illustration showing the link between remote sensing and ecological mangrove hierarchical organisation; (2) a table of relationships between image spatial resolution, mappable mangrove features and mapping accuracy; and (3) a guideline for selecting image datasets and mapping techniques for mangrove mapping. It linked the image resolution dimensions into the mangrove spatial ecology hierarchy. Specifically, it confirmed that remote sensing spatial and temporal dimensions could be fitted into the spatio-temporal hierarchical organisation of mangroves. It also revealed the relationships between image spatial resolution, level of information detail and the accuracy of the resulted maps. The major outcome of this objective is a guideline that provides an effective and efficient way to select the best image datasets and mapping techniques to map mangrove feature(s) at a relevant spatial and temporal scale. The guidelines facilitate the task of selecting the correct image resolutions to address a particular mapping problem for mangroves at a specific scale.

7.3. Limitations and Future Research

Individual research chapters have addressed the limitations related to the research methods and results. This section will outline some key limitations and future directions.

The primary limitation of this thesis is the transferability of the methods and guideline to other locations with different mangrove environmental settings. The results from the mangrove spatial structure characterisation using semi-variogram was site-specific. It means that in order to obtain a comprehensive pattern of mangrove spatial structure characteristics that is applicable globally, this method needs to be applied to every representative mangrove environment. Another challenge found was the non-transferability of most of the component of GEOBIA mapping rule set developed to map mangrove composition at multiple scales. The detailed component of the rule set was site-, scale- and time-specific. Modifications need to be made to apply the rule set to different locations, images and times. Although the two selected study sites, with very different characteristics and locations, were used in this research, the locations represented a relatively narrow strip of mangrove stands. Therefore, further studies need to be carried out to apply the methods and guidelines to vast and species-rich mangrove forests.

As with any study that involves field survey components, multiple sources of error associated with field data collection can be found. Mangrove forests are not easy to access and sometimes features obstruct the field data collection due to the nature of mangrove forests. This includes the unconsolidated sediment of the base material, unique mangrove root systems (e.g. stilt and knee roots), dense sapling understoreys and tidal fluctuations. Animal threats were also present in some of mangrove forests, such as crocodiles in Northern Queensland (Australia) and tigers in Sundarbans mangroves (Bangladesh). The issue with the tidal fluctuation was the main challenge in this study and previously explained in section 5.2.3. By carefully planning of the fieldwork in regards to the tides, the field data collection periods can be optimised.

Another limitation was the limited number of images and mapping methods investigated in this thesis. The main images available for both sites and used in this thesis were three multi-spectral images selected to represent different spatial resolutions and LiDAR data of the Moreton Bay mangrove sites. Data from TM (30 m), AVNIR-2 (10 m) and WV-2 (2 m) were used for mangrove composition and LAI mapping, while the LiDAR data were used for mangrove composition mapping only. In terms of mapping techniques, this study only assessed the object-based and pixel-based techniques. Future work needs to investigate the utility of a larger number of image datasets (such as aerial photographs, hyper-spectral, high-spatial resolution and RADAR images) for mangrove mapping to improve the applicability of the guidelines. Examination of hybrid approaches and other advanced mapping techniques will enrich the utility of the developed guidelines. The role of the temporal resolution of the images to provide multi-temporal or time series mangrove information also need to be studied specifically in order to enhance the applicability of the image selection guidelines.

The time gaps between the images used, especially for Karimunjawa Island, may have influenced the mapping results. Cloud cover is the main issue in this area and obtaining several cloud-free images at similar times is difficult. The time gaps of the image acquisition of the Karimunjawa Island images were about three years (July 2009, February 2009 and May 2012). In terms of mangrove phenological stages, a period of three years will not alter the mangrove physical appearance much as long as no extreme weather events occur within this time period. However, the presence of natural and anthropogenic disturbance could significantly change the extent and condition of mangrove forest. Fortunately, there was no noticeable disturbance events during this period. The status of the mangrove forest as a National Park also limited human access to the location and kept the mangrove habitat intact.

Finally, the limitation in terms of implementation of the mapping methods is the cost of the software licences for object-based image analysis. The high cost of the standard software for this purpose inhibits the transfer of the multi-scale image-based mapping concept and practice for a wider audience in science and management groups. Some open source softwares have been developed for object-based image analysis such as SPRING, InterImage, and GeoDMA. However, they are more focussed on the image segmentation part and have limited ability to develop the rule sets for image classification. More efforts should be directed to develop a reliable and effective open source software with ability to develop the classification rule set for more robust and repeatable image classification.

7.4. Contribution to Knowledge

The methods and products presented in this thesis provide a fundamental basis for multi-scale image-based mangrove mapping and signify the operational use of remote sensing data for multi-scale mangrove mapping. This study has successfully integrated two different fields, remote sensing and mangrove spatial ecology; and revealed an explicit relationship between image spatial resolution, detail of the mangrove information obtained and the expected product accuracy. Based on the relationships, a guideline for selecting the most appropriate image dataset and mapping techniques for mangrove mapping was developed to produce science- and management-ready environmental information at a relevant spatial and temporal scale. This study has substantially increased our capacity to use object-based image analysis for multi-scale mangrove composition and LAI mapping. The study has also led to an efficient and effective use of remote sensing data for mapping, measuring, and monitoring mangrove environments.

The contributions of this thesis to the body of scientific knowledge are:

- The first ever effort to develop an explicit guideline for selecting image datasets and mapping techniques for mangrove mapping, at specific spatial and temporal scales;
- First effort to integrate the remote sensing data dimensions to the spatio-temporal mangrove ecological organisation;
- Development of a method to estimate the optimum pixel size for accurately mapping different sizes of mangrove features;
- Identification of the relationships between image pixel sizes and mangrove features able to be mapped;
- Definition of an explicit relationship between image spatial resolution, detail of the mangrove features able to be mapped and the mapping accuracy;
- Provision of a fundamental basis for multi-scale image-based mangrove mapping;

- Demonstration of the effectiveness of having a conceptual hierarchical model of objects in place before the object-based image analysis mapping;
- Development of a new object-based approach for mapping mangrove composition at multiple spatial scales;
- Improvements in the accuracy of LAI mapping using object-based estimation; and
- Proof of concept for the use of remote sensing for multi-scale mangrove mapping.

REFERENCES

Addink, EA, deJong, SM & Pebesma, EJ 2007, 'The importance of scale in object-based mapping of vegetation parameters with hyperspectral imagery'. *Photogrammetric Engineering & Remote Sensing,* vol. 73, pp. 905-912.

Al-Habshi, A, Youssef, T, Aizpuru, M & Blasco, F 2007, 'New mangrove ecosystem data along the UAE coast using remote sensing'. *Aquatic Ecosystem Health & Management,* vol. 10, pp. 309-319.

Alongi, DM 2002, 'Present state and future of the world's mangrove forests'. *Environmental Conservation,* vol. 29, pp. 331-349.

Alongi, DM 2008, 'Mangrove forests: resilience, protection from tsunamis, and responses to global climate change'. *Estuarine, Coastal and Shelf Science,* vol. 76, pp. 1-13.

Andrefouet, S, Kramer, P, Torres-Pulliza, D, Joyce, KE, Hochberg, EJ, Garza-Pe´rez, R, Mumby, PJ, Riegl, B, Yamano, H, White, WH, Zubia, M, Brock, JC, Phinn, SR, Naseer, A, Hatcher, BG & Muller-Karger, FE 2003, 'Multi-site evaluation of IKONOS data for classification of tropical coral reef environments'. *Remote Sensing of Environment,* vol. 88, pp. 128-143.

Araújo, RJ, Jaramillo, JC & Snedaker, SC 1997, 'LAI and leaf size differences in two red mangrove forest types in South Florida'. *Bulletin of Marine Science,* vol. 60, pp. 643-647.

Arbia, G, Benedetti, R & Espa, G 1996, 'Effects of the MAUP on image classification'. *Geographical Systems* vol. 3, pp. 123-141.

Atkinson, PM & Curran, PJ 1997, 'Choosing an appropriate spatial resolution for remote sensing investigations'. *Photogrammetric Engineering & Remote Sensing,* vol. 63, pp. 1345-1351.

Atzberger, C 2004, 'Object-based retrieval of biophysical canopy variables using artificial neural nets and radiative transfer models'. *Remote Sensing of Environment,* vol. 93, pp. 53-67.

Baatz, M & Schäpe, A. 'Object-oriented and multi-scale image analysis in semantic networks', Proceedings of the 2nd International Symposium on Operationalization of Remote Sensing, 16-20 August, ITC, The Netherland, pp. 1-7.

Baatz, M & Schape, A. 'Multiresolution segmentation: an optimization aproach for high quality multiscale image segmentation', *In:* Strobl, J, Blaschke, T & Griesebner, G, eds, Proceedings of the Angewandte Geographische Informationsverarbeitung XII, Heidelberg: Wichmann-Verlag, pp. 12-23.

Bailey, TC & Gatrell, AC 1995, *Interactive Spatial Data Analysis,* Longman Scientific & Technical, Harlow, Essex, UK.

Benfield, SL, Guzman, HM & Mair, JM 2005, 'Temporal mangrove dynamics in relation to coastal development in Pacific Panama'. *Journal of Environmental Management,* vol. 76, pp. 263-276.

Bengen, DG 2002, *Pedoman Teknis Pengenalan dan Pengelolaan Ekosistem Mangrove,* PKSPL IPB, Bogor.

Benz, UC, Hofmann, P, Willhauck, G, Lingenfelder, I & Heynen, M 2004, 'Multi-resolution, object-oriented fuzzy analysis of remote sensing data for GIS-ready information'. *ISPRS Journal of Photogrammetry and Remote Sensing,* vol. 58, pp. 239-258.

Berger, U, Rivera-Monroy, VH, Doyle, TW, Dahdouh-Guebas, F, Duke, NC, Fontalvo-Herazo, ML, Hildenbrandt, H, Koedam, N, Mehlig, U, Piou, C & Twilley, RR 2008, 'Advances and limitations of individual-based models to analyze and predict dynamics of mangrove forests: a review'. *Aquatic Botany,* vol. 89, pp. 260-274.

Bhattarai, B & Giri, C 2011, 'Assessment of mangrove forests in the Pacific region using Landsat imagery'. *Journal of Applied Remote Sensing,* vol. 5, pp. 053509-053511.

Bian, L & Butler, R 1999, 'Comparing effects of aggregation methods on statistical and spatial properties of simulated spatial data '. *Photogrammetric Engineering & Remote Sensing,* vol. 65, pp. 73-84.

Birth, GS & McVey, GR 1968, 'Measuring the color of growing turf with a reflectance spectrophotometer'. *Agronomy Journal*, vol. 60, pp. 640-643.

Blaschke, T, Lang, S, Lorup, E, Strobl, J & Zeil, P 2000, Object-oriented image processing in an integrated GIS/remote sensing environment and perspectives for environmental applications. *In:* Cremers, A & Greve, K (eds.), *Environmental Information for Planning, Politics and the Public*, Metropolis Verlag, Marburg.

Blaschke, T & Strobl, J 2001, 'What's wrong with pixels? Some recent development interfacing remote sensing and GIS'. *GeoBIT/GIS*, vol. 6, pp. 12-17.

Blaschke, T. 'Multiscale image analysis for ecological monitoring of heterogeneous, small structured landscapes', *In:* Conradi, M & Lang, S, eds, Proceedings of the SPIE 4545, Remote Sensing for Environmental Monitoring, GIS Applications, and Geology, 25 January: SPIE, pp. 35-44.

Blaschke, T 2010, 'Object based image analysis for remote sensing'. *ISPRS Journal of Photogrammetry and Remote Sensing*, vol. 65, pp. 2-16.

Blaschke, T, Hay, GJ, Kelly, M, Lang, S, Hofmann, P, Addink, E, Queiroz Feitosa, R, van der Meer, F, van der Werff, H, van Coillie, F & Tiede, D 2014, 'Geographic Object-Based Image Analysis - towards a new paradigm'. *ISPRS Journal of Photogrammetry and Remote Sensing*, vol. 87, pp. 180-191.

Blasco, F, Gauquelin, T, Rasolofoharinoro, M, Denis, J, Aizpuru, M & Caldairou, V 1998, 'Recent advances in mangrove studies using remote sensing data'. *Marine and Freshwater Research*, vol. 49, pp. 287-296.

Bolstad, PV & Lillesand, TM 1991, 'Rapid maximum likelihood classification'. *Photogrammetric Engineering & Remote Sensing*, vol. 57, pp. 67-74.

BoM. 2013, '*Australian Bureau of Meteorology*' [Online]. Available: http://www.bom.gov.au/ [Accessed February 2013.

Bouvet, M, Goryl, P, Chander, G, Santer, R & Saunier, S. 'Preliminary radiometric calibration assessment of ALOS AVNIR-2', Proceedings of the IEEE International Geoscience and Remote Sensing Symposium, 2007. IGARSS 2007., 23-28 July 2007, pp. 2673-2676.

Bréda, NJJ 2008, Leaf Area Index. *In:* Editors-in-Chief: Sven Erik, J & Brian, F (eds.), *Encyclopedia of Ecology*, Academic Press, Oxford.

BTNK 2001, 'Rencana Pengelolaan 25 Tahun Taman Nasional Karimunjawa Periode 2002-2027', Balai Taman Nasional Karimunjawa, Semarang.

BTNK 2008, 'Statistik Balai Taman Nasional Karimunjawa (BTNK) 2008', BTNK, Dirjen Perlindungan Hutan dan Konservasi Alam, Departemen Kehutanan, Semarang.

BTNK 2011, *Interpretasi Trekking Mangrove Taman Nasional Karimunjawa*, Balai Taman Nasional Karimunjawa, Semarang.

Bunt, JS, Williams, WT & Duke, NC 1982, 'Mangrove distributions in North-East Australia'. *Journal of Biogeography*, vol. 9, pp. 111-120.

Bunting, P & Lucas, R 2006, 'The delineation of tree crowns in Australian mixed species forests using hyperspectral Compact Airborne Spectrographic Imager (CASI) data'. *Remote Sensing of Environment*, vol. 101, pp. 230-248.

Burnett, C & Blaschke, T 2003, 'A multi-scale segmentation/object relationship modelling methodology for landscape analysis'. *Ecological Modelling*, vol. 168, pp. 233-249.

Campbell, JB 2002, *Introduction to Remote Sensing*, The Guilford Press, New York.

Cao, C & Lam, NS-N 1997, Understanding the scale and resolution effects in remote sensing and GIS. *In:* Quattrochi, DA & Goodchild, MF (eds.), *Scale in Remote Sensing and GIS*, CRC Press, Boca Raton.

Carlson, TN & Ripley, DA 1997, 'On the relation between NDVI, fractional vegetation cover, and leaf area index'. *Remote Sensing of Environment*, vol. 62, pp. 241-252.

Carter, GA 1994, 'Ratios of leaf reflectances in narrow wavebands as indicators of plant stress'. *International Journal of Remote Sensing*, vol. 15, pp. 697-703.

Castilla, G & Hay, GJ 2008, Image objects and geographic objects. *In:* Blaschke, T, Lang, S & Hay, GJ (eds.), *Object-Based Image Analysis - Spatial Concepts for Knowledge-Driven Remote Sensing Applications*, Springer-Verlag, Berlin.

Chadwick, J 2011, 'Integrated LiDAR and IKONOS multispectral imagery for mapping mangrove distribution and physical properties'. *International Journal of Remote Sensing,* vol., pp. 1-17.

Chander, G, Markham, BL & Helder, DL 2009, 'Summary of current radiometric calibration coefficients for Landsat MSS, TM, ETM+, and EO-1 ALI sensors'. *Remote Sensing of Environment*, vol. 113, pp. 893-903.

Chen, D. 2001, '*Multi-resolution image analysis and classification for improving urban land use/cover mapping using high resolution imagery',* PhD, Thesis, SDSU and UCSB.

Chen, W & Henebry, GM 2009, 'Change of spatial information under rescaling: a case study using multi-resolution image series'. *ISPRS Journal of Photogrammetry and Remote Sensing,* vol. 64, pp. 592-597.

Cho, MA & Skidmore, AK 2006, 'A new technique for extracting the red edge position from hyperspectral data: The linear extrapolation method'. *Remote Sensing of Environment,* vol. 101, pp. 181-193.

Chusnie, JL 1987, 'The interactive effect of spatial resolution and degree of internal variability within land-cover types on classification accuracies'. *International Journal of Remote Sensing,* vol. 8, pp. 15-29.

Clark, CD, Ripley, HT, Green, EP, Edwards, AJ & Mumby, PJ 1997, 'Mapping and measurement of tropical coastal environments with hyperspectral and high spatial resolution data'. *International Journal of Remote Sensing,* vol. 18, pp. 237-242.

Clough, BF 1992, Primary Productivity and Growth of Mangrove Forests. *In:* Robertson, AI & Alongi, DM (eds.), *Tropical Mangrove Ecosystem*, American Geophysical Union, Washington DC.

Clough, BF, Ong, JE & Gong, WK 1997, 'Estimating leaf area index and photosynthetic production in canopies of the mangrove *Rhizophora apiculata*'. *Marine Ecology Progress Series,* vol. 159, pp. 285-292.

Cohen, WB, Spies, TA & Bradshaw, GA 1990, 'Semivariograms of digital imagery for analysis of conifer canopy structure'. *Remote Sensing of Environment,* vol. 34, pp. 167-178.

Colombo, R, Bellingeri, D, Fasolini, D & Marino, CM 2003, 'Retrieval of leaf area index in different vegetation types using high resolution satellite data'. *Remote Sensing of Environment,* vol. 86, pp. 120-131.

Colombo, S, Chica-Olmo, M, Abarca, F & Eva, H 2004, 'Variographic analysis of tropical forest cover from multi-scale remotely sensed imagery'. *ISPRS Journal of Photogrammetry & Remote Sensing,* vol. 58, pp. 330-341.

Conchedda, G, Durieux, L & Mayaux, P. 'Object-based monitoring of land cover changes in mangrove ecosystems of Senegal', Proceedings of the International Workshop on the Analysis of Multi-temporal Remote Sensing Images, 2007. MultiTemp 2007. , 18-20 July 2007, pp. 1-6.

Conchedda, G, Durieux, L & Mayaux, P 2008, 'An object-based method for mapping and change analysis in mangrove ecosystems'. *ISPRS Journal of Photogrammetry and Remote Sensing,* vol. 63, pp. 578-589.

Congalton, RG 1991, 'A review of assessing the accuracy of classifications of remotely sensed data'. *Remote Sensing of Environment,* vol. 37, pp. 35-46.

Cullinan, VI, Simmons, MA & Thomas, JM 1997, 'A bayesian test of hierarchy theory: scaling up variability in plant cover from field to remotely sensed data'. *Landscape Ecology,* vol. 12, pp. 273-285.

Culvenor, DS 2002, 'TIDA: an algorithm for the delineation of tree crowns in high spatial resolution remotely sensed imagery'. *Computers & Geosciences,* vol. 28, pp. 33-44.

Culvenor, DS 2003, Extracting individual tree information: A survey of techniques for high spatial resolution imagery. *In:* Wulder, MA & Franklin, SE (eds.), *Remote Sensing of Forest Environments: Concepts and Case Studies*, Kluwer Academic Publishers, Boston.

Curran, PJ 1988, 'The semivariogram in remote sensing: an introduction'. *Remote Sensing of Environment,* vol. 24, pp. 493-507.

Curran, PJ & Atkinson, PM 1998, 'Geostatistics and remote sensing'. *Progress in Physical Geography,* vol. 22, pp. 61-78.

Cutini, A, Matteucci, G & Mugnozza, GS 1998, 'Estimation of leaf area index with the Li-Cor LAI 2000 in deciduous forests'. *Forest Ecology and Management,* vol. 105, pp. 55-65.

Da Cruz, C, Mendoza, U, Queiroz, J, Berrêdo, J, Da Costa Neto, S & Lara, R 2013, 'Distribution of mangrove vegetation along inundation, phosphorus, and salinity gradients on the Bragança Peninsula in Northern Brazil'. *Plant and Soil*, vol. 370, pp. 393-406.

Dahdouh-Guebas, F, Verheyden, A, Kairo, JG, Jayatissa, LP & Koedam, N 2006, 'Capacity building in tropical coastal resource monitoring in developing countries: a re-appreciation of the oldest remote sensing method'. *International Journal of Sustainable Development & World Ecology,* vol. 13, pp. 62-76.

Davis, BA & Jensen, JR 1998, 'Remote sensing of mangrove biophysical characteristics'. *Geocarto International*, vol. 13, pp. 55-64.

de Jong, SM & van der Meer, FD (eds.) 2005. *Remote Sensing Image Analysis: Including the Spatial Domain*, Kluwer Academic Publishers, Dordrecht

de Oliveira Vasconcelos, A, Landau, L & de Miranda, FP. 'Multi-temporal analysis of a mangrove ecosystem in Southeastern Brazil using object-based classification applied to IKONOS II data', *In:* Bruzozne, L & Bovolo, F, eds, Proceedings of the 2011 6th International Workshop on the Analysis of Multi-temporal Remote Sensing Images (Multi-Temp 2011), 12-14 July, Trento, Italy, pp. 169-172.

Delcourt, HR, Delcourt, PA & Webb III, T 1983, 'Dynamic plant ecology: the spectrum of vegetational change in space and time'. *Quaternary Science Reviews,* vol. 1, pp. 153-175.

Demuro, M & Chisholm, L. 2003, 'Assessment of Hyperion for characterizing mangrove communities'. Available: ftp://popo.jpl.nasa.gov/pub/docs/workshops/03_docs/Demuro_AVIRIS_2003_web.pdf [Accessed 28 October 2007].

Díaz, BM & Blackburn, GA 2003, 'Remote sensing of mangrove biophysical properties: evidence from a laboratory simulation of the possible effects of background variation on spectral vegetation indices'. *International Journal of Remote Sensing,* vol. 24, pp. 53-73.

DigitalGlobe. 2013. Available: https://www.digitalglobe.com/downloads/Imagery_Support_Data_Documentation.pdf [Accessed 27 February 2013].

Dowling, R & Stephens, K 1998, 'Coastal Wetlands of South East Queensland: Volume 1 Mapping and Survey', Queensland Herbarium, Brisbane.

Dowling, RM 1986, 'The mangrove vegetation of Moreton Bay'. *Queensland Botany Bulletin,* vol. 6, pp. 1-45.

Dowling, RM & Stephen, K 2001, *Coastal Wetlands of South-Eastern Queensland Maroochy Shire to New South Wales Border,* Queensland Herbarium, Environmental Protection Agency, Brisbane, Australia.

Duke, N 1992, Mangrove floristics and biogeography. *In:* Robertson, AI & Alongi, DM (eds.), *Tropical Mangrove Ecosystem*, American Geophysical Union, Washington DC.

Duke, N 2006, *Australia's Mangroves: The authoritative guide to Australia's mangrove plants,* University of Queensland, Brisbane.

Duke, NC, Ball, MC & Ellison, JC 1998, 'Factors influencing biodiversity and distributional gradients in mangroves'. *Global Ecology and Biogeography Letters,* vol. 7, pp. 27-47.

Duke, NC, Meynecke, J-O, Dittmann, S, Ellison, AM, Anger, K, Berger, U, Cannicci, S, Diele, K, Ewel, KC, Field, CD, Koedam, N, Lee, SY, Marchand, C, Nordhaus, I & Dahdouh-Guebas, F 2007, 'A world without mangroves?'. *Science,* vol. 317, pp. 41-42.

Ellison, AM, Mukherjee, BB & Karim, A 2000, 'Testing patterns of zonation in mangroves: scale dependence and environmental correlates in the Sundarbans of Bangladesh'. *Journal of Ecology,* vol. 88, pp. 813-824.

English, S, Wilkinson, C & Baker, V 1997, *Survey manual for tropical marine resources,* Australian Institute of Marine Science, Townsville.

Environment Australia 2001, *A Directory of Important Wetlands in Australia,* Environment Australia, Canberra, Australia.

Eslami-Andargoli, L, Dale, P, Sipe, N & Chaseling, J 2009, 'Mangrove expansion and rainfall patterns in Moreton Bay, Southeast Queensland, Australia'. *Estuarine, Coastal and Shelf Science,* vol. 85, pp. 292-298.

Everitt, JH, Yang, C, Sriharan, S & Judd, FW 2008, 'Using high resolution satellite imagery to map black mangrove on the Texas Gulf coast'. *Journal of Coastal Research,* vol. 24, pp. 1582-1586.

Fang, H & Liang, S 2008, Leaf Area Index Models. *In:* Editors-in-Chief: Sven Erik, J & Brian, F (eds.), *Encyclopedia of Ecology,* Academic Press, Oxford.

FAO 2007, 'The World's Mangroves 1980-2005', *FAO Forestry Paper 153.* FAO, Rome, Italy.

Farnsworth, EJ 1998, 'Issues of spatial, taxonomic and temporal scale in delineating links between mangrove diversity and ecosystem function'. *Global Ecology and Biogeography Letters,* vol. 7, pp. 15-25.

Fassnacht, KS, Gower, ST, MacKenzie, MD, Nordheim, EV & Lillesand, TM 1997, 'Estimating the leaf area index of North Central Wisconsin forests using the Landsat Thematic Mapper'. *Remote Sensing of Environment,* vol. 61, pp. 229-245.

Feller, IC, Lovelock, CE, Berger, U, McKee, KL, Joye, SB & Ball, MC 2010, 'Biocomplexity in mangrove ecosystems'. *Annual Review of Marine Science,* vol. 2, pp. 395-417.

Feng, Y, Li, Z & Tokola, T 2010, 'Estimation of stand mean crown diameter from high-spatial-resolution imagery based on a geostatistical method'. *International Journal of Remote Sensing,* vol. 31, pp. 363-378.

Filella, I & Penuelas, J 1994, 'The red edge position and shape as indicators of plant chlorophyll content, biomass and hydric status'. *International Journal of Remote Sensing,* vol. 15, pp. 1459-1470.

Fisher, P 1997, 'The pixel: a snare and a delusion'. *International Journal of Remote Sensing,* vol. 18, pp. 679-685.

Forshaw, MRB, Haskell, A, Miller, PF, Stanley, DJ & Townshend, JRG 1983, 'Spatial resolution of remotely sensed imagery: a review paper'. *International Journal of Remote Sensing,* vol. 4, pp. 497-520.

Fox, J 1992, 'The problem of scale in community resource management'. *Environmental Management,* vol. 16, pp. 289-297.

Gamanya, R, De Maeyer, P & De Dapper, M 2007, 'An automated satellite image classification design using object-oriented segmentation algorithms: a move towards standardization'. *Expert Systems with Applications,* vol. 32, pp. 616-624.

Gao, J 1998, 'A hybrid method toward accurate mapping of mangroves in a marginal habitat from SPOT multispectral data'. *International Journal of Remote Sensing,* vol. 19, pp. 1887-1899.

Gao, J 1999, 'Evaluation of SPOT HRV data in mapping mangrove forests in a temperate zone'. *Geocarto International,* vol. 14, pp. 45-52.

Garrigues, S, Allard, D, Baret, F & Weiss, M 2006, 'Quantifying spatial heterogeneity at the landscape scale using variogram models'. *Remote Sensing of Environment,* vol. 103, pp. 81-96.

Gholz, HL 1982, 'Environmental limits on aboveground net primary production, leaf area, and biomass in vegetation zones of the Pacific Northwest'. *Ecology,* vol. 63, pp. 469-481.

Gholz, HL, Vogel, SA, Cropper, WP, McKelvey, K, Ewel, KC, Teskey, RO & Curran, PJ 1991, 'Dynamics of canopy structure and light interception in *Pinus elliottii* stands, North Florida'. *Ecological Monographs*, vol. 6, pp. 33-51.

Gilman, EL, Ellison, J, Duke, NC & Field, C 2008, 'Threats to mangroves from climate change and adaptation options: a review'. *Aquatic Botany*, vol. 89, pp. 237-250.

Giri, C, Pengra, B, Zhu, Z, Singh, A & Tieszen, LL 2007, 'Monitoring mangrove forest dynamics of the Sundarbans in Bangladesh and India using multi-temporal satellite data from 1973 to 2000'. *Estuarine, Coastal and Shelf Science*, vol. 73, pp. 91-100.

Giri, C, Zhu, Z, Tieszen, LL, Singh, A, Gillette, S & Kelmelis, JA 2008, 'Mangrove forest distributions and dynamics (1975–2005) of the tsunami-affected region of Asia'. *Journal of Biogeography*, vol. 35, pp. 519-528.

Giri, C & Muhlhausen, J 2008, 'Mangrove forest distributions and dynamics in Madagascar (1975–2005)'. *Sensors*, vol. 8, pp. 2104-2117.

Giri, C, Ochieng, E, Tieszen, LL, Zhu, Z, Singh, A, Loveland, T, Masek, J & Duke, N 2011, 'Status and distribution of mangrove forests of the world using earth observation satellite data'. *Global Ecology and Biogeography*, vol. 20, pp. 154-159.

Glenn, E, Huete, A, Nagler, P & Nelson, S 2008, 'Relationship Between Remotely-sensed Vegetation Indices, Canopy Attributes and Plant Physiological Processes: What Vegetation Indices Can and Cannot Tell Us About the Landscape'. *Sensors*, vol. 8, pp. 2136.

Goodchild, MF & Quattrochi, DA 1997, Scale, multiscaling, remote sensing, and GIS. *In:* Quattrochi, DA & Goodchild, MF (eds.), *Scale in Remote Sensing and GIS*, CRS Press, Boca Raton.

Gopal, B & Chauhan, M 2006, 'Biodiversity and its conservation in the Sundarban mangrove ecosystem'. *Aquatic Sciences - Research Across Boundaries*, vol. 68, pp. 338-354.

Gougeon, FA 1995, 'A crown-following approach to the automatic delineation of individual tree crowns in high spatial resolution aerial images'. *Canadian Journal of Remote Sensing*, vol. 21, pp. 274-284.

Gougeon, FA & Leckie, DG 2006, 'The individual tree crown approach applied to IKONOS images of a coniferous plantation area'. *Photogrammetric Engineering & Remote Sensing*, vol. 72, pp. 1287-1297.

Green, EP, Mumby, PJ, Edwards, AJ, Clark, CD & Ellis, AC 1997, 'Estimating leaf area index of mangroves from satellite data'. *Aquatic Botany*, vol. 58, pp. 11-19.

Green, EP, Mumby, PJ, Edwards, AJ, Clark, CD & Ellis, AC 1998a, 'The assessment of mangrove areas using high resolution multispectral airborne imagery'. *Journal of Coastal Research*, vol. 14, pp. 433-443.

Green, EP, Clark, CD, Mumby, PJ, Edwards, AJ & Ellis, AC 1998b, 'Remote sensing techniques for mangrove mapping'. *International Journal of Remote Sensing*, vol. 19, pp. 935-956.

Green, EP & Mumby, PJ 2000, Mapping mangroves. *In:* Edwards, AJ (ed.) *Remote Sensing Handbook for Tropical Coastal Management*, UNESCO Publishing, Paris.

Haboudane, D, Miller, JR, Pattey, E, Zarco-Tejada, PJ & Strachan, IB 2004, 'Hyperspectral vegetation indices and novel algorithms for predicting green LAI of crop canopies: Modeling and validation in the context of precision agriculture'. *Remote Sensing of Environment*, vol. 90, pp. 337-352.

Hardisky, MA, Gross, MF & Klemas, V 1986, 'Remote sensing of coastal wetlands'. *BioScience*, vol. 36, pp. 453-460.

Hasegawa, K, Matsuyama, H, Tsuzuki, H & Sweda, T 2010, 'Improving the estimation of leaf area index by using remotely sensed NDVI with BRDF signatures'. *Remote Sensing of Environment*, vol. 114, pp. 514-519.

Hay, GJ, Blaschke, T, Marceau, DJ & Bouchard, A 2003, 'A comparison of three image-object methods for the multiscale analysis of landscape structure'. *ISPRS Journal of Photogrammetry and Remote Sensing*, vol. 57, pp. 327-345.

Hay, GJ, Castilla, G, Wulder, MA & Ruiz, JR 2005, 'An automated object-based approach for the multiscale image segmentation of forest scenes'. *International Journal of Applied Earth Observation and Geoinformation,* vol. 7, pp. 339-359.

He, Y, Guo, X, Wilmshurst, J & Si, BC 2006, 'Studying mixed grassland ecosystems II: optimum pixel size'. *Canadian Journal of Remote Sensing,* vol. 32, pp. 108-115.

Heenkenda, M, Joyce, K, Maier, S & Bartolo, R 2014, 'Mangrove species identification: comparing WorldView-2 with aerial photographs'. *Remote Sensing,* vol. 6, pp. 6064-6088.

Held, A, Ticehurst, C, Lymburner, L & Williams, N 2003, 'High resolution mapping of tropical mangrove ecosystems using hyperspectral and radar remote sensing'. *International Journal of Remote Sensing,* vol. 24, pp. 2739-2759.

Herrmann, I, Pimstein, A, Karnieli, A, Cohen, Y, Alchanatis, V & Bonfil, DJ 2011, 'LAI assessment of wheat and potato crops by VENμS and Sentinel-2 bands'. *Remote Sensing of Environment,* vol. 115, pp. 2141-2151.

Heumann, BW 2011a, 'An object-based classification of mangroves using a hybrid decision tree - Support Vector Machine approach'. *Remote Sensing,* vol. 3, pp. 2440-2460.

Heumann, BW 2011b, 'Satellite remote sensing of mangrove forests: recent advances and future opportunities'. *Progress in Physical Geography,* vol. 35, pp. 87-108.

Hirano, A, Madden, M & Welch, R 2003, 'Hyperspectral image data for mapping wetland vegetation'. *Wetlands,* vol. 23, pp. 436-448.

Holling, CS 1992, 'Cross-scale morphology, geometry, and dynamics of ecosystems'. *Ecological Monographs,* vol. 62, pp. 447-502.

Huete, A, Didan, K, Miura, T, Rodriguez, EP, Gao, X & Ferreira, LG 2002, 'Overview of the radiometric and biophysical performance of the MODIS vegetation indices'. *Remote Sensing of Environment,* vol. 83, pp. 195-213.

Huete, AR 1988, 'A soil-adjusted vegetation index (SAVI)'. *Remote Sensing of Environment,* vol. 25, pp. 295-309.

Huete, AR 2012, 'Vegetation indices, remote sensing and forest monitoring'. *Geography Compass,* vol. 6, pp. 513-532.

Hutchings, P & Saenger, P 1987, *Ecology of Mangroves,* University of Queensland Press, Brisbane.

Hyppanen, H 1996, 'Spatial autocorrelation and optimal spatial resolution of optical remote sensing data in boreal forest environment'. *International Journal of Remote Sensing,* vol. 17, pp. 3441-3452.

INRA. 2013, '*CAN-EYE imaging software'* [Online]. Available: https://www4.paca.inra.fr/can-eye [Accessed 10 November 2012].

Ishil, T & Tateda, Y. 'Leaf area index and biomass estimation for mangrove plantation in Thailand', Proceedings of the IEEE International Geoscience and Remote Sensing Symposium, 2004. IGARSS '04., 20-24 Sept. 2004, pp. 2323-2326.

Jayanth, J, Kumar, TA & Koliwad, S 2012, Comparative Analysis of Image Fusion Techniques in Remote Sensing. *In:* Hassanien, AE, Salem, AM, Ramadan, R & Kim, T (eds.), *Advanced Machine Learning Technologies and Applications*, Springer Berlin Heidelberg.

Jean-Baptiste, N & Jensen, JR 2006, 'Measurement of mangrove biophysical characteristics in The Bocozelle ecosystem in Haiti using ASTER multispectral data'. *Geocarto International,* vol. 21, pp. 3-8.

Jelinski, D & Wu, J 1996, 'The modifiable areal unit problem and implications for landscape ecology'. *Landscape Ecology,* vol. 11, pp. 129-140.

Jensen, JR, Lin, H, Yang, X, Ramsey, E, Davis, BA & Thoemke, CW 1991, 'The measurement of mangrove characteristics in Southwest Florida using SPOT multispectral data'. *Geocarto International,* vol. 6, pp. 13-21.

Jensen, JR 2005, *Introductory Digital Image Processing: a remote sensing perspective,* Pearson prentice Hall, Upper Saddle river, New Jersey.

Jensen, R, Mausel, P, Dias, N, Gonser, R, Yang, C, Everitt, J & Fletcher, R 2007, 'Spectral analysis of coastal vegetation and land cover using AISA+ hyperspectral data'. *Geocarto International*, vol. 22, pp. 17-28.

Jensen, RR & Binford, MW 2004, 'Measurement and comparison of Leaf Area Index estimators derived from satellite remote sensing techniques'. *International Journal of Remote Sensing*, vol. 25, pp. 4251-4265.

Johansen, K & Phinn, S 2006, 'Linking riparian vegetation spatial structure in Australian tropical savannas to ecosystem health indicators: semi-variogram analysis of high spatial resolution satellite imagery'. *Canadian Journal of Remote Sensing*, vol. 32, pp. 228-243.

Johansen, K, Phinn, S, Witte, C, Philip, S & Newton, L 2009, 'Mapping banana plantations from object-oriented classification of SPOT-5 imagery'. *Photogrammetric Engineering & Remote Sensing*, vol. 75, pp. 1069-1081.

Jupp, DLB, Strahler, AH & Woodcock, CE 1988, 'Autocorrelation and regularization in digital images. I. Basic theory'. *IEEE Transactions on Geoscience and Remote Sensing*, vol. 26, pp. 463-473.

Jupp, DLB, Strahler, AH & Woodcock, CE 1989, 'Autocorrelation and regularization in digital images. II. Simple image models'. *IEEE Transactions on Geoscience and Remote Sensing*, vol. 27, pp. 247-258.

Justice, C, Belward, A, Morisette, J, Lewis, P, Privette, J & Baret, F 2000, 'Developments in the 'validation' of satellite sensor products for the study of the land surface'. *International Journal of Remote Sensing*, vol. 21, pp. 3383-3390.

Kamal, M & Phinn, SR 2011, 'Hyperspectral data for mangrove species mapping: a comparison of pixel-based and object-based approach'. *Remote Sensing*, vol. 3, pp. 2222-2242.

Kamal, M, Phinn, S & Johansen, K. 2013, 'Assessment of mangrove spatial structure using high-spatial resolution image data', Proceedings of the IEEE International Geoscience and Remote Sensing Symposium (IGARSS), 21-26 July 2013, Melbourne, Australia, pp. 2609-2612.

Kamal, M, Phinn, S & Johansen, K 2014, 'Characterizing the spatial structure of mangrove features for optimizing image-based mangrove mapping'. *Remote Sensing*, vol. 6, pp. 984-1006.

Kathiresan, K & Bingham, BL 2001, Biology of mangroves and mangrove ecosystems. *Advances in Marine Biology*, Academic Press.

Kayitakire, F, Hamel, C & Defourny, P 2006, 'Retrieving forest structure variables based on image texture analysis and IKONOS-2 imagery'. *Remote Sensing of Environment*, vol. 102, pp. 390-401.

Key, T, Warner, TA, McGraw, JB & Fajvan, MA 2001, 'A comparison of multispectral and multitemporal information in high spatial resolution imagery for classification of individual tree species in a temperate Hardwood forest'. *Remote Sensing of Environment*, vol. 75, pp. 100-112.

Kitamura, S, Anwar, C, Chaniago, A & Baba, S 2004, *Handbook of Mangroves in Indonesia: Bali & Lombok*, International Society of Mangrove Ecosystem (ISME), Okinawa, Japan.

Koedsin, W & Vaiphasa, C 2013, 'Discrimination of tropical mangroves at the species level with EO-1 Hyperion data'. *Remote Sensing*, vol. 5, pp. 3562-3582.

Kovacs, J, King, J, Flores de Santiago, F & Flores-Verdugo, F 2009, 'Evaluating the condition of a mangrove forest of the Mexican Pacific based on an estimated leaf area index mapping approach'. *Environmental Monitoring and Assessment*, vol. 157, pp. 137-149.

Kovacs, J, de Santiago, F, Bastien, J & Lafrance, P 2010, 'An assessment of mangroves in Guinea, West Africa, using a field and remote sensing based approach'. *Wetlands*, vol. 30, pp. 773-782.

Kovacs, JM, Wang, J & Blanco-Correa, M 2001, 'Mapping disturbances in a mangrove forest using multi-date Landsat TM imagery'. *Environmental Management*, vol. 27, pp. 763-776.

Kovacs, JM, Flores-Verdugo, F, Wang, J & Aspden, LP 2004, 'Estimating leaf area index of a degraded mangrove forest using high spatial resolution satellite data'. *Aquatic Botany*, vol. 80, pp. 13-22.

Kovacs, JM, Wang, J & Flores-Verdugo, F 2005, 'Mapping mangrove leaf area index at the species level using IKONOS and LAI-2000 sensors for the Agua Brava Lagoon, Mexican Pacific'. *Estuarine, Coastal and Shelf Science*, vol. 62, pp. 377-384.

Kovacs, JM, Lu, XX, Flores-Verdugo, F, Zhang, C, Flores de Santiago, F & Jiao, X 2013, 'Applications of ALOS PALSAR for monitoring biophysical parameters of a degraded black mangrove (*Avicennia germinans*) forest'. *ISPRS Journal of Photogrammetry and Remote Sensing*, vol. 82, pp. 102-111.

Krause, G, Bock, M, Weiers, S & Braun, G 2004, 'Mapping land-cover and mangrove structures with remote sensing techniques: a contribution to a synoptic GIS in support of coastal management in North Brazil'. *Environmental Management*, vol. 34, pp. 429-440.

Kuenzer, C, Bluemel, A, Gebhardt, S, Quoc, TV & Dech, S 2011, 'Remote sensing of mangrove ecosystems: a review'. *Remote Sensing*, vol. 3, pp. 878-928.

LAADS. 2012, '*Level 1 and Atmosphere Archive and Distribution System. Website of NASA – Goddard Space Flight Center* ' [Online]. Available: http://ladsweb.nascom.nasa.gov/data/search.html [Accessed 5 March 2012 2012].

Laben, CA & Brower, BV. 2000. *Process for enhancing the spatial resolution of multispectral imagery using pan-sharpening*. US patent application US 09/069,232. 4 Jan 2000.

Lam, N, Catts, D, Quattrochi, D, Brown, D & McMaster, R 2004, Scale. *In:* Usery, EL & Mcmaster, RB (eds.), *A Research Agenda for Geographic Information Science*, CRC Press, Boca Raton, Florida.

Lam, NS-N & Quattrochi, DA 1992, 'On the issues of scale, resolution, and fractal analysis in the mapping sciences'. *The Professional Geographer*, vol. 44, pp. 88-98.

Lang, S 2008, Object-based image analysis for remote sensing applications: modeling reality – dealing with complexity. *In:* Blaschke, T, Lang, S & Hay, G (eds.), *Object-Based Image Analysis*, Springer Berlin Heidelberg.

Laongmanee, W, Vaiphasa, C & Laongmanee, P 2013, 'Assessment of spatial resolution in estimating leaf area index from satellite images: a case study with *Avicennia marina* plantations in Thailand'. *International Journal of Geoinformatics*, vol. 9, pp. 69-77.

Lee, D & Grant, W 1995, 'A hierarchical approach to fisheries planning and modeling in the Columbia River Basin'. *Environmental Management*, vol. 19, pp. 17-25.

Lefsky, MA & Cohen, WB 2003, Selection of Remotely Sensed Data. *In:* Wulder, MA & Franklin, SE (eds.), *Remote Sensing of Forest Environments*, Kluwer Academic Publishers, Dordrecht, The Netherlands.

LI-COR 2009, *LAI-2200 Plant Canopy Analyzer*, LI-COR Inc., Lincoln, Nebraska.

Lucas, RM, Mitchell, AL, Rosenqvist, A, Proisy, C, Melius, A & Ticehurst, C 2007, 'The potential of L-band SAR for quantifying mangrove characteristics and change: case studies from the tropics'. *Aquatic Conservation: Marine and Freshwater Ecosystems*, vol. 17, pp. 245-264.

Lucas, RM, Lee, AC & Bunting, PJ 2008, 'Retrieving forest biomass through integration of CASI and LiDAR data'. *International Journal of Remote Sensing*, vol. 29, pp. 1553-1577.

Lucas, RM, Bunting, P, Clewley, D, Proisy, C, Filho, PWMS, Viergever, K, Woodhouse, I, Ticehurst, C, Carreiras, J, Rosenqvist, A, Accad, A & Armston, J. 2010, 'Characterisation and Monitoring of Mangroves Using ALOS PALSAR Data'. *JAXA Kyoto and Carbon (K&C) Initiative Report* [Online]. Available: http://www.eorc.jaxa.jp/ALOS/en/kyoto/phase_1/KC-Phase1-report_Lucas_WT.pdf [Accessed 19 March 2012].

Lugo, AE & Snedaker, SC 1974, 'The ecology of mangroves'. *Annual Review of Ecology and Systematics*, vol. 5, pp. 39-64.

Lugo, AE 1997, 'Old-growth mangrove forests in the United States'. *Conservation Biology*, vol. 11, pp. 11-20.

Lymburner, L, Beggs, PJ & Jacobson, CR 2000, 'Estimation of canopy-average surface-specific leaf area using Landsat TM data'. *Photogrammetric Engineering & Remote Sensing*, vol. 66, pp. 183-191.

MacKay, H, Finlayson, CM, Fernández-Prieto, D, Davidson, N, Pritchard, D & Rebelo, LM 2009, 'The role of Earth Observation (EO) technologies in supporting implementation of the Ramsar convention on wetlands'. *Journal of Environmental Management,* vol. 90, pp. 2234-2242.

Malthus, TJ & Mumby, PJ 2003, 'Remote sensing of the coastal zone: an overview and priorities for future research'. *International Journal of Remote Sensing,* vol. 24, pp. 2805-2815.

Manson, FJ, Loneragan, NR, McLeod, IM & Kenyon, RA 2001, 'Assessing techniques for estimating the extent of mangroves: topographic maps, aerial photographs and Landsat TM images'. *Marine and Freshwater Research*, vol. 52, pp. 787-792.

Manson, FJ, Loneragan, NR & Phinn, SR 2003, 'Spatial and temporal variation in distribution of mangroves in Moreton Bay, subtropical Australia: a comparison of pattern metrics and change detection analyses based on aerial photographs'. *Estuarine, Coastal and Shelf Science*, vol. 57, pp. 653-666.

Marceau, DJ, Howarth, PJ & Gratton, DJ 1994a, 'Remote sensing and the measurement of geographical entities in a forested environment. 1. The scale and spatial aggregation problem'. *Remote Sensing of Environment,* vol. 49, pp. 93-104.

Marceau, DJ, Gratton, DJ, Fournier, RA & Fortin, J-P 1994b, 'Remote sensing and the measurement of geographical entities in a forested environment. 2. The optimal spatial resolution'. *Remote Sensing of Environment*, vol. 49, pp. 105-117.

Marceau, DJ & Hay, GJ 1999, 'Remote sensing contributions to the scale issue'. *Canadian Journal of Remote Sensing,* vol. 25, pp. 357-366.

Marceau, DJ 1999, 'The scale issue in social and natural sciences'. *Canadian Journal of Remote Sensing,* vol. 25, pp. 347-356.

Markham, BL & Townshend, JRG. 'Land cover classification accuracy as a function of sensor spatial resolution', Proceedings of the The 15th International Symposium on Remote Sensing of Environment, 11-15 May, Ann Arbor, MI, pp. 1075-1090.

Mather, PM & Koch, M 2011, *Computer Processing of Remotely-Sensed Images: An Introduction,* John Wiley & Sons, Chichester, West Sussex.

McCloy, KR 2005, *Resource Management Information Systems: Remote Sensing, GIS and Modelling,* CRC Press, Boca Raton, FL.

McFadden, L, Nicholls, RJ & Penning-Rowsell, E (eds.) 2007. *Managing Coastal Vulnerability,* Elsevier, Oxford

Menges, CH, Hill, GJE & Ahmad, W 2001, 'Use of airborne video data for the characterization of tropical savannas in northern Australia: the optimal spatial resolution for remote sensing applications'. *International Journal of Remote Sensing,* vol. 22, pp. 727-740.

Meyers, TP & Paw, UKT 1986, 'Testing of a higher-order closure model for modeling airflow within and above plant canopies'. *Boundary-Layer Meteorology*, vol. 37, pp. 297-311.

Meyers, TP & Paw, UKT 1987, 'Modelling the plant canopy micrometeorology with higher-order closure principles'. *Agricultural and Forest Meteorology,* vol. 41, pp. 143-163.

Morgan, JL, Gergel, SE & Coops, NC 2010, 'Aerial photography: a rapidly evolving tool for ecological management'. *BioScience,* vol. 60, pp. 47-59.

Müller, F 1992, 'Hierarchical approaches to ecosystem theory'. *Ecological Modelling,* vol. 63, pp. 215-242.

Müller, F 1997, 'State-of-the-art in ecosystem theory'. *Ecological Modelling*, vol. 100, pp. 135-161.

Mumby, PJ, Green, EP, Edwards, AJ & Clark, CD 1999, 'The cost-effectiveness of remote sensing for tropical coastal resources assessment and management'. *Journal of Environmental Management,* vol. 55, pp. 157-166.

Murray, MR, Zisman, SA, Furley, PA, Munro, DM, Gibson, J, Ratter, J, Bridgewater, S, Minty, CD & Place, CJ 2003, 'The mangroves of Belize: Part 1. distribution, composition and classification'. *Forest Ecology and Management*, vol. 174, pp. 265-279.

Myint, SW, Giri, CP, Wang, L, Zhu, Z & Gillette, SC 2008, 'Identifying mangrove species and their surrounding land use and land cover classes using an object-oriented approach with a lacunarity spatial measure'. *GIScience & Remote Sensing,* vol. 45, pp. 188-208.

Naveh, Z & Lieberman, A 1994, *Landscape Ecology: Theory and Application,* Springer-Verlag New York.

Navulur, K 2007, *Multispectral Image Analysis Using the Object-Oriented Paradigm,* CRS Press, Boca Raton, Florida.

Neukermans, G, Dahdouh-Guebas, F, Kairo, JG & Koedam, N 2008, 'Mangrove species and stand mapping in Gazi Bay (Kenya) using Quickbird satellite imagery'. *Journal of Spatial Science,* vol. 53, pp. 75-86.

Nguyen, H-H, McAlpine, C, Pullar, D, Johansen, K & Duke, NC 2013, 'The relationship of spatial–temporal changes in fringe mangrove extent and adjacent land-use: case study of Kien Giang coast, Vietnam'. *Ocean & Coastal Management,* vol. 76, pp. 12-22.

Openshaw, S 1984, *The Modifiable Areal Unit Problem,* Geo Books, Norwich, United Kingdom.

Phinn, S, Franklin, J, Hope, A, Stow, D & Huenneke, L 1996, 'Biomass distribution mapping using airborne digital video imagery and spatial statistics in a semi-arid environment'. *Journal of Environmental Management,* vol. 47, pp. 139-164.

Phinn, SR 1998, 'A framework for selecting appropriate remotely sensed data dimensions for environmental monitoring and management'. *International Journal of Remote Sensing,* vol. 19, pp. 3457-3463.

Phinn, SR, Menges, C, Hill, GJE & Stanford, M 2000, 'Optimizing remotely sensed solutions for monitoring, modeling, and managing coastal environments'. *Remote Sensing of Environment,* vol. 73, pp. 117-132.

Pierce, LL & Running, SW 1988, 'Rapid estimation of coniferous forest leaf area index using portable integrating radiometer'. *Ecology,* vol. 69, pp. 1762-1767.

Proisy, C, Couteron, P & Fromard, F 2007, 'Predicting and mapping mangrove biomass from canopy grain analysis using Fourier-based textural ordination of IKONOS images'. *Remote Sensing of Environment,* vol. 109, pp. 379-392.

Pu, R, Gong, P, Biging, GS & Larrieu, MR 2003, 'Extraction of red edge optical parameters from Hyperion data for estimation of forest leaf area index'. *Geoscience and Remote Sensing, IEEE Transactions on,* vol. 41, pp. 916-921.

Qi, J, Kerr, YH, Moran, MS, Weltz, M, Huete, AR, Sorooshian, S & Bryant, R 2000, 'Leaf Area Index Estimates Using Remotely Sensed Data and BRDF Models in a Semiarid Region'. *Remote Sensing of Environment,* vol. 73, pp. 18-30.

Raffy, M 1994, 'Change of scale theory: a capital challenge for space observation of earth'. *International Journal of Remote Sensing,* vol. 15, pp. 2353-2357.

Ramsey III, EW & Jensen, JR 1996, 'Remote sensing of mangrove wetlands: relating canopy spectra to site-specific data'. *Photogrammetric Engineering & Remote Sensing,* vol. 62, pp. 939-948.

Rasolofoharinoro, M, Blasco, F, Bellan, MF, Aizpuru, M, Gauquelin, T & Denis, J 1998, 'A remote sensing based methodology for mangrove studies in Madagascar'. *International Journal of Remote Sensing,* vol. 19, pp. 1873-1886.

Richter, K, Atzberger, C, Vuolo, F, Weihs, P & D'Urso, G 2009, 'Experimental assessment of the Sentinel-2 band setting for RTM-based LAI retrieval of sugar beet and maize'. *Canadian Journal of Remote Sensing,* vol. 35, pp. 230-247.

Robertson, AI & Duke, NC 1987, 'Mangroves as nursery sites: comparisons of the abundance and species composition of fish and crustaceans in mangroves and other nearshore habitats in tropical Australia'. *Marine Biology,* vol. 96, pp. 193-205.

Rocchini, D 2007, 'Effects of spatial and spectral resolution in estimating ecosystem α-diversity by satellite imagery'. *Remote Sensing of Environment*, vol. 111, pp. 423-434.
Roelfsema, CM & Phinn, SR 2013, Validation. *In:* Goodman, JA, Purkis, SJ & Phinn, SR (eds.), *Coral Reef Remote Sensing*, Springer, Dordrecht.
Rouse, JW, Jr., Haas, RH, Schell, JA & Deering, DW. 'Monitoring vegetation systems in the Great Plains with ERTS', *In:* Freden, SC, Mercanti, EP & Becker, MA, eds, Proceedings of the Third Earth Resources Technology Satellite-1 Symposium, Washington, D.C.: NASA, pp. 309-317.
Ruddell, D & Wentz, EA 2009, 'Multi-tasking: scale in geography'. *Geography Compass*, vol. 3, pp. 681-697.
Saito, H, Bellan, MF, Al-Habshi, A, Aizpuru, M & Blasco, F 2003, 'Mangrove research and coastal ecosystem studies with SPOT-4 HRVIR and TERRA ASTER in the Arabian Gulf'. *International Journal of Remote Sensing*, vol. 24, pp. 4073-4092.
Schaeffer-Novelli, Y, Cintrón-Molero, G, Cunha-Lignon, M & Coelho Jr, C 2005, 'A conceptual hierarchical framework for marine coastal management and conservation: a "Janus-like" approach'. *Journal of Coastal Research*, vol. SI 42, pp. 191-197.
Schopfer, E & Lang, S 2006, 'Object fate analysis - a virtual overlay method for the categorisation of object transition and object-based accuracy assessment', paper presented to the 1st International Conference on Object-based Image Analysis (OBIA 2006), Salzburg, 4-5 July.
Shapiro, LG & Stockman, GC 2001, *Computer Vision*, Prentice–Hall, Upper Saddle River.
Skidmore, AK, Franklin, J, Dawson, TP & Pilesjö, P 2011, 'Geospatial tools address emerging issues in spatial ecology: a review and commentary on the Special Issue'. *International Journal of Geographical Information Science*, vol. 25, pp. 337-365.
Smith, TJ 1992, Forest structure. *In:* Robertson, AI & Alongi, DM (eds.), *Tropical Mangrove Ecosystems*, American Geophysical Union, Washington DC.
Song, C, Woodcock, CE, Seto, KC, Lenney, MP & Macomber, SA 2001, 'Classification and change detection using Landsat TM data: when and how to correct atmospheric effects?'. *Remote Sensing of Environment*, vol. 75, pp. 230-244.
Soudani, K, François, C, le Maire, G, Le Dantec, V & Dufrêne, E 2006, 'Comparative analysis of IKONOS, SPOT, and ETM+ data for leaf area index estimation in temperate coniferous and deciduous forest stands'. *Remote Sensing of Environment*, vol. 102, pp. 161-175.
Souza-Filho, PWM & Paradella, WR 2003, 'Use of synthetic aperture radar for recognition of coastal geomorphological features, land-use assessment and shoreline changes in Bragança Coast, Pará, Northern Brazil'. *Anais da Academia Brasileira de Ciências*, vol. 75, pp. 341-356.
Spalding, M, Kainuma, M & Collins, L 2010, *World Atlas of Mangroves*, Earthscan, London.
Specht, RL, Specht, A, Whelan, MB & Hegarty, EE 1995, *Conservation Atlas of Plant Communities in Australia*, Southern Cross University Press, Lismore.
Strahler, AH, Woodcock, CE & Smith, JA 1986, 'On the nature of models in remote sensing'. *Remote Sensing of Environment*, vol. 20, pp. 121-139.
Teillet, PM, Staenz, K & William, DJ 1997, 'Effects of spectral, spatial, and radiometric characteristics on remote sensing vegetation indices of forested regions'. *Remote Sensing of Environment*, vol. 61, pp. 139-149.
Thom, BG 1982, Mangrove Ecology: A Geomorphological Perspective. *In:* Clough, BF (ed.) *Mangrove Ecosystems in Australia*, Australian National University Press, Canberra.
Tian, Y, Woodcock, CE, Wang, Y, Privette, JL, Shabanov, NV, Zhou, L, Zhang, Y, Buermann, W, Dong, J, Veikkanen, B, Häme, T, Andersson, K, Ozdogan, M, Knyazikhin, Y & Myneni, RB 2002, 'Multiscale analysis and validation of the MODIS LAI product: II. Sampling strategy'. *Remote Sensing of Environment*, vol. 83, pp. 431-441.
Tobler, W. 'Measuring spatial resolution', Proceedings of the Land Resources Information Systems Conference, Beijing, China, pp. 12-16.
Tomlinson, PB 1994, *The Botany of Mangroves*, Cambridge University Press, Cambridge.

Townshend, JRG 1981, 'The spatial resolving power of earth resources satellites'. *Progress in Physical Geography,* vol. 5, pp. 32-55.
Treitz, P & Howarth, P 2000, 'High spatial resolution remote sensing data for forest ecosystem classification: an examination of spatial scale'. *Remote Sensing of Environment,* vol. 72, pp. 268-289.
Trimble 2011, *eCognition Developer 8.7 User Guide,* Trimble Germany GmbH, Munchen, Germany.
Turner, MG, O'Neill, RV, Gardner, RH & Milne, BT 1989, 'Effects of changing spatial scale on the analysis of landscape pattern'. *Landscape Ecology,* vol. 3, pp. 153-162.
Twilley, RR, Snedaker, SC, Yanez-Arancibia, A & Medina, E 1996, Biodiversity and Ecosystem Processes in Tropical Estuaries: Perspectives of Mangrove Ecosystems. *In:* Mooney, HA, Cushman, JH, Medina, E, Sala, OE & Schulze, E-D (eds.), *Functional Roles of Biodiversity: A Global Perspective*, John Wiley & Sons, Chichester, UK.
Twilley, RR, Rivera-Monroy, VH, Chen, R & Botero, L 1999, 'Adapting an ecological mangrove model to simulate trajectories in restoration ecology'. *Marine Pollution Bulletin,* vol. 37, pp. 404-419.
Updike, T & Comp, C 2010, 'Radiometric use of WorldView-2 imagery', DigitalGlobe Inc., Longmont, Colorado, USA.
Vaiphasa, C, Ongsomwang, S, Vaiphasa, T & Skidmore, AK 2005, 'Tropical mangrove species discrimination using hyperspectral data: a laboratory study'. *Estuarine, Coastal and Shelf Science,* vol. 65, pp. 371-379.
Vaiphasa, C, Skidmore, AK & de Boer, WF 2006, 'A post-classifier for mangrove mapping using ecological data'. *ISPRS Journal of Photogrammetry and Remote Sensing,* vol. 61, pp. 1-10.
Valiela, I, Bowen, JL & York, JK 2001, 'Mangrove forests: one of the world's threatened major tropical environments'. *BioScience,* vol. 51, pp. 807-815.
Verrelst, J, Rivera, JP, Veroustraete, F, Muñoz-Marí, J, Clevers, JGPW, Camps-Valls, G & Moreno, J (in press), 'Experimental Sentinel-2 LAI estimation using parametric, non-parametric and physical retrieval methods – A comparison'. *ISPRS Journal of Photogrammetry and Remote Sensing,* vol.
Vijayaraj, V, O'Hara, CG & Younan, NH. 'Quality analysis of pansharpened images', Proceedings of the The IEEE International Geoscience and Remote Sensing Symposium, 20-24 September 2004, Anchorage, Alaska, USA, pp. 85-88.
Wang, L, Sousa, WP, Gong, P & Biging, GS 2004a, 'Comparison of IKONOS and QuickBird images for mapping mangrove species on the Caribbean coast of Panama'. *Remote Sensing of Environment,* vol. 91, pp. 432-440.
Wang, L, Sousa, WP & Gong, P 2004b, 'Integration of object-based and pixel-based classification for mapping mangroves with IKONOS imagery'. *International Journal of Remote Sensing,* vol. 25, pp. 5655-5668.
Wang, L, Silván-Cárdenas, JL & Sousa, WP 2008, 'Neural network classification of mangrove species from multi-seasonal Ikonos imagery'. *Photogrammetric Engineering & Remote Sensing*, vol. 74, pp. 921-927.
Wang, L & Sousa, WP 2009a, 'Distinguishing mangrove species with laboratory measurements of hyperspectral leaf reflectance'. *International Journal of Remote Sensing,* vol. 30, pp. 1267 - 1281.
Wang, L & Sousa, WP 2009b, Remote sensing of coastal mangrove forest. *In:* Yang, X (ed.) *Remote Sensing and Geospatial Technologies for Coastal Ecosystem Assessment and Management*, Springer-Verlag, Berlin Heidelberg.
Wang, L, Dong, T, Zhang, G & Niu, Z 2013, 'LAI retrieval using PROSAIL model and optimal angle combination of multi-angular data in wheat'. *IEEE Journal of Selected Topics in Applied Earth Observations and Remote Senisng,* vol. 6, pp. 1730-1736.

Wang, Y, Woodcock, CE, Buermann, W, Stenberg, P, Voipio, P, Smolander, H, Häme, T, Tian, Y, Hu, J, Knyazikhin, Y & Myneni, RB 2004c, 'Evaluation of the MODIS LAI algorithm at a coniferous forest site in Finland'. *Remote Sensing of Environment,* vol. 91, pp. 114-127.

Wannasiri, W, Nagai, M, Honda, K, Santitamnont, P & Miphokasap, P 2013, 'Extraction of mangrove biophysical parameters using airborne LiDAR'. *Remote Sensing,* vol. 5, pp. 1787-1808.

Warner, TA, Nellis, MD & Foody, GM 2009, Remote Sensing Scale and Data Selection Issues. *In:* Warner, TA, Nellis, MD & Foody, GM (eds.), *The SAGE Handbook of Remote Sensing,* SAGE Publications Ltd, London.

Webster, R 1985, 'Quantitative spatial analysis of soil in the field'. *Advances in Soil Science,* vol. 3, pp. 1-70.

Weiss, M & Baret, F 1999, 'Evaluation of canopy biophysical variable retrieval performances from the accumulation of large swath satellite data'. *Remote Sensing of Environment,* vol. 70, pp. 293-306.

Weiss, M, Baret, F, Smith, GJ, Jonckheere, I & Coppin, P 2004, 'Review of methods for in situ leaf area index (LAI) determination: Part II. Estimation of LAI, errors and sampling'. *Agricultural and Forest Meteorology,* vol. 121, pp. 37-53.

Welles, JM & Norman, JM 1991, 'Instrument for indirect measurement of canopy architecture'. *Agronomy Journal,* vol. 83, pp. 818-825.

Welles, JM & Cohen, S 1996, 'Canopy structure measurement by gap fraction analysis using commercial instrumentation'. *Journal of Experimental Botany,* vol. 47, pp. 1335-1342.

Wen, Z, Zhang, C, Zhang, S, Ding, C, Liu, C, Pan, X, Li, H & Sun, Y 2012, 'Effects of Normalized Difference Vegetation Index and related wavebands' characteristics on detecting spatial heterogeneity using variogram-based analysis'. *Chinese Geographical Science,* vol. 22, pp. 188-195.

Whiteside, T, Boggs, G & Maier, S. 'Area-based validity assessment of single- and multi-class object-based image analysis', Proceedings of the 15th Australasian Remote Sensing and Photogrammetry Conference, 13-17 September 2010, Alice Spring, Australia, pp. 1-16.

Wiens, JA 1989, 'Spatial scaling in ecology'. *Functional Ecology,* vol. 3, pp. 385-397.

Wolter, PT, Townsend, PA & Sturtevant, BR 2009, 'Estimation of forest structural parameters using 5 and 10 meter SPOT-5 satellite data'. *Remote Sensing of Environment,* vol. 113, pp. 2019-2036.

Woodcock, C & Harward, VJ 1992, 'Nested-hierarchical scene models and image segmentation'. *International Journal of Remote Sensing,* vol. 13, pp. 3167-3187.

Woodcock, CE & Strahler, AH 1987, 'The factor of scale in remote sensing'. *Remote Sensing of Environment,* vol. 21, pp. 311-332.

Woodcock, CE, Strahler, AH & Jupp, DLB 1988a, 'The use of variograms in remote sensing: I. Scene models and simulated images'. *Remote Sensing of Environment,* vol. 25, pp. 323-348.

Woodcock, CE, Strahler, AH & Jupp, DLB 1988b, 'The use of variograms in remote sensing: II. Real digital images'. *Remote Sensing of Environment,* vol. 25, pp. 349-379.

Wu, H & Li, Z-L 2009, 'Scale issues in remote sensing: a review on analysis, processing and modeling'. *Sensors,* vol. 9, pp. 1768-1793.

Wu, J 1999, 'Hierarchy and scaling: extrapolating information along a scaling ladder'. *Canadian Journal of Remote Sensing,* vol. 25, pp. 367-380.

Yang, S-C, Shih, S-S, Hwang, G-W, Adams, JB, Lee, H-Y & Chen, C-P 2013, 'The salinity gradient influences on the inundation tolerance thresholds of mangrove forests'. *Ecological Engineering,* vol. 51, pp. 59-65.

Zarco-Tejada, PJ, Ustin, SL & Whiting, ML 2005, 'Temporal and Spatial Relationships between Within-Field Yield Variability in Cotton and High-Spatial Hyperspectral Remote Sensing Imagery'. *Agronomy Journal,* vol. 97, pp. 641-653.

Zhan, Q, Molenaar, M, Tempfli, K & Shi, W 2005, 'Quality assessment for geo-spatial objects derived from remotely sensed data'. *International Journal of Remote Sensing*, vol. 26, pp. 2953-2974.

Zhang, K 2008, 'Identification of gaps in mangrove forests with airborne LIDAR'. *Remote Sensing of Environment*, vol. 112, pp. 2309-2325.

Zheng, G & Moskal, LM 2009, 'Retrieving Leaf Area Index (LAI) using remote sensing: theories, methods and sensors'. *Sensors*, vol. 9, pp. 2719-2745.

APPENDICES

Appendix 1.

Structural formations in Australia (Specht 1995)

Life form and height of tallest stratum		Foliage Projective Cover of the Tallest Stratum (%) 100-70 (4)#	70-30** (3)	30-10 (2)	<10 (1)
Trees* > 30m	(T)#	tall closed-forest	tall open-forest	tall woodland	-
Trees 10-30m	(M)	closed-forest	open-forest	woodland	open-woodland
Trees 5-10m	(l)	low closed-forest	low open-forest	low woodland	low open-woodland
Trees < 5m	(VL)	v. low closed-forest	v. low open-forest	v. low woodland	v. low open-woodland
Shrubs* > 2m	(S)	closed-scrub	open-scrub	tall shrubland	tall open-shrubland
Shrubs 0.25-2m sclerophyllous & semi-sclerophyllous	(Z)	closed heathland	heathland	open-heathland	sparse heathland
non-sclerophyllous	(C)	low closed-scrub	low open-scrub	low shrubland	low open-shrubland
Shrubs < 0.25m sclerophyllous & semi-sclerophyllous	(D)	-	-	dwarf open-heathland (fell-field)	dwarf sparse-heathland (fell-field)
non-sclerophyllous	(W)	-	-	dwarf open-shrubland	dwarf sparse-shrubland
Hummock grasses	(H)	-	dense hummock grassland	hummock grassland	open hummock grassland
Herbaceous layer					
graminoids & grass	(G)	closed (tussock) grassland	(tussock) grassland	open (tussock) grassland	sparse (tussock) grassland
sedges	(Y)	closed-sedgeland	sedgeland	open-sedgeland	sparse-sedgeland
herbs	(X)	closed-herbland	herbland	open-herbland	sparse-herbland
ferns	(f)	closed-fernland	fernland	-	-
reeds/rushes	®	closed-reedland	reedland	-	-

* a tree is defined as a woody plant usually with a single stem; a shrub is a woody plant with many stems arising at or near the base
\# Symbols and numbers given in parentheses may be used to describe the formation, e.g. tall closed-forest = T4
** this cover class may be subdivided into cover intervals 70-50% and 50-30% to distinguish commercial forests

Appendix 2.

Table A2.1. List of mangrove species found during fieldwork.

Location	Species name
Moreton Bay, Australia	*Avicennia marina* *Rhizophora stylosa* *Ceriops tagal* *Aegiceras corniculatum*
Karimunjawa Island, Indonesia	*Aegiceras corniculatum* *Avicennia marina* *Bruguiera cylindrica* *Bruguiera gymnorrhiza* *Ceriops tagal* *Excoecaria agallocha* *Heritiera littoralis* *Lumnitzera littorea* *Lumnitzera racemosa* *Nypa fruticans* *Rhizophora apiculata* *Rhizophora stylosa* *Scyphiphohra hydrophyllacea* *Sonneratia alba* *Sonneratia ovata* *Xylocarpus granatum* *Xylocarpus moluccensis*

Appendix 3.

Statistical examination of pan-sharpened WorldView-2 images was performed for mangroves at Whyte Island and Fisherman Island with three samples of different tonal appearance; dark, medium, and bright mangrove features. The tables shown below are the average values of these three image tonal variation.

Table A3.1. Basic statistics of pan-sharpened WorldView-2 image of mangrove areas.

Minimum and maximum of pixel values

Methods	Band 1		Band 2		Band 3		Band 4	
	min	max	min	max	min	max	min	max
Original	**317.67**	**763.67**	**319.00**	**838.33**	**310.00**	**1094.33**	**316.67**	**1098.67**
Principal component	284.00	713.00	282.67	786.00	293.67	1136.67	319.67	1083.67
Multiplicative	63294.00	284302.00	60625.00	313684.00	56751.33	463044.67	57774.00	441934.33
Brovey	8.07	31.67	8.20	35.57	10.38	39.77	9.55	42.12
Wavelet	242.05	754.75	238.35	846.29	313.26	1146.45	73.23	1100.04
Gram-schmidt	284.67	748.00	287.00	822.67	306.67	1136.67	316.00	1108.67
Colour normalisaton	64.67	253.67	65.67	284.67	83.33	318.33	76.33	337.00

Methods	Band 5		Band 6		Band 7		Band 8	
	min	max	min	max	min	max	min	max
Original	249.00	958.00	487.00	2868.67	737.33	5298.00	664.33	4694.67
Principal component	196.33	920.33	218.33	3297.33	195.00	5754.67	189.00	5367.00
Multiplicative	46011.33	378645.67	89691.00	1294740.33	135414.33	2374598.67	129662.00	2085763.00
Brovey	7.11	39.41	22.44	88.05	33.93	153.07	28.26	138.53
Wavelet	-268.88	1042.30	438.82	2913.76	523.95	5365.76	508.71	4878.69
Gram-schmidt	225.33	965.00	468.33	3146.33	633.00	5595.67	604.67	5063.00
Colour normalisaton	57.00	315.33	179.33	704.33	271.33	1224.33	226.00	1108.00

Mean of pixel values

Methods	Band 1	Band 2	Band 3	Band 4	Band 5	Band 6	Band 7	Band 8
Original	475.86	509.04	708.99	654.14	526.12	1780.62	3047.42	2787.84
Principal component	475.87	509.04	708.99	654.14	526.12	1780.62	3047.42	2787.84
Multiplicative	154221.93	165096.47	232832.42	213775.09	170894.58	594812.03	1021356.93	933816.41
Brovey	15.26	16.34	22.44	20.85	16.92	54.88	93.30	85.36
Wavelet	474.68	508.94	706.99	647.12	515.36	1780.26	3045.11	2784.86
Gram-schmidt	475.86	509.04	708.99	654.14	526.12	1780.62	3047.42	2787.84
Colour normalisaton	122.08	130.74	179.56	166.83	135.34	439.07	746.38	682.85

The statistical measures used to assess the quality of pan-sharpened images were:

1. Standard deviation of the histogram (σ)

$$\sigma = \sqrt{\frac{\sum\left(MS_{i,j} - \overline{MS}\right)^2}{n-1}}$$

Where $MS_{i,j}$ is the individual band pixel value at row i and column j, and n is the total pixel number of MS band.

2. Relative shift of the histogram mean (RM)

$$RM = \frac{output\ mean - original\ mean}{original\ mean}\%$$

3. Root Mean Square Error (RMSE)

$$RMSE = \sqrt{\frac{1}{n}\sum_{i=1}^{n}\left(MS_{output} - MS_{original}\right)^2}$$

Where MS_{output} is the multispectral band pixel value of pan-sharpened image, and $MS_{original}$ is the pixel value of original multispectral image.

4. Correlation coefficient of multi-spectral bands (CC)

$$r = \frac{n\sum xy - (\sum x)(\sum y)}{\sqrt{n(\sum x^2) - (\sum x)^2}\sqrt{n(\sum y^2) - (\sum y)^2}}$$

Where x and y are the two images being compared, and n is the number of pairs of data.

Table A3.2. Statistical measures for evaluating pan-sharpening methods of mangrove image.

Standard deviation of the histogram

Methods	Band 1	Band 2	Band 3	Band 4	Band 5	Band 6	Band 7	Band 8
Original	**69.62**	**83.46**	**95.59**	**103.30**	**112.39**	**429.15**	**882.86**	**791.69**
Principal component	58.54	70.17	102.04	96.29	95.07	452.34	879.83	786.71
Multiplicative	27172.71	31668.61	54065.79	47954.33	40201.98	201799.51	385041.35	345883.10
Brovey	4.22	4.79	4.41	5.29	5.68	10.69	23.04	20.79
Wavelet	65.61	78.97	101.72	121.26	140.57	**428.36**	**882.78**	**792.69**
Gram-schmidt	**70.48**	**84.56**	**94.49**	**103.98**	**107.36**	424.89	846.70	758.32
Colour normalisation	33.74	38.31	35.31	42.33	45.44	85.49	184.31	166.29

Relative shift of the histogram mean

Methods	Band 1	Band 2	Band 3	Band 4	Band 5	Band 6	Band 7	Band 8
Principal component	1.2E-06	1.4E-06	**-1.3E-06**	**-8.5E-08**	-6.1E-07	1.3E-06	-3.0E-08	1.7E-07
Multiplicative	3.2E+02	3.2E+02	3.3E+02	3.3E+02	3.2E+02	3.3E+02	3.3E+02	3.3E+02
Brovey	-9.7E-01	-9.7E-01	-9.7E-01	-9.7E-01	-9.7E-01	-9.7E-01	-9.7E-01	-9.7E-01
Wavelet	-2.5E-03	-1.8E-04	-2.8E-03	-1.1E-02	-2.0E-02	-2.2E-04	-7.4E-04	-1.0E-03
Gram-schmidt	**-9.6E-07**	**-1.1E-06**	-1.7E-06	1.3E-07	**-3.7E-07**	**1.1E-07**	**-1.1E-08**	**-2.0E-08**
Colour normalisation	-7.4E-01	-7.4E-01	-7.5E-01	-7.5E-01	-7.4E-01	-7.5E-01	-7.6E-01	-7.6E-01

RMSE

Methods	Band 1	Band 2	Band 3	Band 4	Band 5	Band 6	Band 7	Band 8
Principal component	29.83	33.15	**15.68**	14.86	40.26	307.01	650.79	580.13
Multiplicative	156158.21	167646.95	238378.70	218497.68	175106.29	626880.70	1089354.97	994175.65
Brovey	465.61	499.41	692.91	641.17	520.58	1777.89	3080.82	2815.48
Wavelet	40.59	48.25	63.93	88.86	113.80	288.82	583.01	525.68
Gram-schmidt	**17.47**	**18.14**	27.31	**5.89**	**19.47**	**274.86**	**558.06**	**496.86**
Colour normalisation	356.40	381.95	535.07	492.90	397.71	1389.51	2412.35	2204.01

Coefficient of correlation of multi-spectral bands

Methods	Band 1	Band 2	Band 3	Band 4	Band 5	Band 6	Band 7	Band 8
Principal component	0.908	0.923	**0.986**	0.991	0.938	0.749	0.716	0.717
Multiplicative	0.611	0.678	0.846	0.776	0.788	**0.954**	**0.957**	**0.954**
Brovey	0.885	0.895	0.667	0.817	0.918	0.879	0.925	0.918
Wavelet	0.823	0.827	0.772	0.681	0.617	0.773	0.784	0.782
Gram-schmidt	**0.966**	**0.974**	0.958	**0.998**	**0.983**	0.783	0.784	0.785
Colour normalisation	0.885	0.895	0.667	0.817	0.918	0.879	0.925	0.918

Appendix 4.

Tabel A4.1. Rule set for mangrove composition mapping at Karimunjawa Island.

Level	Information		Landsat TM	ALOS AVNIR-2	WorldView-2
1	Vegetation		Layer arithmetics Multi-threshold seg. FDI > 100	Layer arithmetics Multi-threshold seg. FDI > 500	Layer arithmetics Multi-threshold seg. FDI > 10000
	Non-vegetation		Not "Vegetation"	Not "Vegetation"	Not "Vegetation"
2	Mangroves		Within "Vegetation" Multiresolution seg. (SP:15, s:0.1, c:0.5) Mean *5* = 750-1160 Manual editing	Within "Vegetation" Multiresolution seg. (SP:50, s:0.1, c:0.5) Brightness*Mean *3* = 15-30 Manual editing	Within "Vegetation" Multiresolution seg. (SP:100, s:0.1, c:0.5) (*7*/*6*)**4* = 620-900 (*7*/*6*)**5* = 450-680 Manual editing
	Non-mangroves		Not "Mangroves"	Not "Mangroves"	Not "Mangroves"
3	Zonation bands			Within "Mangroves" Chess board segmentation: 1	Within "Mangroves" Multiresolution seg. (SP:25, s:0.1, c:0.5)
		Zone 1	-	8 ≤ *4*/(*3*+*1*) < 12	1.55 ≥ *7*/(*5*+*6*) < 1.85
		Zone 2	-	6 ≤ *4*/(*3*+*1*) < 8	1.4 ≥ *7*/(*5*+*6*) < 1.55
		Zone 3	-	4 ≤ *4*/(*3*+*1*) < 6	1.2 ≥ *7*/(*5*+*6*) < 1.4
		Zone 4	-	0 ≤ *4*/(*3*+*1*) < 4	*7*/(*5*+*6*) < 1.2
4	Tree canopy	Canopy gaps	-	-	-
		Tree crowns	-	-	-
5	Individual species		-	-	-

FDI: Forest Discrimination Index, NIR: near-infrared, MIR: mid-infrared, PC: principal component, SP: scale parameter, s: shape, c: compactness, italic numbers represent band order for the associated images, the conditional operator used on each membership rule was "and (min)".

Appendix 5.

Mangrove composition maps of Karimunjawa Island derived from LANDSAT TM image

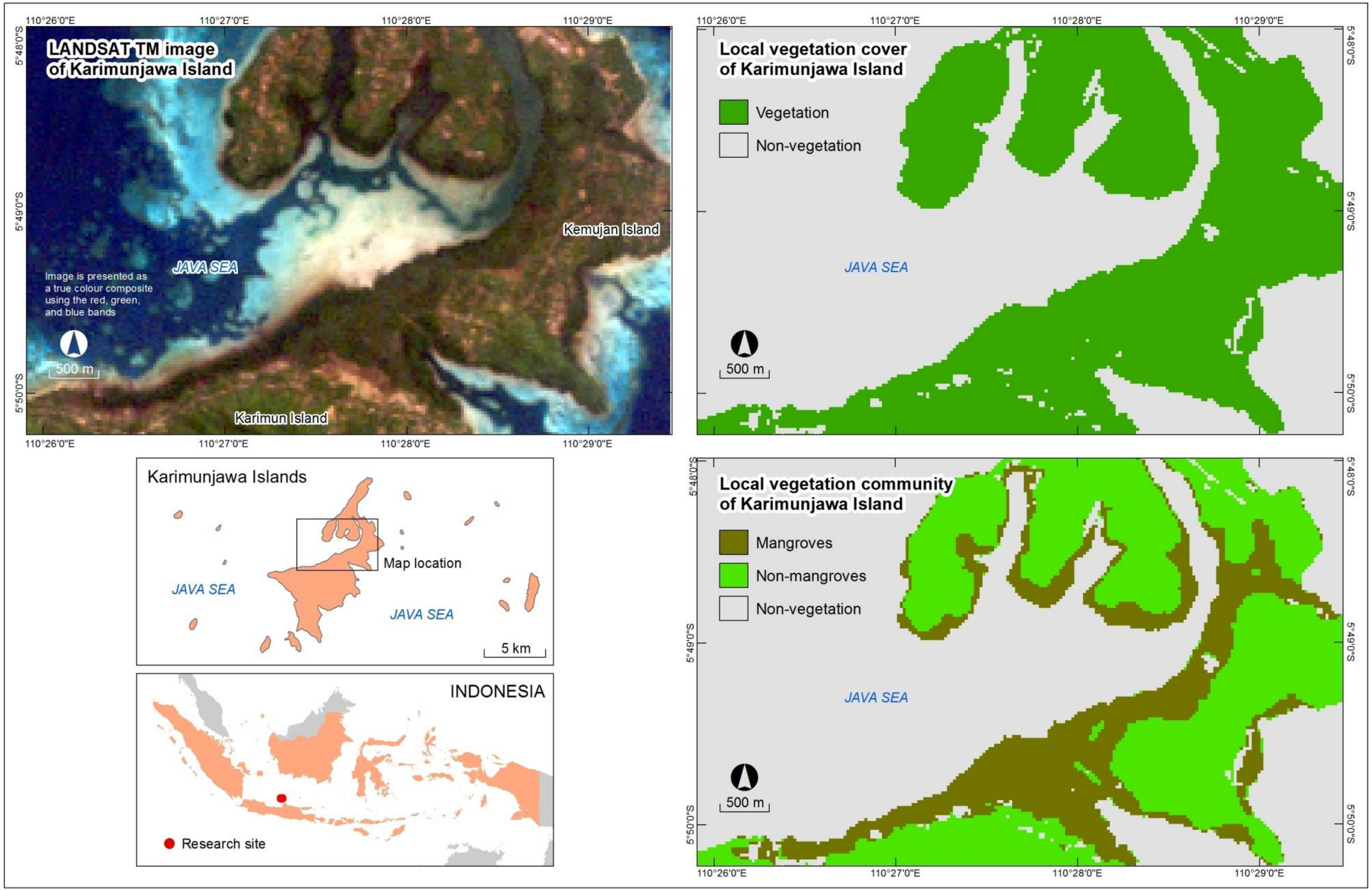

Mangrove composition maps of Karimunjawa Island derived from ALOS AVNIR-2 image

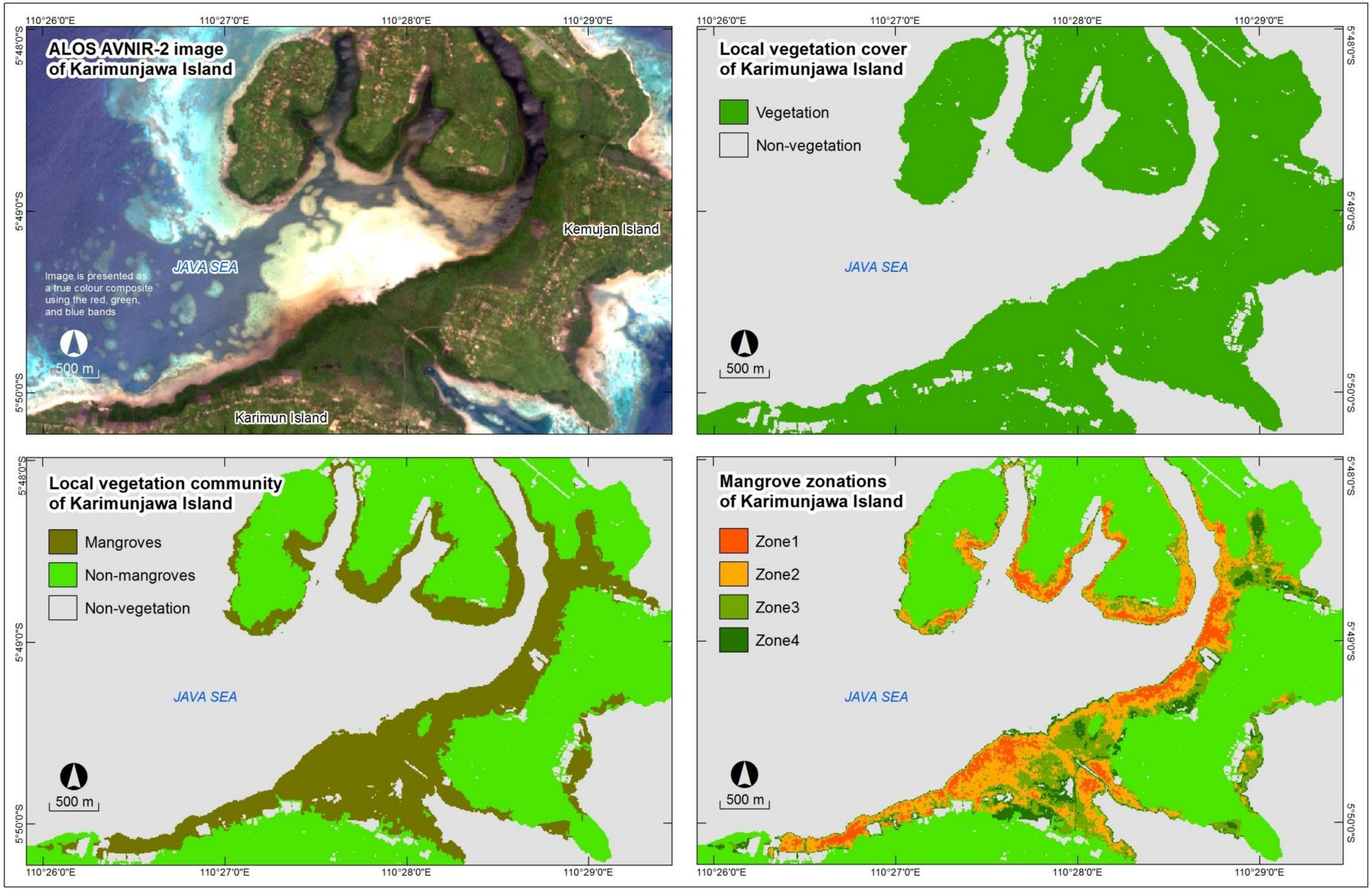

Mangrove composition maps of Karimunjawa Island derived from WorldView-2 image

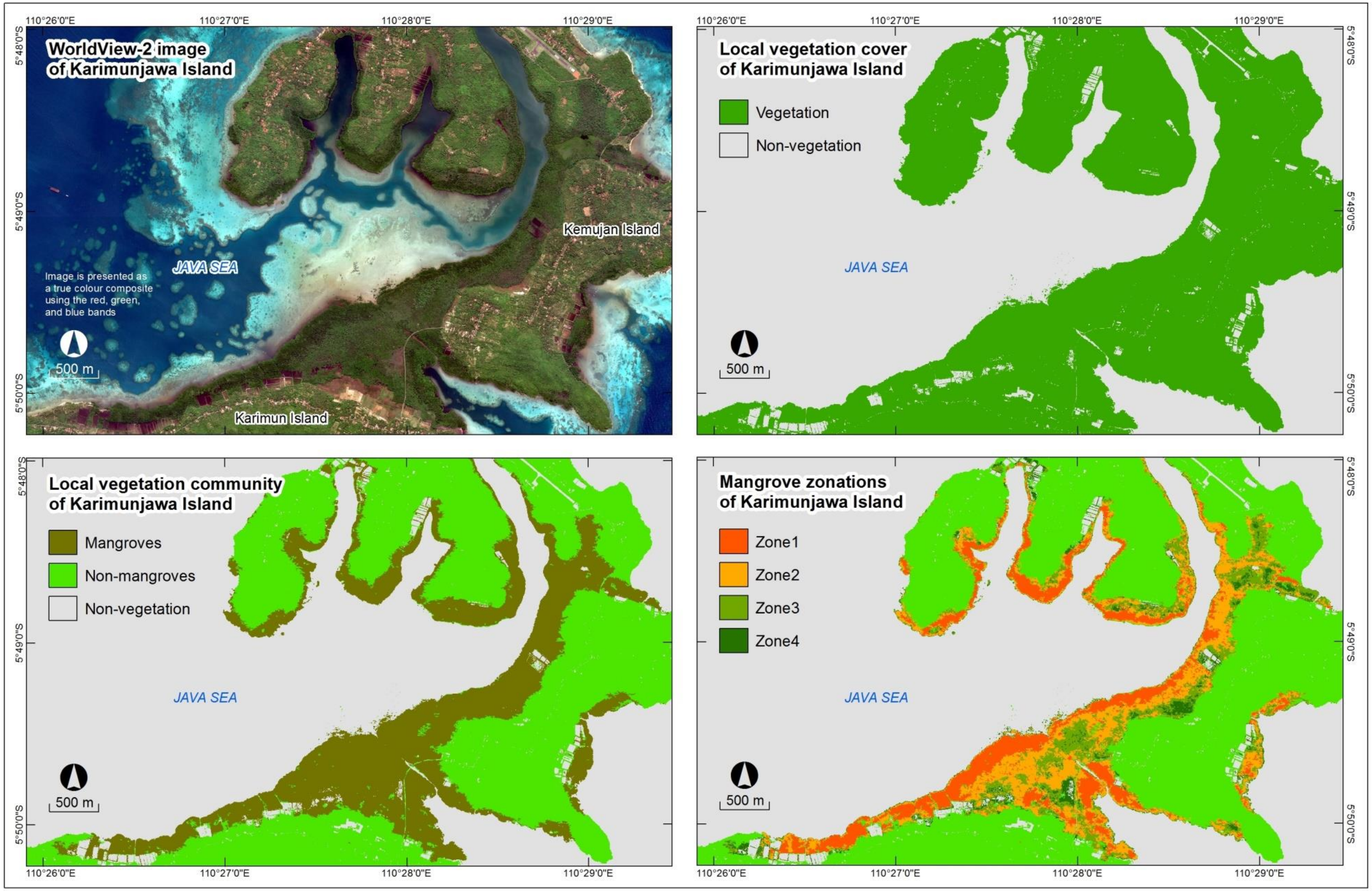

Appendix 6.

Tabel 6.1. LAI models derived from SVIs for Moreton Bay site

Image	SVIs	Best regression model	R^2
Landsat TM	SR	LAI = 2.3018 ln (SR) – 0.761	0.68
	NDVI	LAI = 3.3327 ln (NDVI) + 4.1114	0.70
	SAVI	LAI = 2.568 ln (SAVI) + 4.3968	0.71
	EVI	LAI = 2.1203 ln (EVI) + 4.0223	0.70
ALOS AVNIR-2	SR	LAI = 2.39 ln (SR) – 1.67	0.81
	NDVI	LAI = 5.00 ln (NDVI) + 4.22	0.83
	SAVI	LAI = 7.79 SAVI – 0.98	0.81
	EVI	LAI = 2.29 ln (EVI) + 4.97	0.81
WorldView-2	SR	LAI = 1.5175 ln (SR) – 0.6827	0.63
	NDVI	LAI = 5.937 NDVI – 2.1748	0.63
	SAVI	LAI = 4.2354 SAVI – 0.1382	0.55
	EVI	LAI = 1.4214 ln (EVI) + 3.0913	0.50
Segmentation Scale Parameter 10	SR	LAI = 1.5317 ln (SR) – 0.715	0.64
	NDVI	LAI = 6.0326 NDVI – 2.2496	0.65
	SAVI	LAI = 4.2411 SAVI – 0.139	0.57
	EVI	LAI = 1.4478 ln (EVI) + 3.1099	0.53
Segmentation Scale Parameter 20	SR	LAI = 1.4848 ln (SR) – 0.6116	0.62
	NDVI	LAI = 5.7543 NDVI – 2.032	0.63
	SAVI	LAI = 4.0026 SAVI + 0.0007	0.54
	EVI	LAI = 3.0902 EVI + 0.5406	0.52
Segmentation Scale Parameter 30	SR	LAI = 1.5996 ln (SR) – 0.8232	0.66
	NDVI	LAI = 6.2641 NDVI – 2.4027	0.67
	SAVI	LAI = 4.3212 SAVI – 0.1692	0.57
	EVI	LAI = 3.3418 EVI + 0.4126	0.55
Segmentation Scale Parameter 40	SR	LAI = 1.6958 ln (SR) – 0.9998	0.70
	NDVI	LAI = 4.6372 ln (NDVI) + 3.6422	0.72
	SAVI	LAI = 2.3854 ln (SAVI) + 3.6548	0.64
	EVI	LAI = 1.7296 ln (EVI) + 3.3096	0.61
Segmentation Scale Parameter 10	SR	LAI = 1.6819 ln (SR) – 0.9594	0.69
	NDVI	LAI = 4.517 ln (NDVI) + 3.6167	0.71
	SAVI	LAI = 4.6956 SAVI – 0.352	0.61
	EVI	LAI = 3.6663 EVI + 0.2659	0.59
Pixel average 3x3	SR	LAI = 1.6586 ln (SR) – 0.9476	0.69
	NDVI	LAI = 4.496 ln (NDVI) + 3.5834	0.72
	SAVI	LAI = 2.521 ln (SAVI) + 3.7243	0.69
	EVI	LAI = 1.8448 ln (EVI) + 3.3708	0.68
Pixel average 5x5	SR	LAI = 1.8199 ln (SR) – 1.2516	0.73
	NDVI	LAI = 5.0039 ln (NDVI) + 3.7378	0.75
	SAVI	LAI = 2.9186 ln (SAVI) + 3.9672	0.76
	EVI	LAI = 2.1633 ln (EVI) + 3.5777	0.76
Pixel average 7x7	SR	LAI = 1.9553 ln (SR) – 1.5031	0.74
	NDVI	LAI = 5.443 ln (NDVI) + 3.8744	0.77
	SAVI	LAI = 3.1415 ln (SAVI) + 4.1051	0.78
	EVI	LAI = 2.3121 ln (EVI) + 3.6763	0.77
Pixel average 9x9	SR	LAI = 1.6586 ln (SR) – 0.9476	0.70
	NDVI	LAI = 5.7244 ln (NDVI) + 3.9596	0.77
	SAVI	LAI = 3.2855 ln (SAVI) + 4.1906	0.78
	EVI	LAI = 2.3992 ln (EVI) + 3.7305	0.77

Tabel 6.2. LAI models derived from SVIs for Karimunjawa Island site

Image	SVIs	Best regression model	R^2
Landsat TM	SR	LAI = 4.9907 ln (SR) – 3.2185	0.63
	NDVI	LAI = 8.9644 ln (NDVI) + 8.3408	0.65
	SAVI	LAI = 6.0047 ln (SAVI) + 9.1097	0.69
	EVI	LAI = 4.8146 ln (EVI) + 8.8605	0.69
ALOS AVNIR-2	SR	LAI = 2.70 ln (SR) – 1.78	0.80
	NDVI	LAI = 0.17 $e^{3.99\ NDVI}$	0.82
	SAVI	LAI = 10.19 SAVI – 1.01	0.77
	EVI	LAI = 11.27 EVI – 0.15	0.77
WorldView-2	SR	LAI = 2.4134 ln (SR) – 1.8929	0.58
	NDVI	LAI = 0.0911 $e^{4.5009\ NDVI}$	0.62
	SAVI	LAI = 0.5777 $e^{3.0643\ SAVI}$	0.60
	EVI	LAI = 3.4252 ln (EVI) + 5.4616	0.60
Segmentation Scale Parameter 10	SR	LAI = 2.3663 ln (SR) – 1.7594	0.59
	NDVI	LAI = 0.0933 $e^{4.4838\ NDVI}$	0.63
	SAVI	LAI = 0.597 $e^{3.0084\ SAVI}$	0.59
	EVI	LAI = 3.377 ln (EVI) + 5.428	0.59
Segmentation Scale Parameter 20	SR	LAI = 2.4745 ln (SR) – 1.9836	0.57
	NDVI	LAI = 0.0802 $e^{4.678\ NDVI}$	0.68
	SAVI	LAI = 0.5466 $e^{3.1546\ SAVI}$	0.64
	EVI	LAI = 0.8829 $e^{2.2931\ EVI}$	0.61
Segmentation Scale Parameter 30	SR	LAI = 2.6671 ln (SR) – 2.4007	0.64
	NDVI	LAI = 0.0625 $e^{4.9924\ NDVI}$	0.71
	SAVI	LAI = 0.496 $e^{3.3283\ SAVI}$	0.65
	EVI	LAI = 3.7533 ln (EVI) + 5.6233	0.65
Segmentation Scale Parameter 40	SR	LAI = 2.4953 ln (SR) – 1.9565	0.59
	NDVI	LAI = 0.09 $e^{4.5654\ NDVI}$	0.66
	SAVI	LAI = 0.5709 $e^{3.1159\ SAVI}$	0.64
	EVI	LAI = 3.3784 ln (EVI) + 5.4649	0.62
Segmentation Scale Parameter 10	SR	LAI = 2.4189 ln (SR) – 1.7795	0.55
	NDVI	LAI = 0.0968 $e^{4.4773\ NDVI}$	0.64
	SAVI	LAI = 0.6117 $e^{2.9955\ SAVI}$	0.60
	EVI	LAI = 3.1937 ln (EVI) + 5.3587	0.57
Pixel average 3x3	SR	LAI = 2.5893 ln (SR) – 2.2702	0.64
	NDVI	LAI = 0.077 $e^{4.7163\ NDVI}$	0.68
	SAVI	LAI = 0.5186 $e^{3.2599\ SAVI}$	0.68
	EVI	LAI = 3.6344 ln (EVI) + 5.5853	0.68
Pixel average 5x5	SR	LAI = 2.6018 ln (SR) – 2.2406	0.64
	NDVI	LAI = 0.0811 $e^{4.6745\ NDVI}$	0.70
	SAVI	LAI = 0.4956 $e^{3.362\ SAVI}$	0.71
	EVI	LAI = 7.2041 EVI – 0.6118	0.70
Pixel average 7x7	SR	LAI = 2.574 ln (SR) – 2.1353	0.61
	NDVI	LAI = 0.0849 $e^{4.6347\ NDVI}$	0.68
	SAVI	LAI = 0.4633 $e^{3.5046\ SAVI}$	0.70
	EVI	LAI = 0.7345 $e^{2.6808\ EVI}$	0.69
Pixel average 9x9	SR	LAI = 2.5347 ln (SR) – 2.0263	0.59
	NDVI	LAI = 0.0926 $e^{4.5347\ NDVI}$	0.66
	SAVI	LAI = 0.4396 $e^{3.6084\ SAVI}$	0.70
	EVI	LAI = 0.695 $e^{2.7902\ EVI}$	0.68

Appendix 7.

Comparison of mangrove LAI maps of Karimunjawa Island estimated from different image datasets

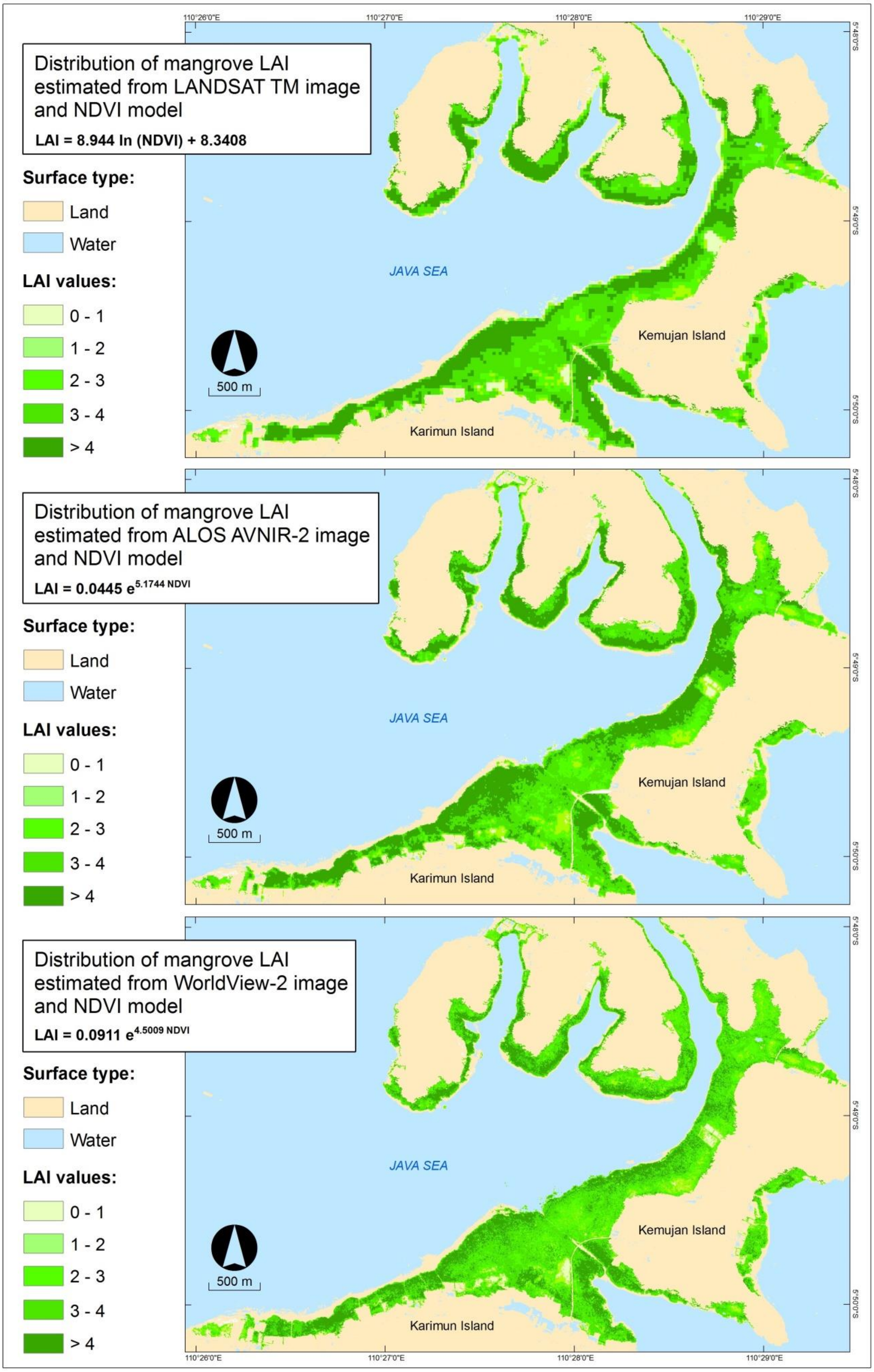

Comparison of mangrove LAI maps of Moreton Bay estimated from different SVIs applied to ALOS AVNIR-2 image

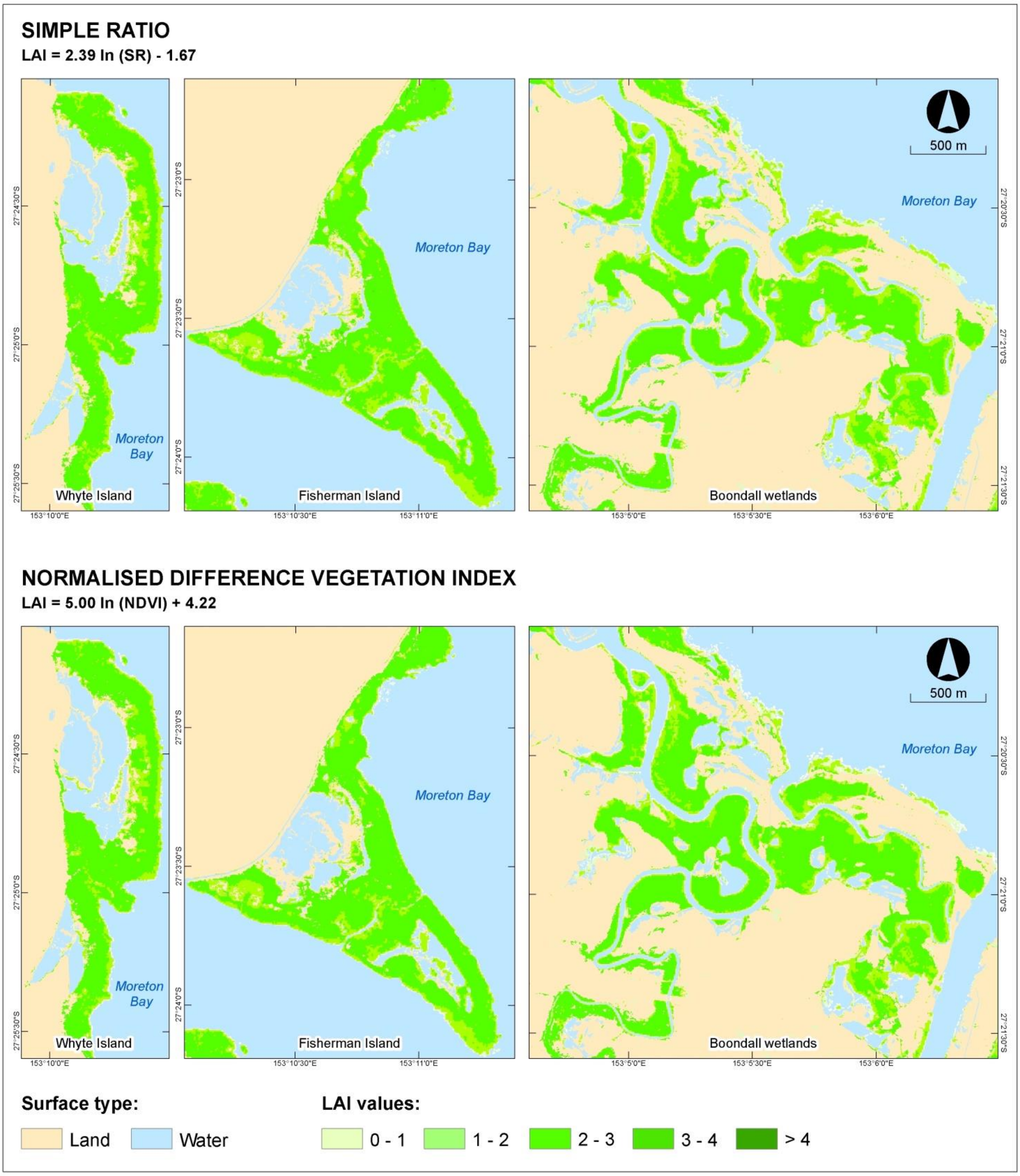

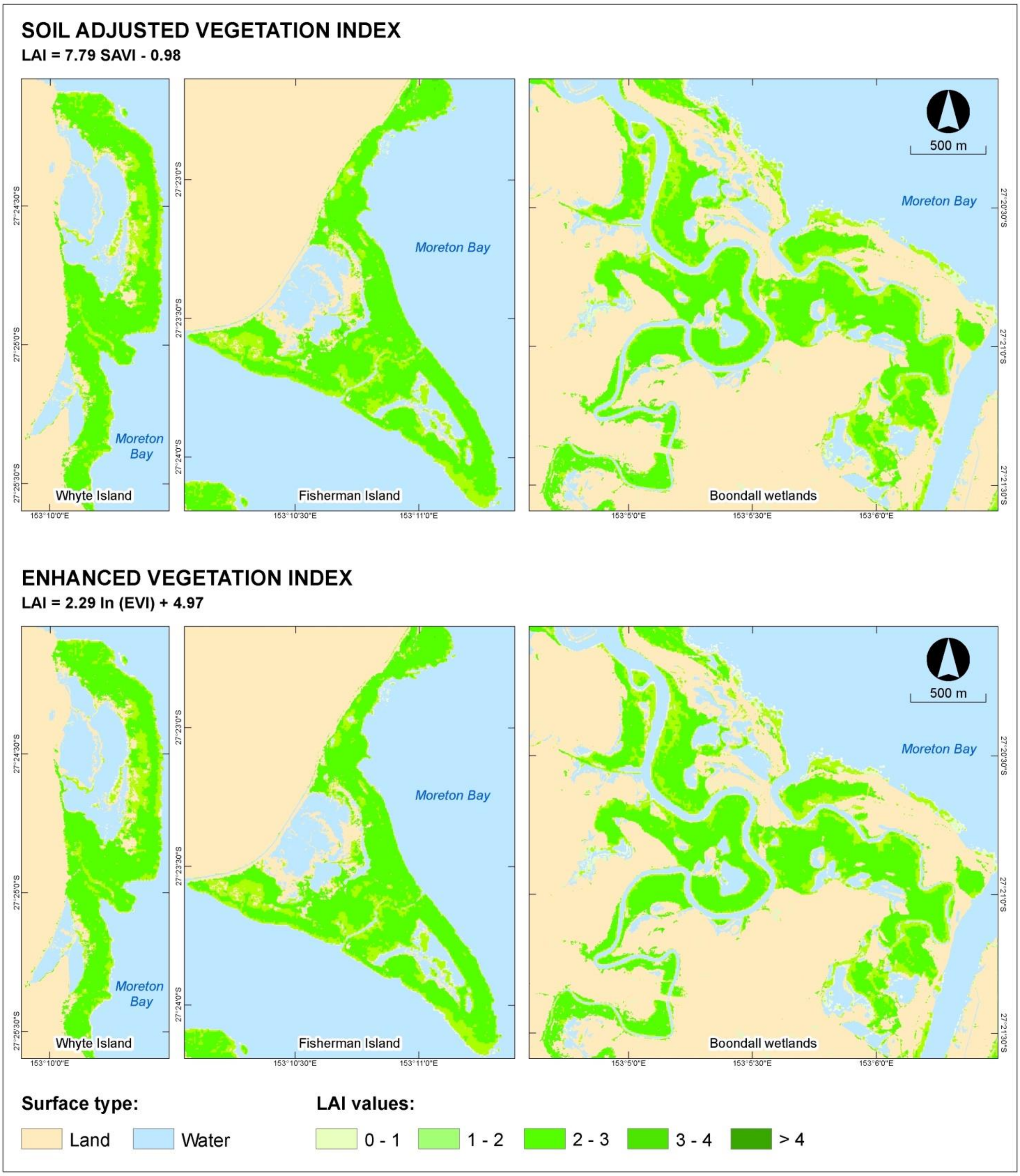
SOIL ADJUSTED VEGETATION INDEX
LAI = 7.79 SAVI - 0.98
Whyte Island
Fisherman Island
Boondall wetlands
Moreton Bay
500 m
ENHANCED VEGETATION INDEX
LAI = 2.29 ln (EVI) + 4.97
Surface type:
Land
Water
LAI values:
0 - 1
1 - 2
2 - 3
3 - 4
> 4

Appendix 8.

Table A5.1. Characteristics of image datasets used as an example in Figure 6.2.

Satellite	Resolution				Revisit time (days)	Altitude (km)	Swath width (km)	Equatorial crossing time	Launch year	End year
	Spatial (m)	Spectral	Radiometric (bits)	Temporal (days)						
Landsat 5	VNIR 30, TIR 120	4 VNIR, 2 SWIR, 1 TIR	8	16	16	705	185	09:30-10:00 AM	1984	2013
Landsat 7	VNIR 30, TIR 60, Pan 15	4 VNIR, 2 SWIR, 1 TIR, 1 Pan	8	16	16	705	185	10:00-10:15 AM	1999	
Landsat 8/ LDCM	VNIR 30, SWIR 30, Pan 15	5 VNIR, 3 SWIR, 1 Pan	12	16	16	705	185	10:00 AM	2013	
SPOT 4	VNIR 20, Pan 10	4 VNIR, 1 Pan	8	26	1-4	832	60	10:30 AM	1998	2013
SPOT 5	VNIR 10, SWIR 20, Pan 5	3 VNIR, 1 SWIR, 1 Pan	8	26	1-4	832	60	10:30 AM	2002	
SPOT 6/7	VNIR 6, Pan 1.5-2.5	4 VNIR, 1 Pan	12	1-5	1	695	60	10:00 AM	2012/14	
ASTER-Terra	VNIR 15, SWIR 30, TIR 90	3 VNIR, 6 SWIR, 5 TIR	8, 12 (TIR)	16	16	705	60	10:30 AM	1999	
ALOS-1	AVNIR-2 10, PRISM 2.5, PALSAR 10-100	4 VNIR, 1 Pan, 4 SAR	8, 5 (SAR)	46	2	692	70	10:30 AM	2006	2011
Sentinel-2	Mixed VNIR-SWIR 10, 20, 60	10 VNIR, 3 SWIR	12	10	5	786	290	10:30 AM	2015	
FORMOSAT-2	VNIR 8, Pan 2	4 VNIR, 1 Pan	12	1	1	888	24	09:26 AM	2004	
RapidEye	VNIR 5	5 VNIR	12	1	1	630	77	11:00 AM	2008	
Flock-1 (Planet Labs)	Vis 3-5	3 Vis	NA	Planned to be daily	Planned to be daily	430			2014	
IKONOS-2	VNIR 3.2, Pan 0.82	4 VNIR, 1 Pan	11	14	1-3	681	11.3	10:30 AM	1999	
Pléiades	VNIR 2.8, Pan 0.7	4 VNIR, 1 Pan	12	26	1	694	20	10:30 AM	2011	
QuickBird-2	VNIR 2.44, Pan 0.61	4 VNIR, 1 Pan	11	~5	1-3.5	450	16.8	10:25 M	2001	2015
GeoEye-1	VNIR 1.64, Pan 0.41	4 VNIR, 1 Pan	11	11	1-3	681	15.2	10:30 AM	2008	
WorldView-2	VNIR 1.84, Pan 0.31	8 VNIR, 1 Pan	11	1.1	1.1	770	16.4	10:30 AM	2009	
WorldView-3	VNIR 1.24, SWIR 3.7, CAVIS 30, Pan 0.31	8 VNIR, 8 SWIR, 12 CAVIS, 1 Pan	11	<1	<1	617	13.1	01:30 PM	2014	
Skysat-2 (SkyBox)	VNIR 2, Pan 1.1	4 VNIR, 1 Pan	16	Variable	Variable	450	8	10:30 AM	2014	
	Videos are full motion black and white 30 frames per second, duration up to 90 seconds									
Aerial photograph	Variable	Variable	Variable	Variable	Variable	Variable	Variable	Variable		
LiDAR	Variable			Variable	Variable	Variable	Variable	Variable		
TerraSAR-X	SAR 1-18.5		8	11	4.5	514	10-100		2007	

Sources: https://directory.eoportal.org/web/eoportal/satellite-missions/ and http://www.geoimage.com.au/satellites/satellite-overview

Mangrove fieldwork at Whyte Island, Moreton Bay; background picture is tall and dense *Avicennia marina* trees. Photo was taken by Kamal on 15 April 2012 (left to right: Novi, Stuart and Kamal).

Terrestrial Laser Scanner trial at Whyte Island, Moreton Bay; background picture is low-closed forest of *Avicennia marina* trees. Photo was taken by Kamal on 21 January 2013 (left to right: Yinyin, Kasper, Sabrina and Kamal).

LICOR LAI 2200 set up at Karimunjawa Island; background picture is short *Avicennia marina* scrub. Photo was taken by Hafizt on 26 July 2012 (left to right: Prama, Dimar, Kamal and Tukiman).

Mangrove fieldwork at Karimunjawa Island; background picture is tall *Rhizophora apiculata* tree. Photo was taken by Kamal on 30 July 2012 (left to right: Dimar, Hafizt, Kamal and Tukiman).

Wallaahu a'lam